Electronic Theses and Dissertations

Theses, Dissertations, and Major Papers

2009

Design of novel chemical oscillators

Mohammad Harati
University of Windsor

NOTE TO USERS

This reproduction is the best copy available.

UMI®

Design of Novel Chemical Oscillators

by

Mohammad Harati

A Dissertation
Submitted to the Faculty of Graduate Studies
through the Department of Chemistry and Biochemistry
in Partial Fulfillment of the Requirements for
the Degree of Doctor of Philosophy at the
University of Windsor

Windsor, Ontario, Canada

2008

Canada

Declaration of Co-Authorship / Previous Publication

I. Co-Authorship Declaration

I hereby declare that two chapters of this thesis incorporate material that is the result of joint research with Dr. James R. Green research group on identifying of intermediate compounds. The collaboration is covered in chapters 4 and 5 of this thesis. In all cases, the key ideas, primary contributions, and experimental designs were performed by the author, and the contribution of co-authors was primarily through the provision of mass spectrometry and NMR analysis.

I am aware of the University of Windsor Senate Policy on Authorship and I certify that I have properly acknowledged the contribution of other researchers to my thesis, and have obtained written permission from each of the co-author(s) to include the above material(s) in my thesis.

I certify that, with the above qualification, this thesis, and the research to which it refers, is the product of my own work.

II. Declaration of Previous Publication

This thesis includes 8 chapters which 5 of them are original papers that have been previously published or submitted for publication in peer reviewed journals, as follows:

Thesis Chapter	Publication title/full citation	Publication status
Chapter 2	Chemical Oscillations in the Uncatalyzed Bromate - Pyrocatechol Reaction, M. Harati and J. Wang, Z. Phys. Chem., 222, 2008, 997.	Published
Chapter 3	Chemical Oscillations and Waves in the Catalyzed Bromate-Pyrocatechol Reaction, M. Harati and J. Wang, J. Phys. Chem. A, 112, 2008, 4241.	Published
Chapter 4	Chemical Oscillations in the 4-Aminophenol - Bromate Photoreaction, M. Harati, S. Amiralaei, J. Green and J. Wang, Chem. Phys. Lett., 439, 2007, 337.	Published
Chapter 5	Nonlinear Instabilities in the Light-Mediated Bromate - 4-Aminophenol Reaction, M. Harati, S. Amiralaei, J. R. Green and J. Wang, J. Photochem. Photobiol. A: Chem., 198, 2008, 92.	Published
Chapter 6	Breathing, Merging, and Packing Pulses in the Ferroin-Bromate-Pyrocatechol Reaction, Chaos (submitted)	Submitted

I certify that I have obtained a written permission from the copyright owner(s) to include the above published material(s) in my thesis. I certify that the above material describes work completed during my registration as graduate student at the University of Windsor.

I declare that, to the best of my knowledge, my thesis does not infringe upon anyone's copyright nor violates any proprietary rights and that any ideas, techniques, quotations, or any other material from the work of other people included in my thesis, published or otherwise, are fully acknowledged in accordance with the standard referencing practices. Furthermore, to the extent that I have included copyrighted material that surpasses the bounds of fair dealing within the meaning of the Canada Copyright Act, I certify that I have obtained a written permission from the copyright owner(s) to include such material(s) in my thesis.

I declare that this is a true copy of my thesis, including any final revisions, as approved by my thesis committee and the Graduate Studies office, and that this thesis has not been submitted for a higher degree to any other University or Institution.

Abstract

Designing new chemical and/or electrochemical oscillatory systems is an important area in nonlinear chemical dynamics. We successfully designed two new chemical oscillators, the pyrocatechol-bromate-sulfuric acid and aminophenol-bromate-sulfuric acid systems. Both chemical systems exhibit a very rich oscillatory behavior and we obtained their phase diagrams in uncatalyzed and ferroin-catalyzed systems. Phase diagrams in the bromate – pyrocatechol – sulfuric acid concentration space illustrate that the observed chemical oscillations strongly depend on the ratio of [bromate]/[pyrocatechol] rather than their actual concentrations. Also, in both uncatalyzed and catalyzed systems kinetics and mechanisms have been investigated. In mechanistic studies, we have tried to determine intermediate species with various analytical techniques such as: FTIR, ^{1}H NMR, ^{13}C NMR, Mass spectroscopy, TLC, Elemental Analysis, etc.

The aminophenol system is found to be a photo-mediated oscillatory system which does not exhibit spontaneous oscillations in the absence of light. Investigation of the role of illumination, in particular the wavelength of light responsible for the oscillatory behaviour, in the aminophenol-acidic bromate system has been carried out. Study shows that the long induction time in this photochemical oscillator has an exponential dependence on the light intensity. On the other hand, the pyrocatechol system is a photosensitive oscillatory system which light is capable of quenching and inducing oscillation in the system.

Furthermore, chemical wave activities in the ferroin-catalyzed pyrocatechol system have been investigated, in 2-dimensional (2-D) beads and homogeneous systems, and

in a 1-dimensional (1-D) medium. In the 1-D pyrocatechol system, we observed various types of pulse instabilities such as: breathing, propagation failure, merging pulses, and packing phenomena. In the homogeneous 2-D medium, the pyrocatechol system exhibited two stages of wave activity. Spontaneous transitions to complex spatiotemporal patterns, as a result of anomalous dispersions, have also been observed. In the beads pyrocatechol system, variation of wave propagation speeds and spiral tip trajectories versus four different factors including concentrations of bromate, acid, and ferroin concentration and beads mass have been characterized.

Wave studies in the 1-D aminophenol system showed different types of pulse instabilities as well, where global breathing phenomena lasted for more than 48 hours in most cases. In 2-D reaction diffusion media in bead, the ferroin-catalyzed aminophenol system is capable of supporting slow waves even in the absence of light.

In loving memory of my father,

Ali-Asghar Harati

Who sadly passed away in the fall of 2004, although he is no longer physically present,

his spirit has continued to inspire me through the tough times I have encountered.

DEDICATION

This work is dedicated to my wife, Maryam Sameie Alalani, for her unwavering support, love and encouragement throughout my doctoral journey. I could not have achieved this life long goal without you! To my son, Masoud Harati, thank you for being such a wonderful baby boy! I hope that I can one day support you in your own quest for higher education. I love you both so very much!

ACKNOWLEDGEMENTS

Foremost, I would like to express my gratitude to Dr. Jichang Wang, my supervisor, for his support and encouragement throughout this entire doctoral journey. His insights regarding both stirred batch oscillatory systems and chemical wave studies have always encouraged me and I am very fortunate to have him as a supervisor who is not only enthusiastic and caring, but also friendly.

Particular thanks to Dr. Robert Schurko, internal examiner, for his priceless advice during comprehensive exam and proposal exam. Also, for his support and encouragement throughout these years, especially I am thankful for his review of my research proposal and thesis and for valuable comments he provided.

One of my most memorable doctoral courses was "Kinetic and Photochemistry." Prof. Ricardo Aroca who taught this course is an excellent, very knowledgeable and incredibly friendly teacher and researcher in the field of surface and photochemistry.

My appreciation also goes to Dr. David Ting, internal dissertation examination committee. I am thankful for his careful review of my thesis and for the valuable comments he provided.

It was an honour to have Prof. Irving R. Epstein as my external examiner. Prof. Epstein's vast experience in and depth of knowledge regarding oscillatory chemical reactions and chemical pattern formations made the oral defence of this thesis incredibly exciting and enlightening experience for me. Thank you for a rich discussion that allowed me to reflect deeply upon my doctoral experiences and think ahead to my future scholarly pursuits.

I would also like to express my gratitude to Dr. James R. Green and his PhD student Sheida Amiralaei. Dr. Green's vast experience in and depth of knowledge regarding

separation, and identifying intermediate chemicals made this PhD journey successful. I am also thankful to him for teaching me how to carry out Mass spect., analyze data and how to separate and identify unknown chemicals in a mixture. Undoubtedly, he is one of the best teachers and researchers I have ever met.

Finally, I would like to thank to all faculty, staff members and the fellow graduate students in Chemistry and Biochemistry Department. Particular thanks to Marlene Bezaire, for her support at every stage during my PhD study.

TABLE OF CONTENTS

LIST OF TABLES

LIST OF FIGURES

LIST OF ABBREVIATIONS

1-D	1-Dimensional
2-D	2-Dimensional
3-D	3-Dimensional
AOT	Sodium bis(2-ethylhexyl) sulfosuccinate
AP	4-Aminophenol
ATP	Adenosine-5'-triphosphate
BR	Briggs-Rauscher
BZ	Belousov-Zhabotinsky
c	Normal velocity
c_∞	Speed of the planar wave front
Ce^{4+}	Ceric ion
Ce^{3+}	Cerous ion
CDIMA	Chlorine dioxide-iodine-malonic acid
CIMA	Chlorite-iodide-malonic acid
CSTR	Continuous-flow stirred tank reactor
CHD	1,4-cyclohexanedione
D	Diffusion coefficient
DA	Dopamine
F_i	Ferricyanide
F_e	Ferrocyanide
FP	Frontal polymerization
G	Glucose
GO	Glucose oxidase
HEA	2-hydroxyethylacrylate
IT	Induction time
IFP	Isothermal frontal polymerization

JO	Jumping oscillons
k_{1st}	Pseudo-first order rate coefficient
MRI	Magnetic resonance imaging
MGSG	methylene glycol-sulfite-gluconolactone
N	Number of oscillation peaks
NAD(P)H	Nicotinamide dinucleotide phosphate
PEO	Poly(ethylene oxide)
Q	Quinone
QH_2	Hydroquinone
SN	Sensorimotor substantia nigra
SO	Slow oscillation
TFP	Thermal frontal polymerization
TLC	Thin layer chromatography
TCA	Tricarboxylic acid cycle
UBO	Uncatalyzed bromate oscillator
VTA	Ventral tegmental area
w/o	Water-in-oil

LIST OF APPENDICES

Chapter 1 Introduction

1. History

Chemical reactions are divided into two main categories: simple reactions and complex reactions [1]. Simple reactions are similar to men's brains in a manner that their brains are constructed of several boxes with the regulations that there is no interaction between these boxes and they are not in contact with each other, e.g., there is a box for work, a box for girlfriend/wife, a box for sport, a box for food and so on. However, complex reactions are like women's brains which presumably are made of wires and these wires are all connected to each other. Everything is connected to everything, e.g., work is connected to car, car is connected to food, food is connected to kids, and kids are connected to in-laws mother and so on. Oscillatory reactions are a subdivision of complex reactions and they are more than laboratory inquisitiveness [1]. There are many examples of oscillatory systems in biochemical reactions and biological systems [2-16]. For example, they occur in the glycolytic cycle, in which one molecule of glucose converts to two molecules of adenosine-5'-triphosphate (ATP) [17-19]. They are present in hair follicles, in the heart, in the brain, the nervous system, and they are responsible for the biological clock [20-43].

Hair follicles in mammalian skin undergo constant regenerative cycles: growth, involution, and resting phases in which periodic activation of β-catenin is responsible for their cyclic activity [20-23]. Present studies clarified that dopamine plays an important role in the core molecular mechanism of the circadian clock in the suprachaismatic nucleus of the hypothalamus, which consists of autoregulatory transcription-translation

loops with a periodicity of about 24 hours [36-43]. Circadian clocks in animals regulate the timing of molecular, physiological, and behavioural rhythms [39]. Circadian clocks are the biological timekeepers that control metabolic and behavioural activities through the cycle of day and night. The sleep-wake cycle also controls a cascade of oscillatory electrical activity in the brain. These neural oscillations take place on time scales ranging from seconds for slow oscillations to hours for the regulation of slow wave sleep.

Coenzyme Q_{10}, also known as ubiquinone, is a benzoquinone, where Q refers to the quinone chemical group. If coenzyme Q is reduced by two equivalents, the compound becomes a ubiquinol, denoted QH_2. Brain research results indicate that coenzyme Q1 (CoQ1) recycling depletes nicotinamide dinucleotide phosphate (NAD(P)H) and inhibits ascorbate recycling when cellular energy metabolism is limited by glucose deprivation [28-31]. The oscillating, age-related reduction of ferricytochrome c is sensitive to superoxide dismutase, is inhibited by coenzyme Q and it is reduced or absent from sera of younger individuals. The presence of this enzyme at the cell surface and the demonstration of its ability to oxidize reduced quinones of the plasma membrane, e.g. ubiquinol, has offered an opportunity to formulate, for the first time, a complete electron transport chain from the cytosol to oxygen at the cell surface with the NADH oxidase (NOX) protein acting as the terminal oxidase. The hydroquinone (NADH) oxidase activity and the protein disulfide-thiol interchange activity alternate to generate the 24 min period [30]. The mechanism by which coenzyme Q blocks the oscillating reduction of ferricytochrome c is unclear. The oscillations are given by both the oxidation of NADH and by the oxidation of ubiquinol.

Neuronal oscillations have been suggested to play an important role in the information processing of the brain [32-35]. Midbrain dopamine (DA) neurons receive inputs from

widely distributed brain areas. Information from these areas are integrated at the DA cell soma and then transmitted in the form of spike trains, to DA terminals. Oscillations may also play a role in information processing at the soma and dendrites. Dopamine neurons in the midbrain are spontaneously active. The amplitude of the slow oscillation (SO) is much reduced in the sensorimotor substantia nigra (SN) compared with the ventral tegmental area (VTA) and so is the number of dopamin neurons qualified as high-SO cells. The functional significance of oscillatory activities of DA neurons remains to be fully understood.

In 1828, Fechner described an electrochemical cell that produced an oscillating current, which is presumably the first published report of oscillations in a chemical system [44]. In 1899, Ostwald observed that the rate of chromium dissolution in acid periodically increased and decreased [45]. Since both systems were inhomogeneous, it was believed in the past and much through of our own century, that homogeneous oscillating reactions were impossible. While the study of oscillating reactions was well established in the mid-1970s, theoretical discussions go back to at least 1910 [3]. In the early 1900's Alfred Lotka worked on a number of theoretical chemical oscillators [46, 47]. Later, Vito Volterra continued Lotka's work and applied it to ecological systems in a predator-prey relationship. In what is now known as the Lotka-Volterra model, the equations consist of three irreversible steps that describe oscillations in population size of the predator and prey [3]. This set of reactions exhibit autocatalysis in which the products of one reaction are the reactants of another.

$$A + X \rightarrow 2X \qquad\qquad\qquad [1]$$

$$X + Y \rightarrow 2Y \qquad\qquad\qquad [2]$$

$$Y \rightarrow P \qquad\qquad\qquad\qquad [3]$$

In this model, X represents the prey and Y is the predator. A is the food source of the prey and P is the dead predator. As the prey population increases, the predators have a greater food source. The predator population is then able to increase, which in turn causes the prey population size to decrease. Once the prey population size decreases, the predators lose some of their food source and their population decreases. Once the predator population decreases, the prey population is able to increase. These oscillations in population size are somewhat analogous to chemical oscillations.

1.1 The Bray Reaction

William C. Bray, and later his student Herman Liebhafsky at the University of California, Berkeley, were the first to show chemical oscillations under isothermal conditions [48]. With their reaction consisting of hydrogen peroxide, iodate and iodine, they were able to show that the oxygen gas evolution and iodine concentration varied periodically under isothermal conditions [48-51].

Nonetheless, for the next fifty years, this result was met with serious skepticism from chemists who would argue that the reaction was not really homogeneous and that the oscillations were an artifact of dust or bubbles. Although Bray tried to disprove the skeptics by using carefully filtered and stirred solutions so that gas evolution would occur faster than bubble formation, his results were still not accepted. It was not until Noyes et al. in 1975 developed mathematical models that the scientific community became convinced of the validity of Bray's oscillator [52].

1.2 The Belousov-Zhabotinsky Reaction

Without any doubt, the most well-known oscillatory reaction is the Belousov-Zhabotinsky (BZ) reaction [53-86]. In 1950, Boris Pavlovich Belousov (1893-1970) discovered this reaction when he was trying to develop an inorganic analog of the Krebs cycle [87-89]. The citric acid cycle, also known as the tricarboxylic acid cycle (TCA cycle) or the Krebs cycle, (or rarely, the Szent-Györgyi-Krebs cycle) is a series of enzyme-catalysed chemical reactions of central importance in all living cells that use oxygen as part of cellular respiration. In aerobic organisms, the citric acid cycle is part of a metabolic pathway involved in the chemical conversion of carbohydrates, fats and proteins into carbon dioxide and water to generate a form of usable energy.

The Belousov reaction mixture consists of potassium bromate, citric acid, sulphuric acid and ceric ions as the catalyst [3]. When conducting these experiments, he expected to see the monotonic conversion of yellow (ceric ions) Ce^{4+} into colorless (cerous ions) Ce^{3+}. Instead, he found that in a well-stirred solution, the colour changed periodically from a pale yellow to clear. This colour change was attributed to the periodic oxidation and reduction of the cerium ions between Ce^{4+} and Ce^{3+}. Belousov also noted that if the reaction remained unstirred, propagating waves of colour could be seen in the media [3, 4]. In the past, and even during, the development of the BZ reaction, a number of papers were written in the West on why true homogeneous oscillating reactions were impossible. Belousov's work, like previous work in chemical oscillations was completely rejected and never published in a scientific journal.

In 1961, Anatol Zhabotinsky continued Belousov's work by using the original recipe for oscillations that Belousov had reported. By experimenting with different organic acids,

Zhabotinsky discovered that if malonic acid was used in place of citric acid, precipitate would not form [3]. This discovery gave birth to the current form of the BZ reaction. Eventually Zhabotinsky began using ferroin and found that ferroin alone, in the absence of cerium, could catalyze the reaction [90]. The distinct red colour of ferroin and blue colour of the oxidized ferroin and feriin provided better visualization. The use of ferroin allowed for direct observation of unstirred reaction to occur in thin layers thus presenting the first propagating chemical waves [4, 5, 90].

The oscillatory behaviour in the ferroin-catalzyed system differs significantly from those obtained in the cerium catalyzed BZ system, which motivated people to execute systematic investigations on this system. The ferroin-catalyzed BZ reaction does not have the same mechanism as cerium-catalyzed system. It could be due to the fact that these standard potential of BrO_3^-/BrO_2^- couple in sulfuric acid is about 1.15V, which is slightly higher than that of ferriin/ferroin couple but much lower than $Ce(IV)/Ce(III)$ redox pair.

1.3 Other Chemical Oscillators

New chemical oscillators that were neither naturally occurring nor variations of the BZ or Bray reactions were difficult to build [91-113]. The use of the continuous-flow stirred tank reactor (CSTR) in the 1980's by Epstein and co-workers enabled the discovery of many new chemical oscillators by using a systematic approach [114, 115]. Based on their proposed approach, no knowledge of the underlying kinetics is required [3]. However, the first thing that needs to be done is to work in an open reactor. Their approach can be summarized as follows: first there is need to choose a reaction that produces a species x autocatalytically. Then we have to run the reaction in a flow reactor and find conditions under which the system is bistable as a function of some parameter such as the flow rate.

Then, add to the flow a species z that perturbs the system on a time scale that is slow with respect to the relaxation of the bistable system to its steady state and by different amounts in the two bistable states. Then, increasing the amounts of z added and observing if the range of bistability narrows down and the steady state maintains its character. If we succeed to narrow down the range of bistability by continuously increase the amounts of z, the bistability will vanish eventually and oscillation will appear. If we fail to get to the oscillatory region by this technique, we have to try a different feedback species.

The first oscillatory reaction discovered by using this method was the chlorite-iodate-arsenite system [116]. Later, the first sulphur based chemical oscillator was discovered along with a series of manganese based reactions involving phosphate intermediates [91-103]. More recently, periodicities in hydrogen ion concentration have been discovered where the main oscillatory components are hydronium ions [117]. With the development of these newer systems, more mechanistic and elementary steps have been proposed. The rapid expansion in the number of new oscillators and variations of known oscillators created a need for a classification system. This led to a definition of a minimal oscillator, that is "that member of a family of chemical oscillations whose components are found as reactants, or intermediates in all members of the family," as well as taxonomy to group the chemical oscillators [3, 4].

Although the classical BZ reaction which uses malonic acid as its organic substrate has been well studied and well-known to be model for chemical wave studies, the production of bubbles, carbon dioxide, obstructs its application in studying chemical waves in reaction-diffusion media. Replacing malonic acid with 1,4-cyclohexanedione (CHD) successfully generated new chemical oscillators which were also bubble free [118-136]. In 1982, Farage and Janjic first reported that CHD could react with acidic bromate and

give rise to oscillations without metal catalyst [118, 119]. Szalai and Körös constructed a mechanistic model which could simulate the experimental results very well [129-131]. Similar to the classic BZ reaction, ferroin could also be added in the CHD-bromate system as an indicator [127, 131].

1.4 Chemical Oscillations and Autocatalysis

Complex reactions that exhibit temporal and spatial oscillatory behaviour almost always require some form of feedbacks in their kinetics; that is, the concentration of some species which affect the rates of its own production [1-5]. The feedback can either increase or decrease the rate of reaction. When the product of a reaction acts as a catalyst for the reaction, the process is known as autocatalysis. In autocatalysis, the rate is proportional to the product concentration and is known as a form of positive feedback. One of the most common examples of autocatalysis is thermal feedback, in which the heat evolved in an exothermic chemical reaction increases the rate of that reaction, thereby increasing the rate of heat production. Many biochemical reactions exhibit negative feedback, in which the rate of the production of a species decreases as the concentration of that species rises. This form of regulation has obvious advantages in living systems, which need to be able to cut off production of proteins, hormones, and other key molecules when their concentrations reach appropriate levels [2-6]. If oscillations are occurring in an open system they can occur indefinitely as long as reactants are continuously supplied and products are removed [1, 3, 4].

In the BZ reaction, bromous acid is a reactant in one reaction and a product in the other as shown below:

$$BrO_3^- + HBrO_2 + H_3O^+ \rightarrow 2BrO_2^- + 2H_2O \qquad [4]$$

$$2BrO_2^- + 2\ Ce(III) + 2H_3O^+ \rightarrow 2HBrO_2 + 2Ce(IV) + 2H_2O \qquad [5]$$
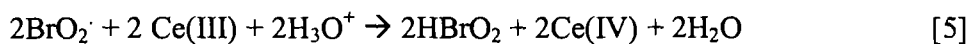
The $HBrO_2$ is therefore an intermediate of the reaction that is responsible for the autocatalysis leading to oscillations [1].

1.5 Clock Reaction

The BZ and other batch oscillatory systems are capable of supporting an important class of reaction behaviour known as clock reactions, which are the simplest manifestations of nonlinear kinetics [137-142]. A clock reaction exhibits an identifiable "induction time," during which the overall reaction rate may be practically identical to zero, followed by a comparatively sharp reaction during which reactants are converted more or less directly to the final products (this depends on the initial concentrations of the major reactants). A schematic evolution of clock reaction behaviour in the aminophenol-bromate oscillatory system is represented in Figure 1.1.
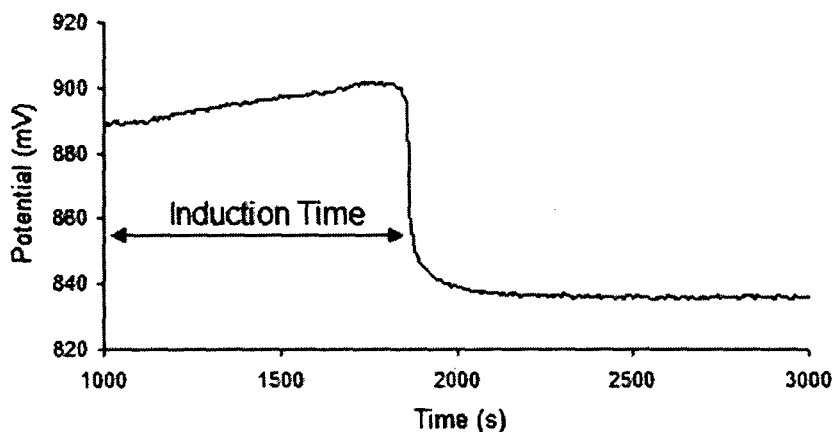
Figure 1.1 Characteristics of a clock reaction in the aminophenol-bromate reaction

1.6 Complex Oscillations

Oscillations can be very complex with more than one maximum or minimum within one cycle. In mixed-mode type oscillations, each period contains a mixture of large-amplitude and small-amplitude peaks. Mixed-mode oscillations are perhaps the most commonly occurring form of complex oscillations in chemical systems [143-153].

Probably the first example of complex periodic oscillations in chemistry is the BZ reaction in a CSTR studied in the mid-1970s [3]. In these experiments, a number of investigators also observed bursting, a form of oscillation commonly seen in neurons, but previously unobserved in simple chemical reactions. Bursting consists of stages of relatively quiescent period, in which concentrations change very little, alternating with periods of large-amplitude oscillations.

Maselko and Swinney find it convenient to characterize the complex mixed-mode patterns by the ratio of small-amplitude oscillations to total oscillations per period [153]. When the period, measured in terms of the number of oscillations per cycle increases by 1, it is called period-adding. Complex oscillations often arise via a scenario known as period-doubling. In this case, instead of observing 1, 2, 3, 4...oscillations per cycle as the control parameter is varied, one sees 1, 2, 4, 8, ...

1.7 Chemical Chaos

In some cases, chemical oscillations exhibit seemingly random fluctuations in frequency and amplitude [152-158]. This type of behaviour is frequently referred as "chaos". For instance, if a heart suddenly begins chaotic non-periodic oscillations, it can result in death [1, 7]. The path of these systems can be described but they are incredibly sensitive to initial conditions. A chaotic system may be defined as one having three

properties: deterministic dynamics, aperiodicity, and sensitivity to initial conditions [3]. Deterministic dynamics implies that there exists a set of laws that govern evolution of the system. It is not necessary that we are able to write down these laws, but they must be specifiable. The requirement of aperiodicity means that the behaviour of a chaotic system in time never repeats. A truly chaotic system neither reaches a stationary state nor behaves periodically; in its phase space, it traverses an infinite path, never passing more than once through the same point. Related to, but distinct from, the property of aperiodicity is the sensitivity, also known as "butterfly catastrophe," of a chaotic system to its initial conditions.

The BZ reaction in a flow reactor shows chaotic behaviour in two different regions, generally referred to as the high-flow-rate and the low-flow-rate regions. Three different routes to chaos, say, period-doubling, period-chaotic sequences and intermittency have been observed in the BZ reaction. The notion of controlling chaos is obviously an attractive and remarkable one; chaos can be controlled in a certain sense. We can control chaos by stabilizing a single, unstable periodic orbit embedded within a chaotic attractor. In view of the appearance of chaos in systems ranging from chemical reactions to lasers, to flames, to hearts, and to brains, our ability first to understand and then to control this ubiquitous phenomenon is likely to have important consequences.

1.8 Influence of External Factors

It is feasible to control and manipulate oscillations by changing external factors such as stirring rate, light illumination in photosensitive and/or photo-induced systems, the presence of oxygen, and temperature [159-189].

Macromixing and micromixing occur on two different time scales. In the faster process, macromixing, lumps of fluid having different compositions come together and become mixed in such a way that the system becomes homogeneous on a macroscopic scale. The rate of macromixing is largely controlled by the average velocity of fluid in the reactor, which can be enhanced by increasingly rapid stirring while micromixing depends on molecular diffusion. Micromixing is the process whereby the fluid becomes mixed on a molecular scale and generally requires significantly more time than macromixing. Mixing can serve as an additional, more subtle control parameter. In addition, the interaction of mixing with nonlinearity, and especially with autocatalysis, can give rise to new phenomena, such as chiral symmetry-breaking and stochasticity in both open and closed systems [3, 4, 159-164]. What is already clear is that the interaction of nonlinear chemical dynamics with imperfect mixing leads to a rich variety of phenomena.

Stirring effects have been observed in bromated oscillators with both malonic acid and CHD acting as the organic substrate independently [159-164]. Menzinger et al. have investigated stirring rate effect on the cerium-catalyzed BZ reaction and ascertained that under anaerobic conditions, stirring rate can modify the oscillation parameters such as frequency and amplitude of peaks [161]. Their following experimental research showed that in a stirred batch reactor, large concentration fluctuations which were spatially distributed rather than homogeneous existed in the ferroin-catalyzed BZ system ubiquitously [164]. They also reported that the fluctuation was dramatically diminished if the gas space above the liquid was eliminated in an open batch reactor [164]. They suggested that the exchange between the liquid and gas phase and concentration gradients due to the bromine adsorption at the wall of the reactor might be the source of concentration fluctuation. Farage and Janjic have studied stirring rate effect on the

uncatalyzed CHD system and observed that the increase of stirring rate in a low range could cause increase of oscillation amplitude while decreasing the stirring rate revived spontaneous oscillations after chemical oscillations have disappeared at a higher stirring rate [119].

Researchers are also fascinated by the influence of light on chemical oscillators since light is very convenient for exploring such interactions [165-180]. Photosensitive and/or photo-controlled oscillatory systems provide an exceptional means to understand the interaction between intrinsic dynamics and external forcing. The ruthenium catalyzed BZ reaction is one of the most studied photochemical oscillators. Kuhnert and co-workers discovered that photoexcited $Ru(bpy)_3^{2+}$ reacts with bromate to produce the bromide ion [183]. Also, Hanazaki et al. found that light has an accelerating effect on autocatalytically oxidizing $Ru(bpy)_3^{2+}$ to produce bromide ions [178, 179]. Sørensen and co-workers reported that the Ru-catalyzed BZ reaction can be quenched by light and concluded that bromide ions and bromous acid were produced under illumination [177]. Ruoff has proposed two major responses when illuminating Ru-catalyzed BZ reaction with light: one is the photoproduction of bromous acid at the beginning of the reaction when little amount of brominated malonic acid (BrMA) was present in the system, and the second one is the photoproduction of bromide ions in the presence of a large amount of BrMA [181].

Another external factor which has influence on oscillatory dynamics is the presence of oxygen [181-187]. The oxygen flux can be controlled in two different ways: controlling the oxygen concentration by using mass flow controller at a constant stirring rate or fixing the oxygen concentration by controlling the influx of oxygen with the stirring rate [3]. Several research groups have tried to establish the influence of oxygen on oscillatory

systems so far. Among them, Hadad et al., was the first to report that the presence of oxygen could enhance the reduction of ceric ions by malonic acid [188]. De Kepper and co-workers have found that the flow of oxygen could change phase diagram of the BZ reaction [3]. Strizhak and co-workers investigated the oxygen effects on the BZ reaction in a closed system. They explained how oxygen affects the oxidation of organic compounds and their intermediates [145]. They suggested that at first, oxygen reacts with malonyl radicals, to produce peroxymalonyl radicals and the next step is associated with chain reaction of peroxymalonyl transformation.

The last external factor which will be discussed here is temperature that has pronounced effects on bromate-based oscillations [189]. Szalai and Körös discovered that increasing temperature shortened the induction period in the CHD-bromate reaction [129]. This is caused by the slow reaction of CHD with bromate at room temperature, which is a key step to influence the induction time. Elevating temperature could speed up this reaction. Nagy et al. reported that the temperature dependence of the BZ reaction is associated to the original compositions of the reaction [192]. Generally, the increase of temperature leads to the increase in the frequency of oscillations.

1.9 Chemical Waves

Our understanding of the world is not complete until we understand the nature and properties of waves [1-7, 193-238]. Waves and wavelike phenomena are all over the universe and we encounter them on a daily basis whether we notice them or not. There are different varieties of waves such as: sound waves, electromagnetic waves, water waves, sine and cosine waves, stadium waves, and earthquake waves are just a few to name. In addition to these, we can consider the "Hello, Good Morning!" wave of the hand

as a wavelike phenomenon. The first thought of waves for many people is a picture of a wave moving across the surface of a lake, pond, or a river. The water waves may appear to be traveling together as a front in a straight-line direction, perhaps towards a sandy shore. The waves may also be circular waves which originate from the point where the disturbances occur; such circular waves travel across the surface of the water in all directions; however their amplitude decreases as they are moving forward.

The thought of waves often brings to mind a baseball stadium when the enthusiastic fans are doing the wave! When performed with reasonably good timing, a noticeable ripple is produced which travels around the stadium. This ripple appears when a group of fans rise up from their seats, swing their arms up high, and then sit back down. The first row of fans abruptly rises up to begin the wave; as they sit back down, next row begins its motion. The wave is passed from row to row as each individual member of the row becomes temporarily displaced out of their seat, only to return to it as the wave passes by.

Then there is the "Hello, Good Morning!" wave. Whether in the driveway as you begin your trip to school, on the street on the way to school, or in the hallway on the way to your first class, the "Hello, Good Morning!" wave provides a simple example of wave. The hand is raised, moved to the left, then back to the far right and finally returns to its original position. And we call the process of doing it "waving!"

Chemical waves are concentration profiles which can maintain their amplitude in time [3-7]. There are two types of chemical waves: the first type is the propagating front, which occurs very frequently in the reaction-diffusion medium. The second type is the static profile and their formation requires very specific conditions on the relative diffusivities of the activator and inhibitor [3-7].

In order to initiate a chemical wave, having a perturbation is vital; however where it

comes from is a question that still needs to be addressed. One possibility is that the experimenter can make the initial perturbation intentionally [7]. A system can be pushed to wave activity by chemical means (such as adding a drop of acid to a pH-sensitive reaction), by electrical stimulation, by thermally increasing the rate of a reaction or by illuminating the system at the appropriate wavelength in photosensitive systems.

A very interesting question is how chemical waves can arise spontaneously. The onset of waves has largely been attributed to the presence of macroscopic heterogeneities in the system such as dust or bubbles [3, 7]. The mechanism by which these macroscopic particles initiate waves has yet to be explained. This leads to the question of what will happen if a system reaches oscillatory conditions but there is no macroscopic particle to initiate waves? It has been shown that these waves cannot start based on thermal internal fluctuation because those types of fluctuations are small and would require time to reach macroscopic level to cause waves [3, 7]. The point of nucleation is currently thought to be one of two possibilities. The first is that it is a result of spontaneous concentration changes. These changes exceed the threshold of excitability at a point and then initiate waves from there [7]. The alternative to this idea is the presence of a heterogeneous particle such as a dust particle. These particles, referred to as pacemakers or catalytic site, can be reduced with careful filtration and conditions but they cannot be completely eliminated [193]. The time before wave initiation can be increased by applying seemingly "dust free" conditions and careful filtration, but waves cannot be suppressed indefinitely [3]. It is still up for debate as to whether or not these waves can form without pacemakers. When the solution oscillates, it generates a phase wave, which ultimately turns into a trigger wave that can propagate through the excitable bulk of the medium. The next front starts after the oscillatory region has gone through its cycle and the excitable part has

returned to its resting state after the refractory period. Thus, we see a series of repeated waves. As Tyson and Keener pointed out, the oxidizing wavefront in the BZ system is a trigger wave propagated via the reaction and diffusion of bromous acid, while the reducing waveback is actually a phase wave that follows behind the gradient created by the wavefront [194]. Pagola and co-workers suggest that dust particles do serve as pacemakers, but it remains an open question as to whether waves can arise from random concentration fluctuations or whether it was simply too difficult to eliminate all heterogeneities from the system [193].

1.10 Reaction-Diffusion Fronts

The simplest type of chemical wave is a "front" which is a thin layer of reaction that propagates through a mixture, converting the initial reactants to final products. The front wave consists of a single point or a very narrow interval where concentrations jump from one nearly constant level to another. It is essentially a clock reaction happening in space. The mixture ahead of the front is kinetically frozen in its unreacted state. For autocatalytic reactions, this may arise due to the absence of the autocatalytic species in the original reaction mixture. Behind the front, the reaction rate is again zero as the mixture has attained its final thermodynamic equilibrium state. A flame is one of the most familiar types of chemical wave and it has a narrow zone in which a chemical reaction is taking place and which separates unconsumed reactants ahead from the final products behind [3, 195]. A flame will propagate through the reactant mixture with a constant speed which depends on the chemistry and kinetic parameters of reactants. The front wave is driven by a combination of chemical feedback coupling with molecular transport processes such as diffusion.

Fronts propagate through combination of diffusion and reaction kinetics, typically adopting a constant velocity which depends on the diffusion coefficient and the rate coefficient for the reaction. In each case, the speed c has the form

$$c = A\sqrt{Dk_{1st}}$$

[6]

where A is a constant, D is the diffusion coefficient for the autocatalytic species and k_{1st} is the pseudo-first order rate coefficient for the autocatalytic reaction. The evolution of a chemical wave is governed by the reaction-diffusion equation, which combines Fick's law of diffusion with chemical reaction rate law. Reaction diffusion equation is as follows:

$$\frac{\partial c}{\partial t} = D\frac{\partial^2 c}{\partial x^2} + r(c)$$

[7]

For a quadratic autocatalytic reaction A + B $\rightarrow$ 2B with $r = kab$, two reaction-diffusion equations are

$$\frac{\partial a}{\partial t} = D_A\frac{\partial^2 a}{\partial x^2} - kab \qquad \frac{\partial b}{\partial t} = D_B\frac{\partial^2 b}{\partial x^2} + kab$$

[8]

where D_A and D_B are the diffusion coefficients for the reactant and autocatalyst respectively.

For conditions just outside those required for spontaneous oscillatory behaviour, the BZ system shows a property known as excitability. An excitable system is characterised by first, having a steady state; second, the steady state is unaffected by small perturbations; and third, if the perturbation exceeds some critical or threshold value, the system responds by exhibiting an excitation. Following the excitation, the system eventually returns to the initial steady state and recovers its excitability. During the recovery period, the system is insensitive to further disturbances and is said to be

refractory until it has regained its excitability. Excitability is found widely throughout

biological systems with important examples in nerve signal transmission and co-ordinated

muscle contraction, and brain tissues [2-43].

1.11 Waves in 2-D

Waves in two dimensions can look very much like those seen in biological systems [2].

If a thin layer of reaction solution is spread over an area such as a Petri dish, and the

medium is left undisturbed, chemical waves may begin to propagate across the medium

[196-212]. The single propagating front is the most common type of wave. The simplest

type of wave in 2-dimentional (2-D) reaction-diffusion system is known as "pulse" and

they are regularly found in excitable systems. Circular wave is a result of the reaction

occurring at the same speed in all directions and all initiating at the same point. Figure 1.2

shows a single circular wave in the aminophenol-bromate system:
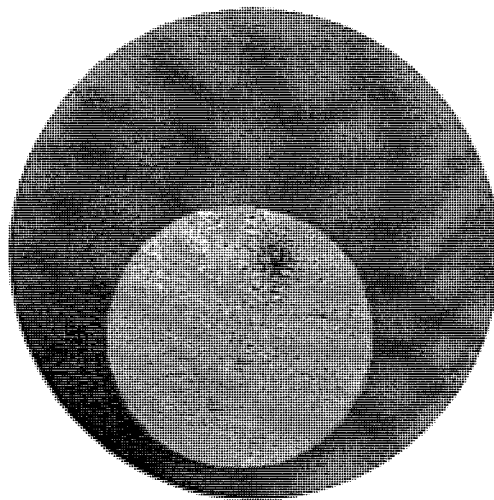
Figure 1.2 Circular wave in the aminophenol-bromate system

A wave train is a series of pulses that travel one after the other. If the solution is spread as a thin film (*e.g.* in petri dish) and initiation is from a point source, the natural geometry will be for a series of concentric, circular wave pulses, i.e., a target. The greater the separation between fronts in a given target, the longer the solution has to recover from the passage of one wave before the next front arrives. During this period, the concentration of the inhibitor is decreasing, so widely spaced waves are propagating into solutions of lower [Br⁻] than closely-spaced waves.

In Figure 1.3, in the first picture, two pacemaker sites can be seen, one at the top and the other at the bottom of the dish. In frame 2, sometime later, the third pacemaker has developed in the middle of the Petri dish. When wave fronts from different pacemakers meet, they annihilate. Chemical waves cannot pass through each other or 'bounce off' each other, as the solution immediately behind a wave is refractory and will not support wave propagation until it has recovered. In frame 4, the central pacemaker apparently has disappeared and has been overtaken by the other two pacemakers from the top and the bottom of the dish. In frame 5, the waves emanating from the bottom pacemaker that has the highest frequency have virtually overtaken the top pacemaker site and entrained the whole dish.
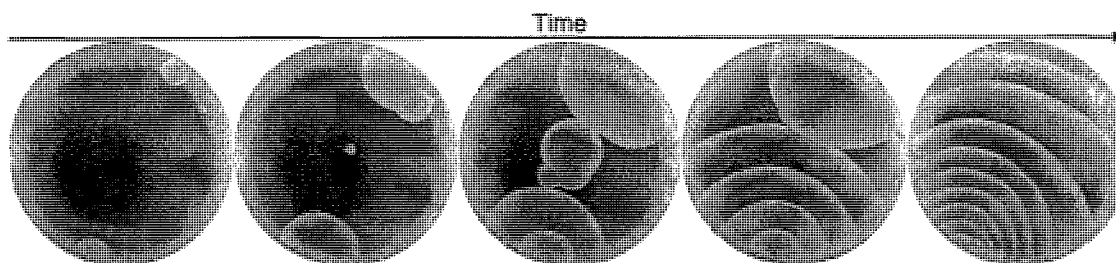
Figure 1.3 Wave evolutions during the course of wave activity in the aminophenol-bromate system

Different pacemaker sites, corresponding to different heterogeneities, have different natural oscillatory frequencies, so waves are initiated at different periods from each site. This leads to a variation from target to target in the wavelength/frequency and in the velocity of the fronts. For any given target, the three quantities are related by the simple condition

velocity × period = wavelength   [9]

This equation is known as the dispersion relationship. The frequency of a wave refers to how often a wave passes through a point in the medium.

In two- (and three) dimensional waves there is the possibility that the front wave may be curved. Investigators have shown theoretically and experimentally that the velocity of a curved front depends on the curvature [213-217]. The dependence of the speed of a wave on the curvature of the front is given by the eikonal equation, which has the form

$$c = c_\infty - \frac{D}{r}$$
                                                                                      [10]

Here c is the normal velocity of the curved front wave, c_∞ is the speed of the corresponding planar wave front, D is the diffusion coefficient of the autocatalytic species and r is the radius of the wave segment. For a circular front, the radius is positive and is simply equal to the radius of the circle. Because of this, the wave speed is reduced from the planar wave speed.

Breaking a propagating wave will make two free ends which subsequently lead to the creation of spiral [218-232]. An example showing a spiral is shown below.
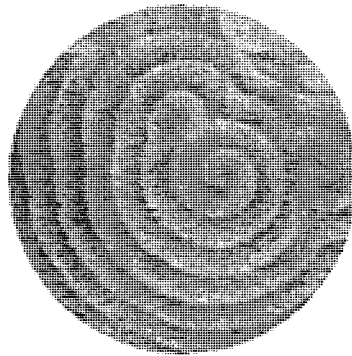
Figure 1.4 Spiral formed in the pyrocatechol-acidic bromate system in a Petri dish

There are some differences between spirals and targets, e.g., the location of the spiral core does not depend on the existence of any heterogeneity in the system. In contrast, targets require a repetitive stimulus to produce new waves: if the heterogeneity at a pacemaker site is removed, no new waves will be initiated. In nature, spirals are found far more often than targets due to the large number of irregularities in natural systems. Spiral waves are seen in a number of different oscillatory systems including carbon monoxide oxidation on platinum crystals [233], aggregation of slime moulds [234], and the myocardium of the heart [235].

The center or core of a spiral has approximately uniform concentration out of which the spirals form, and if you watch a single spiral wave carefully over a long period of time, you may see something surprising. Under certain circumstances, the core of the spiral moves around! This spiral core actually moves in the media [3-5]. The core motion is not regular and in fact can be very complex ranging from simple circular and semicircular patterns to flower-like petal paths [227-232]. This motion of the spiral core is known as

meandering, and was first discovered in numerical experiments on the Oregonator model [231] and then confirmed by experiments in the ferroin-catalyzed BZ reaction [232].

1.12 Waves in 3-D

Three-dimensional (3-D) waves are much more difficult to observe and conduct computations on in comparison to two-dimensional waves. The large number of variables, including things like bubbles and convection currents make three-dimensional waves very difficult to study experimentally [3-5]. Some success, however, has been achieved when these experiments are performed in gels by Steinbock et al. [236-238]. Current knowledge of three dimensional wave formations is still limited but this type of pattern formation would be seen in many natural systems including the heart and brain [3]. The target patterns and spiral waves seen in two dimensions would become spherical and scroll patterns in three dimensions.

1.13 Turing Patterns

Waves are propagating reaction-diffusion structures that depend on the existence of an excitable medium and a sustained initiation source. Alan Turing, the British mathematician, in 1952 proposed a theoretical model for the development of spatial form on the basis of diffusion-driven instability [239]. Turing patterns are also called stationary waves which are stationary in time but periodic in space [240-248].

The systems' requirements for exhibiting a Turing pattern are: it must involve nonlinear feedbacks and the feedback species must have a lower diffusivity than the other species, and for spatial patterns to be indefinitely sustained, it is necessary to have an open system. Chlorite-iodide-malonic acid (CIMA) reaction has shown the first experimental evidence

of Turing pattern in 1990 [240]. In order to allow a continuous flow to the reaction

domain, reaction is carried out in a gelled medium. The large starch molecules become

immobilised by being trapped in the cross-linked structure. The I_3^- is immobilised

whenever it complexes to the starch, thus effectively reducing the diffusivity of the

feedback species I^- through this complexation.

2. New Trends and Developments

2.1 Chemical Wave

Target and spiral waves were discovered about 30 years ago and have been observed in

a variety of chemical, biological, and physical systems [1-7]. One part of Epstein and

co-workers' work deals with wave studies on the BZ reaction in water-in-oil AOT

microemulsion [249-251]. Microemulsions are thermodynamically stable mixtures of

water, oil, and surfactant which also contain micelles. The role of the surfactant is to

make a connection between two immiscible fluids. Microemulsions have an oil phase in a

continuous water phase. However, in reverse microemulsion droplets of water are

dispersed in an oil phase. One of the most commonly used water-in-oil (w/o) reverse

microemulsions uses the surfactant sodium bis (2-ethylhexyl) sulfosuccinate (Aerosol-OT,

AOT). The BZ reaction reagents, which are polar, are dissolved in the water droplets. By

starting the reaction, nonpolar species such as bromine and bromine dioxide which are

produced in water can diffuse into oil. Droplets communicate through the oil phase via

fast diffusion of these small molecules or during droplet collision/fusion/fission. Epstein

and co-workers reported the observation of segmented spiral and target waves in the

BZ-AOT system that were highly ordered and regularly separated by gaps [249]. They

have noticed that segmented spirals have several breaks and only the segment closest to the spiral tips curls while in the trigger waves the end part of broken wave curls. Lifetimes of segmented waves in this system are about 3 hours in the best case. A proposed mechanism suggests that segmented spirals are Turing structures in a system possessing multiple steady states such as excitable and pseudo-Turing unstable. More recently, they discovered that adding poly(ethylene oxide) (PEO) stabilizes the formation of clusters in the system by adsorbing on the water/oil interface of droplets and therefore increasing lifetime of dashed waves for 12-14 hours [250]. However, if the microemulsion is prepared 24 hours before starting the reaction, the system does not display dashed wave in the absence of PEO while dashed waves are present in PEO added system. Their experiments reveal that the presence of at least two droplet populations with different sizes is vital for the appearance of dashed waves. PEO stabilizes these populations and thereby prolongs the duration of the dashed waves.

Recently, a new type of traveling waves, the inwardly propagating concentric waves (antitargets) and the inwardly rotating spirals (antispirals) were observed by Vanag et al. in BZ-AOT [251]. In antispirals, the waves propagate in toward to the center and they appear when the system is far from the boundary between the reduced steady state and oscillatory state. This makes it very easy to change the type of spiral by a small variation in the structure of the either microemulsion or the chemical composition. They also present another novel type of solitary traveling wave called jumping oscillons (JO) [252]. JO waves propagate in such a manner that the pulses periodically disappear from its original position and then reemerge at a fixed distance. This phenomenon is a combination of both solitons and oscillons, i.e., constant motion and sustained oscillation. The existence of this kind of wave activity requires a high value of inhibitor diffusion

coefficient in comparison with other species' coefficients. This wave activity may be achievable in water-in-oil system. Ouyang et al. also reported their experimental and theoretical studies of inwardly propagating waves (antiwaves) in an open spatial reactor using a chlorite-iodide-malonic acid reaction [253]. Antiwaves appear spontaneously when the system was set to near a hopf bifurcation point and it changed to ordinary waves when the system was moved away from the hopf onset. In most of their experiments antitargets dominate the system because they had longer oscillation periods and thus suppressed antispirals with smaller periods.

In 2008, Taylor et al. used water-in-oil (w/o) microemulsions with neutral (Triton X-100, TX) or cationic (CTAB) surfactants in order to study an acidic autocatalytic reaction of bromate-sulfite [254]. This reaction is an acid autocatalytic reaction that displays both clock and front type behaviour. They determined the effect of the composition of the water-in-oil microemulsion on the reaction, and the propagating acid front shows dependency on w/o composition, propagating 10 times faster in the aqueous phase than in microemulsion environment. The pH is reduced in the TX system and both the initial and final pH is shifted to higher values in the CTAB system.

Despite our increased knowledge on vortices in oscillatory and excitable systems over the past decade, we still have very restricted information on their three-dimensional analogues [255-258]. The latter structures are known as scroll waves which are three dimensional spiral waves that rotate around circular filaments. In three dimensional systems, spiral rotates around one dimensional space rather than a point and these curves are commonly referred to as filaments. These filaments are boundary- or wave-terminated lines, closed rings, chains and knots. Generally, they are not stationary and they move,

stretch, bend according to their shape, phase gradients in spiral station, and system specific parameters.

In 2006, Steinbock et al. described a novel nucleation mechanism of scrolling waves in 3-D with anomalous dispersion relations [255]. Their experimental results suggest that formation of scroll waves does not rely on external obstacles but it is closely related to the system's anomalous dispersion relation. In 2007, they found that these filaments can expand, buckle, and build up gradients in rotation phase [256]. The rotation of scroll waves happens around tubular regions which can be represented by 1-D space curves.

Steinbock et al. also analyzed 3-D reconstructions of merging waves in the CHD-BZ reaction [257]. They discovered that filaments of scroll waves can terminate in the back of travelling waves. It corrects previous belief that filaments end only at the system's boundary or close in on themselves. This finding is important because it extends knowledge on topological constraints that governs the basic characteristics of scroll wave filaments. One of the results of wave termination is the steady growth of the phase differences along the expanding filaments. This result is the first experimental report of increasing phase differences in a homogeneous, gradient-free medium. However, there is need to do more work in order to answer questions such as response of wave filaments to the annihilation of their anchoring wave pulse.

In 2008, Steinbock et al. reported that in excitable media with anomalous dispersion, filaments could be pinned to the wake of travelling wave pulses [258]. They have studied this pinning in experiments with the CHD-BZ reaction and a three-variable reaction-diffusion model. Their numerical results show that wave merging can allow the pinning of scroll wave filaments to traveling wave pulses. They also studied pattern formation by filling capillary tube with BZ reaction mixture [259]. They characterized

excitation pulses by a high concentration of bromous acid that is accompanied by a trailing of refractory zone. This refractory zone not only influences the specific velocity of subsequent waves but also defines the direction of pulse propagation. The observed patterns were not stable over a long time. However, most of pulses reveal oscillatory changes in their width and speed and these changes were happening around mean values that are very similar or identical to the constant width and speed of the leading pulse. These breathing pulses were subject to propagation failure. They observed breathing pulses only in Ce/Fe and Mn/Fe catalyzed CHD-BZ reaction. Stefan Müller et al. have studied the BZ reaction by filling capillary tubes with gel-immobilized catalyst [260]. They immersed these filled capillary tubes into BZ reaction solution which creates an open capillary reactor free of perturbations. The most interesting phenomenon observed was spontaneously arising of quantized propagation of waves along with the length of the capillary tube and 3-D helix waves. These helix waves emerge under macroscopically unperturbed conditions in a catalyst-immobilized cylindrical gel system.

Showalter's research group reported a new type of wave source in excitable media which is a resonance induced pacemaker [261]. They carried out experiments with a photosensitive BZ reaction with varied excitability according to the illumination intensity. Initiation of chemical waves happened in an excitable medium by resonance with local periodic forcing of the excitability. Oscillatory pacemakers depend on the systems' parameters while initiation of resonance wave relies only on small amplitude modulations of the local excitability. Their experiments and simulation indicate that small, local modulations of excitability give rise to wave initiation in a quiescent excitable medium. In a separate publication, they reported a network of excitable nodes based on the photosensitive BZ reaction in which local and nonlocal links were possible, through both

experiment and simulation [262]. These networks are important and common in biological systems such as interacting neurons in brain tissue. They also reported a systematic investigation of wave mediated synchronization of oscillatory cellular media in experiments and simulations [263]. They characterized the spatiotemporal evolution of a medium that is made up of an array of oscillatory cells with controllable coupling at the cell boundaries and randomly distributed frequencies. The medium evolves from an initial state of multiple wave sources to a synchronized state which occurs via a competition between the sources, which arise when the oscillators are distinguishable but have slightly different natural frequencies. Epstein et al. investigated the evolution of fronts in a nonlinear wave equation with global feedbacks [264]. They studied the motion of one and quasi-two dimensional fronts and found a much richer dynamics than for the cases without any global feedback, leading in most cases to the stabilization of one phase inside the other. The nature of localized solutions depends on the strength of the global feedback as well as model parameters.

Magnetic resonance imaging (MRI) is a powerful tool for monitoring chemical reactions in porous medium in which chemical concentration gradients can be visualized, and diffusion and flow properties are simultaneously determined. MRI has the advantage of being able to determine the pore network of the medium and the chemical composition over other types of imaging techniques such as x-ray. Taylor and co-workers presented their studies on MRI technique and its application to studying formation of chemical waves [265]. According to their studies 3-D structure of stationary concentration patterns formed via the flow-distributed oscillation mechanism is determined to reflect the local hydrodynamics in the packed bed.

2.2 Turing Pattern

Until recently the only observed stationary patterns were hexagonal lattices, parallel stripes, and black eye patterns which all of them arise from random initial concentrations in experiments and simulations [242-248]. Epstein's group reported the formation of hexagonal and square superlattice patterns in a photosensitive chlorine dioxide-iodine-malonic acid (CDIMA) reaction [266]. They found out that in the CDIMA, illumination patterned as a simple hexagonal or square pattern creates initial conditions leading to development of superlattice patterns with a wavelength close to a multiple of the intrinsic Turing pattern's wavelength and they lasted for 10 hours. The square superlattice was the first example of time-independent square Turing patterns.

The human brain may be thought of as a reaction-diffusion system. Epstein et al. illustrated that a photosensitive BZ-AOT system is capable of storing spatial information for up to an hour, even without refreshing of reactants [267]. They have shown that this chemical system can be used not only for image processing but also for image storage. They have found conditions between a homogeneous steady state and stationary Turing pattern under which the system displays bistability. Their results implied that the BZ-AOT system in a continuous reactor can be used for restoring images indefinitely. This photosensitive reaction can thus be used to create readable and rewritable chemical memory. Another useful application suggested by Epstein is constructing a "thinking device" [268-270]. Encoding information and performing logic operations like those in a computer can be done by flowing of bubbles through narrow channels. As mentioned by Epstein, it is like the traveler in Robert Frost's poem "The Road Not Taken," bubbles must choose a path; however, a solitary bubble or droplet forced to settle on one of two paths will pick the channel with lowest resistance to flow. Fuerstman et al. were able to

restore the initial series of intervals and therefore decoding the signal through either the direction of flow or passing the stream through a second loop [269]. However, Prakash and Gershenfeld represented a bit of information as bubbles in a channel, and made circuits that can be linked together to produce more elaborate arrangements capable of acting as counters, oscillators, or memory arrays [270]. The demonstration of two components flow system make one wonder how far it is possible to go in constructing "thinking devices." One way to enhance the capability of these thinking devices is to combine them with a bistability, oscillations, and waves in a nonlinear chemical dynamics.

2.3 Silica Gardens

Chemical gardens are familiar to every child with a chemistry set. They are obtainable from precipitation reaction via adding crystals of soluble metal salts to aqueous solution containing anions such as aluminate, silicate, borate, and so on. Silica gardens have been studied since the 17th century. These gardens consist of hollow tubular structures that appear from salt crystals seeded into silicate solution. In 19th century some researchers considered silica gardens as pre-biotic life forms and models for the genesis of the life. Studies on silica gardens have been resumed in modern research and many of their intriguing chemical and physical aspects have been discovered in recent years [271-276].

All earlier studies on silica gardens carried out in flow-controlled tube growth involved the injection of salt solution into waterglass. Recently, Steinbock and co-workers analyzed tube formation under reverse conditions, i.e., a condition in which waterglass was injected into a large reservoir of cupric sulfate solution [271]. This flow injection creates single, downward growing precipitation tubes because the waterglass is denser

than the employed cupric sulfate solutions. These tubes have diameter in the range of 0.8-2.4 mm and can grow several centimeters in length. They have successfully observed four distinct growth regimes and have examined tubes stability in terms of flow rate and cupric sulfate concentration. While three of the four observed regimes have been reported before, including reverse jetting, popping, and budding, they found a new regime in which the growth dynamics are affected by the repetitive break-off of large tube segments. In a following publication, they investigated the structure and elemental composition of these tubes [272]. They employed micro-Raman spectroscopy along with energy dispersive X-ray fluorescence data and identified amorphous silica and copper (II) hydroxide as the main compound within the inner and outer tube surfaces, respectively. Moreover, S.E.M. analysis shows that the wall is more sophisticated than a simple two-layer structure. In particular, they found that the outside surface has a texture with stripes of unknown origin.

2.4 Enzyme and pH Oscillators

The design of pH oscillators is very interesting as they can be coupled with pH sensitive polymers for the novel chemomechanical and biomimetic devices [277-279]. They also may provide less aggressive environments for use in conjunction with pH sensitive gels. Scott's et al. have tried to design an organic pH oscillator. In 2005, they reported a minimal model based on formaldehyde-sulfite reaction which is an acid to alkali clock reaction in a batch reactor and demonstrated that a base-catalyzed rate-determining step coupled with a negative feedback can result in bistability and oscillations [277]. Generally, in a pH oscillator, the hydronium ion is produced autocatalytically from the oxidation of sulfur species, arsenite, or hydroxylamine by

inorganic oxidants [3]. The negative feedback can be provided by the use of reductants, such as ferricyanide, thiosulfate, and thiourea. Two years later, they reported the first experimental example that shows how the base catalysis of methylene glycol coupled with hydrolysis of gluconolactone can create an organic-base pH oscillator [278]. In this system, the base-catalyzed dehydration of methylene glycol acts as a source of hydroxyl ion and gluconolactone is a source of hydronium production. This oscillatory reaction displays large amplitude oscillations of pH between 7 and 10 when performed in a CSTR. Methylene glycol can be replaced by other organic molecules with carbonyl group and stable hydrated forms. Besides, gluconolactone can be replaced by glucose-glucose oxidase enzyme which produces gluconolactone.

As Taylor et al. demonstrated that a clock reaction can be coupled with the hydrolysis of gluconolactone to create an organic pH oscillator, they reported the first example of an organic pH oscillator: the methylene glycol-sulfite-gluconolactone (MGSG) [279]. They described this system in both batch and CSTR configurations and proposed a mechanism for it. This reaction displays small amplitude oscillations in redox potential along with large amplitude oscillations in the concentration of hydroxide ion, which indicates that this oscillatory system is not driven by redox processes. From the mechanistic point of view, in this reaction dehydration of methylene glycol is a base-catalyzed rate-determining step which is coupled with the hydrolysis of gluconolactone, a base-catalyzed reaction. The clock behaviour in this reaction involves the consumption of the sulfite/bisulfite buffer.

Cardiac muscle waves, calcium waves in cells, and glycolytic waves have been the subject of many investigations because of their importance in living systems [2, 6]. Waves in living systems are often driven by biochemical reactions with enzymes as the

catalysts. Biological and chemical wave systems share several features in common, in spite of their very different origin. There have been enormous efforts to find enzymatic pH oscillators. Discovery of a simple, inexpensive, enzymatic pH oscillator is an attractive subject as it will give impetus not only for studies of pattern formation but also for better understanding of enzymatic oscillators.

During past years Epstein and co-workers tried to design a simple, inexpensive enzymatic pH oscillator [280-282]. They have studied and presented the first experimental and theoretical results on an enzymatic autocatalytic reaction between glucose (G) and ferricyanide (F_i), catalyzed by the enzyme glucose oxidase (GO) in a CSTR [281]. It is well known that a bistable system in CSTR can be transformed to an oscillatory reaction by adding an appropriate negative feedback to the system. For example, a large group of autocatalytic H^+ producing reactions can oscillate upon introducing H^+ consumption process to the system. This reaction gave rise to a wide range of bistability when changing flow rate and they added inflow of hydroxide ion to the system that caused the system to show oscillatory behaviour. They would be able to create a batch oscillator if the negative feedback can be replaced with another enzymatic reaction or a chemical reaction to serve as negative feedback, and using additional reactions to regenerate ferricyanide. The concentration of glucose and ferricyanide oscillate in this system while the amplitude of glucose is higher since the concentration of glucose is higher than the concentration of ferricyanide.

They have also reported that this system is able to support fronts and pulses propagation in a reaction-diffusion medium as a result of introducing a reaction that can restore the product, F_e, to its initial form, F_i, by adding hydrogen peroxide to the system through the following reaction [280]:

$$H_2O_2 + 2F_e + 2H^+ \quad \rightarrow \quad 2F_i + 2H_2O \qquad\qquad [1]$$
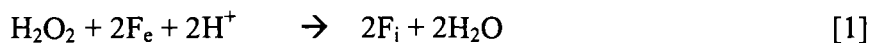
Addition of this negative feedback into the reaction transformed the front to a pulse. This reaction can also be replaced by another proton-consuming enzymatic reaction. The front moves by producing hydrogen ion and ferrocyanide via consuming ferricyanide. Experiments at various pH showed that the front velocity is almost independent of pH in the manner that changing the pH from 10 to 5 just produced an increase of the front velocity by only a factor of two.

2.5 Front Polymerization

In recent years, the study of frontal polymerization (FP) has attracted an ever increasing attention because of its potential as a promising technique for synthesizing uniform polymers and polymeric networks with spatially-controlled microstructures [284-289]. It is a mode of converting monomers into a polymer via a localized reaction zone that propagates by coupling of thermal diffusion and reaction. There are three types of frontal polymerization: thermal frontal polymerization (TFP), photofrontal polymerization, and isothermal frontal polymerization (IFP). TFP uses an outside heat source to initiate the front. Photofrontal polymerization is driven by an external UV source and IFP is driven by monomer and inhibitor diffusing into a small piece of polymer as a seed.

One active research group in the investigation of frontal polymerization is Pojman's group. In 2006, they reported for the first time synthesizing urethane-acrylate macromonomer and copolymerized it with 2-hydroxyethylacrylate (HEA) [284]. They also added persulfate to their reaction system to avoid bubbles from peroxide or nitrile inhibitors. In a typical run, they have mixed urethane-acrylate, 2-hydroxyethylacrylate,

and ammonium persulfate in dimethyl sulfoxide. FP was started with heating the wall of the tube which resulted in starting FP. Once FP started, no further heating was required for the polymerization to continue. In this system, in contrast to other investigated polymer systems, front velocity shows a linear dependence on the inhibitor concentration. Also, this system has produced the least amount of thermal FP front temperature to date due to that large amount of DMSO acts as a heat sink. They also have studied the influence of initiator concentration on the front velocity and front temperature.

In the same year, they have also reported an IFP which consists of a solution of methyl methacrylate [285]. They contacted this solution with thermal inhibitor in the presence of a polymer seed. For the first time, they have used poly(methyl methacrylate) as the seeds and found out that there is a critical molecular weight necessary to seed a front. They also found that higher molecular weight increases the induction period and propagation distance. In this system, oxygen acts as a bulk polymerization inhibitor.

As the inspiration for greener world is rapidly raising and so does green chemistry, organic chemists are trying solvent-free processes. Pojman et al. reported a solvent-free FP process using N-methylolacrylamide and ammonium persulfate [286]. In this report, they also determined the dependence of the front velocity and front temperature on the monomer and inhibitor concentrations. In this system if the inhibitor concentration is too high, then the pot life is too short and if it is too low the front will be extinguished because of heat loss. For the first time, they also have investigated FP with ionic liquid monomers [287]. They synthesized a series of compounds from the neutralization reaction between trialkylamines and acrylic or methacrylic acid. They determined the minimum conditions to obtain frontal polymerization with mono- and di-functional (meth)acrylate ionic liquid monomers. The front velocity is slower in the presence of

diacrylate than dodecyl acrylate. Also, monofunctional monomers from (meth)acrylate could not support FP alone; however, with adding another monomer with a lower molecular weight frontal polymerization could be achieved. On the contrary, difunctional ionic liquids were able to support the FP without extra addition.

They also reported the film preparation by the photopolymerization of a reverse microemulsion [288]. They created hydrophobic polymer films with an aqueous phase which covered throughout the matrix as droplets. The organic phase consisted of dodecyl acrylate and 1,6-hexanediol diacrylate with water drops in separated phase stabilized with anodic surfactant sodium bis(2-ethylhexyl) sulfosuccinate (AOT). The solution turned from clear to opaque upon polymerization which is due to aggregation of water droplets from nanosized micelle in the microemulsion into micro-sized aggregates in the film.

Snell's law governs light refraction and it also describes the behaviour of any steadily propagating fronts when they cross the boundary of two media with unequal constant velocity of propagation. Pojman et al. studied chemical fronts sustained by an exothermic polymerization reaction [289]. They demonstrated that Snell's law can be applied to fronts propagating through a boundary between regions that support distinct frontal velocities. In those experiments, they placed two or three stripes with different concentrations of the peroxide initiator side-by-side in contact with each other. The sines of the incident angle between domains were approximately equal to 1 and they verified that the reaction front propagation in these systems follows Snell's law of refraction.

References

1. P. Atkins and J. de Paula, Physical Chemistry, Oxford University Press, 2002.

2. A. Goldbeter, Biochemical Oscillations and Cellular Rhythms, Cambridge University Press, 1996.

3. I. R. Epstein and J. A. Pojman, An Introduction to Nonlinear Chemical Dynamics, Oxford University Press, New York, 1998.

4. R. J. Field and M. Burger, Oscillations and Traveling Waves in Chemical Systems, Wiley-Interscience, New York, 1985.

5. R. Kapral and K. Showalter, Chemical Waves and Patterns, Kluwer Academic Publishers, Netherlands, 1995.

6. A. T. Winfree, The Geometry of Biological Time, Springer, Heidelberg, 2000.

7. S. K. Scott, Chemical Chaos, Oxford University Press, 1994.

8. H. Y. Lin and P. Neubauer, J. Biotech., 79, 2000, 27.

9. N. J. Abram, M. K. Gagan, Z. Liu, W. S. Hantoro, M. T. McCulloch and B. W. Suwargadi, Nature, 445, 2007, 299.

10. P. Mohanty, Nature, 437, 2005, 325.

11. E. Fung, W. W. Wong, J. K. Suen, T. Bulter, S. Lee and J. C. Liao, Nature, 435, 2005, 118.

12. K. Horikawa, K. Ishimatsu, E. Yoshimoto, S. Kondo and H. Takeda, Nature, 441, 2006, 719.

13. W. W. Wong, T. Y. Tsai and J. C. Liao, Mol. Syst. Biol., 3, 2007, 1.

14. B. Blasius, A. Huppert and L. Stone, Nature, 399, 1999, 354.

15. S. Danø, P. G. Sørensen and F. Hynne, Nature, 402, 1999, 320.

16. T. Hideshima and Y. Kato, Biophys. Chem., 124, 2006, 100.

17. E. Kolb and I. Harris, Proc. Biochem. Soc., 30, 1972, 26.

18. A. Goldbeter, Nature, 420, 2002, 238.

19. M. Calvin, Science, 219, 1983, 24.

20. W. E. Lowry, C. Blanpain, J. A. Nowak, G. Guasch, L. Lewis and E. Fuchs, Genes and Dev., 19, 2005, 1596.

21. J. Huelsken, R. Vogel, B. Erdmann, G. Cotsarelis and W. Birchmeier, Cell, 105, 2001, 533.

22. C. L. Celso, D. M. Prowse and F. M. Watt, Development, 131, 2003, 1787.

23. M. V. Plikus, J. A. Mayer, D. Cruz, R. E. Baker, P. K. Maini, R. Maxson and C. Chuong, Nature, 451, 2008, 340.

24. A. V. Holden, Nature, 392, 1998, 20.

25. S. H. Strogatz, Nature, 394, 1998, 316.

26. M. Hastings, Nature, 376, 1995, 296.

27. T. Podzuweit, G. C. J. Louw and B. C. Shanley, Advances in Myocardiology, University Park Press, Baltimore, 1980.

28. M. G. Murer, K. Y. Tseng, F. Kasanetz, M. Belluscio and L. A. Riquelme, Cell. Mol. Neurobiol., 22, 2002, 611.

29. C. D. Fiorillo, P. N. Tobler and W. Schultz, Behav. Brain Func., 1, 2005, 7.

30. D. J. Morré, R. Pogue and D. M. Morré, BioFactors, 9, 1999, 179.

31. M. Dragan, S. J. Dixon, E. Jaworski, T. S. Chan, P. J. O'Brien and J. X. Wilson, Brain Res., 1078, 2006, 9.

32. V. E. Shashoua, Intern. J. Neuroscience, 3, 1972, 299.

33. S. Zeng and P. Jung, Phys. Rev. E, 71, 2005, 011910.

34. W. Shi, J. Neurophysiol., 94, 2005, 3516.

35. D. Zhang, S. Yang, G. Jin, B. S. Bunney and W. Shi, Synapse, 62, 2008, 169.

36. D. J. Morré, P. Chueh, J. Pletcher, X. Tang, L. Wu and D. Morré, Biochemistry, 41, 2002, 11945.

37. V. Yuferov, E. R. Butelman and M. J. Kreek, Eur. J. Hum. Genet., 13, 2005, 1101.

38. D. M. Morré, F. Guo and D. J. Morré, Mol. Cell. Biochem., 254, 2003, 101.

39. I. H. Riedel-Kruse, C. Müller and A. C. Oates, Science, 317, 2007, 1911.

40. C. B. Green and M. Menaker, Science, 301, 2003, 319.

41. J. D. Levine, P. Funes, H. B. Dowse and J. C. Hall, Science, 298, 2002, 2010.

42. J. C. Dunlap, Science, 311, 2006, 184.

43. M. U. Gillette and T. J. Sejnowski, Science, 309, 2005, 1196.

44. A. T. Fechner, Schweigg. J., 53, 1828, 61.

45. W. Ostwald, Phys. Zeitsch, 8, 1899, 87.

46. A. J. Lotka, J. Phys. Chem., 14, 1910, 271.

47. A. J. Lotka, J. Am. Chem. Soc., 42, 1920, 1595.

48. W. C. Bray, J. Phys. Chem. Soc., 43, 1921, 1262.

49. W. C. Bray and H. A. Liebhafsky, J. Phys. Chem., 53, 1931, 38.

50. D. Edelson and R. M. Noyes, J. Phys. Chem., 83, 1979, 212.

51. D. R. Stanisavljev, A. R. Djordjević and V. D. Likar-Smiljanić, Chem. Phys. Lett., 412, 2005, 420.

52. K. R. Sharma and R. M. Noyes, J. Am. Chem. Soc., 91, 1975, 202.

53. I. R. Epstein, Faraday Discuss., 120, 2001, 421.

54. H. Försterling and V. Margit, J. Phys. Chem., 97, 1993, 7932.

55. R. J. Field, E. Körös and R. M. Noyes, J. Am. Chem. Soc., 94, 1972, 8649.

56. J. L. Hudson, M. Hart and D. Marinko, J. Chem. Phys., 71, 1979, 1601.

57. J. Horváth, Z. Nagy-Ungvárai and S. C. Müller, Phys. Chem. Chem. Phys., 3, 2001, 218.

58. K. Pelle, M. Wittmann, Z. Noszticzius, R. Lombardo, C. Sbriziolo and M. L. Turco Liveri, J. Phys. Chem. A, 107, 2003, 2039.

59. L. Onel, G. Bourceau, I. Bitter, M. Wittmann and Z. Noszticzius, J. Phys. Chem., 110, 2006, 990.

60. I. Gonda and G. A. Rodley, J. Phys. Chem., 94, 1990, 1516.

61. V. K. Vanag and D. V. Boulanov, J. Phys. Chem., 98, 1994, 1449.

62. V. K. Vanag and I. Hanazaki, J. Phys. Chem., 99, 1995, 6944.

63. V. K. Vanag and I. Hanazaki, J. Phys. Chem., 100, 1996, 10609.

64. L. Treindl, T. Hemmingsen and P. Ruoff, Chem. Phys. Lett., 269, 1997, 263.

65. Y. Jiang, S. Zhong and H. Xin, J. Phys. Chem. A, 104, 2000, 8521.

66. Y. Gao and H. Försterling, J. Phys. Chem., 99, 1995, 8638.

67. J. Wang, P. G. Sørensen and F. Hynne, Z. Phys. Chem., 192, 1995, 63.

68. E. Körös, M. Orbán and I. Habon, J. Phys. Chem., 84, 1980, 559.

69. M. Varga, L. Györgyi and E. Körös, React. Kinet. Catal. Lett., 42, 1990, 375.

70. Z. Noszticzius and J. Bódiss, J. Am. Chem. Soc., 101, 1979, 3177.

71. R. P. Rastogi, G. P. Misra, I. Das and A. Sharma, J. Phys. Chem.., 97, 1993, 2571.

72. Y. Hara and R. Yoshida, J. Chem. Phys., 128, 2008, 224904.

73. R. M. Noyes, J. Am. Chem. Soc., 102, 1980, 4644.

74. D. Edelson, R. M. Noyes and R. J. Field, Int. J. Chem. Kinet., 11, 1979, 155.

75. R. M. Noyes and R. J. Field, Acc. Chem. Res., 10, 1977, 273.

76. P. Herbine and R. J. Noyes, J. Phys. Chem., 84, 1980, 1330.

77. R. M. Noyes, J. Phys. Chem., 94, 1990, 4404.

78. L. Györgyi, T. Turányi and R. J. Field, J. Phys. Chem., 94, 1990, 7162.

79. J. Liu and S. K. Scott, J. Phys. Chem., 96, 1992, 9870.

80. T. Turányi, L. Györgyi and R. J. Field, J. Phys. Chem., 97, 1993, 1931.

81. S. Kéki, I. Magyar, M. T. Beck and V. Gáspár, J. Phys. Chem., 96, 1992, 1725.

82. R. P. Rastoi, M. M. Husain, P. Chand, G. P. Misra and M. Das, Chem. Phys. Lett., 353, 2002, 40.

83. P. Ruoff, M. Varga and E. Körös, J. Phys. Chem., 91, 1987, 5332.

84. E. Körös and M. Orbán, Nature, 273, 1978, 371.

85. M. Orbán and E. Körös, J. Phys. Chem., 82, 1978, 1672.

86. M. Orbán and E. Körös, React. Kinet. Catal. Lett, 8, 1978, 273.

87. J. M. Berg, J. L. Tymoczko, L. Stryer, Biochemistry, W. H. Freeman and Company, 2002.

88. J. D. Johnson, J. G. Mehus, K. Tews, B. I. Milavetz, J. Biol. Chem., 273, 1998, 27580.

89. D. Voet and J. G. Voet, Biochemistry, John Wiley & Sons, Inc., NewYork, 2004.

90. A. N. Zaikin and A. M. Zhabotinsky, Nature, 225, 1970, 535.

91. C. J. Doona, K. Kustin, M. Orban and I. R. Epstein, J. Am. Chem. Soc., 113, 1991, 7484.

92. M. Melicherčík, Mrákavová, A. Nagy, A. Olexová and L. Treindl, J. Phys. Chem., 96, 1992, 8367.

93. A. Nagy, A. Olexová and L. Treindl, J. Phys. Chem., 95, 1991, 5809.

94. M. Orban and I. R. Epstein, J. Am. Chem. Soc., 112, 1990, 1812.

95. A. Nagy and L. Treindl, J. Phys. Chem., 93, 1989, 2807.

96. M. Tóthová, A. Nagy and L. Treindl, Chem. Phys. Lett., 299, 1999, 243.

97. A. Nagy, P. G. Sørensen and F. Hynne, J. Phys. Chem. A, 101, 1997, 1317.

98. N. Okazaki, G. Rábai and I. Hanazaki, J. Phys. Chem. A, 103, 1999, 10915.

99. C. J. Doona, K. Kustin, M. Orbán and I. R. Epstein, J. Am. Chem. Soc., 113, 1991, 7484.

100. M. Orbán and I. R. Epstein, J. Am. Chem. Soc., 111, 1989, 8543.

101. K. Kurin-Csörgei, I. R. Epstein and M. Orbán, J. Phys. Chem. B, 108, 2004, 7352.

102. J. A. Pojman, H. Dedeaux and D. Fortenberry, J. Phys. Chem., 96, 1992, 7331.

103. H. Li, X. Huang and J. Deng, Chem. Phys. 208, 1996, 229.

104. M. Orbán and I. R. Epstein, J. Am. Chem. Soc., 114, 1992, 1252.

105. G. Marlovits, M. Wittmann, Z. Noszticzius and V. Gáspár, J. Phys. Chem., 99, 1995, 5359.

106. G. Rábai and I. Hanazaki, J. Phys. Chem., 98, 1994, 10550.

107. R. P. Rastogi and P. Chand, Chem. Phys. Lett., 369, 2003, 434.

108. F. Cortés-Salazar, D. Barragán and M. F. Suárez, Electrochem. Commun. 6, 2004, 470.

109. L. Adamčíková, Z. Farbulová and P. Ševčík, New J. Chem., 25, 2001, 487.

110. M. Orbán, K. Kurin-Csörgei, A. M. Zhabotinsky and I. R. Epstein, Faraday Discuss., 120, 2001, 11.

111. M. J. B. Hauser and L. F. Olsen, Biochemistry, 37, 1998, 2458.

112. A. K. Horváth, I. Nagypál and I. R. Epstein, J. Am. Chem. Soc., 124, 2002, 10956.

113. R. H. Simoyi, J. Phys. Chem., 90, 1986, 2802.

114. I. R. Epstein, J. Chem. Edu., 66, 1989, 191.

115. I. R. Epstein, K. Kustin, P. DeKepper and M. Orbán, Science, 248, 1983, 112.

116. P. DeKepper, I. R. Epstein, and K. Kustin, J. Am. Chem. Soc., 103, 1981, 2133.

117. G. Rábai, M. Orbán and I. R. Epstein, Acc. Chem. Res., 23, 1990, 258.

118. V. J. Farage and D. Janjic, Chem. Phys. Lett., 88, 1982, 301.

119. V. J. Farage and D. Janjic, Chem. Phys. Lett., 93, 1982, 621.

120. C. T. Hamik, N. Manz and O. Steinbock, J. Phys. Chem. A, 105, 2001, 6144.

121. S. Shah and J. Wang, J. Phys. Chem. C, 111, 2007, 10639.

122. D. S. Huh, M. S. Kim and S. J. Choe, Bull. Korean Chem. Soc., 22, 2001, 867.

123. L. Yang and I. R. Epstein, J. Phys. Chem. A, 106, 2002, 11676.

124. B. T. Ginn and O. Steinbock, Phys. Rev. Lett., 93, 2004, 158301.

125. K. Kurin-Csörgei, A. M. Zhabotinsky, M. Orbán and I. R. Epstein, J. Phys. Chem. 100, 1996, 5393.

126. J. Wang, K. Yadav, B. Zhao, Q. Gao and D. S. Huh, J. Chem. Phys., 121, 2004, 10138.

127. I. Szalai, K. Kurin-Csörgei, I. R. Epstein and M. Orbán, J. Phys. Chem. A, 107, 2003, 10074.

128. K. Kurin-Csörgei, I. Szalai, I. Molnár-Perl and E. Körös, React. Kinet. Catal. Lett., 53, 1994, 115.

129. I. Szalai and E. Körös, J. Phys. Chem. A, 102, 1998, 6892.

130. I. Szalai, E. Körös and L. Györgyi, J. Phys. Chem. A, 103, 1999, 243.

131. I. Szalai, K. Kurin-Csörgei and M. Orbán, Phys. Chem. Chem. Phys., 4, 2002, 1271.

132. M. M. Britton, J. Phys. Chem. A, 107, 2003, 5033.

133. K. Keresztúri and I. Szalai, Chem. Phys. Lett., 428, 2006, 288.

134. A. Komlósi, I. P. Nagy, G. Bazsa and J. A. Pojman, J. Phys. Chem. A, 102, 1998, 9136.

135. N. Manz, S. C. Müller and O. Steinbock, J. Phys. Chem. A, 104, 2000, 5896.

136. D. S. Huh, Y. J. Kim, H. S. Kim, J. K. Kang and S. J. Choe, Bull. Korean Chem. Soc., 25, 2004, 267.

137. H. Landolt, Ber. Dtsch. Chem. Ges., 19, 1886, 1317.

138. E. C. Edblom, M. Orbán and I. R. Epstein, J. Am. Chem. Soc., 108, 1986, 2826.

139. E. C. Edblom, L. György, M. Orbán and I. R. Epstein, 109, 1987, 4876.

140. V. Gáspár and K. Showalter, J. Am. Chem. Soc., 109, 1987, 4869.

141. I. Szalai and P. De Kepper, Phys. Chem. Chem. Phys., 8, 2006, 1105.

142. K. Benyaich, T. Erneux, S. Métens, S. Villain and P. Borckmans, Chaos, 16, 2006, 037109.

143. J. Boissonade, J. Chim. Phys., 73, 1976, 540.

144. D. Barkley, J. Chem. Phys., 89, 1988, 5547.

145. P. E. Strizhak and A. L. Kawczyński, J. Phys. Chem., 99, 1995, 10830.

146. J. Zhao, Y. Chen and J. Wang, J. Chem. Phys., 122, 2005, 114514.

147. Q. Gao and J. Wang, Chem. Phys. Lett., 391, 2004, 349.

148. M. Orbán and I. R. Epstein, J. Phys. Chem., 98, 1994, 2930.

149. J. Ross and M. O. Vlad, Annu. Rev. Phys. Chem., 50, 1999, 51.

150. S. K. Scott, B. R. Johnson, A. F. Taylor and M. R. Tinsley, Chemical Engineering Science, 55, 2000, 209.

151. K. Nielsen, P. G. Sørensen, F. Hynne and H. G. Busse, Biophys. Chem., 72, 1998, 49.

152. G. Schmitz, L. Kolar-Anić, S. Anić, T. Grozdić and V. Vukojević, J. Phys. Chem. A, 110, 2006, 10361.

153. J. Maselko, H. L. Swinny, J. Chem. Phys., 85, 1986, 6430.

154. G. Biosa, M. Masia, N. Marchettini and M. Rustici, Chem. Phys., 308, 2005, 7.

155. R. Wackerbauer and K. Showalter, Phys. Rev. Lett., 91, 2003, 174103.

156. F. Argoul, A. Arneodo, P. Richetti and J. C. Roux, Acc. Chem. Res., 20, 1987, 436.

157. M. Rustici, R. Lombardo,M. Mangone, C. Sbriziolo, V. Zambrano and M. L. Turco Liveri, Faraday Discuss., 120, 2001, 39.

158. I. R. Epstein and K. Showalter, J. Phys. Chem., 100, 1996, 13132.

159. P. Ševčík, L. Adamčíkivá, J. Chem. Phys., 91, 1989, 1012.

160. A. K. Dutt and M. Menzinger, J. Phys. Chem., 94, 1990, 4867.

161. M. Menzinger and P. Jankowski, J. Phys. Chem., 90, 1986, 1217.

162. J. Wang, J. Phys. Chem. A, 107, 2003, 8774.

163. L. Györgyi and R. J. Field, J. Phys. Chem., 96, 1992, 1220.

164. F. Ali and M. Menzinger, J. Phys. Chem. A, 101, 1997, 2304.

165. M. K. Ram Reddy, Z. Szlávik, Z. Nagy-Ungvarai and S.C. Müller, J. Phys. Chem., 99, 1995, 15081.

166. K. P. Zeyer and F. W. Schneider, J. Phys. Chem. A, 102, 1998, 9702.

167. L. Treindl, D. Knudsen, T. Nakamura, T. Matsumura-Inoue, K. B. Jørgensen and P. Ruoff, J. Phys. Chem. A, 104, 2000, 10788.

168. I. Cassidy and S. C. Müller, Phys. Rev. E, 74, 2006, 026206.

169. L. Hegedüs, H. D. Försterling, E. Kókai, K. Pelle, G Taba, M. Wittmann and Z. Noszticzius, Phys. Chem. Chem. Phys., 2, 2000, 4023.

170. H. D. Försterling, S. Murányi and Z. Noszticzius, React. Kinet. Catal. Lett., 42, 1990, 217.

171. T. Amemiya, T. Yamamoto, T. Ohmori and T. Yamaguchi, J. Phys. Chem. A, 106, 2002, 612.

172. D. S. Huh, Y. M. Choe, D. Y. Park, S. H. Park, Y. S. Zhao and S. J. Choe, Bull. Korean Chem. Soc., 26, 2005, 219.

173. E. Koros, G. Putirskaya and M. Varga, Acta. Chim. Acad. Sci. Hung., 110, 1982, 295.

174. D. S. Huh, H. S. Kim, J. K. Kang, Y. J. Kim, D. H. Kim, S. H. Park, K. Yadav and J. Wang, Chem. Phys. Lett., 378, 2003, 78.

175. D. S. Huh, Y. J. Kim, H. S. Kim, J. K. Kang and J. Wang, Phys. Chem. Chem. Phys., 5, 2003, 3188.

176. B. Zhao and J. Wang, Chem. Phys. Lett., 430, 2006, 41.

177. P. G. Sørensen, T. Lorenzen and F. Hynne, J. Phys. Chem., 100, 1996, 19192.

178. I. Hanazaki, Y. Mori, T. Sekiguchi and G. Rábai, Physica D, 84, 1995, 228.

179. V. K. Vanag and I. Hanazaki, J. Phys. Chem. A, 101, 1997, 2147.

180. S. Kéki, G. Székely and M. T. Beck, J. Phys. Chem. A, 107, 2003, 73.

181. P. Ruoff and R. M. Noyes, J. Phys. Chem. 93, 1989, 7394.

182. O. Steinbock and S. C. Müller, J. Phys. Chem. A, 102, 1998, 6485.

183. H. Krug, L. Pohlmann and L. Kuhnert, J. Phys. Chem. 94, 1990, 4862.

184. O. Steinbock, C. T. Hamik and B. Steinbock, J. Phys. Chem. A, 104, 2000, 6411.

185. L. Treindl, P. Ruoff and P. O. Kvernberg, J. Phys. Chem. A, 101, 1997, 4606.

186. A. Petrascu, M. H. J. Koch, H. D. Försterling, J. Phys. Chem. A, 103, 1999, 6757.

187. J. Wang, F. Hynne, P. G. Sørensen and K. Nielsen, J. Phys. Chem., 100, 1996, 17593.

188. K. Bar-Eli and S. Haddad, J. Phys. Chem., 83, 1979, 2952.

189. G. Rabai, Tibor G. Szanto and K. Kovacs, J. Phys. Chem. 112, 2008, 12007.

190. M. Masia, N. Marchettini, V. Zambrano and M. Rustici, Chem. Phys. Lett., 341, 2001, 285.

191. F. Rossi, F. Pulselli, E. Tiezzi, S. Bastianoni and M. Rustici, Chem. Phys., 313, 2005, 101.

192. G. Nagy, E. Körös, N. Oftedal, K. Telflaat and P. Ruoff,Chem. Phys. Lett., 250, 1996, 255.

193. A. Pagola and C. Vidal, J. Phys. Chem., 91, 1987, 501.

194. J. J. Tyson and J. P. Keener, Physica D, 32, 1988, 327.

195. M. Harati, S. Amiralaei, J. Green and J. Wang, Chem. Phys. Lett., 439, 2007, 337.

196. L. Kuhnert, Nature, 319, 1986, 393.

197. A. E. Bugrim, M. Dolnik, A. M. Zhabotinsky and I. R. Epstein, J. Phys. Chem., 100, 1996, 19017.

198. L. Kuhnert, H. J. Krug and L. Pohlmann, J. Phys. Chem., 89, 1985, 2022.

199. C. Oosawa, Y. Fukuta, K. Natsume and K. Kometani, J. Phys. Chem., 100, 1996, 1043.

200. S. Wehner, P. Hoffmann, D. Schmeißer, H. R. Brand and J. Küppers, Phys. Rev. Lett., 95, 2005, 038301.

201. J. Wang, Chem. Phys. Lett., 339, 2001, 357.

202. V. K. Vanag and I. R. Epstein, Phys. Rev. lett., 87, 2001, 228301.

203. K. Showalter, J. Phys. Chem., 85, 1981, 440.

204. S. B. Shin, S. J. Choe, D. S. Huh and K. Showalter, Bull. Korean Chem. Soc., 20, 1999, 411.

205. P. A. Bechmann, P. L. Luisi and J. Lang, Nature, 357, 1992, 57.

206. A. Yen, A. L. Lin, Y. L. Koo, B. Vilensky, H. Taitelbaum and R. Kopelman, J. Phys. Chem. A, 101, 1997, 2819.

207. H. Fukuda, N. Tamari, H. Morimura and S. Kai, J. Phys. Chem. A, 109, 2005, 11250.

208. D. S. Huh, J. K. Kang, Y. J. Kim and R. Yoshida, Polym. Bull., 54, 2005, 215.

209. M. Orbán, J. Am. Chem. Soc., 102, 1980, 4311.

210. B. R. Johnson, S. K. Scott and A. F. Taylor, J. Chem. Soc., Faraday Trans., 93, 1997, 3733.

211. A. N. Zaikin and A. M. Zhabotinsky, Nature, 225, 1970, 535.

212. Z. Nagy-Ungvarai, S. C. Müller, J. J. Tyson and B. Hess, J. Phys. Chem., 93, 1989, 2760.

213. Z. Nagy-Ungvarai, J. J. Tyson and B. Hess, J. Phys. Chem., 93, 1989, 707.

214. L. Kuhnert and H. J. Krug, J. Phys. Chem., 91, 1987, 730.

215. R. J. Field and R. M. Noyes, J. Am. Chem. Soc., 96, 1974, 2001.

216. P. M. Wood and J. Ross, J. Chem. Phys., 82, 1985, 1924.

217. N. Manz and S. C. Müller, Rev. Sci. Instrum., 74, 2003, 5161.

218. H. Guo, L. Li, Q. Ouyang, J. Liu and Z. She, J. Chem. Phys., 118, 2003, 5038.

219. K. Rohlf, L. Glass and R. Kapral, Chaos, 16, 2006, 037115.

220. D. E. Strier and J. Boissonade, Phys. Rev. E, 70, 2004, 016210.

221. K. J. Lee, Phys. Rev. Lett., 79, 1997, 2907.

222. H. J. Zhang, P. Y. Wang and Y. Y. Zhao, Chin. Phys. Lett., 22, 2005, 287.

223. V. Zykov and H. Engel, Phys. Rev. E, 70, 2004, 016201.

224. O. Rudzick and A. S. Mikhailov, Phys. Rev. Lett., 96, 2006, 018302.

225. S. Grill, V. S. Zykov and S. C. Müller, J. Phys. Chem., 100, 1996, 19082.

226. C. Luengviriya, U. Storb, M. J. B. Hauser and S. C. Müller, Phys. Chem. Chem. Phys., 8, 2006, 1425.

227. N. Manz, B. T. Ginn and O. Steinbock, J. Phys. Chem. A, 107, 2003, 11008.

228. S. Grill, V. S. Zykov and S. C. Müller, Phys. Rev. Lett., 75, 1995, 3368.

229. H. M. Liao, L. Q. Zhou, C. X. Zhang and Q, Ouyang, Phys. Rev. Lett., 95, 2005, 238301.

230. O. Steinbock and S. C. Müller, Phys. Rev. E, 47, 1993, 1506.

231. A. T. Winfree, Science, 175, 1972, 634.

232. T. Plesser, S. C. Müller and B. Hess, J. Phys. Chem., 94, 1990, 7501.

233. S. Jakubith, H. H. Rotermund, W. Engel, A. V. Oertzen and G. Ertl, Phys. Rev. Lett., 65, 1990, 3013.

234. F. Seigert and C. Weijer, J. Cell. Sci., 93, 1989, 325.

235. J. M. Davidenko, A. V. Pertsov, R. Salomonsz, W. Baxter and J. Jalife, 355, 1992, 349.

236. W. Jahnke, C. Henze and A. T. Winfree, Nature, 336, 1988, 662.

237. S. Mironov, M. Vinson, S. Mulvey and A. Pertsov, J. Phys. Chem., 100, 1996, 1975.

238. A. F. Taylor, B. R. Johnson and S. K. Scott, Phys. Chem. Chem. Phys., 1, 1999, 807.

239. A. M. Turing, Philos. Trans. R. Soc. London B, 237, 1952, 37.

240. V. Castets, E. Dulos, J. Boissonade and P. De Kepper, Phys. Rev. Lett., 64, 1990, 2953.

241. I. R. Epstein, I. B. Berenstein, M. Dolnik, V. K. Vanag, L. Yang and A. M. Zhabotinsky, Phil. Trans. R. Soc. A, 366, 2008, 397.

242. I. Szalai and P. De Kepper, J. Phys. Chem. A, 108, 2004, 5315.

243. L. Yang and I. R. Epstein, Phys. Rev. Lett., 90, 2003, 178303.

244. W. Horsthemke, K. Lam and P. K. Moore, Phys. Lett. A, 328, 2004, 444.

245. Y. Almirantis, Comp. Chem., 24, 2000, 159.

246. Y. Abe and R. Yoshida, J. Phys. Chem. A, 109, 2005, 3773.

247. D. G. Míguez, E. M. Nicola, A. P. Munuzuri, J. Casademunt, F. Sagués and L. Kramer, Phys. Rev. Lett., 93, 2004, 048303.

248. I. Berenstein, L. Yang, M. Dolnik, A. M. Zhabotinsky and I. R. Epstein, J. Phys. Chem. A, 109, 2005, 5382.

249. V. K. Vanag and I. R. Epstein, Proc. Nat. Acad. Sci., 100, 2003, 14635.

250. J. Carballido-Landeira, I. Berenstein, P. Taboada, V. Mosquera, V. Vanag, I. R. Epstein, V. Pérez-Villar and A. P. Muñuzuri, Phys. Chem. Chem.. Phys., 10, 2008, 1094.

251. V. K. Vanag and I. R. Epstein, Science, 294, 2001, 835.

252. L. Yang, A. M. Zhabotinsky and I. R. Epstein, Phys. Chem. Chem. Phys., 8, 2006, 4647

253. X. Shao, Y. Wu, J. Zhang, H. Wang and Q. Ouyang, Phys. Rev. Lett., 100, 2008, 198304

254. R. E. McIlwaine, H. Fenton, S. K. Scott and A. F. Taylor, J. Phys. Chem. C, 112, 2008, 2499

255. T. Bánsági and O. Steinbock, Phys. Rev. Lett., 97, 2006, 198301

256. T. Bánsági and O. Steinbock, Phys. Rev. E, 76, 2007, 045202

257. T. Bánsági, C. Palczewski and O. Steinbock, J. Phys. Chem. A, 111, 2007, 2492

258. T. Bánsági, K. J.Meyer and O. Steinbock, J. Chem. Phys., 128, 2008, 094503

259. N. Manz and O. Steinbock, Chaos, 16, 2006, 037112

260. P. Kettunen, T. Yamaguchi, H. Hashimoto, T. Amemiya, B. Steinbock and S. C. Müller, Chaos, 16, 2006, 037111

261. T. R. Chigwada, P. Parmananda and K. Showalter, Phys. Rev. Lett., 96, 2006, 244101

262. A. J. Steele, M. Tinsley and K. Showalter, Chaos, 16, 2006, 015110

263. O. Kheowan, E. Mihaliuk, B. Blasius, I. Sendiña-Nadal and K. Showalter, Phys. Rev. Lett., 98, 2007, 074101

264. H. G. Rotstein, A. M. Zhabotinsky and I. R. Epstein, Phys. Rev. E, 74, 2006, 016612

265. A. F. Taylor and M. M. Britton, Chaos, 16, 2006, 037103

266. L. Yang, M. Dolnik, A. M. Zhabotinsky and I. R. Epstein, Chaos, 16, 2006, 037114

267. A. Kaminaga, V. K. Vanag and I. R. Epstein, Angew. Chem. Int. Ed., 45, 2006, 3087

268. I. R. Epstein, Science, 315, 2007, 775

269. M. J. Fuerstman, P. Garstecki and G. M. Whitesides, Science, 315, 2007, 828

270. M. Prakash and N. Gershenfeld, 315, 2007, 832

271. J. J. Pagano, T. Bánsági and O. Steinbock, J. Phys. Chem. C, 111, 2007, 9324

272. J. J. Pagano, S. Thouvenel-Romans and O. Steinbock, Phys. Chem. Chem. Phys., 9, 2007, 110

273. J. Maselko and P. Strizhak, J. Phys. Chem. B, 108, 2004, 4937

274. L. S. Dent Glasser, Chem. Br., 18, 1982, 33

275. C. Collins, W. Zhou and J. Klinowski, J. Chem. Phys. Lett., 306, 1999, 145

276. D. Balköse, F. Özkan, U. Köktürk, S. Ulutan, S. Ülkü and G. Nişli, J. Sol-Gel Sci. Technol., 23, 2002, 253

277. R. McIlwaine, K. Kovacs, S. K. Scott and A. F. Taylor, Chem. Phys. Lett., 417, 2006, 39

278. K. Kovacs, R. E. McIlwaine, S. K. Scott and A. F. Taylor, J. Phys. Chem. A, 111, 2007, 549

279. K. Kovacs, R.E. McIlwaine, S. K. Scott and A. F. Taylor, Phys. Chem. Chem. Phys., 9, 2007, 3711

280. D. G. Míguez, V. K. Vanag and I. R. Epstein, Proc. Nat. Acad. Sci., 104, 2007, 6992

281. V. K. Vanag, D. G. Míguez and I. R. Epstein, J. Chem. Phys., 125, 2006, 194515

282. I. R. Epstein, Proc. Nat. Acad. Sci., 103, 2006, 15727

283. T. D. Campbell, R. P. Washington and O. Steinbock, J. Polym. Sci. Part A: Polym. Chem., 45, 2007, 2593

284. T. Hu, S. Chen, Y. Tian, J. A. Pojman and L. Chen, J. Polym. Sci. Part A: Polym. Chem., 44, 2006, 3018

285. S. I. Evstratova, D. Antrim, C. Fillingane and J. A. Pojman, J. Polym. Sci. Part A: Polym. Chem., 44, 2006, 3601

286. L. Chen, T. Hu, H. Yu, S. Chen and J. A. Pojman, J. Polym. Sci. Part A: Polym. Chem., 45, 2007, 4322

287. Z. Jiménez and J. A. Pojman, J. Polym. Sci. Part A: Polym. Chem., 45, 2007, 2745

288. J. E. Marszalek, J. A. Pojman, K. L. Aultman, C. E. Hoyle and J. B. Whitehead, J. Appl. Polym. Sci., 106, 2007, 1957

289. J. A. Pojman, V. Viner, B. Binici, S. Lavergne, M. Winsper, D. Golovaty and L. Gross, Chaos, 17, 2007, 033125

Chapter 2 Chemical Oscillations in the Uncatalyzed Bromate - Pyrocatechol Reaction

Introduction

Chemical reactions can be conveniently manipulated through adjusting their initial concentrations, temperature, or flow rate in a continuously flow stirred tank reactor (CSTR). As a result, chemical oscillators have played an important role in gaining insight into various nonlinear behaviors encountered in nature [1-16]. The vast majority of reported chemical oscillators rely on a few elements that possess multiple oxidation states, such as halogens, sulfur and some transition metals [17-20]. In 1978, Orbán and Körös carried out an extensive search to explore chemical oscillations in the oxidations of aromatic compounds by acidic bromate [21-23]. Among the 50 compounds tested, they found that 23 aromatic reagents could show oscillatory behavior [22]. Because of the absence of metal catalysts, systems reported by Orbán and Körös in 1978 and those discovered more recently by other groups have been frequently referred as the uncatalyzed bromate oscillator (UBO) [5, 6, 23, 24]. In general, reactions of UBOs represent the parallel running of oxidation and bromination of the organic substrates, which result in the production of a variety of substances [25].

In this study, we investigated nonlinear kinetics of the uncatalyzed bromate-pyrocatechol reaction in a stirred batch reactor. The uncatalyzed bromate-pyrocatechol reaction has been investigated earlier by Orbán and Körös, but no oscillatory behavior was observed [21, 22]. The failure of achieving oscillations in the pyrocatechol system

has been attributed to the following two major points: First, the reaction between acidic bromate and aromatic compounds such as pyrocatechol immediately results in the production of bromine, which inhibits autocatalytic reactions; secondly, the oxidation product of pyrocatechol is a stable quinone. Recent progress in the study of uncatalyzed bromate-aromatic compounds reactions, especially the achievement of oscillations in the light-mediated bromate-1,4-benzoquinone reaction, renew our interests in the uncatalyzed bromate-pyrocatechol system [26]. As is shown in the following, after an extensive search in the concentration phase space, the bromate-pyrocatechol reaction is found to be capable of exhibiting spontaneous oscillations in a stirred batch reactor. The established phase diagram in the bromate-pyrocatechol concentration phase space sheds light on why finding chemical oscillations in this system is such a challenging task. Same as reported for other UBOs, the uncatalyzed bromate-pyrocatechol reaction exhibits subtle responses to illumination, where, depending on the reaction conditions, either light-induced or light-quenched oscillatory phenomena could be observed.

Experimental Procedure

All reactions were carried out in a thermal-jacketed 50 ml glass beaker purchased from ChemGlass and temperature was kept at 25.0 ± 0.1 °C by a circulating water bath (Thermo NesLab RTE 7). The reactor was sealed with a Teflon stopcock, which also served as the holder of electrodes. The solution level was about 1.0 cm below the bottom of the stopcock. The reaction solution was stirred with an octagonal magnetic bar driven by a magnetic stirrer (Fisher Isotemp). Influences of stirring on the oscillatory behavior were characterized, which show that under the protection of nitrogen increasing stirring rate from 500 rpm to 1200 rpm does not have significant effects on the oscillatory

behavior. Without the protection of nitrogen, however, the number of oscillation peak decreases significantly with increasing stirring rate.

Reactions were monitored with a platinum electrode (M231Pt-9 Radiometer Analytical) coupled with a Hg|Hg$_2$SO$_4$|K$_2$SO$_4$ reference electrode (XR200 Radiometer Analytical). All measurements were recorded with a pH/potential meter (Radiometer PHM220) connected to a personal computer through a PowerLab/4SP data logger. When investigating influences of light, a halogen lamp with dual bifurcated optic fibers and continuous variable light level was used as the light source (Fisher Scientific, Model DLS-100HD, 150 W). The illumination was implemented by placing the two fibers either on the opposite or the same side of the reactor and no difference in the reaction behavior was observed, implying that the mixing was fast enough to generate a situation of homogeneous illumination.

Stock solutions NaBrO$_3$ (Aldrich, 99%), 0.6 M, and sulfuric acid (Aldrich, 95-98%), 4.0 M, were prepared with double-distilled water. Pyrocatechol (Sigma, 99%) was directly dissolved in the reaction mixture. Bromine stock solution was prepared by dissolving 0.5 ml of bromine liquid (Aldrich) into 500.0 ml of double-distilled water. Hydrogen peroxide solution (30%) was purchased from ACP Chemical Inc. The volume of the reaction mixture was fixed at 30.0 cm^3 in all experiments. Results reported in the following were conducted without nitrogen protection at the stirring rate of 500 rpm. Absorption spectra were measured with a UV-visible spectrophotometer (Ocean Optics, 2000 USB). A quartz cuvette (10 mm light path, HELLMA) containing 2.5 ml of sample mixture was placed in the CUV sample holder which has two water jackets connected to a circulating water bath (Thermo NesLab RTE 7). The cuvette was stirred with a small magnetic bar.

Results and Discussions

Temporal evolutions of the bromate-pyrocatechol (pyrocatechol) reaction under different initial concentrations of pyrocatechol: (a) 0.038 M, (b) 0.044 M, and (c) 0.047 M. Other reaction conditions are $[BrO_3^-]$ = 0.085 M and $[H_2SO_4]$ = 1.4 M as shown in Figure 2.1. Shortly after mixing all chemicals together, Pt potential in Fig. 2.1a exhibits a clock reaction, followed by gradual decrease for several hours. The clock variation of the Pt potential is accompanied by a dramatic color change of the reaction solution from transparent to deep red. The color change occurs upon the addition of bromate, which is always introduced to the reactor in the last step. After the rapid color change, which has been observed in all of the following experiments, the red color gradually turns into yellow within the next two hours. When pyrocatechol concentration is increased to 0.044 M in Fig. 2.1b, spontaneous oscillations take place at about 2 hours after the solution has turned into yellow. Further increase of pyrocatechol concentration results in some irregularity in those transient oscillations such as the one shown in Fig. 2.1c. To show details of the chemical oscillations time scale in Fig. 2.1c is different from that used in Figs. 2.1a and 2.1b. There is an extremely long induction time period in both Figs. 2.1b and 2.1c. Such a dynamic feature is similar to what was reported in other uncatalyzed bromate oscillators [24-26].

Variations of the number of oscillation peaks (N) and the induction time (IP) as a function of pyrocatechol concentration are summarized in Fig. 2.2. Fig. 2.2a shows that the total number of oscillation peak increases rapidly as pyrocatechol concentration is above the bifurcation threshold (c.a. 0.040 M), which is followed by a more gradual decrease as pyrocatechol concentration is increased further. Eventually, the system moves out of the oscillatory parameter window at [pyrocatechol] $\approx$ 0.055 M. Fig. 2.2b illustrates

that within the oscillatory window the induction time of spontaneous oscillations decreases monotonically as pyrocatechol concentration is increased.
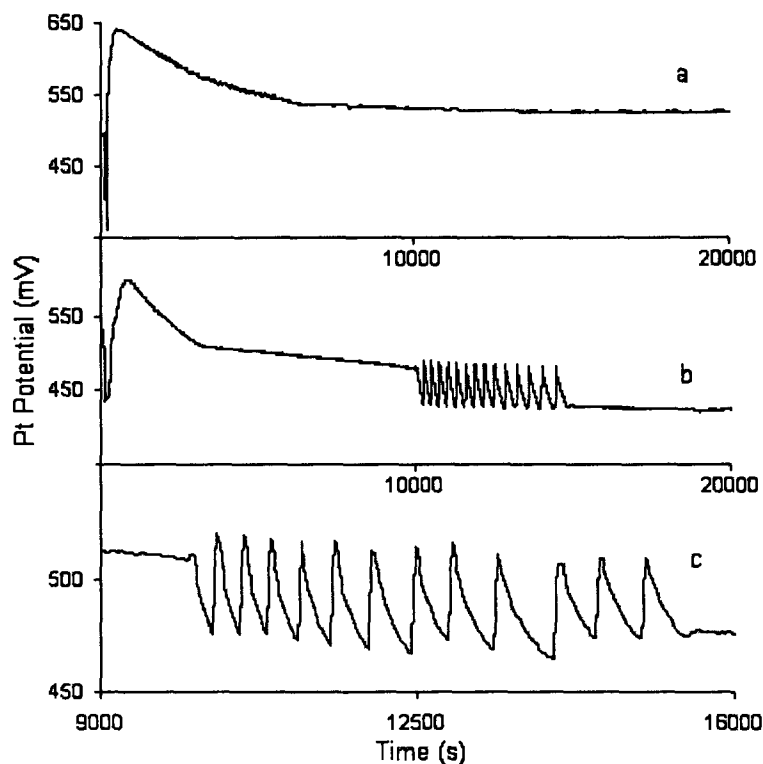
Figure 2.1 Time series of the bromate - pyrocatechol reaction at different initial concentrations of pyrocatechol: (a) 0.038 M, (b) 0.044 M, and (c) 0.047M. Other reaction conditions are [BrO₃⁻] = 0.085 M and [H₂SO₄] = 1.4 M.

Within the oscillation window, the induction time decreases monotonically with the increase of pyrocatechol concentration. On the other hand, the total number of oscillation peak increases rapidly as pyrocatechol concentration is just above the lower bifurcation threshold and then decreases as pyrocatechol concentration is increased further.
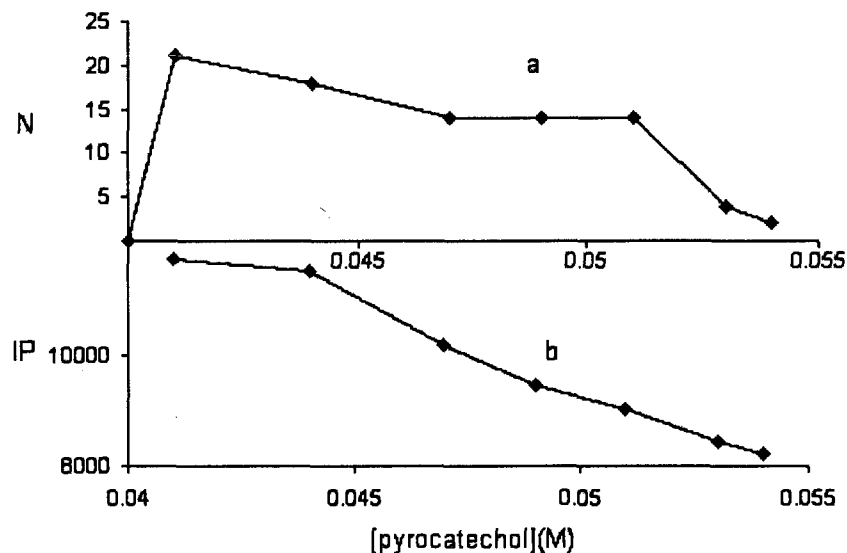
Figure 2.2 Dependence of the number of oscillations (N) and induction period (IP) on the initial concentration of pyrocatechol. Other reaction conditions are the same as those used in Fig. 2.1.

Time series performed under different initial concentrations of BrO_3^- show similar trends as those in Fig. 2.1. Figure 2.3 presents three time series performed under different initial concentrations of BrO_3^-: (a) 0.085 M, (b) 0.093 M, and (c) 0.095 M. Other reaction conditions are [pyrocatechol] = 0.057 M and [H_2SO_4] = 1.4 M. For low bromate concentrations (<0.09 M), the Pt potential of the system decreased monotonically after its initial excursion, the same as the one shown in Fig. 2.3a. Transient oscillations were obtained when bromate concentration was increased to 0.093 M. Further increase of bromate concentration led to irregular oscillations in Fig. 2.3c, where not only the amplitude but also the frequency of oscillation fluctuates irregularly. To show modulations in the oscillation frequency clearly, only the oscillation window is plotted in

Fig. 2.3c, in which the long induction time period, similar to the ones plotted in Figs. 2.3a

and 2.3b, is omitted. As bromate concentration was increased continuously, the system

underwent reverse bifurcations leading the system back to non-oscillatory states where

the evolution of Pt potential was the same as that in Fig. 2.3a. For conditions employed in

Fig. 2.3, spontaneous oscillations have been obtained when bromate concentration was

between 0.09 and 0.11 M.
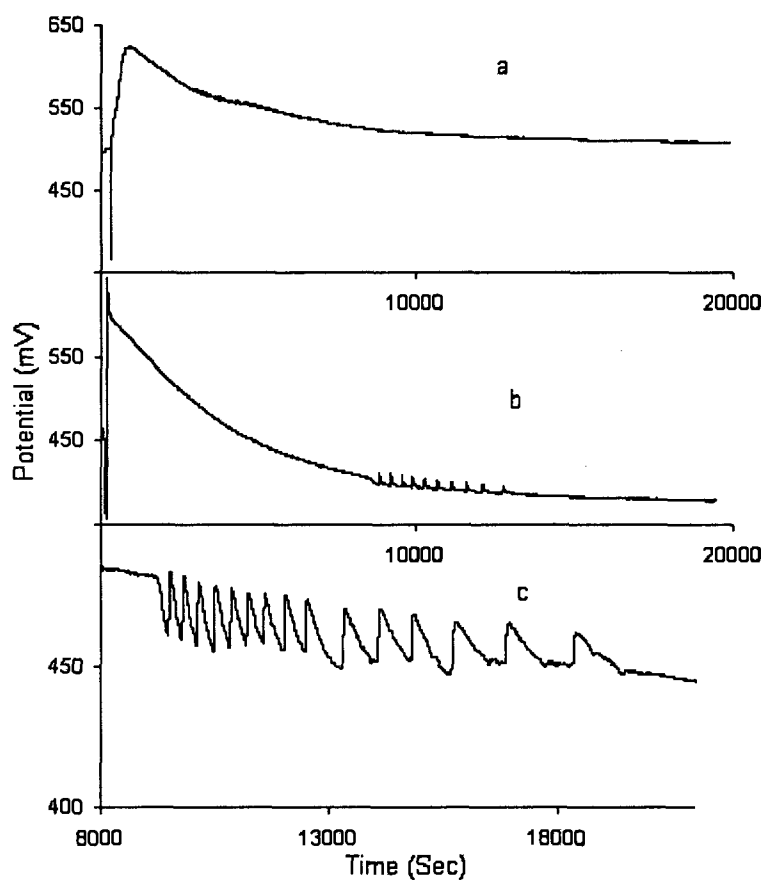
Figure 2.3 Time series of the pyrocatechol – bromate reaction at different initial concentrations of bromate: (a) 0.085 M, (b) 0.093 M, and (c) 0.095M. Other reaction conditions are [pyrocatechol] = 0.057 M, and [H$_2$SO$_4$] = 1.4 M.

Fig. 2.4a shows that the number of oscillation peak increased with bromate concentration and then dropped sharply as the system moved out of the oscillation window from the high bromate concentration end. This result demonstrates that increasing of bromate concentration has opposite effects on the oscillatory behavior as increasing pyrocatechol concentration. Yet, similar to what was seen in Fig. 2.2b, Fig. 2.4b shows that as the number of oscillation peaks increases, their induction time also grows.
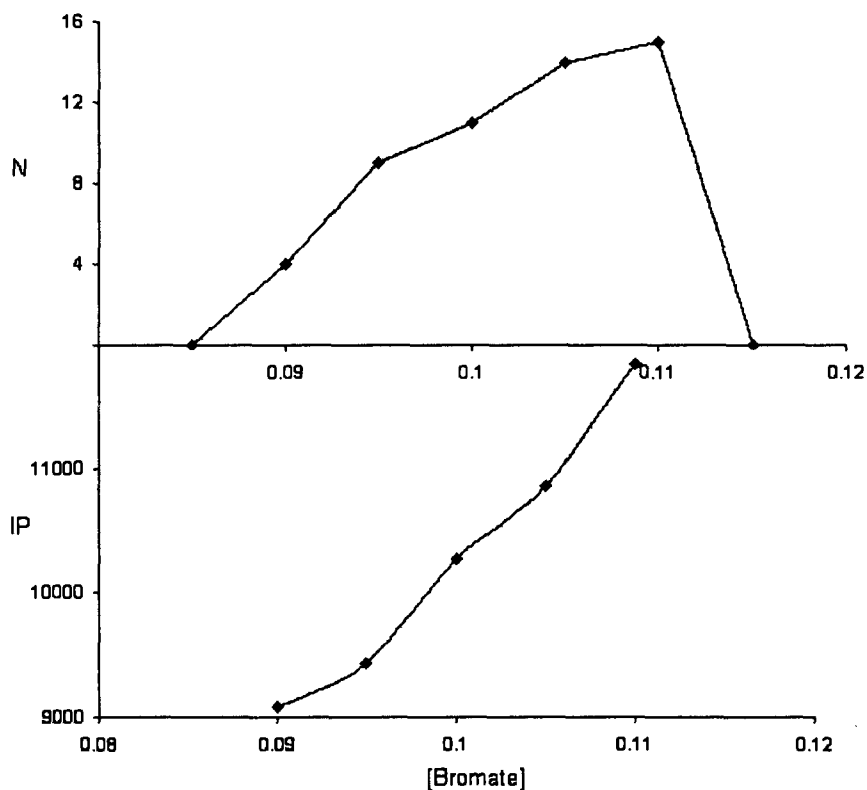
Figure 2.4 Dependence of the number of oscillations (N) and induction period (IP) on the initial concentration of bromate. Other reaction conditions are [pyrocatechol] = 0.057 M, and [H_2SO_4] = 1.4 M.

Figure 2.5 is a phase diagram in the pyrocatechol-bromate concentration phase plane, where filled triangles and squares denote that the system exhibits spontaneous oscillations. Here, the concentration of H_2SO_4 is fixed at 1.4 M. First glance of this phase diagram indicates that the oscillatory behavior can be obtained over broad concentrations of pyrocatechol and bromate. However, at a given concentration of bromate (or pyrocatechol) there is only a narrow range of pyrocatechol (or bromate) concentration within that the system oscillates. This diagonal narrow band window sheds light on the difficulty of achieving chemical oscillations in this system [21, 22]. Conditions under which oscillations exhibit some irregularities such as seen in Fig. 2.1c are denoted by those filled squares in this phase diagram.
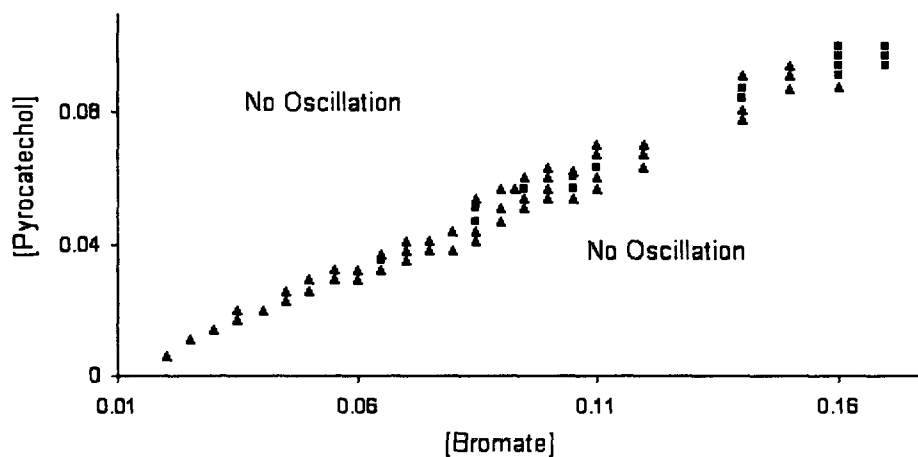
Figure 2.5 Phase diagram of the bromate - pyrocatechol reaction in the pyrocatechol – bromate concentration plane. (■) denotes where the system exhibits transient complex oscillations, whereas simple periodic oscillations are represented by (▲). $[H_2SO_4]$ = 1.4 M.

Dependence of the above chemical oscillations on H_2SO_4 and bromate concentrations

is summarized in Figure 2.6, in which pyrocatechol concentration is fixed at 0.057 M.

Filled triangles and squares indicate the conditions under which the system exhibits

spontaneous oscillations. This phase diagram shows that when the concentration of

H_2SO_4 is larger than 2.5 M or smaller than 0.9 M, no oscillations can be obtained

regardless bromate concentration. On the other hand, the range of H_2SO_4 concentration

over which the system exhibits spontaneous oscillations is broader at low bromate

concentration. Filled squares indicate where oscillations show slight irregularities as seen

in Fig. 2.1c.
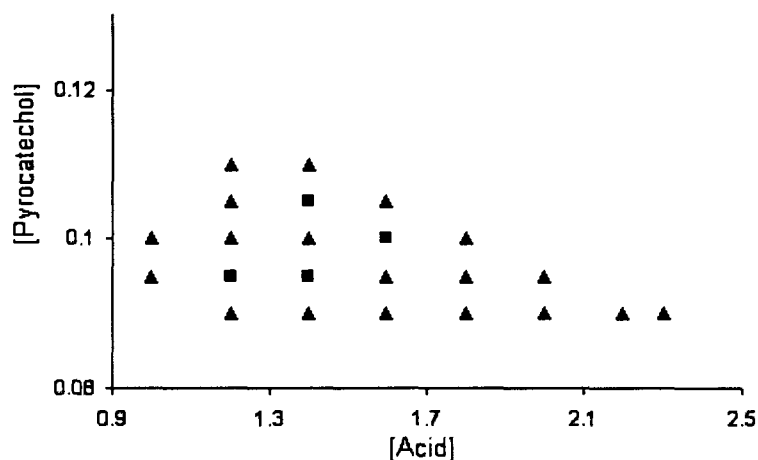
Figure 2.6 Phase diagram of the bromate - pyrocatechol reaction in the bromate – H_2SO_4 concentration plane. (■) denotes where the system exhibits transient complex oscillations, whereas simple periodic oscillations are represented by (▲). The concentration of pyrocatechol is 0.057 M.

Figure 2.7 shows the response of the pyrocatechol-bromate reaction to the addition of

Br⁻. Reaction conditions are $[BrO_3^-] = 0.078$ M, $[H_2SO_4] = 1.3$ M, and [pyrocatechol] =

0.043 M. Here the evolution of the system is monitored simultaneously by Pt and bromide selective electrodes. For the bromide electrode, our calibration indicates that the more negative potential value corresponds to a higher concentration of bromide ions. The time series in Fig. 2.7b illustrates that at the initial stage of the reaction, there is a sudden drop in bromide concentration, which resembles an autocatalytic reaction process. The bromide concentration increases gradually through the long induction time period and then starts oscillating, similar to the behavior reported in the uncatalyzed bromate-1,4-cyclohexanedione and bromate-1,4-benzoquinone reactions [25, 26]. The arrow indicates the moment that a 0.01 ml of Br⁻ solution is injected into the reaction mixture, which leads to [Br⁻] = 5×10⁻⁵ M after mixing. As shown in the Figure, the addition of bromide temporally stops the spontaneous oscillations, similar to quenching behavior reported in the Belousov-Zhabotinsky (BZ) reaction [35].
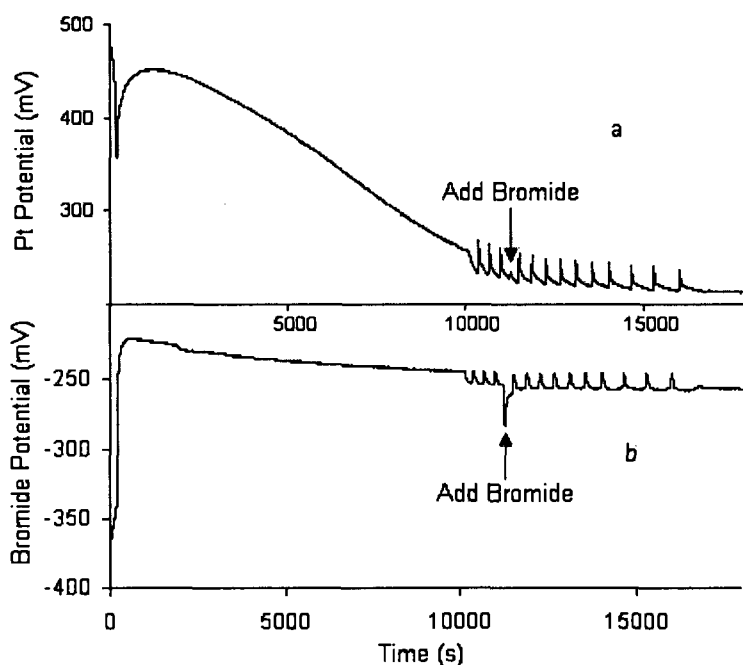
Figure 2.7 Responses of the pyrocatechol-bromate reaction to the addition of Br⁻. Reaction conditions are [BrO₃⁻] = 0.078 M, [H₂SO₄] = 1.3 M, and [pyrocatechol] = 0.043 M.

Time series measured with a bromide selective electrode show that bromide concentration increases slowly during the long induction time and then starts oscillating (see fig. 2.8). It is similar to the behavior reported in earlier studies of the uncatalyzed bromate reactions, in which the accumulation of bromide precursors has been suggested to be responsible for the long induction time [25, 26].
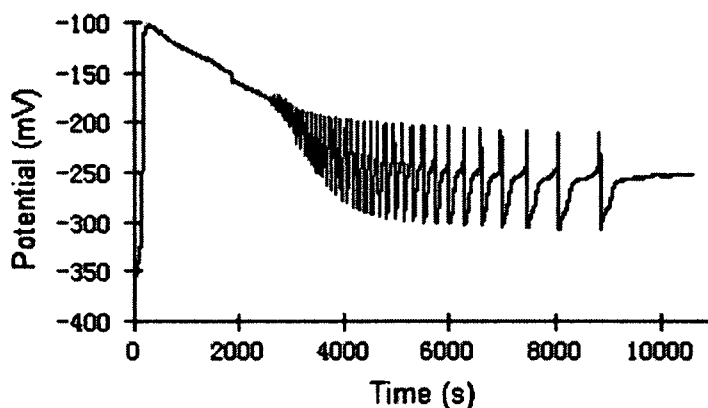
Figure 2.8 Time series of pyrocatechol-bromate system with bromate selective under condition: [pyrocatechol] = 0.057 M, [acid] = 1.3 M, [bromate] = 0.078 M.

Fig. 2.9 shows that the initial addition of bromide into the system, which leads to the rapid production of bromine and the subsequent bromination of pyrocatechol (confirmed by UV/vis and mass spectrometry experiments), does not affect the induction time. A slight decrease of the induction time is seen at high bromide concentration, but such a decline might result from decreases in pyrocatechol and BrO_3^- concentrations due to their reactions with bromide. The insensitivity of the induction time to the presence of brominated substrates suggests that the governing mechanism of this bromate-oscillator

could be different from the UBOs reported earlier, in which the accumulation of bromide

precursor has been suggested to be responsible for the long induction time [6, 25, 26].
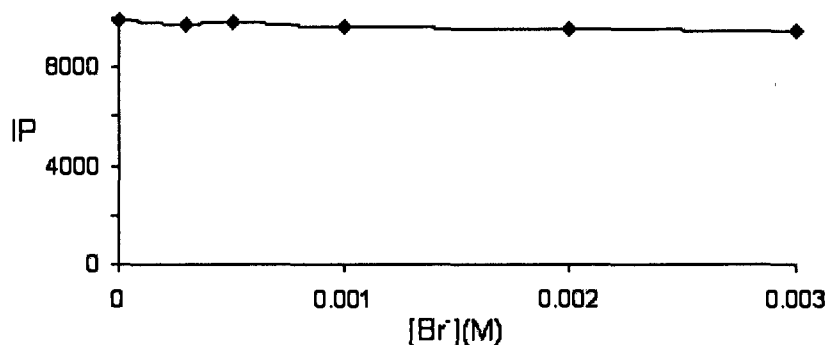
Figure 2.9 The variation of the induction time as a function of the initial concentration of bromide ions. Other reaction conditions are: [pyrocatechol] = 0.047 M, [BrO$_3^-$] = 0.09 M, and [H$_2$SO$_4$] = 1.4 M.

In this study, however, the initial addition of bromide, which leads to the rapid

production of bromine and then causes the bromination of organic substrates i.e.

pyrocatechol (evidenced by mass spectrometry study in Fig. 2.11), does not shorten the

induction time. The slight decrease of the induction time at very high bromide

concentration may result from decreases in pyrocatechol and BrO$_3^-$ concentrations due to

reactions with bromide. The insensitivity of the induction time to the initial presence of

brominated substrates suggests that the governing mechanism of this oscillator may be

different from UBOs reported earlier [6, 24-28]; for instance, the brominated

pyrocatechol products may not participate in further reactions.

Fig. 2.10 presents two time series of pyrocatechol and Br_2 reactions collected at 400 nm at which Br_2 has a strong absorption [36]. As is shown in this Figure, the presence of acid greatly accelerates the reaction process.
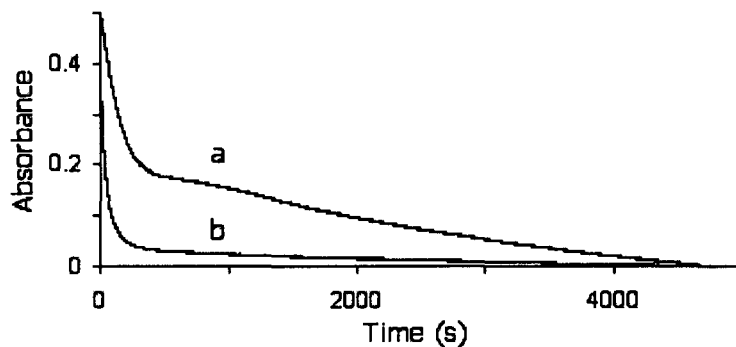
Figure 2.10 Time series of the bromine-pyrocatechol reaction collected at 400 nm. Reaction conditions are $[Br_2]$ = 0.0039 M, [pyrocatechol] = 0.078 M, and $[H^+]$ = (a) 0, and (b) 2.0 M.

The mass spectrum of the above reaction is presented in Fig. 2.11, in which the largest peak belongs to a 109 m/e, the unreacted pyrocatechol. There is an accompanying peak at 188/190 with appropriate isotopic ratios, suggesting the production of monobrominated 1,2-benzoquinone. The following step, $2Br_2 + HAr(OH)_2 \rightarrow BrArO_2 + 3Br^- + 3H^+$, is suggested to account for the above oxidation and bromination of pyrocatechol by bromine. The influence of acid on the oxidation rate may arise from its effects on the deprotonation of pyrocatechol. We have employed initial rate approach to measure the effective rate constant of the above process, in which a series of reactions has been conducted in the presence of excessive amount of one of the two species while the concentration of the other was adjusted gradually. The experiments indicate that the reaction between bromine

and pyrocatechol is first order with respect to both species. The effective rate constant is

calculated from Fig. 2.10 as 0.014 $M^{-2}s^{-1}$ in water and 0.035 $M^{-2}s^{-1}$ in acidic solution.
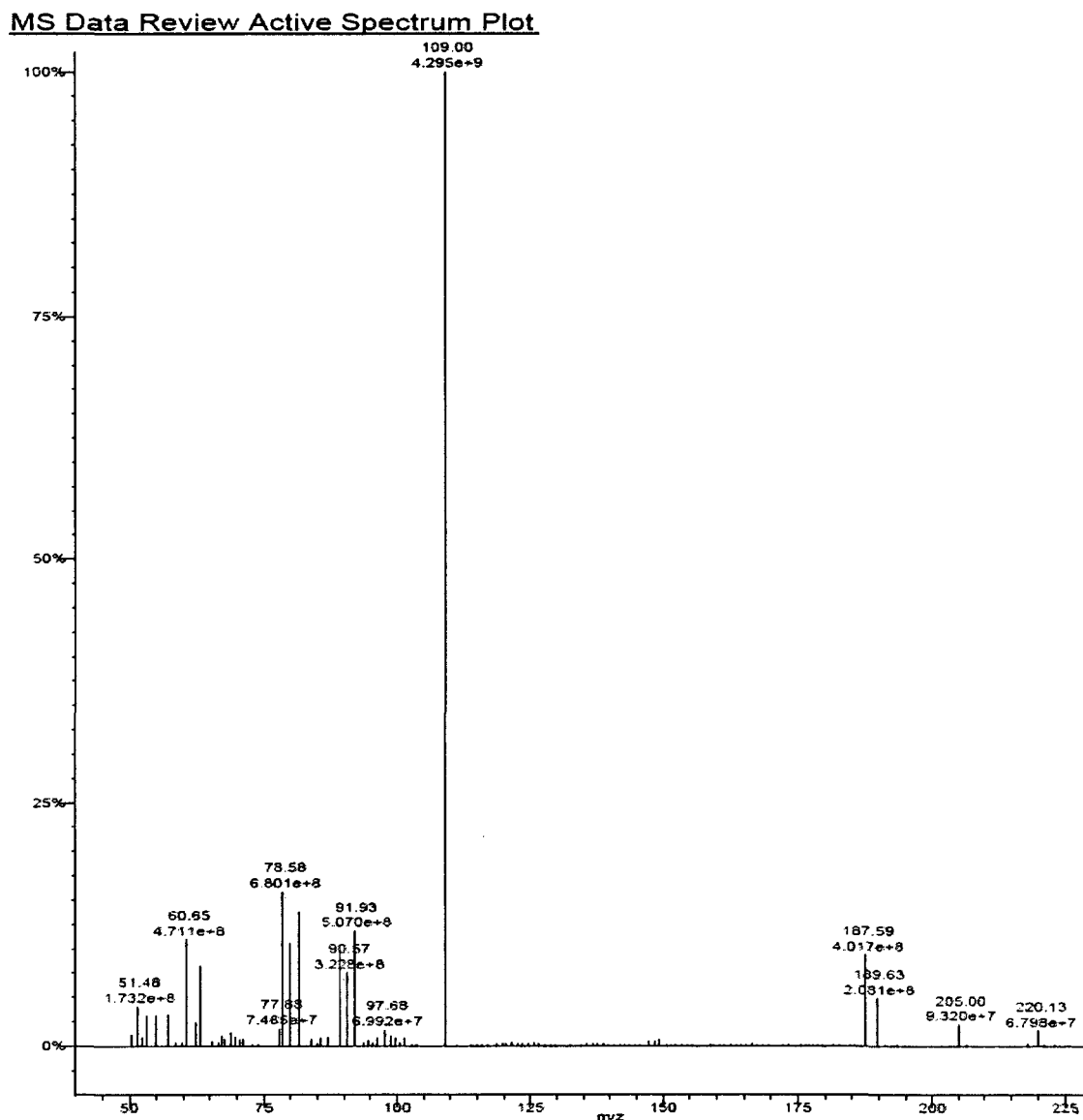
Figure 2.11 The mass spectrum of the bromine and pyrocatechol reaction. Reaction conditions are [pyrocatechol] = 0.006 M, and [Br$_2$] = 0.0078 M.

In addition to being quenched by bromide ions, Fig. 2.12 shows that the bromate-pyrocatechol oscillations can also be quenched by ethanol, which is employed primarily as a radical scavenger [29]. Fig. 2.12a shows that upon the addition of a small amount of ethanol (1.0 x 10^{-4} M), the oscillation amplitude becomes smaller. In Fig. 2.12b spontaneous oscillations are completely quenched as a result of adding larger amounts of ethanol (1.0 x 10^{-3} M). Different from quenching by bromide ions, spontaneous oscillations in Fig. 2.12b do not revive. Such a result suggests that the uncatalyzed bromate-pyrocatechol oscillator is also radical-controlled. However, one cannot preclude the effect of ethanol from its reaction with acidic bromate which produces HOBr.
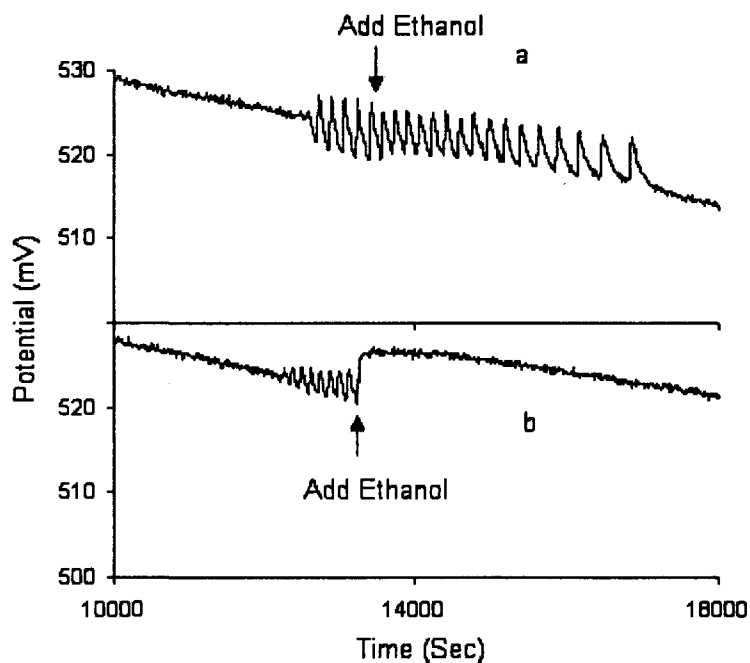
Figure 2.12 Perturbations of the spontaneous oscillations by ethanol. Arrows indicate the moment ethanol is injected into the reaction mixture. In (a) 1.0 x 10^{-4} M ethanol is added, whereas 1.0x10^{-3} M ethanol is added in (b). Other reaction conditions are [pyrocatechol] = 0.047 M, [BrO_3^-] = 0.09 M, and [H_2SO_4] = 1.4 M.

The oscillatory oxidation of pyrocatechol by acidic bromate has one important difference with BZ reaction. Orbán et al. reported that chloride ion inhibited oscillatory behaviour in concentrations higher than 10^{-4} M [21]. In this system, initial added chloride ions cannot suppress the oscillation (Fig. 2.13a). It will inhibit the oscillation just when its concentration reaches 0.01 M which also will form a large amount of precipitations in the system. When we add chloride ions during the oscillatory period in concentrations higher than 5×10^{-4} M, oscillations are quenched. Perturbing system with lower concentrations will inhibit oscillations just for a short time and after that system will continue showing oscillatory behavior, Fig. 2.13b.
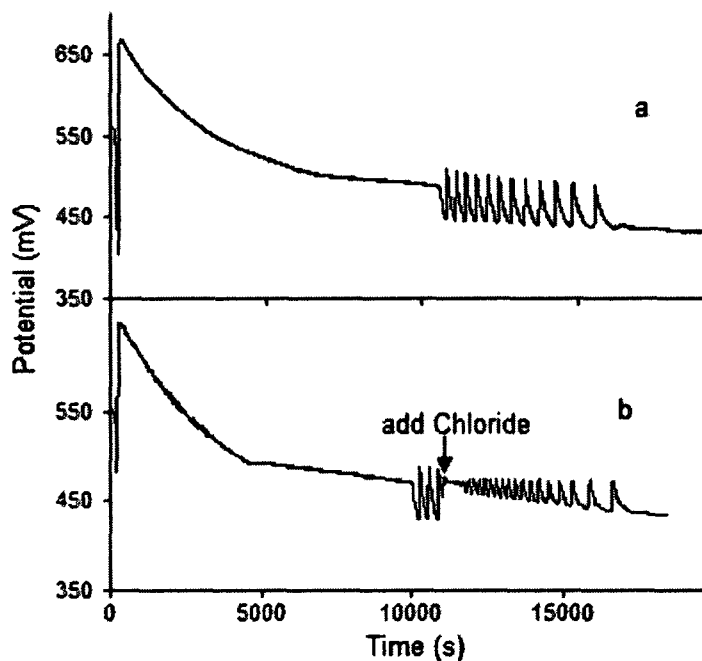
Figure 2.13 Chloride effect on pyrocatechol–Bromate system under conditions: [Bromate] = 0.07 M, [Acid] = 1.40 M, [pyrocatechol] = 0.038 M, and [Chloride] = 10^{-4} M in both cases

Fig. 2.14a shows that in the absence of illumination the Pt potential only exhibits a large excursion at the beginning of the reaction and then decreases smoothly. When the same reaction system is exposed to a constant illumination from the beginning (the intensity = 70 mW/cm^2), however, three oscillation peaks appear in Fig. 2.14b at about 5500 s after the reaction starts.
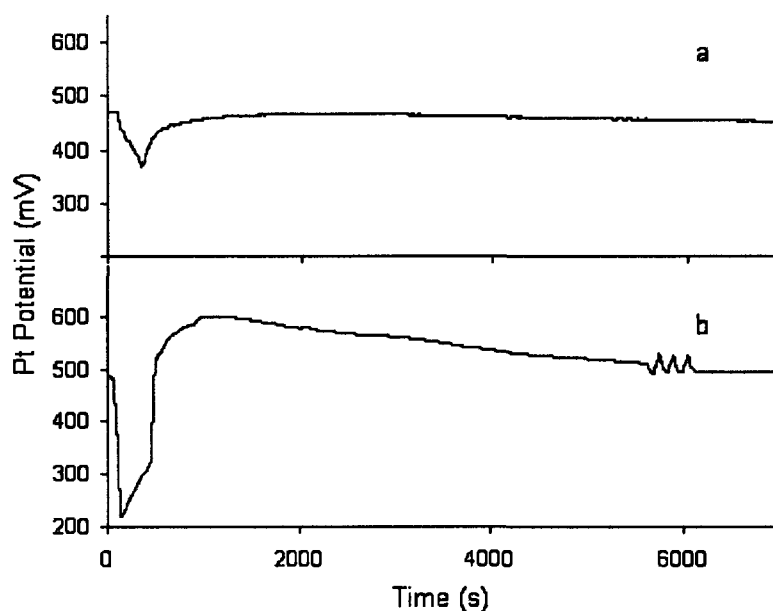
Figure 2.14 The bromate – pyrocatechol reaction in the absence (a) and presence (b) of illumination. Other reaction conditions are [pyrocatechol] = 0.026 M, [BrO$_3^-$] = 0.05 M, and [H$_2$SO$_4$] = 2.0 M. The light intensity in (b) is equal to 70 mW/cm^2.

Fig. 2.15 illustrates that spontaneous oscillations can be quenched by light and then revive immediately upon turning-off the light. Frequencies of these revived oscillations become significantly different, implying that illumination causes irreversible impacts on the reaction dynamics. Results presented in Figs. 2.14 and 2.15 illustrate that the

bromate-pyrocatechol system can be a model system to explore interactions of complex

intrinsic dynamics and external forcing.
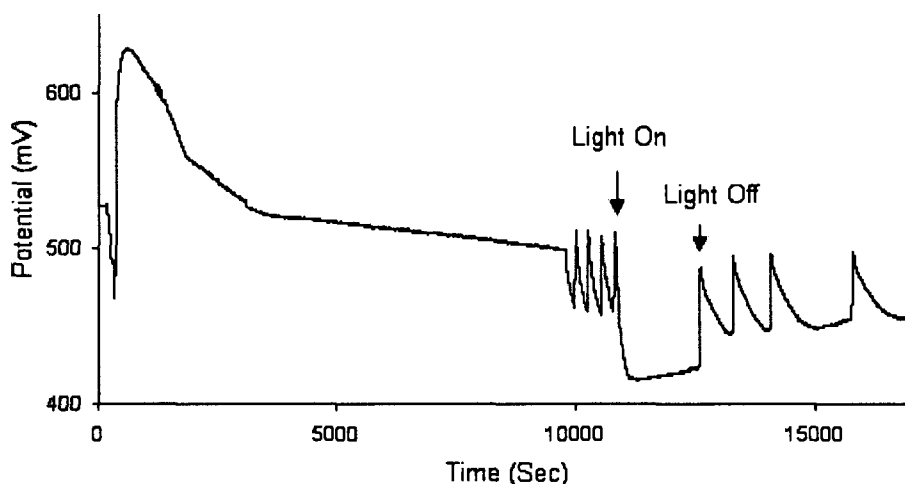
Figure 2.15 Quenching of the bromate - pyrocatechol oscillations with light. Other reaction conditions are [pyrocatechol] = 0.057 M, [BrO$_3^-$] = 0.10 M, and [H$_2$SO$_4$] = 1.4 M. The light intensity is equal to 80 mW/cm^2.

Preliminary mechanistic characterizations have been carried out to determine products

and possible elementary steps of the bromate-pyrocatechol reaction. Fig. 2.16 presents the

UV-Vis spectra of (a) pyrocatechol, (b) 1,2-benzoquinone (1,2-Q), (c) the bromate-

pyrocatechol reaction mixture, and (d) the light source. The spectrum in Fig. 2.16a shows

that pyrocatechol has two large absorption peaks centered, respectively, at 225 nm and

275 nm. When the pyrocatechol concentration is high, such as 0.01 M, there is only one

broad peak spanning 220 and 290 nm in the spectrum. The absorption peak of 1,2-Q in

Fig. 2.16b was obtained via oxidizing 5.0 x 10^{-4} M pyrocatechol with excess amount of

H$_2$O$_2$, in which the concentrated H$_2$O$_2$ (0.12 M) solution was used as the reference and

thus its absorption does not interfere with 1,2-Q. This result illustrates that 1,2-Q has one

large absorption peak at 275 nm.
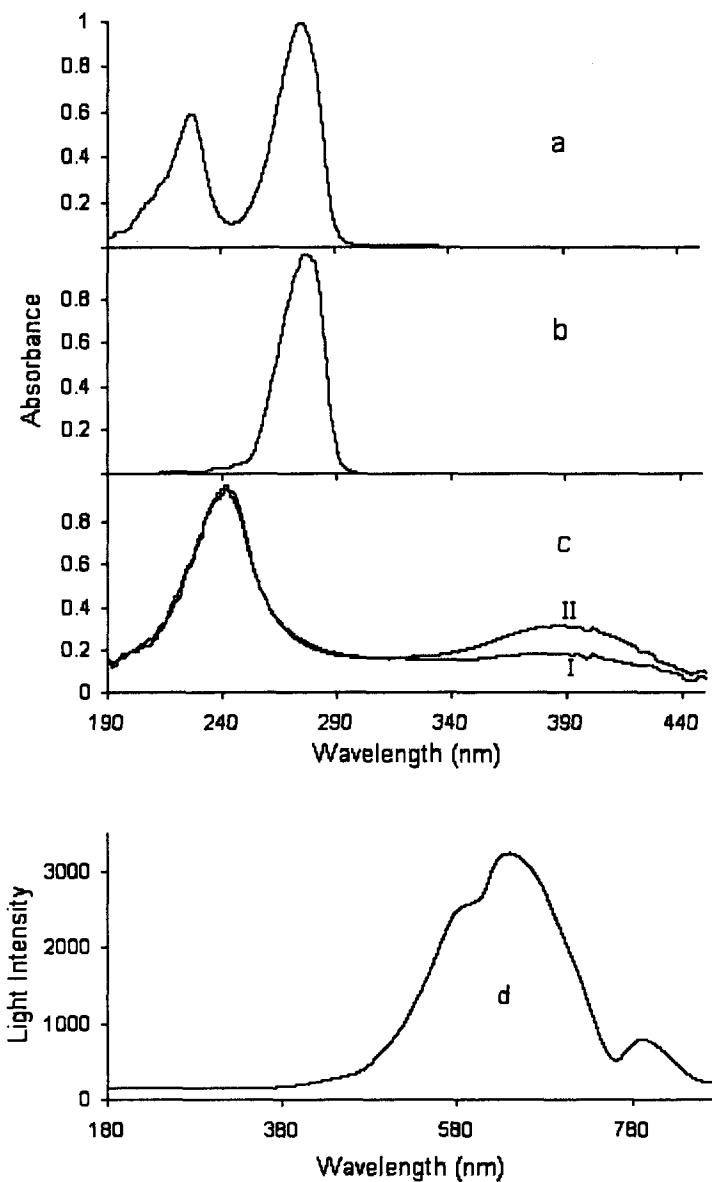
Figure 2.16 Spectra of (a) pyrocatechol, (b) 1,2-benzoquinone, (c) the bromate-pyrocatechol reaction solution, and (d) light source. The concentration of pyrocatechol equals 5×10^{-4} M in (a). In (b) 5×10^{-4} M pyrocatechol was added to 0.12 M H_2O_2 solution and 0.12 M H_2O_2 solution was used as the reference solution in the spectroscopic measurement. In (c) the reaction mixture was diluted 12 times and before the dilution it contained $[BrO_3^-]$ = 0.085 M, $[H_2SO_4]$ = 1.4 M, [pyrocatechol] = 0.041 M. The spectra in (c) were collected at I) 2 min., and II) 120 minute after mixing all reagent together.

Spectra in Fig. 2.16c were collected by using $[BrO_3^-] = 0.085$ M and $[H_2SO_4] = 1.4$ M

solution as the reference and thus their absorption effects were eliminated. The spectrum

(I) was collected right after the solution has turned into red (i.e. after the occurrence of the

first excursion in the Pt potential). Here, a broad absorption peak is seen at 390 nm, which

reflects the formation of the red colored substance. Such an absorption peak coincides

with the absorption peak of bromine. An earlier study by Kumli and co-workers on the

catalyzed bromate-sorbitol reaction also showed the red color change at the beginning of

the reaction, which has been suggested due to the formation of bromine [36]. Notably,

here the absorption at 225 nm is also greatly reduced, suggesting that a portion of

pyrocatechol has undergone reactions or structure changes through, possibly, the

formation of dimer or trimmers with the pyrocatechol radicals produced through the

initial excursion. The red color substance with absorption at 390 nm has decreased

significantly before oscillations commence.

Fig. 2.16d shows that the power of the halogen light source concentrates within the

visible region. Here the measured light intensity corresponds to 20 mW/cm^2. In order to

have a detectable amount of UV light the overall light intensity needs to be above 50

mW/cm^2. The mismatch between the absorptions of pyrocatechol and its derivatives and

the distribution of light power could be responsible for the intensive illumination required

in Fig. 2.15.

To shed light on the above issue, mass spectrometry study was conducted with the

solution (I). The analysis was performed by adding 30 ml diethyl ether to the 30.0 ml

reaction mixture and the subsequent separation of the organic phase. The remaining

aqueous phase was then extracted twice, respectively, with 30 ml diethyl ether. Later, a

rotavac was used to dry the diethyl ether sample, which took about 60 minutes.
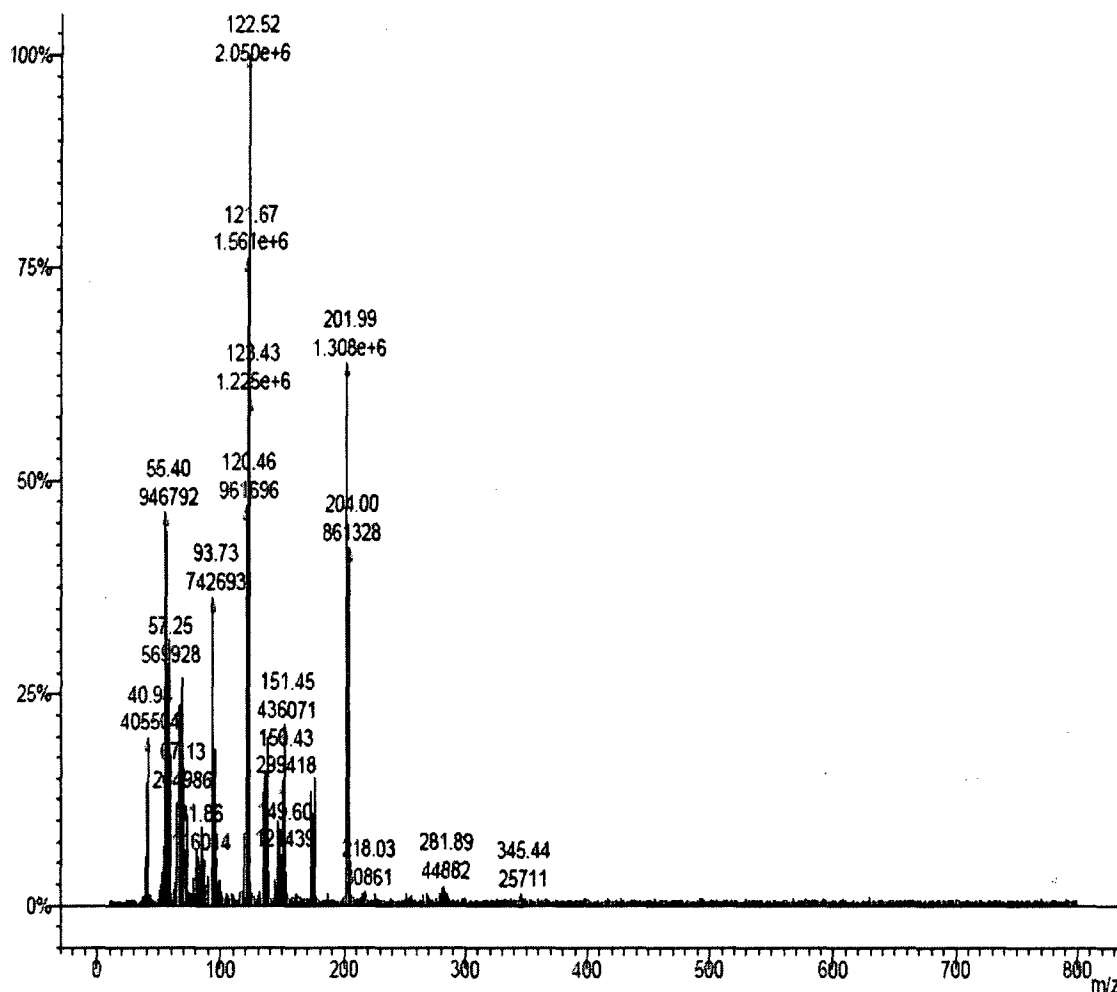
Figure 2.17 Mass Spectrum (EI, 20 eV) of a sample extracted from the reaction mixture of $[BrO_3^-]$ = 0.085 M, $[H_2SO_4]$ = 1.4 M, [pyrocatechol] = 0.041 M. The extraction was conducted at 10 minutes after mixing the above reagents together.

Finally, the dried sample was analyzed. The mass spectrum in Fig. 2.17, illustrates the formation of larger molecules, in particular, there is a small peak with 218 m/e, which strongly suggests the presence of pyrocatechol and 1,2-benzoquinone dimer. The largest peak at 123 m/e cannot be identified at this time. As illustrated by the spectra (II) and (III) in Fig. 2.16c, the substance with the absorption between 300 and 400 nm decreases in

time. To account for the above reversible changes in the absorption spectra, we propose a reversible formation of catechol complex through pyrocatechol and pyrocatechol radicals (see step 11 in the following model). It is useful to point out that bromine, an intermediate in the studied system, may also contribute to the absorption peak around 390 nm in the spectra (I, II and III).

Experiments in Fig. 2.12 have demonstrated that the addition of ethanol to the reaction mixture has irreversible influences on the reaction behavior. Fig. 2.18 shows the reaction between ethanol and acidic bromate, where the evolution was followed at 330 nm by assuming the formation of HOBr [29]. The absorption curve in Fig. 2.18 exhibits a maximum at approximately 2000 seconds, indicating the existence of a direction reaction between ethanol and bromate.
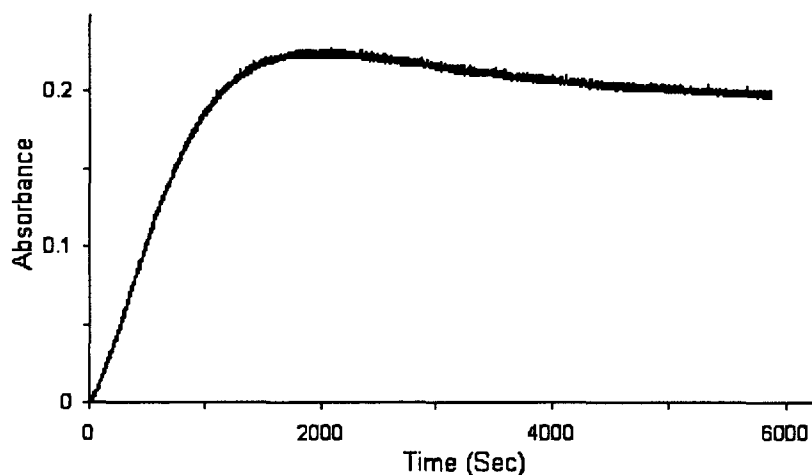
Figure 2.18 Time evolution of the ethanol and acidic bromate reaction. It is collected at 330 nm, which is due to the absorption of HOBr. Initial conditions are $[CH_3CH_2OH]$ = 0.01 M, $[BrO_3^-]$ = 0.3 M, and $[H_2SO_4]$ = 1.0 M.

In addition, the curve in Fig. 2.18 suggests that the reaction between ethanol and bromate is a complicated one, in which HOBr may proceed to react with ethanol further, similar to the case discussed in the methanol and acidic bromate system [29]. Thus, it is suggested that ethanol may have been involved in the oscillatory process through the following step:

$$CH_3CH_2OH + BrO_3^- + H^+ \rightarrow CH_3COOH + HOBr + H_2O \quad (a)$$

Notably, including the above reaction in the model can qualitatively reproduce the quenching phenomena seen in Fig. 2.12.

The model is developed based on the mechanism proposed for the 1,4-cyclohexanedione-bromate system and a skeleton mechanism proposed by Orban, Körös and Noyes (OKN) for the uncatalyzed reactions of aromatic compounds and acidic bromate 25, 31]. Listed in Table 2.1, reactions 1 to 5 form an autocatalytic feedback, which is the core of a chemical oscillator. Different from catalyzed bromate-oscillators [32-34], the organic substrate pyrocatechol replaces reduced metal ions to reduce bromine dioxide radicals in step 4. Spectroscopic measurements in Fig.2.16c suggest that the formation and dissociation of catechol dimer might be involved in the reaction process. To account for such a complicated process, an abstract step is included in the model (see reaction 11). As such a process remains largely unknown, its rate constant is chosen in a way that the model could generate spontaneous oscillations under the experimental conditions. An important feature of the proposed model is that the brominated pyrocatechol species are final products, which appears to agree with our experimental observation that the induction time is insensitive to the initial presence of brominated substrates.

The mass spectrometry study illustrates that the bromine and pyrocatechol reaction leads to the oxidation and bromination of the substrate. Such a process is represented by step 9 in the model, i.e. $2Br_2 + HAr(OH)_2 \rightarrow BrArO_2 + 3Br^- + 3H^+$. Kinetic measurements suggest that the rate constant is $0.014\ M^{-2}s^{-1}$ in water and $0.035\ M^{-2}s^{-1}$ in acidic environment. The value used in the following simulation, $0.05\ M^{-2}s^{-1}$, is slightly higher in order to obtain a longer oscillation train.

Table 2.1 The model proposed for the uncatalyzed bromate – pyrocatechol reaction

No.	Reaction	Rate Constant	Ref.
1	$BrO_3^- + Br^- + 2H^+ \leftrightarrow HBrO_2 + HOBr$	$K_{1f} = 2.1\ M^{-3}s^{-1}$ $K_{1r} = 10000\ M^{-1}s^{-1}$	30
2	$HBrO_2 + Br^- + H^+ \rightarrow 2HOBr$	$K_2 = 2\times10^9\ M^{-2}s^{-1}$	30
3	$BrO_3^- + HBrO_2 + H^+ \leftrightarrow 2BrO_2^\bullet + H_2O$	$K_{3f} = 10000\ M^{-2}s^{-1}$ $K_{3r} = 2\times10^7\ M^{-2}s^{-1}$	30
4	$BrO_2^\bullet + HAr(OH)_2 \rightarrow HBrO_2 + HAr(OH)O^\bullet$	$K_4 = 700\ M^{-1}s^{-1}$	30
5	$2HBrO_2 \rightarrow BrO_3^- + HOBr + H^+$	$K_5 = 4\times10^7\ M^{-1}s^{-1}$	30
6	$HOBr + HAr(OH)O^\bullet \leftrightarrow Br^\bullet + HArO_2 + H_2O$	$K_{6f} = 5500\ M^{-1}s^{-1}$ $K_{6r} = 2\times10^6\ M^{-1}s^{-1}$	a
7	$Br^\bullet + HAr(OH)O^\bullet \leftrightarrow Br^- + HArO_2 + H^+$	$K_{7f} = 55\times10^5\ M^{-1}s^{-1}$ $K_{7r} = 1050\ M^{-2}s^{-1}$	a
8	$HOBr + Br^- + H^+ \leftrightarrow Br_2 + H_2O$	$K_{8f} = 8\times10^9\ M^{-2}s^{-1}$ $K_{8r} = 110\ M^{-1}s^{-1}$	30
9	$2Br_2 + HAr(OH)_2 \rightarrow BrArO_2 + Br^- + H^+$	$K_9 = 0.05\ M^{-2}s^{-1}$	b
10	$HOBr + HAr(OH)_2 \rightarrow BrAr(OH)_2 + H_2O$	$K_{10} = 1\ M^{-1}s^{-1}$	30
11	$HAr(OH)O^\bullet + HAr(OH)_2 \leftrightarrow Complex$	$K_{11f} = 1\times10^6\ M^{-1}s^{-1}$ $K_{11r} = 1\ s^{-1}$	a
12	$HAr(OH)O^\bullet + BrO2^\bullet \rightarrow HBrO_2 + HArO_2$	$K_{12} = 5000\ M^{-1}s^{-1}$	a

a: adjusted in this study; b: measured in this study. Here notations $HAr(OH)_2$ and $HArO_2$ represent, respectively, pyrocatechol and 1,2-benzoquinone. $BrArO_2$ represents bromo-1,2-benzoquinone

Fig. 2.19 presents two time series calculated under different initial concentrations of pyrocatechol. Numerical integrations were carried out with commercial software (Berkeley Madonna software). Rate constants used in the simulation were taken from the literature or chosen in such a way that the best agreement between experiments and simulations could be achieved [30]. Similar to what were seen in experiments, Fig. 2.19a shows that the system does not oscillate at the low pyrocatechol concentration. Spontaneous oscillations with a long induction time (> 5000 s) were obtained in Fig. 2.19b, where a higher pyrocatechol concentration was employed in the calculation. Spontaneous oscillations disappeared when pyrocatechol concentration became too high, in agreement with experiments, but it has to be above 0.77 M, which is significantly larger than 0.078 M seen in experiments.

To account for the photo-manipulated reaction behavior presented in Figs. 2.14 and 2.15, the following reaction step is included into the reaction scheme listed in Table 2.1.

$$Br_2 + h\nu \rightarrow 2Br^{\cdot} \qquad\qquad (b)$$

Fig. 2.20 presents the simulation results after incorporating the above photo-dissociation of bromine. In Fig. 2.20a, k_b equals 0, corresponding to the absence of illumination. Same as the experimental result, the system does not exhibit spontaneous oscillations. In Fig. 2.20b, the rate constant k_b equals 10.0 s^{-1} and spontaneous oscillations are achieved after a long induction time. Other conditions used in the above simulation are [H$_2$SO$_4$] = 1.4 M, [pyrocatechol] = 0.90 M, and [BrO$_3^-$] = 0.10 M. While photo-induced oscillations are reproduced here, the initial concentration of pyrocatechol is 20 times larger than that used in experiments.
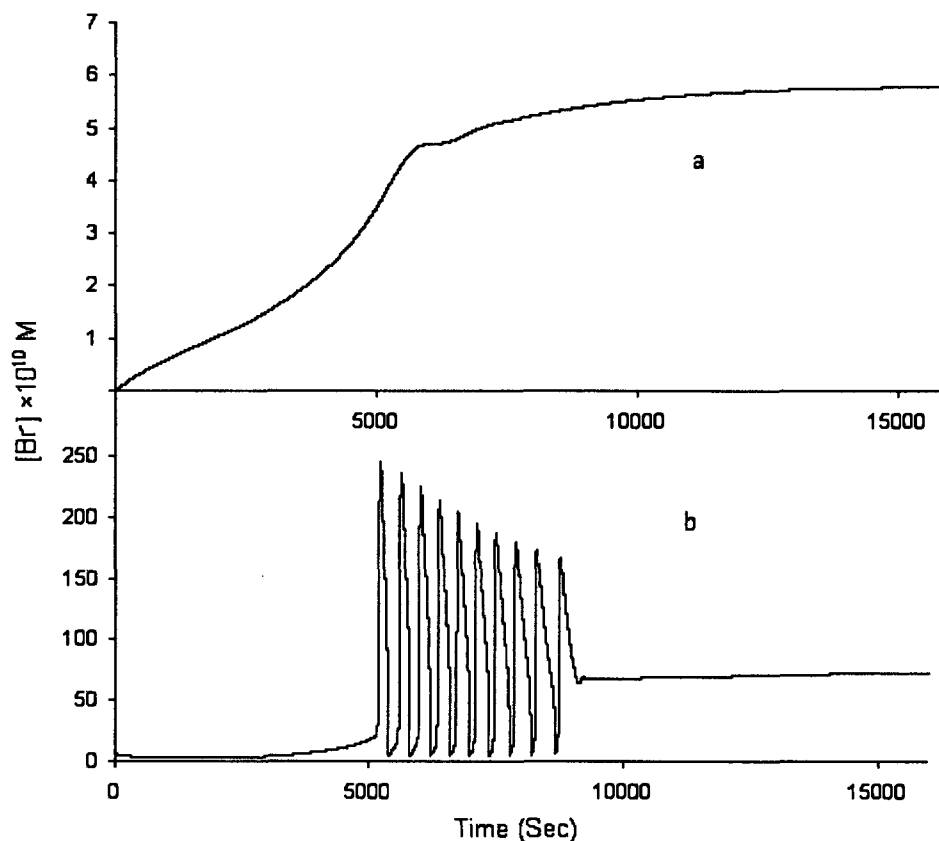
Figure 2.19 Time series calculated from the model listed in Table 2.1. The initial concentration of pyrocatechol is varied as (a) 0.0008 M, and (b) 0.041 M. Other initial conditions are $[BrO_3^-]$ = 0.085 M and $[H_2SO_4]$ = 1.4 M, the same as used in experiments. In the simulation the initial concentration of Br- was set at 1.0×10^{-10} M. Other intermediates were set to 0.

Quenching of the bromate-pyrocatechol oscillations by light is reproduced in Fig. 2.21, in which the system exhibits spontaneous oscillations in the absence of light (k_b = 0). After spontaneous oscillations appear, the system is exposed to light by temporally setting k_b = 0.14 s^{-1}. Such a temporal change in the reaction dynamic results in an immediate

quenching of oscillation. After the illumination is turned off (i.e. resetting k_b to 0.0), a few more oscillations appear, similar to the revival behavior seen in Fig. 2.15.
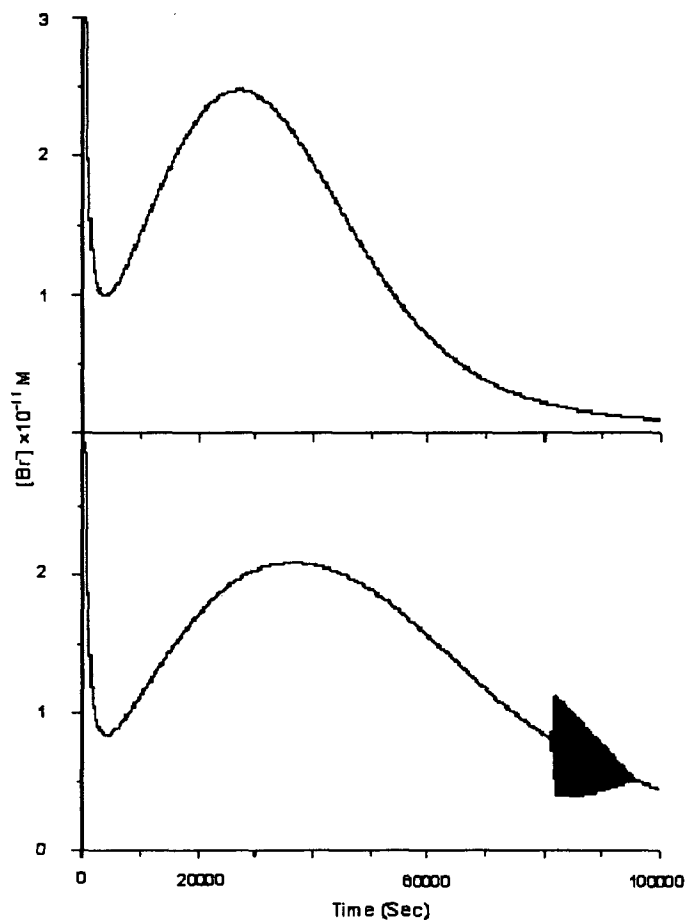
Figure 2.20. Light-induced oscillations in the bromate – pyrocatechol reaction: (a) k_b = 0 s^{-1} and (b) k_b = 10.0 s^{-1}. Other initial conditions are [pyrocatechol] = 0.9 M, [BrO_3^-] = 0.10 M, and [H_2SO_4] = 1.4 M.

The above model can also qualitatively reproduce effects of bromate concentration on the oscillations seen in experiments, but is unable to account for variations of the induction time with respect to bromate concentration. Time series presented in Fig. 2.19

show that bromide concentration increases slowly during the induction time and then starts oscillating after reaching a critical value, which agrees well with experiments. Such a scenario generally implies that the production of bromide is the bottle neck. Yet, the initial presence of brominated species shows no influence on the long induction time.
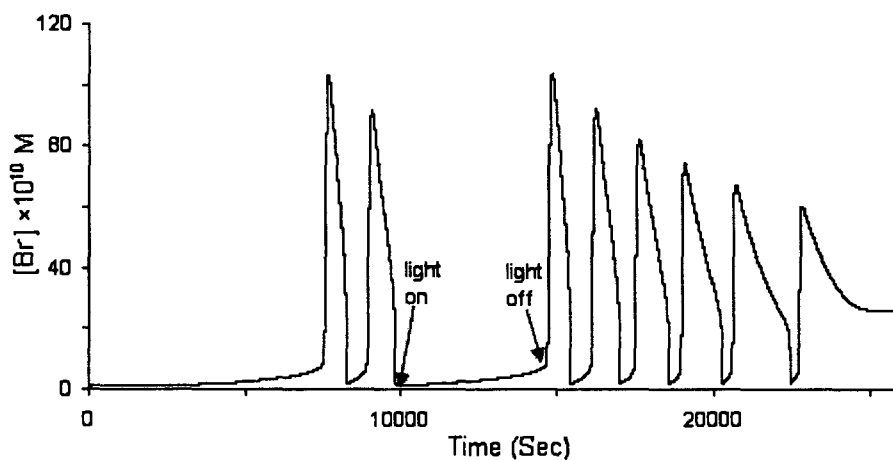
Figure 2.21. Quenching of chemical oscillations by light. Rate constant k_b is temporally increased from 0 to 0.14 s^{-1} during the illumination period. Other initial conditions are [pyrocatechol] = 0.021 M, [BrO$_3^-$] = 0.040 M, and [H$_2$SO$_4$] = 1.4 M.

Conclusion

This chapter discussed and investigated nonlinear kinetics of the uncatalyzed bromate-pyrocatechol reaction in a stirred batch reactor and discovered chemical oscillations in the studied system. The parameter regime within which the system oscillates is a diagonal narrow band in the pyrocatechol and BrO$_3^-$ concentration phase plane, suggesting that the oscillatory behavior is more sensitive to the ratio of [pyrocatechol]/[BrO$_3^-$] rather than

their actual concentrations. The achievement of both light-induced and light-inhibited oscillatory phenomena demonstrates that this chemical oscillator could be potentially employed to explore interactions of intrinsic complex reaction dynamics and external forcing. Our simulations suggest that photo-induced dissociation of bromine may be responsible for the observed photosensitivity.

Understanding the suitable Br⁻ production in the UBOs remains a challenging task. It has been speculated that some intermediate of bromide accumulates until an autocatalytic process begins to destroy it. The system is then quiescent until a suitable amount of this intermediate again accumulates, and another pulse occurs, and so forth. The experiment illustrates that the induction time is independent of the initial presence of brominated pyrocatechol species. The proposed model successfully reproduced spontaneous oscillations and the insensitivity of the induction time to the brominated species. The preliminary spectroscopic characterization suggests the possible formation/dissociation of catechol dimers/trimers. The simulation indicates that the accumulation of pyrocatechol radical (increases up to 10^{-5} M) and catechol complex may be responsible for the long induction as both reagents increase throughout the induction time and then oscillate. Understanding the significance of dimer formation could be critical in the further understanding of this as well as other uncatalyzed bromate–aromatic compounds reactions and shall be investigated in future mechanistic research.

References

1. A. Goldbeter, Biochemical Oscillations and Cellular Rhythms, Cambridge University Press, 1996.

2. V. K. Vanag and I. R. Epstein, J. Chem. Phys., 119, 2003, 7297.

3. F. X. Witkowski, L. J. Leon, P. A. Penkoske, W. R. Giles, M. L. Spanol, W. L. Ditto, and A. T. Winfree, Nature, 392, 1998, 78.

4. I. R. Epstein and J. A. Pojman, An Introduction to Nonlinear Chemical Dynamics, Oxford University Press, New York, 1998.

5. K. R. Kim, K. J. Shin, and D. J. Lee, J. Chem. Phys., 121, 2004, 2664.

6. L. Adamčíková, Z. Farbulová, and P. Ševčík, New J. Chem., 25, 2001, 487.

7. S. K. Scott, Chemical Chaos, Oxford University Press, 1994.

8. V. K. Vanag, D. G. Míguez, and I. R. Epstein, J. Chem. Phys., 125, 2006, 194515.

9. H. Guo, L. Li, Q. Ouyang, J. Liu, and Z. She, J. Chem. Phys., 118, 2003, 5038.

10. A. P. Dhanarajan, G. P. Misra, and R. A. Siegel, J. Phys. Chem. A, 106, 2002, 8835.

11. W. L. C. Alan, S. S. Jahromi, H. Khosravani, L. P. Carlen, and L. B. Bardakjian, J. Neural Eng., 3, 2006, 9.

12. J. Zhao, Y. Chen, and J. Wang, J. Chem. Phys., 122, 2005, 114514.

13. I. Schreiber, P. Hasal, and M. Marek, Chaos, 9, 1999, 43.

14. P. Carlsson, V. P. Zhdanov, and M. Skoglundh, Phys. Chem. Chem. Phys., 8, 2006, 2703.

15. K. M. Beutel and E. Peacock-López, J. Chem. Phys., 125, 2006, 024908.

16. D. S. Huh, Y. J. Kim, H. S. Kim, J. K. Kang, and J. Wang, Phys. Chem. Chem. Phys., 5, 2003, 3188.

17. K. Kurin-Csörgei, I. R. Epstein, and M. Orbán, J. Phys. Chem. B 108, 2004, 7352.

18. R. McIlwaine, K. Kovacs, S. K. Scott, and A. F. Taylor, Chem. Phys. Lett., 417, 2006, 39.

19. A. K. Dutt and M. Menzinger, J. Chem. Phys., 110, 1999, 7591.

20. A. K. Horváth, I. Nagypál, and I. R. Epstein, J. Am. Chem. Soc., 124, 2002, 10956.

21. E. Körös and M. Orbán, Nature, 273, 1978, 371.

22. M. Orbán and E. Körös, J. Phys. Chem., 82, 1978, 1672.

23. M. Orbán and E. Körös, React. Kinet. Catal. Lett., 8, 1978, 273.

24. V. J. Farage and D. Janjic, Chem. Phys. Lett., 88, 1982, 301.

25. I. Szalai and E. Körös, J. Phys. Chem. A, 102, 1998, 6892.

26. B. Zhao and J. Wang, Chem. Phys. Lett., 430, 2006, 41.

27. J. Horváth, Z. Nagy-Ungvarai, and S. C. Müller, Phys. Chem. Chem. Phys., 3, 2001, 218.

28. Z. Nagy-Ungvarai and I. Zimányi, React. Kinet. Catal. Lett., 31, 1986, 249.

29. K. Pelle, M. Wittman, Z. Noszticzius, R. Lombardo, C. Sbriziolo, and M. L. T. Liveri, J. Phys. Chem. A, 107, 2003, 2039.

30. P. Herbine and R. J. Field, J. Phys. Chem., 84, 1980, 1330.

31. M. Orbán, E. Körös, and R. M. Noyes, J. Phys. Chem., 83, 1979, 3056.

32. R. J. Field and M. Bueher (Eds.), Oscillations and Traveling Waves in Chemical Systems, Wiley-Interscience, New York, 1985.

33. L. Gyorgyi, T. Turanyi, and R. J. Field, J. Phys. Chem., 94, 1990, 7162.

34. K. Kereszturi, and I. Szalai, Chem. Phys. Lett., 428, 2006, 288.

35. P. G. Sørensen, F. Hynne, and K. Nielsen, React. Kinet. Catal. Lett., 42, 1990, 309.

36. P. I. Kumli, M. Burger, M. J. B. Hauser, S. C. Müller, and Z. Nagy-Ungvarai, Phys. Chem. Chem. Phys., 5, 2003, 5454.

Chapter 3 Chemical Oscillations and Waves in the Catalyzed Bromate-Pyrocatechol Reaction

Introduction

The study of chemical oscillations and wave formation has blossomed in the past three decades, and has led to the observation of various nonlinear spatiotemporal behaviours such as both simple and complex oscillations in stirred systems [1-4], Turing patterns [5-7], target and spiral waves in a two-dimensional reaction-diffusion media [8-13], and scroll waves in a 3-dimensional system [14]. Understanding the onset of those exotic phenomena in chemical systems has provided important insight into the formation of similar patterns in nature [15-21]. One of the most frequently studied and, arguably, the best characterized chemical oscillators is the Belousov-Zhabotinsky (BZ) reaction, which is the oxidation and bromination of malonic acid in acidic solution catalyzed by metal ions or complexes [2-4, 22-24]. To facilitate the observation of propagating waves, ferroin or a ruthenium complex is usually employed as the metal catalyst [24-31]. In particular, the photosensitivity of ruthenium complex provides a convenient approach for studying perturbed nonlinear dynamics [29-31], which has led to the observation of a number of interesting behaviours which do not exist in perturbation free environments such as avalanche phenomena [32], stochastic resonances [33], oscillatory standing waves [34, 35], etc.

The development of nonlinear spatiotemporal structures depends both on the local temporal kinetics and diffusive transport [2-4]. As most chemical reagents have similar

diffusion coefficients in solution, finding new chemical systems which exhibit novel nonlinear dynamics becomes increasingly desired in the study of nonlinear chemical dynamics [36-38]. The discovery of the bromate-1,4-cyclohexanedione oscillator in 1982 [39], for example, has allowed the recent observation of anomalous dispersion relationship of chemical waves and sequential pattern formation [40, 41]. This research aims to develop a new chemical reaction system which is capable of showing a long time series of periodic color changes (i.e., temporal oscillations) in a stirred medium and thus can be a promising model system for the investigation of chemical waves.

De Kepper, Kustin, and Epstein have developed a systematic approach of designing chemical oscillators in a continuous flow stirred tank reactor (CSTR). Their method includes four steps: finding an autocatalytic system, running the reaction in a CSTR, finding a bistability region and then perturbing the system by adding another species to induce oscillations [42]. To facilitate its transformation to the study of chemical waves, this research focuses on nonlinear reaction dynamics in a closed system. Following the observation of oscillatory behaviour in the uncatalyzed pyrocatechol-bromate system, nonlinear kinetics of the Mn^{2+}-, Ce^{3+}-, and ferroin-catalyzed bromate-pyrocatechol reactions were explored in a stirred batch reactor. The influence of light on all three catalyzed systems was also carried out. Rate constants related to the pyrocatechol-ferriin and pyrocatechol-Ce^{4+} reactions were determined to gain a better understanding of the chemistry of the system. Preliminary investigations of the spatially extended system show the feasibility of studying wave formation in the ferroin-catalyzed bromate-pyrocatechol medium.

Experimental Procedure

All reactions were carried out in a thermal-jacketed 50 ml glass beaker (ChemGlass), in which temperature was kept constant at 25.0 ± 0.1 °C by a circulating water bath (Thermo NesLab RTE 7). A Teflon cap was placed on top of the reactor to hold the electrodes. The solution level was about 1 cm below the Teflon cap. The reaction solution was stirred by a magnetic stirrer (Fisher Isotemp). Reactions were monitored with a platinum electrode coupled with a $Hg|Hg_2SO_4|K_2SO_4$ reference electrode (Radiometer Analytical, XR200 and M231Pt-9). All measurements were recorded through a pH/potential meter (Radiometer PHM220) connected to a personal computer through a PowerLab/4SP data logger. The perturbation of light was implemented with a halogen lamp equipped with dual bifurcated optic fibers and continuous variable light level (Fisher Scientific, Model DLS-100HD, 150 W). The illumination was implemented by placing the two fibers either on the opposite or the same sides of the reactor and no difference in the reaction behaviour was observed, implying that mixing was fast enough to generate a situation of homogeneous illumination.

Stock solutions of $NaBrO_3$ (Aldrich, 99%), 0.6 M, sulfuric acid (Aldrich, 95-98%), 4.0 M, $Ce_2(SO_4)_3$ (Aldrich, 97%), 0.025 M, and $MnSO_4 \cdot H_2O$ (Aldrich, 98+%), 0.025 M, were prepared with double-distilled water. Ferroin, 0.025 M, was prepared from a calculated amount of $FeSO_4 \cdot 7H_2O$ (Aldrich, 99+%) and 1,10-phenanthroline (Aldrich, 99+%). Pyrocatechol (Sigma, 99%) was directly dissolved in the reaction mixture. The volume of the reaction mixture was fixed at 30.0 ml in all experiments. Absorption spectra were measured with a UV-visible spectrophotometer (Ocean Optics, 2000 USB), in which a quartz cuvette (10 mm light path, HELLMA) containing 2.5 ml sample mixture was placed in a CUV sample holder which has two water jackets connected to a circulating

water bath (Thermo NesLab RTE 7). The cuvette was stirred with a small magnetic bar. All kinetic runs were carried out at least three times. Infinity values of absorbance (A_∞) were experimentally determined in all cases by running the reaction for up to 3 hours in each trial. Regression coefficients of all the reaction rate calculations were higher than 0.980.

Chemical waves were investigated by injecting the reaction solution into a narrow space between two microscope slides, forming a 0.5 mm (or 0.3 mm) thick solution layer without a free surface. The evolution of chemical waves was monitored with a CCD camera equipped with a zoom lens. The CCD camera was connected to a personal computer running a frame grabber program (Matrox Imaging Library).

Results and Discussions

Figure 3.1 presents time series of the (a) uncatalyzed, (b) ferroin-, (c) cerium-, and (d) manganese-catalyzed bromate-pyrocatechol reactions. In all four cases, there is a large excursion in the Pt potential occurring shortly after mixing all reagents together. Through out this research, bromate is the last reagent added to the reactor. In the uncatalyzed system, the Pt potential decreases gradually after the initial excursion and then reaches a plateau. In general, one may consider that this closed reaction is over. However, the Pt potential suddenly starts oscillating after another two hours, and the oscillatory process lasts for longer than an hour with about 14 peaks. This result illustrates that the uncatalyzed bromate-pyrocatechol is capable of exhibiting spontaneous oscillations under the conditions investigated here. Similar to existing uncatalyzed bromate oscillators [39], oscillations do not commence right after the reaction begins, i.e. there is a long induction time.
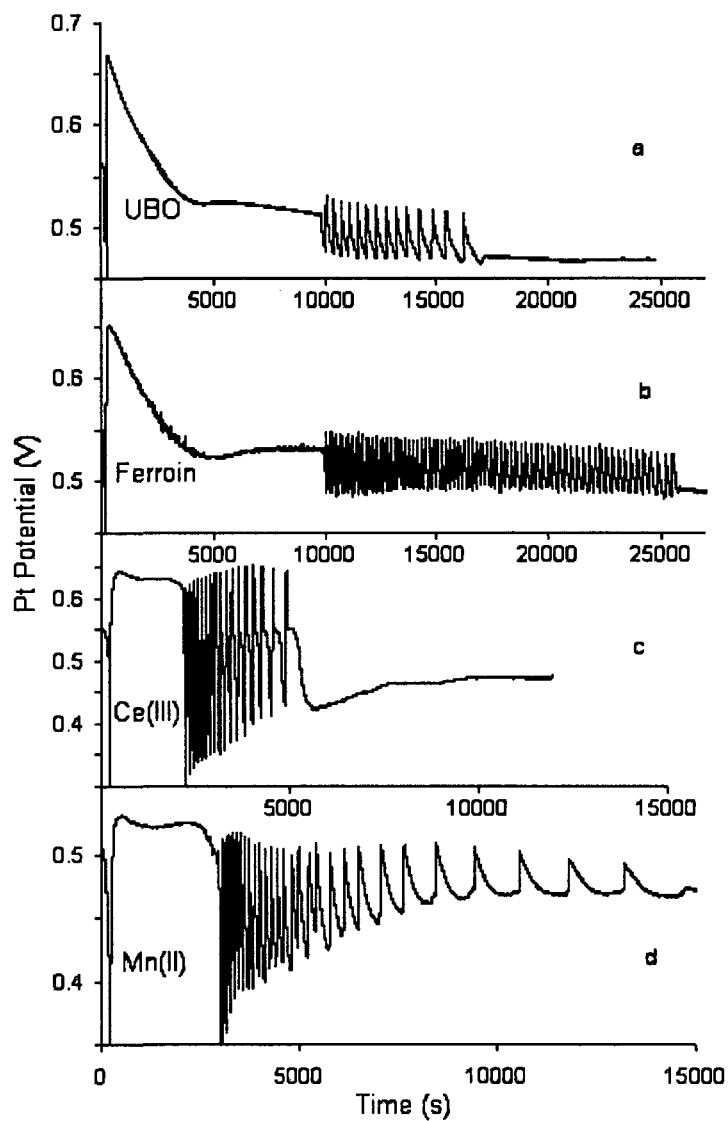
Figure 3.1 Time series of the (a) uncatalyzed, (b) ferroin-, (c) cerium- and (d) manganese-catalyzed bromate-pyrocatechol reaction. Other reaction conditions are: $[H_2SO_4]$ = 1.30 M, [pyrocatechol] = 0.043 M, and $[BrO_3^-]$ = 0.078 M. The concentration of metal catalysts is 1.0×10^{-4} M in all three cases.

Phenomenologically, the color of the reaction solution becomes dark red from transparent during the initial Pt excursion and then slowly turns into yellow during the long induction period. There is no periodic color change during the oscillations and thus this uncatalyzed system is unsuitable for studying chemical waves, despite its capacity of exhibiting oscillatory dynamics. When 1.0×10^{-4} M ferroin is added to the bromate-pyrocatechol reaction, spontaneous oscillations commence at about the same time as in the uncatalyzed system. The most significant changes occur at the frequency of oscillation and the total number of oscillations, which have been increased greatly. Notably, in this catalyzed system the oscillation lasts for longer than 4 hours. Our experiments illustrate that this system exhibits observable periodic color changes from yellowish green to faint pink during the oscillatory period when the concentration of ferroin is above 1.0×10^{-4} M. Further increase of the concentration of ferroin results in a better contrast, but reduces the lifetime of the oscillatory period. Furthermore, when ferroin concentration is higher than 1.0×10^{-3} M no obvious color change could be seen in the stirred system. When oscillations in the ferroin-bromate-pyrocatechol system stop, the solution has a blue color if the concentration of ferroin added is above 1.0×10^{-3} M, or a pink color when the ferroin concentration is less than 5×10^{-4} M. In this bromate-pyrocatechol system, there is an enormous change in the oscillation frequency and number of peaks when the concentration of ferroin added is above 1.0×10^{-5} M; however, there is no noticeable change in the induction time.

For the cerium-catalyzed bromate-pyrocatechol reaction, the Pt potential stays flat after the initial excursion. Spontaneous oscillations occur at about 2000 s after mixing all reactants together. Note that the time scale used for (c) and (d) is different from that used for (a) and (b). The induction time is significantly shortened in comparison to the

uncatalyzed and the ferroin-catalyzed bromate-pyrocatechol reaction. The amplitude of oscillation also become significantly larger than that of the uncatalyzed as well as ferroin-catalyzed system; yet, there is no significant increase in the total number of oscillation peaks when comparing with the uncatalyzed system. Unlike the ferroin-catalyzed system, here no periodic color change is achieved and thus is unfit for studying waves. A short induction time and large oscillation amplitude (> 300 mV), however, make the cerium-catalyzed system suitable for exploring nonlinear dynamics in a CSTR, in particular the oscillations have a broad shoulder which may potential leads to the development of complex oscillations.

The times series of the Mn^{2+}-catalyzed bromate-pyrocatechol reaction is very similar to that of the cerium-catalyzed one, in which the Pt potential stays flat after the initial excursion and the oscillation commences much earlier than in the uncatalyzed system. The number of oscillations in the manganese system is also larger than that of the uncatalyzed system. Overall, Fig. 3.1 demonstrates that chemical oscillations can be achieved in the bromate-pyrocatechol reaction, in which the three metal catalysts, all of which have different redox potentials, have different impacts on the reaction dynamics. Redox potentials of cerium and manganese are above the redox potential of $BrO_2^{\cdot}/HBrO_2$. Adding manganese exhibits almost the same influence on the reaction behavior as cerium.

Figure 3.2 summarizes the dependence of the number of oscillations (N) and the induction time (IP) on the concentrations of ferroin, Mn^{2+} and Ce^{3+}. Other reaction conditions were kept constant at $[H_2SO_4] = 1.30$ M, [pyrocatechol] $= 0.043$ M, and $[BrO_3^{-}] = 0.078$ M. The sharp increase in the number of oscillations at the low concentration of metal catalysts illustrates that the presence of small amounts of metal catalyst favours the oscillatory behaviour. As the amount of catalyst increases, however, the number of

oscillations decreases, which may due to the increased consumption of the reactants. In

general, Mn^{2+} and Ce^{3+} concentrations do not affect the number of peaks as significantly

as ferroin, although they double the number of peaks under optimized conditions. On the

other hand, ferroin shows little effect on the induction time.
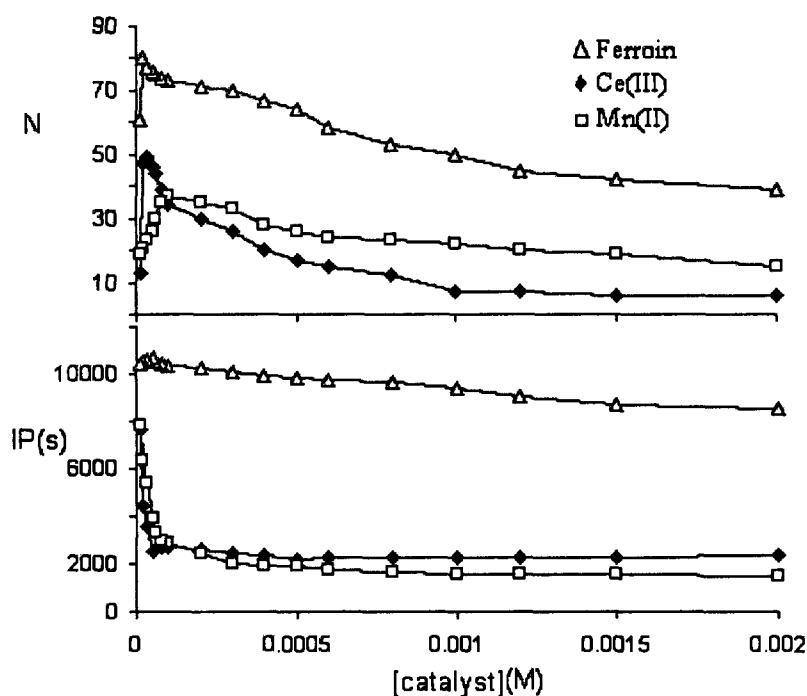
Figure 3.2 Dependence of the number of oscillations (N) and induction period (IP) on the concentration of metal catalysts. Other reaction conditions are: [H₂SO₄] = 1.30 M, [BrO₃⁻] = 0.078 M, and [pyrocatechol] = 0.043 M.

As shown in the Figure 3.2, increasing ferroin concentration to 0.002 M only reduces

the IP by about 10 percent. In contrast, the presence of a small amount of cerium or

manganese dramatically reduces the induction time, where the induction time is shortened

from about 3 hours (in the uncatalyzed system) to approximately half an hour when the

concentration of manganese and cerium are, 2.0×10^{-4} and 5.0×10^{-5} M, respectively. The IP becomes relatively stable when the concentration of manganese or cerium is increased further.

We also examined the response of the three catalyzed systems to the addition of the same catalyst at different reaction stages. It has been reported in the BZ reaction that adding small amounts of ferroin in the middle of the oscillation window has different impact than when it is added at the end of the reaction process. Here, experiments were carried out with the conditions described in Fig. 3.1, and the observed influences are summarized in Table 3.1.

Table 3.1 Effect of adding catalysts at different reaction stages.

Name of the catalyst	Adding catalyst to the studied system	
	During the oscillation process	After oscillations terminated
Fe (phen)$_3{}^{2+}$	Oscillations continue with a higher amplitude	Oscillations are revived when the added amount is higher than 6.0×10^{-4} M
Ce^{3+}	Quenched oscillations	No change
Mn^{2+}	Quenched oscillations	No change

For the cerium and manganese-catalyzed systems, the addition of 2.5×10^{-4} M of the same type of metal catalyst quenches the spontaneous oscillations immediately; but, for the ferroin-catalyzed system, oscillations continue after the addition of 2.5×10^{-4} M ferroin. The amplitude of oscillation in the ferroin system is increased upon the addition of the extra amount of ferroin, yet there is no obvious change in the number of peaks. The

overall response agrees well with the results presented in Fig. 3.2, which show that the number of oscillations decreases as the concentrations of metal catalysts increase. The quenching effect of Ce^{3+} and Mn^{2+} may arise from its reaction with bromate producing bromine, a well-known inhibitor of the autocatalysis in the bromate-based oscillators [43]. Interestingly, when catalysts were added after oscillations have terminated, the addition of 6.0×10^{-4} M ferroin was able to revive the oscillatory behaviour, while adding the same amounts of cerium or magnesium ions at the end of oscillation window does not show any observable influence on the reaction behavior.

As the ferroin-catalyzed bromate-pyrocatechol system is the only one which exhibits observable periodic color changes and thus is suitable for studying chemical waves, the following kinetic investigations are focused on the ferroin system. Figure 3.3 plots the influence of concentrations of bromate and sulfuric acid on the number of peaks (N) and induction period (IP) in the ferroin-catalyzed system, where the concentration of ferroin was fixed at 1.0×10^{-4} M in all the experiments. Figures 3.3a and 3.3b show that increasing bromate concentration prolongs the induction period, which may arise from the production of larger amounts of bromine in the reaction solution. The number of peaks ascends first with bromate concentration and then declines slightly at higher concentrations (>0.081 M). Under the conditions studied here, the concentration of bromate must be between 0.070 and 0.085 M for the system to show oscillations. As shown in Figs. 3.2c and 3.2d, both N and IP increase monotonically with the increase of the acid concentration. The system does not oscillate when the concentration of sulfuric acid is higher than 1.4 M or lower than 1.0 M under these conditions.
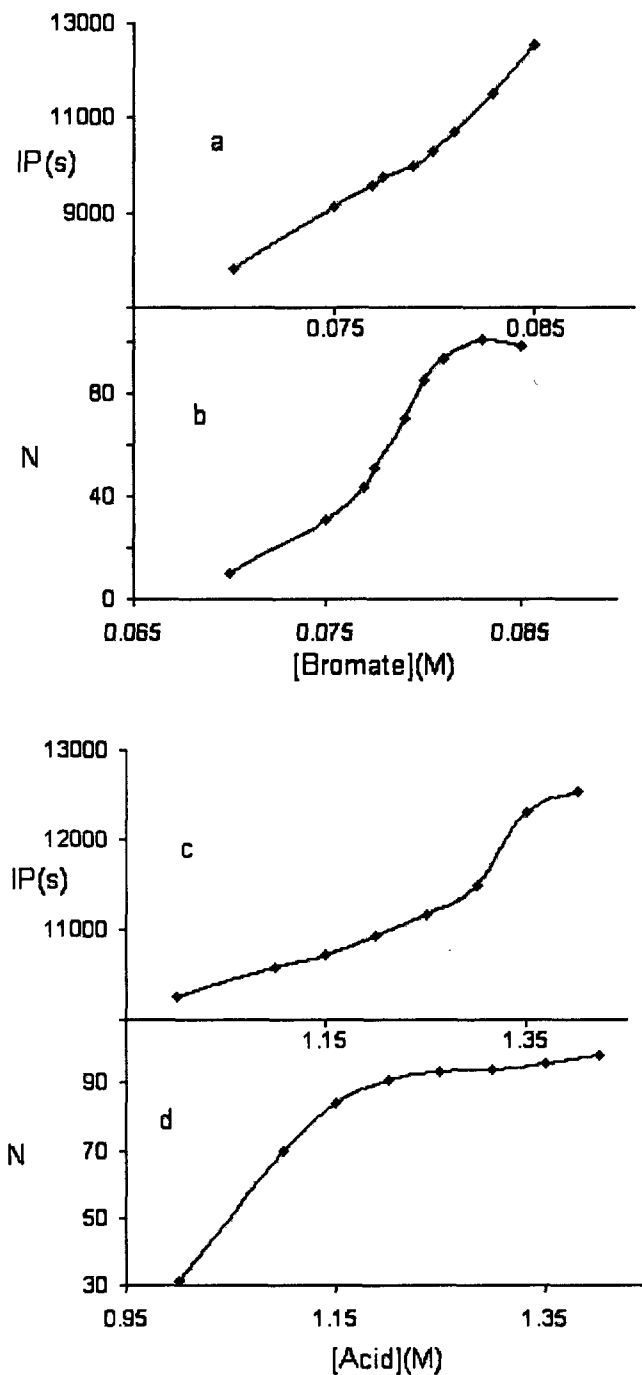
Figure 3.3 Dependence of the number of oscillations (N) and induction time (IP) of the ferroin-catalyzed system on the concentration of bromate and sulfuric acid. Other reaction conditions are: [pyrocatechol] = 0.044 M, [ferroin] = 1.0 x 10^{-4} M, and (a) [H$_2$SO$_4$] = 1.40 M; (c) [BrO$_3^-$] = 0.085 M.

Figure 3.4 is a phase diagram of the ferroin-catalyzed system in the pyrocatechol and

bromate concentration plane, where ($\blacklozenge$) indicates the conditions under which the system

exhibits spontaneous oscillations. A first glance at this Figure indicates that the system is

able to exhibit oscillatory dynamics over a broad range of bromate and pyrocatechol

concentrations. However, at each given concentration of pyrocatechol (or bromate), the

proper concentration of bromate (or pyrocatechol) is quite narrow. This diagonally

structured phase diagram suggests that nonlinear behavior of the system is more sensitive

to the ratio of [pyrocatechol]/[bromate] than their absolute concentrations. In comparison

to the uncatalyzed bromate-pyrocatechol system, the presence of ferroin does not change

the structure of this phase diagram, but makes the area of the oscillation window slightly

bigger since ferroin favors the oscillations.
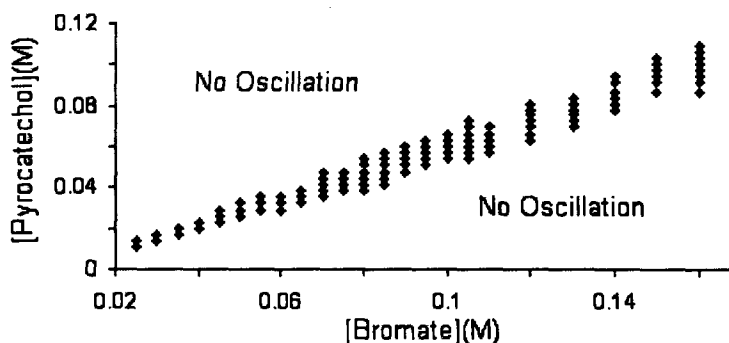
Figure 3.4 Phase diagram of the ferroin-catalyzed reaction in the bromate–pyrocatechol concentration plane. ($\blacklozenge$) denotes where the system exhibits simple periodic oscillations. The concentration of ferroin is 1.0×10^{-4} M.

In Fig. 3.5, the photosensitivity of the ferroin-catalyzed bromate-pyrocatechol reaction is examined, in which the concentration of ferroin was adjusted. As shown in Fig. 3.5a, when the system is exposed to light from the beginning of the reaction, spontaneous oscillations develop earlier, where the induction time is shortened to about 6000 s. However, the oscillatory process lasts for a shorter period of time. The system then goes to non-oscillatory evolution, where turning off the illumination causes the Pt potential to jump to a higher value immediately and, more significantly, another batch of oscillations develops after a long induction time. The above results indicate that the influence of light in the ferroin-catalyzed system is quite subtle, on one hand it seems to favor the oscillation by shortening the induction time, but it later quenches the oscillations.

The system in Fig. 3.5b was illuminated with the same light from the beginning, no oscillation is achieved with this low ferroin concentration; however, there is a sharp drop in the Pt potential at about the same time as that in Fig. 3.5a. Again, after turning off the light, the non-illuminated system exhibits oscillatory behaviour with a long induction time. In Fig. 3.5c, light was applied in the middle of the oscillatory period, in which the illumination of 100 mW/cm^2 light immediately quenches the oscillatory behaviour. Oscillations revive shortly after reducing the light intensity to 30 mW/cm^2. Interestingly, in the above three experiments the influence of light does not go away upon its removal. Carrying out similar experiments with the cerium- and manganese-catalyzed systems under similar reaction conditions shows less photosensitivity, in which no quenching behaviour was obtained although the light does decrease the amplitude of oscillation.
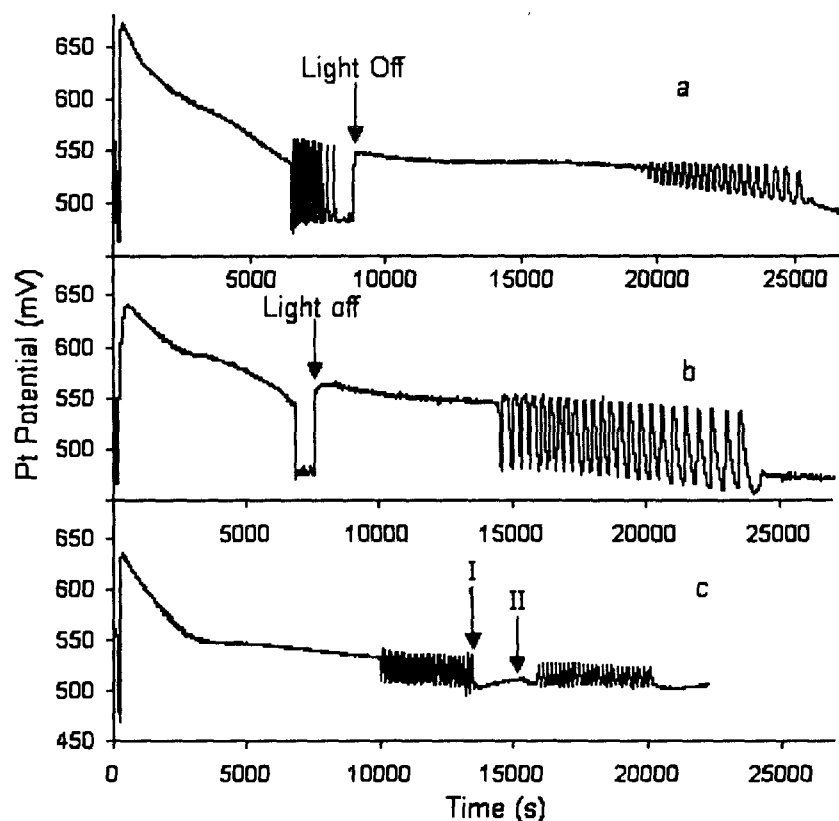
Figure 3.5 Light effects on the ferroin-bromate-pyrocatechol reaction: In (a) and (b), 70 mW/cm^2 light was turned on from the beginning and the reaction conditions are [BrO$_3^-$] = 0.10 M, [H$_2$SO$_4$] = 1.40 M, [pyrocatechol] =0.057 M, and [ferroin] = (a) 5.0 × 10^{-4} M, and (b) 1.0 x 10^{-3} M. In (c), 70 mW/cm^2 light was switched on as indicated by the arrow I and was reduced to 30 W/cm^2 at arrow II. All other reaction conditions are the same as those used in (a) except here [ferroin] = 1.0 x 10^{-4} M.

Preliminary exploration of wave formation in the ferroin system has been performed. To get a better contrast and be visible with bare eyes, the concentration of ferroin used in the reaction-diffusion medium is increased to above 1.0 x 10^{-3} M. As discussed earlier, the homogeneous system has a large excursion in the Pt potential shortly after mixing all reagents together. Such an initial reactivity leads to the formation of propagating fronts and target patterns in a thin layer (see snapshots in Fig. 3.6). Those spatiotemporal

behaviours last between 20 and 150 seconds, depending on the reaction conditions, especially the concentration of ferroin. Increasing ferroin concentration shortens the life time of these initial waves. In this study, the initial chemical wave activities appear normally within the first 5 minutes after starting the reaction. Later, a kind of "wildfire" activity washed out the entire wave activity, resulting in a homogeneous medium with a red color.
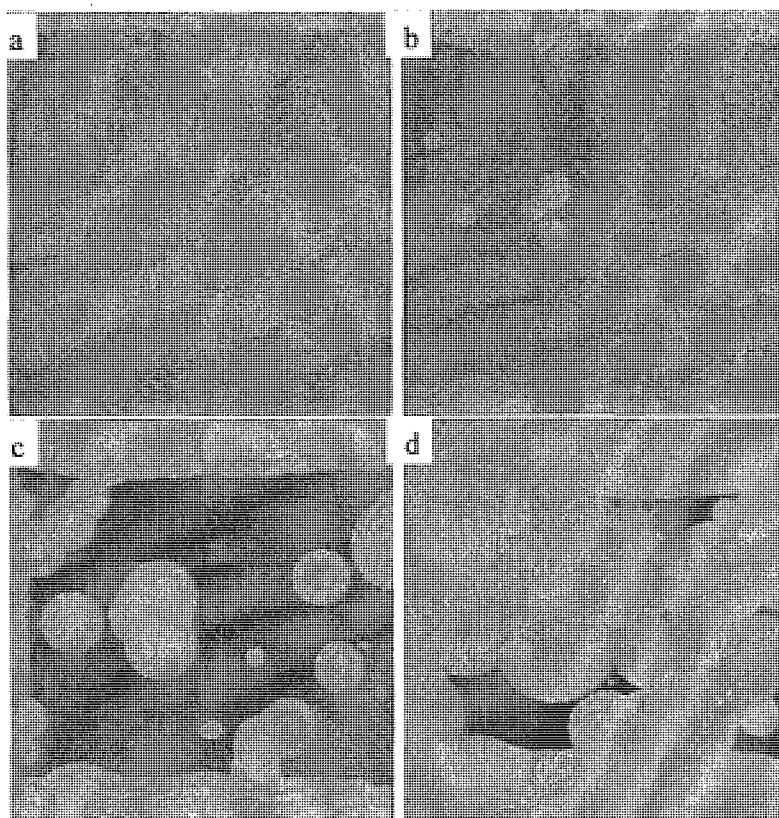
Figure 3.6 Snapshots of waves achieved during the first stage of the ferroin-pyrocatechol-bromate reaction: (a) 58, (b) 71, (c) 83, and (d) 100 s after mixing all reagents together. The initial concentrations are [pyrocatechol] = 0.091 M, [BrO_3^-] = 0.14 M, [H_2SO_4] = 1.40 M, and [ferroin] = 3.0 × 10^{-3} M.

As expected, chemical waves can also be obtained when the system evolves into the oscillation window, which commences typically at three hours after the reaction has

begun. Under the conditions explored, the chemical wave activity could last for up to 10

hours.
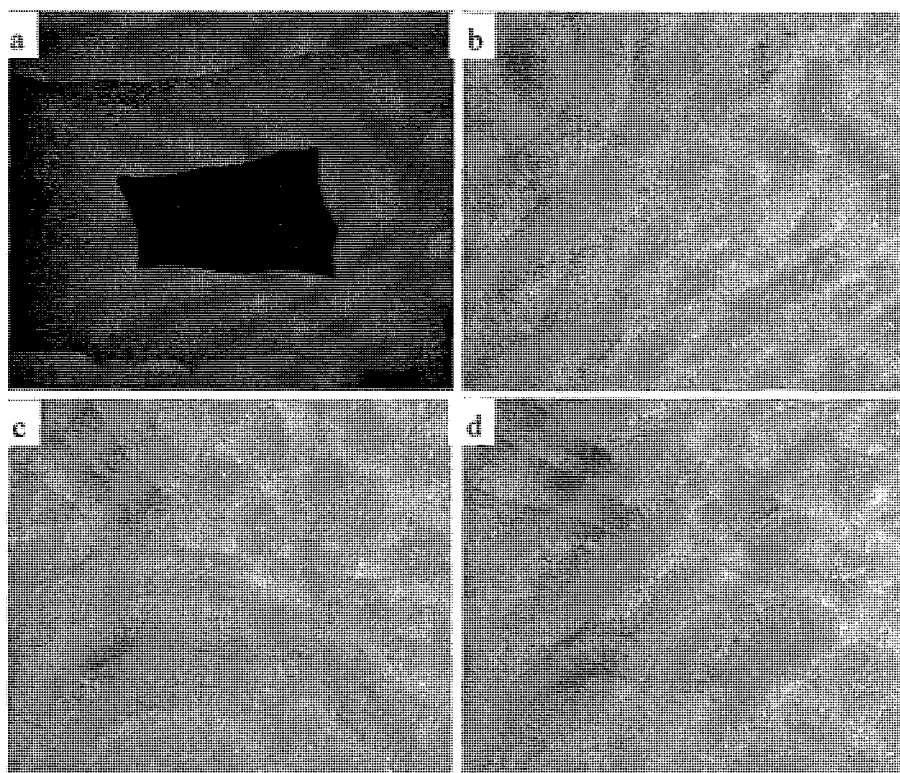
Figure 3.7 Snapshots of wave in the second stage of wave activity in ferroin-pyrocatechol-bromate system: (a) 17, (b) 133, (c) 238 and (d) 345 minute after setting up the reaction-diffusion medium. The initial concentrations are [pyrocatechol] = 0.091 M, [BrO$_3$$^-$] = 0.13 M, [H$_2SO_4$] = 1.40 M, and [ferroin] = 3.0 ×10^{-3} M.

Fig. 3.7 presents several snapshots of the waves collected at (a) 17, (b) 133, (c) 238

and (d) 345 minutes after setting up the reaction-diffusion medium. In a stirred system,

spontaneous oscillations occur at about three hours after mixing all reactants together.

The above reaction-diffusion solution was prepared by allowing the reaction to evolve first in a stirred system for 2.5 hours, which is about half an hour before spontaneous oscillations commence. Yet, as shown in the Figure 3.7, waves emerge from edges even before the reaction system evolves into the oscillation window. Such a result demonstrates that chemical waves can also be achieved in the non-oscillatory (i.e., excitable) ferroin-bromate-pyrocatechol medium.

Conclusions

This research presents a new chemical system capable of showing a long time series of temporal oscillations in a closed system and wave formation in a spatially extended medium. Experiments illustrate that the nonlinear dynamics of the bromate-pyrocatechol system strongly depends on the metal catalysts used. Among the three metal catalysts investigated here, ferroin does not show great influence on the induction time, but significantly increases the number of oscillations. In contrast to the effect of ferroin, the presence of small amounts of Ce(III) and Mn(II) greatly decrease the induction time, e.g. from 3 to half an hour; on the other hand, Ce(III) and Mn(II) can maximally increase the number of oscillations by a factor of 2.

A phase diagram in the pyrocatechol and bromate concentration plane shows that the ferroin-catalyzed system is more sensitive to the ratio of [pyrocatechol]/[BrO_3^-] than their absolute concentrations. The presence of ferroin favors the oscillatory behavior and thus broadens the parameter window within which the system exhibits spontaneous oscillations. In the ferroin-catalyzed system light acts as a quencher, especially at high concentration of ferroin, but significantly shortens the induction time. Preliminary studies on reaction-diffusion media indicate that the ferroin-catalyzed system has the potential of

showing two-stage pattern formation, in which the first stage arises from the single excursion lasting for a couple of minutes, and the second stage emerges from the oscillation window, which can last for as long as 10 hours.

This new system appears to be an appropriate model for exploring nonlinear chemical dynamics. However, a major drawback is that its mechanism remains largely unknown. Quenching experiments with bromide ions suggest that oscillators studied here are bromide-controlled. Based on the similarity between pyrocatechol and organic substrates used in other uncatalyzed bromate-oscillators [39], we speculate that nonlinear feedbacks in the system studied here are through the reaction between bromine dioxide radicals and pyrocatechol forming $HBrO_2$. This may account for why cerium and manganese exhibit similar effects on the reaction behavior but are different from that of ferroin, since the redox potentials of cerium and manganese are both larger, while the redox potential of ferroin is smaller, than that of $BrO_2^{\cdot}/HBrO_2$. To understand how the oxidized metal catalysts are reduced in the studied system, we carried out kinetic measurements on the reactions between pyrocatechol and ferriin and between pyrocatechol and Ce(IV) under different combinations ranging from the concentrations of pyrocatechol (0.01-0.08 M), Ce(IV) and ferriin ($1.0 \times 10^{-4} - 2.0 \times 10^{-3}$ M), and sulfuric acid (0.5 - 2.0 M). The reaction between pyrocatechol and ferriin was followed spectrophotometrically with the absorbance at 600 nm, where ferriin has the largest absorption [21]. Following an approach used in the hydroquinone-metal catalyst reaction [44], the analysis suggests that the oxidation of pyrocatechol by ferriin is first order with respect to both ferriin and pyrocatechol, and is inversely proportional to the concentration of acid. The suggested rate equation is :

$$\text{rate} = k[\text{Fe(phen)}_3^{3+}][\text{pyrocatechol}]/[\text{H}^+] \quad \text{with} \quad k = 16.3 \text{ s}^{-1}$$

The oxidation of pyrocatechol by Ce(IV) was followed spectrophotometrically at 350 nm.[45] Results suggest a rate law: rate $= k[\text{Ce}^{4+}][\text{pyrocatechol}][\text{H}^+]$ with $k = 2.46 \times 10^2$ $\text{M}^{-2}\text{s}^{-1}$.

In summary, the subtle photosensitivity, together with no bubble formation, makes the ferroin-catalyzed bromate-pyrocatechol reaction a new attractive model for exploring novel spatiotemporal dynamics.

References

1. J. L. Hudson, M. Hart and D. Marinko, J. Chem. Phys., 71, 1979, 1601.

2. R. J. Field and Burger (Eds.), M. Oscillations and Traveling Waves in Chemical Systems, Wiley-Interscience, New York, 1985.

3. A. T. Winfree, The Geometry of Biological Time, Springer, Heidelberg, 2000.

4. S. K. Scott, Chemical Chaos, Oxford University Press, 1994.

5. I. Szalai and P. De Kepper, J. Phys. Chem. A, 108, 2004, 5315.

6. V. Castets, E. Dulos, J. Boissonade and P. De Kepper, Phys. Rev. Lett., 64, 1990, 2953.

7. I. Berenstein, L. Yang, M. Dolnik, A. M. Zhabotinsky and I. R. Epstein, J. Phys. Chem. A, 109, 2005, 5382.

8. R. Kapral and K. Showalter (Eds.), Chemical Waves and Patterns, Kluwer Academic Publishers, Netherlands, 1995.

9. A. Bugrim, E. M. Dolnik, A. M. Zhabotinsky and I. R. Epstein, J. Phys. Chem., 100, 1996, 19017.

10. H. Sevcikova, I. Schreiber and M. Marek, J. Phys. Chem., 100, 1996, 19153.

11. O. Rudzick and A. S. Mikhailov, Phys. Rev. Lett., 96, 2006, 018302.

12. V. K. Vanag and I. R. Epstein, Proc. Natl. Acad. Sci., 100, 2003, 14635.

13. H. Guo, L. Li, Q. Quyang, J. Liu and Z. She, J. Chem. Phys., 118, 2003, 5038.

14. C. Luengviriya, U. Storb, M. J. B. Hauser and S. C. Müller, Phys. Chem. Chem. Phys., 8, 2006, 1425.

15. E. Fung, W. W. Wong, J. K. Suen, T. Bulter, S. Lee and J. C. Liao, Nature, 435, 2005, 118.

16. N. J. Abram, M. K. Gagan, Z. Liu, W. S. Hantoro, M. T. McCulloch and B. W. Suwargadi, Naure, 445, 2007, 299.

17. K. Horikawa, K. Ishimatsu, E. Yoshimoto, S. Kondo and H. Takeda, Nature, 441, 2006, 719.

18. W. W. Wong, T. Y. Tsai and J. C. Liao, Mol. Syst. Biol., 3, 2007, 1.

19. B. Blasius, A. Huppert and L. Stone, Nature, 399, 1999, 354.

20. S. Danø, P. G. Sørensen and F. Hynne, Nature, 402, 1999, 320.

21. T. Hideshima and Y. Kato, Biophys. Chem., 124, 2006, 100.

22. E. Körös and M. Orbán, Nature, 273, 1978, 371.

23. V. K. Vanag and I. Hanazaki, J. Phys. Chem. A, 101, 1997, 2147.

24. A. N. Zaikin and A. M. Zhabotinsky, Nature, 225, 1970, 535.

25. K. Kurin-Csörgei, A. M. Zhabotinsky, M. Orbán and I. R. Epstein, J. Phys. Chem., 100, 1996, 5393.

26. C. T. Hamik, N. Manz and O. Steinbock, J. Phys. Chem. A, 105, 2001, 6144.

27. D. S. Huh, Y. J. Kim, H. S. Kim, J. K. Kang and J. Wang, Phys. Chem. Chem. Phys., 5, 2003, 3188.

28. I. Szalai and P. De Kepper, Phys. Chem. Chem. Phys., 8, 2006, 1105.

29. I. Szalai, K. Kurin-Csörgei, V. Horváth and M. J. Orbán, J. Phys. Chem. A, 110, 2006, 6067.

30. L. Kuhnert, K. I. Agladze and V. I. Krinsky, Nature, 337, 1989, 244.

31. Y. Gao and H. D. Försterling, J. Phys. Chem., 99, 1995, 8638.

32. J. Wang, S. Kádár, P. Jung, K. Showalter, Phys. Rev. Lett., 82, 1999, 855.

33. E. Volkov, I. E. Ullner, A. Zaikin and J. Kurths, J. Phys. Rev. E, 68, 2003, 026214.

34. L. Yang and I. R. Epstein, J. Phys. Chem. A, 106, 2002, 11676.

35. V. Petrov, Q. Ouyang and H. L. Swinney, Nature, 388, 1997, 655.

36. M. Orbán, K. Kurin-Csörgei, A. M. Zhabotinsky and I. R. Epstein, Faraday Discuss., 120, 2002, 11.

37. K. Kurin-Csörgei, I. R. Epstein and M. Orbán, Nature, 433, 2005, 139.

38. M. Harati, S. Amiralaei, J. Green and J. Wang, Chem. Phys. Lett., 439, 2007, 337.

39. V. J. Farage and D. Janjic, Chem. Phys. Lett., 93, 1982, 621.

40. N. Manz, S. C. Müller and O. Steinbock, J. Phys. Chem. A, 104, 2000, 5895.

41. D. S. Huh, S. J. Choe and M. S. Kim, React. Kinet. Cataly. Lett., 74, 2001, 11.

42. P. De Kepper, I. R Epstein and K. J. Kustin, J. Am. Chem. Soc., 103, 1981, 2133.

43. E. Körös, M. Orbán and I. Habon, J. Phys. Chem., 84, 1980, 559.

44. I. Szalai, K. Kurin-Csörgei and M. Orbán, Phys. Chem. Chem. Phys., 4, 2002, 1271.

45. F. P. Cavasino, R. Cervellati, R. Lombardo and L. T. Liveri, J. Phys. Chem. B, 103, 1999, 4285.

Chapter 4 Chemical Oscillations in the 4-Aminophenol - Bromate Photoreaction

Introduction

Chemical reactions are known to be capable of exhibiting various interesting nonlinear

dynamical behaviors such as oscillations and the co-existence of multiple stationary states

[1-11]. The appearance of those exotic behaviors requires the existence of nonlinear

feedbacks, which can be either an autocatalytic or an auto-inhibition reaction process [10,

11]. Recent focus in the exploration of new chemical oscillators has been on three areas,

namely, enzyme-catalyzed reactions, pH-oscillators and photochemical systems [12-17].

Due to the convenience of changing intensity and protocol of illumination, which is a

particular advantage in implementing external forcing, photo-sensitive chemical

oscillators have garnered a great deal of attention in the last two decades [18-22]. Indeed,

studies of photochemical oscillators have made significant contributions toward the

understanding of interactions of intrinsic dynamics and external forcing as well as the

control of complex spatial temporal dynamics [18-20]. Various responses of chemical

oscillators to perturbation by UV, visible, and ^{60}Co γ-radiation have been reported. For

example, effects of light have been discussed in the Bray-Liebhafsky reaction [4], the

Briggs-Rauscher (BR) reaction [5,6], the hydrogen peroxide-ferrocyanide system [7,8]

and the Belousov-Zhabotinsky (BZ) reaction [21].

In a recent report, chemical oscillations were achieved in the light-mediated bromate-

1,4-benzoquionone reaction [22]. As evidenced by a flat Pt potential line in the

measurement, the bromate-1,4-benzoquinone system does not react in the absence of light, which distinguishes it from other photosensitive systems. Utilizing the property that aromatic compounds have strong absorption in UV range, in this report we investigated the reaction kinetics of 4-aminophenol (4AP) with acidic bromate in the presence of illumination. A closely related compound, phenol, has been reported to exhibit chemical oscillations in a stirred batch reactor when reacting with acidic bromate [23]. As shown in the following, the existence of an amino group on phenolic ring significantly changes the reactivity and no oscillatory behaviour, indeed not much reactivity, could be seen there. However, upon the application of an above threshold illumination, spontaneous oscillations are obtained over a broad range of 4-aminophenol, bromate and sulphuric acid concentrations.

Experimental Procedure

All reactions were carried out in a thermal-jacketed 50 ml glass beaker (ChemGlass). Reaction temperature was kept constant at 25.0 ± 0.1 °C by a circulating water bath (Thermo NesLab RTE 7). A Teflon cap was placed on top of the reactor to hold the electrodes. The solution level was about 1 cm below the Teflon cap. The reaction solution was stirred with a magnetic stirring bar driven by a magnetic stirrer (Fisher Isotemp). Reactions were monitored with a platinum electrode coupled with a $Hg|Hg_2SO_4|K_2SO_4$ reference electrode (Radiometer Analytical, XR200 and M231Pt-9). All measurements were recorded with a pH/potential meter (Radiometer PHM220) connected to a personal computer through a PowerLab/4SP data logger.

A halogen lamp with dual bifurcated optic fibers and continuous variable light level was used as the light source (Fisher Scientific, Model DLS-100HD, 150 W). The

illumination was implemented by placing the two fibers either on the opposite or the same

sides of the reactor and no difference in the reaction behaviour was observed, implying

that mixing was fast enough to generate a situation of homogeneous illumination. Stock

solutions $NaBrO_3$ (Aldrich, 99%), 0.6 M, and sulfuric acid (Aldrich, 95-98%), 4.0 M,

were prepared with double-distilled water. 4-aminophenol (Aldrich, 98+ %) was directly

dissolved in the reaction mixture. The volume of the reaction mixture was fixed at 30.0

ml in all experiments. Results reported in the following were conducted at a stirring rate

of 500 RPM. Absorption spectra were measured with a UV-visible spectrophotometer

(Ocean Optics, 2000 USB). A quartz cuvette (10 mm light path, HELLMA) containing

2.5 ml sample mixture was placed in a CUV sample holder which has two water jackets

connected to a circulating water bath (Thermo NesLab RTE 7). The cuvette was stirred

with a small magnetic bar.

Results and Discussion

Fig. 4.1 presents two time series of (a) the non-illuminated and (b) illuminated bromate

– 4-aminophenol reactions. In Fig. 4.1a, the Pt potential increases rapidly after mixing all

reactants together. During the above process, the reaction solution turns from colorless to

yellow, which is accompanied by the appearance of yellow precipitate. As more and more

precipitate forms in the solution, the Pt potential dips a little. The mixture of yellow

reaction solution and yellow precipitate then stays stable for several days, as indicated by

a slow decrease of the Pt potential. The reaction behavior seen in Fig. 4.1a is totally

different from what was reported in the non-illuminated bromate - phenol system [23],

demonstrating the dramatic changes in the reactivity caused by the amino group.
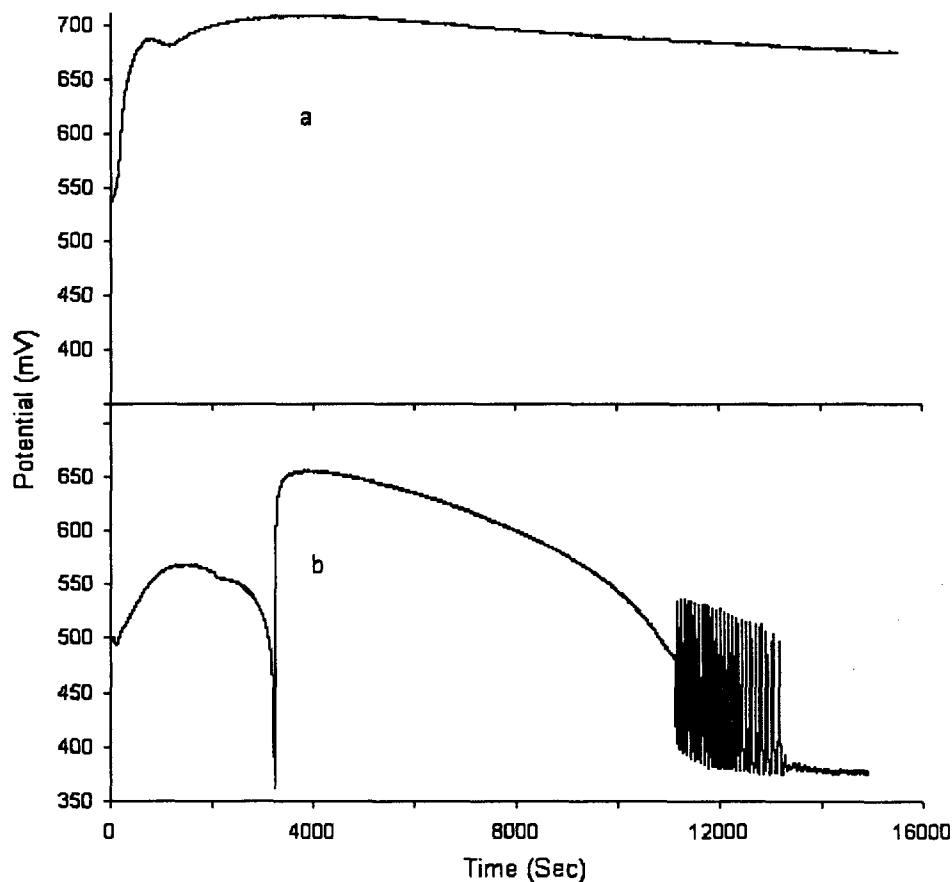
Figure 4.1 Time series of the bromate – 4-aminophenol (4AP) reaction: (a) without illumination, and (b) under a constant illumination of 100 mW/cm^2. Other reaction conditions are [BrO$_3^-$] = 0.050 M, [H$_2$SO$_4$] = 1.70 M, and [4AP] = 0.020 M. The mixture of yellow precipitate and yellow solution in (a) does not exhibit any observable changes in 4 days.

Formation of the yellow precipitate is greatly accelerated and, more importantly, the precipitate disappears quickly in time in the presence of illumination. There is a critical moment at which the murky solution suddenly turns clear, which corresponds to the sharp jump in the Pt potential in Fig. 4.1b. After the solution becomes clear, the Pt potential

decreases again for another 2 hr and then periodic oscillations appear. The oscillatory behavior could last as long as 50 minutes with as many as 40 peaks. Under the conditions used in Fig. 4.1 the solution remains yellow after oscillations have stopped.

While results in Fig. 4.1 clearly demonstrate that light is critical to the progress of the reaction, particularly in the dissolution of the precipitate, its role during the oscillating evolution is yet to be determined. Fig. 4.2a shows how the above chemical oscillations respond to changes of the applied light intensity. The reaction in Fig. 4.2a was started with a constant illumination of 150 mW/cm^2. After the system has exhibited a few oscillations, decreasing the light intensity to 60 mW/cm^2 resulted in an immediate cessation of the oscillatory behaviour. When the intensity was adjusted back to 120 mW/cm^2, oscillations revived instantaneously. This scenario illustrates that light plays a key role in the chemical oscillations in the bromate – 4-aminophenol system. An additional increase of the light intensity led to further changes in the frequency and amplitude of oscillation. Figs. 4.1b and 4.2a illustrate that there is a long induction time before spontaneous oscillations appear. How this induction time varies with the light intensity is plotted in Fig. 4.2b, where an exponential decrease with increasing light intensity is observed. The results in Fig. 4.2b also show that spontaneous oscillations could be obtained for light intensity as low as 40 mW/cm^2, as opposed to no oscillations at 60 mW/cm^2 in Fig. 4.2a. The only difference in compositions of the reaction solutions is that the 4-aminophenol concentration used in Fig. 4.2b is higher than that in Fig. 4.2a. This observation thus suggests that 4-aminophenol and/or its derivatives play an important role in the observed photosensitivity.
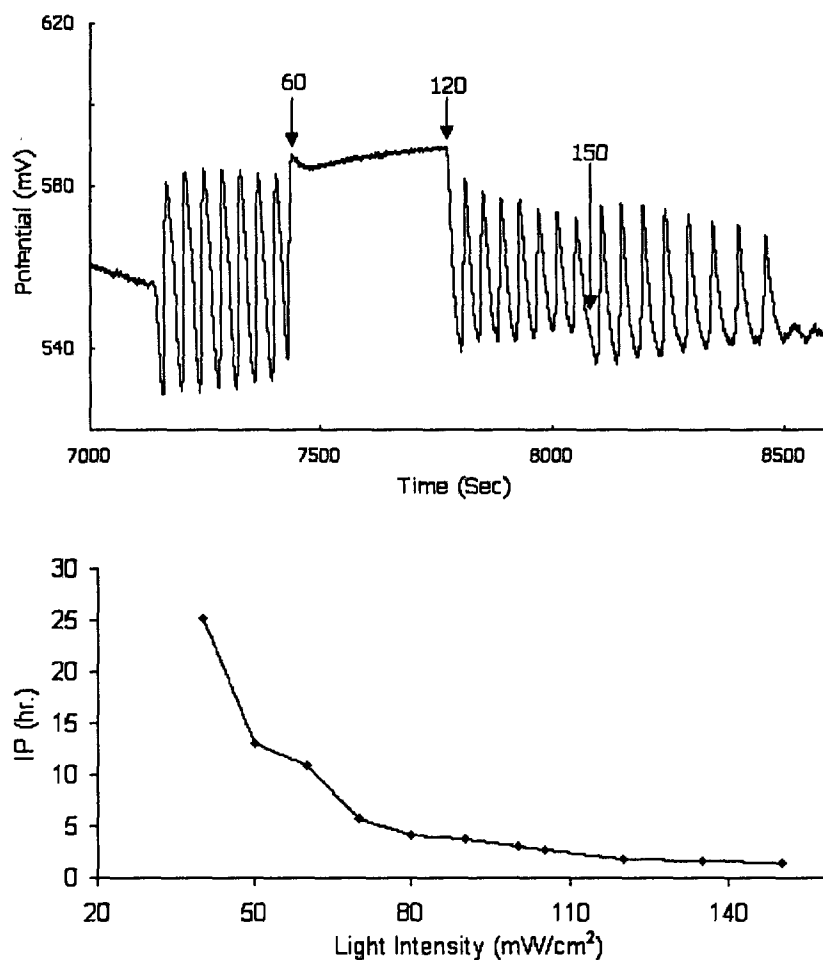
Figure 4.2 (a) Time series showing that oscillations stop and revive instantaneously upon adjusting light intensity around a threshold level; (b) variation of the induction time as a function of the applied light intensity. Reaction conditions are $[BrO_3^-]$ = 0.050 M, $[H_2SO_4]$ = 1.70 M, and [4AP] = (a) 0.013 M and (b) 0.023 M.

To shed light on the underlying reaction mechanism, the yellow precipitate formed at the beginning of the reaction was analyzed with several methods including thin layer chromatography (TLC), mass spectrometry, ^{1}HNMR spectrometry, ^{13}CNMR spectroscopy, and elemental analysis. The TLC analysis (petroleum ether and diethyl

ether solvent mixture (1:1 ratio)) shows that the yellow precipitate is a polar and pure

compound, as supported by the observation that there was just one spot moving on TLC.

Proton NMR decoupling experiments further confirm the above conclusion. In the mass

spectrum (EI, 20 eV) the largest peak belongs to a 185 m/e, with an accompany peak at

187, suggesting that this is a monobrominated compound. The ^{1}H-NMR spectrum shows

4 different hydrogen atoms on the ring at 7.35 ppm (dd, J_1 =10.5 Hz, J_2 = 3.0 Hz, 1H) ,

7.69 ppm (dd, J_1 =10.5 Hz, J_2 = 3.0 Hz, 1H), 6.68 ppm (dd, J_1 =10.5 Hz, J_2 = 1.8 Hz,

1H), and 6.51 ppm (dd, J_1 = 10.5 Hz, J_2 = 1.8 Hz, 1H); as each resonates in the form of a

doublet of doublets, the spectrum suggests that bromination does not occur on the ring.

Elemental analysis shows that the yellow precipitate contains, respectively, 39.04, 2.20,

and 7.48 percent of carbon, hydrogen, and nitrogen. Our analysis strongly suggests that

N-bromo-1,4-benzoquinone-4-imine (C_6H_4BrNO) is the most probable species, as the

theoretical element percentages for carbon, hydrogen and nitrogen are, respectively, 38.74,

2.17, and 7.53, in good agreement with experimental values. This yellow compound

decomposes at 66 °C, whereas the decomposition of N-bromo-1,4-benzoquinone 4-imine

is reported at 67 - 68 °C [25]. Finally, the resonances in the ^{13}C-NMR spectrum of the

precipitate are in agreement with the suggested compound (4 alkene carbon peaks at

130.8, 132.2, 136.1, and 137.7 ppm, one peak at 170.2 ppm and the most downfield one

187.7 ppm).

Fig. 4.3 is a phase diagram in the 4-aminophenol and sulphuric acid concentration

plane, where (♦) indicates the conditions under which the system exhibits spontaneous

oscillations. We would like to point out that no oscillatory phenomena could be seen in

the non-illuminated bromate - 4-aminophenol reaction system. Fig. 4.3 demonstrates that

the presence of a strong illumination allows the system to oscillate over broad

concentrations. In general, increasing 4-aminophenol concentration shifts the suitable

sulphuric acid conditions toward higher concentrations. An important note is that when

the sulphuric acid concentration is lower than 0.6 M, there is no yellow precipitate in the

reactor and the yellow solution gradually evolves into the oscillatory window with a few

broad peaks. No precipitate at low acid concentration is likely because bromate reactions

are slow at low H^+ conditions and the yellow reagent never reaches its saturation level

due to its continuous consumption. Studies performed at lower H_2SO_4 concentrations

illustrate that the formation of the yellow species (C_6H_4BrNO) has the characteristics of

an autocatalytic reaction, where the Pt potential increases slowly for a few minutes and

then makes an exponential jump accompanied by the appearance of yellow color.
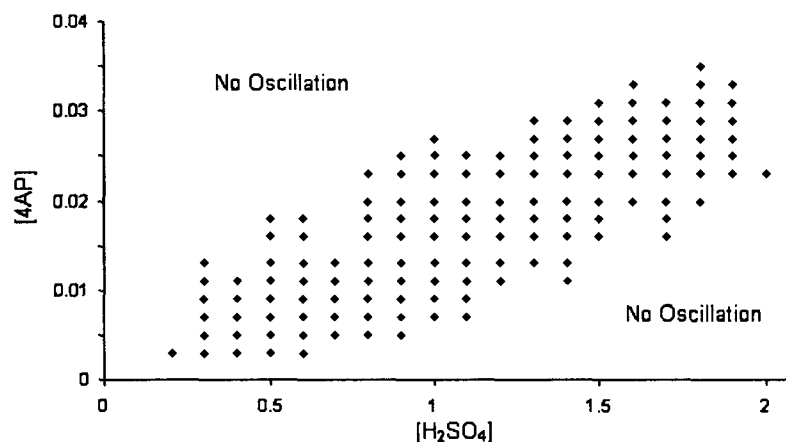
Figure 4.3 Phase diagram in the 4-aminophenol – H_2SO_4 concentration plane. Conditions under which the system shows spontaneous oscillations are indicated by (♦). Other reaction conditions are [BrO_3^-] = 0.060 M and light intensity is 100 mW/cm^2.

Fig. 4.4 presents four snapshots showing the appearance of the yellow reagent in a

spatially extended medium. Here, reaction conditions are [BrO_3^-] = 0.060 M, [4AP] =

0.009 M, and $[H_2SO_4]$ = 0.4 M. The reaction solution was held between two microscope slides to form a 0.5 mm thick solution layer. This experiment shows that the colorless 4-aminophenol and sulphuric acid solution actually turns into purple (dark color in Fig. 4.4) upon the addition of bromate. The purple color survives, depending strongly on sulphuric acid concentration, for a few minutes during which the Pt potential increases slowly in a stirred media; then, the yellow color appears accompanied by an abrupt increase in the Pt potential. In the spatially extended medium, the autocatalytic formation of the yellow reagent leads to the formation of yellow front (white color) propagating in the purple background. When sulphuric acid concentration is high, the above process becomes too fast to be observed.
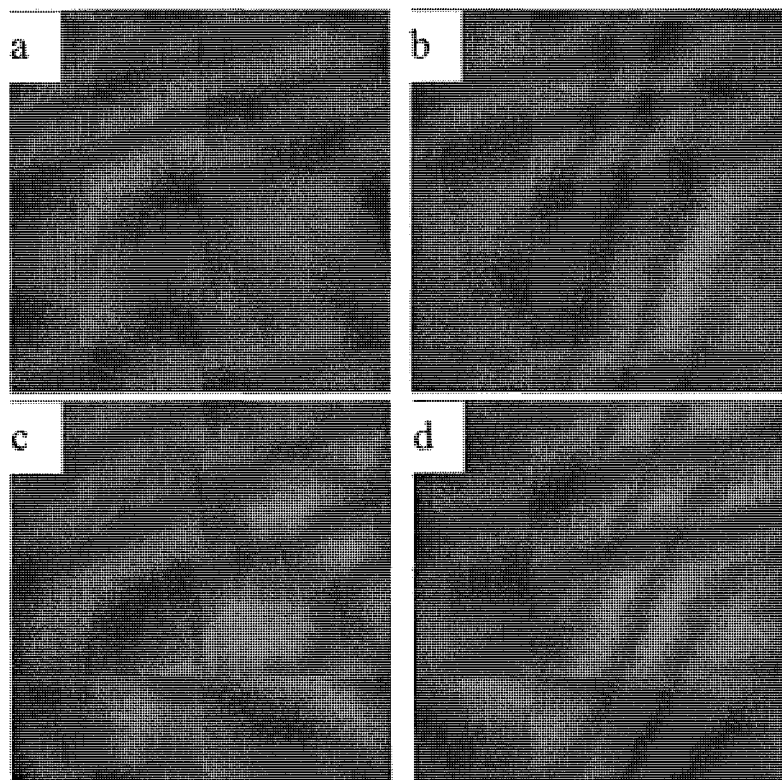
Figure 4.4 Snapshots of the propagating fronts in the bromate - 4-aminophenol reaction recorded at t = (a) 60 s, (b) 61 s, (c) 65 s, and (d) 68 s. The white color indicates where the yellow substance C_6H_4BrNO has been formed.

Fig. 4.5 shows that the addition of a small amount of bromide ion can temporarily quench those spontaneous oscillations. The quenching phenomenon becomes more obvious when the reaction is near the end of the oscillation window, i.e. close to a bifurcation point. The observed Br⁻ effects depend on both the amount and phase at which bromide is added, similar to that reported in other bromate-based oscillators [26]. This result leads us to speculate that autocatalytic productions of $HBrO_2$ proposed for the BZ reaction may also be the nonlinear feedback in this photochemical oscillator, except here organic species replace the metal catalyst [27-29].
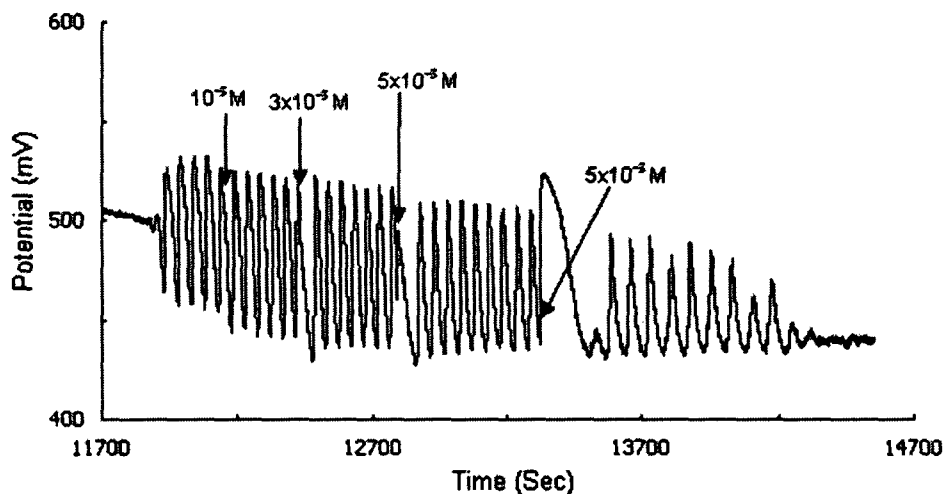
Figure 4.5 Quenching of oscillations with bromide ion. Reaction conditions are [BrO₃⁻] = 0.050 M, [H₂SO₄] = 1.70 M, and [4AP] = 0.016 M. The applied light intensity is 100 mW/cm².

Conclusions

This research presents a new photochemical oscillator, in which the presence of light is critical to the extent of the reaction and the onset of oscillations. Similar to existing bromate - aromatic compounds oscillators [23,24], this bromate – 4-aminophenol oscillator has a long induction time, which exhibits exponential dependence on the light intensity. While the underlying photochemical mechanisms remain to be understood, our experiments show that the threshold light intensity for inducing oscillations decreases with increasing 4-aminophenol concentration, implying that 4-aminophenol and/or its products may be responsible for the photosensitivity. Examination with narrow band filters centered at 250 ± 10 nm and 300 ± 10 nm, where 4-aminophenol shows strong absorbance, failed to confirm the above hypothesis. The failure could be due to the dramatic reduction of the light intensity, as the filter only allows less than 15 percent of the incident light to pass through. Separate spectroscopic studies show that bromine reacts with 4-aminophenol, producing quinone substances which have one maximum absorption peak in the UV range (at 250 nm). Quenching experiments suggest that the nonlinear feedback may arise from the autocatalytic production of $HBrO_2$, similar to the classic BZ reaction [18].

Analytical measurements suggest that an intermediate C_6H_4BrNO (N-bromo-1,4-benzoquinone 4-imine) is produced during the reaction of 4-aminophenol and bromate. This intermediate is responsible for the yellow color of the reaction solution and stays un-reacted in the absence of light. The consumption of this yellow compound is also greatly affected by bromate. For example, the yellow solution becomes colorless at the end of the reaction if the initial concentration of bromate is higher than 0.08 M. Under high acid concentrations, C_6H_4BrNO precipitates in the yellow solution due to its low solubility. If

the C_6H_4BrNO precipitate is purified and mixed with acidic bromate, there was no

reactivity in the absence of light, but oscillations could be observed in the presence of

light. Detailed studies of such a subsystem will be reported in future research.

References

1. J. L. Hudson and J. C. Mankin, J. Chem. Phys., 74, 1981, 6171.

2. L. Onel, G. Bourceanu, I. Bitter, M. Wittmann and Z. Noszticzius, J. Phys. Chem. A, 110, 2006, 990.

3. I. R. Epstein and J. Pojman, An Introduction to Nonlinear Chemical Dynamics, Oxford University Press, New York, 1998.

4. K. R. Sharma and R. M. Noyes, J. Am. Chem. Soc., 97, 1075, 202.

5. E. Dulos and P. DeKepper, Biophys. Chem., 18, 1983, 211.

6. N. Okazaki, Y. Mori and I. Hanazaki, Chem. Lett., 1993, 1135.

7. G. Rábai, K. Kustin and I. R. Epstein, J. Am. Chem. Soc., 111, 1989, 8271.

8. Y. Mori and I. Hanazaki, J. Phys. Chem., 96, 1992, 9083.

9. I. Schreiber, P. Hasal and M. Marek, Chaos, 9, 1999, 43.

10. P. Gray and S. K. Scott, Chemical Oscillations and Instabilities, Clarendon Press, Oxford, 1994.

11. V. K. Vanag, D. G. Miguez and I. R. Epstein, J. Chem. Phys., 125, 2006, 194515.

12. T. Hideshima and Y. Kato, Biophys. Chem., 124, 2006, 100.

13. S. Danø, P. G. Sørensen and F. Hynns, Nature, 402, 1999, 320.

14. K. Nielsen, P. G. Sørensen, F. Hynns and H. G. Busse, Biophys. Chem., 72, 1998, 49.

15. R. E. McIlwaine, K. Kovacs, S. K. Scott and A. F. Taylor, Chem. Phys. Lett., 417, 2006, 39.

16. Q. Gao and J. Wang, Chem. Phys. Lett., 391, 2004, 349.

17. K. Kovacs, R. E. McIlwaine, S. K. Scott and A. F. Taylor, J. Phys. Chem. A, 111, 2007, 549.

18. R. J. Field and M. Burger, Oscillations and Traveling Waves in Chemical Systems, John Wiley & Sons, New York, 1984.

19. S. Kadar, J. Wang and K. Showalter, Nature, 391, 1998, 700.

20. L. Kuhnert, Nature, 319, 1986, 393.

21. M.K. Ram Reddy, Z. Szlávik, Zs. Nagy-Ungvarai and S.C. Müller, J. Phys. Chem., 99, 1995, 15081.

22. B. Zhao and J. Wang, Chem. Phys. Lett., 430, 2006, 41.

23. L. Adamčíková, Z. Farbulová and P. Ševčík, New J. Chem., 25, 2001, 487.

24. I. Szalai and E. Körös, J. Phys. Chem. A, 102, 1998, 6892.

25. E. M. Hodnett, G. Prakash and J. Amirmoazzami, J. Med. Chem., 21, 1978, 11.

26. F. Hynne, P. G. Sørensen and K. Nielsen, J. Chem. Phys., 92, 1990, 1747.

27. M. Orbán and E. Körös, J. Phys. Chem., 82, 1978, 1672.

28. Z. Farbulova, P. Ševčik and L. Adamčikova, Collect. Czech. Chem. Commun., 68, 2003, 2093.

29. R. Cervellati and B. Mongiorgi, Int. J. Chem. Kinet., 30, 1998, 641.

Chapter 5 Nonlinear instabilities in the light-mediated bromate - 4-aminophenol reaction

Introduction

Behavior of an oscillatory reaction system can be conveniently manipulated through varying external parameters such as the flow rate in a continuous flow stirred tank reactor (CSTR), the concentration of a reagent, or, light illumination if the system is photosensitive [1-10]. Perhaps the most beautiful instance of such a controlling influence is the stabilization of unstable limit cycle oscillations in a chaotic Belousov-Zhabotinsky (BZ) system through perturbing the flow rate at which the metal catalyst and bromate solutions are fed into a CSTR [11]. From a practical point of view, using light as the control parameter has great advantages due to the easy regulation of both intensity and illumination protocols, particularly in the study of reaction-diffusion media in which spatially inhomogeneous perturbations are sometimes desired. As a result, photosensitive chemical oscillators have attracted a great deal of attention in the past three decades [12-28].

Based on the function of light in the studied systems, photochemical oscillators can be loosely classified into two groups, namely, photosensitive oscillators and photo-controlled oscillators. For photosensitive chemical systems, illumination merely provides an alternative approach of producing key intermediates and the vast majority of existing investigations on nonlinear photochemical dynamics have been carried out in this

category [12-24]. In the ruthenium-catalyzed BZ reaction, for example, light causes additional production of bromide ions, an inhibitor of the autocatalytic reaction [19]. Vanag and co-workers studied the photosensitivity of the ferroin-catalyzed BZ reaction in the water-in-oil microemulsion system [20]. Extensive studies on the effect of light on the Bray reaction were performed by Noyes et al. [21, 22]. Subtle photosensitive behavior has been observed in both the uncatalyzed and catalyzed bromate-1,4-cyclohexanedione reaction (CHD), in which the response of the reaction to light does not only depend on the compositions of the system but also depends on the light intensity [23,24].

For photo-controlled chemical reactions, light creates an exclusive approach of producing certain intermediates. Therefore, the system does not exhibit any reactivity in the absence of illumination [25-31]. Examples of those systems include the photo-degradation of tetrathionate, and the photo-mediated bromate-1,4-benzoquinone reactions [25-27]. In a recent letter [28], we reported that the bromate-4-aminophenol (AP) reaction also belongs to the group of photo-controlled chemical oscillators, in which significant reactivity, especially chemical oscillations, could be achieved only in the presence of light. In the following, the kinetics and mechanism of the photo-mediated bromate-AP reaction were systematically investigated and characterized with different analytical methods.

Experimental Procedure

All reactions were carried out in a thermal-jacketed 50 ml glass beaker purchased from ChemGlass and temperature was kept at 25.0 ± 0.1 °C by a circulating water bath (Thermo NesLab RTE 7). Reactions were monitored with a platinum electrode coupled with a $Hg|Hg_2SO_4|K_2SO_4$ reference electrode (Radiometer Analytical). All measurements were recorded through a pH/potential meter (Radiometer PHM220) connected to a

personal computer through a PowerLab/4SP data logger. A halogen lamp with dual bifurcated optic fibers and continuous variable light level was used as the light source (Fisher Scientific, Model DLS-100HD, 150 W).

Mass spectrometry studies were performed with a 1200 L single quadrupole MS (Varian) using a direct insertion probe. The mass range was between 10 and 800 amu and electron ionization was used as ionization mode. The probe temperature was controlled independently and changed from 20 to 300 °C with the same steps and durations for all the Mass measurements. The samples have been prepared as follows: the reaction was stopped at different stages by adding 30 ml diethyl ether ($\geq$ 99.0%, purchased from Sigma-Aldrich) to the reaction mixture and subsequently separating the organic phase. The remaining aqueous phase was then extracted twice, respectively, with 30 ml diethyl ether. Later, a rotary evaporator was used to concentrate the diethyl ether sample, which took about 60 minutes. The mass spectra of all samples were recorded at 20 eV electron impact. All ^{1}HNMR and ^{13}CNMR measurements were carried out using Bruker Avance 500 MHz spectrometer and with the same sample that was used for mass spectrometry studies but dissolved in chloroform-d (99.8%) or acetone-d6 (99.9%) purchased from Cambridge Isotope Laboratories.

Stock solutions of $NaBrO_3$ (Aldrich, 99%), 0.6 M, and sulfuric acid (Aldrich, 95-98%), 4.0 M, were prepared with double-distilled water. 4-aminophenol (Aldrich, 98+ %) was directly dissolved in the reaction mixture. The volume of the reaction mixture was kept at 30.0 ml in all experiments. Absorption spectra were measured with a UV-visible spectrophotometer from Ocean Optics (2000 USB), in which a quartz cuvette (10 mm light path, HELLMA) containing 2.5 ml sample mixture was placed in a CUV sample

holder which has two water jackets connected to a circulating water bath (Thermo NesLab RTE 7). The solution in the cuvette was stirred with a small magnetic bar.

Results and Discussions

Figure 5.1 shows the temporal evolution of the illuminated bromate-AP reaction under different initial concentrations of AP: (a) 0.011 M, (b) 0.018 M, and (c) 0.029 M. In all three cases, the reaction evolves through a broad peak in the Pt potential, which is followed by an abrupt potential increase as indicated by the arrows. Depending on the compositions of the reaction, yellow precipitates may occur during the first broad peak, but disappear rapidly and completely by the occurrence of the sharp Pt potential increase. Beyond this point, the evolution of the reaction system becomes qualitatively different from (a) to (c). At the low AP concentration, the Pt potential decreases smoothly in time until a constant value is achieved at about 3 hours after mixing all reagents together. Under a moderate AP concentration, however, periodic oscillations in the Pt potential take place. Notably, there is a long induction time before the spontaneous chemical oscillations occur. When the concentration of AP is too high, the smooth decrease of the Pt potential is interrupted by a sudden decrease at about 10,000 seconds after the reaction has begun, but no oscillation takes place afterwards. This Figure illustrates that, in addition to an above threshold light intensity [28], AP concentration must be within a proper range for this photochemical system to exhibit oscillatory behaviour.
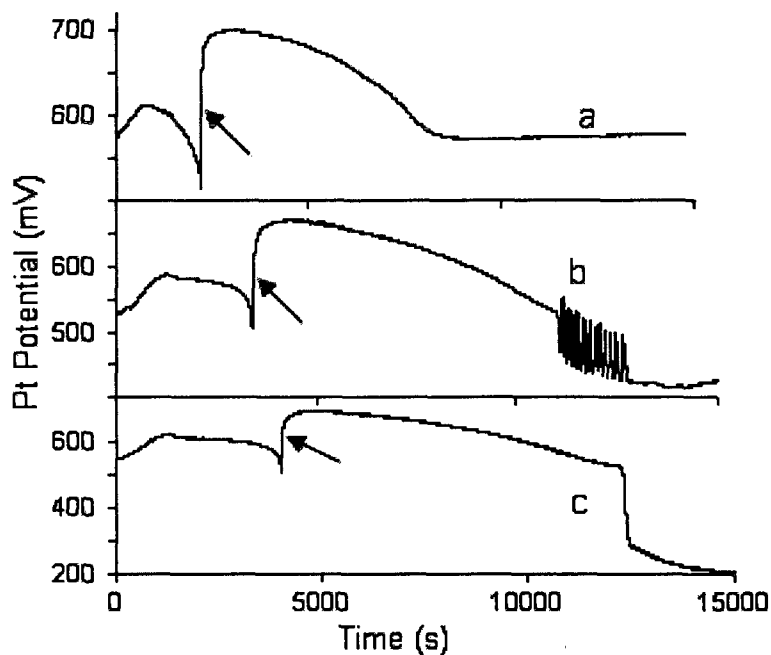
Figure 5.1 Time series of the illuminated bromate-AP reaction under different concentrations of AP: (a) 0.011 M, (b) 0.018 M, and (c) 0.029 M. Other reaction conditions are: $[BrO_3^-] = 0.050$ M, $[H_2SO_4] = 1.70$ M, and light intensity = 100 mW/cm^2.

Fig. 5.2 plots the variation of the induction time and number of oscillations as a function of AP concentration. Under the conditions studied here, chemical oscillations have been found within the range between 0.013 and 0.027 M. Figure 5.2a illustrates that, as the concentration of AP is gradually increased, the total number of oscillations first increases, reaching a maximum of 40 peaks, and then decreases gradually until the system moves out of the oscillation window. On the other hand, as is shown in Fig. 5.2b, the induction time increases monotonically with the concentration of AP, indicating that the induction time is not related to the number of oscillation peaks.
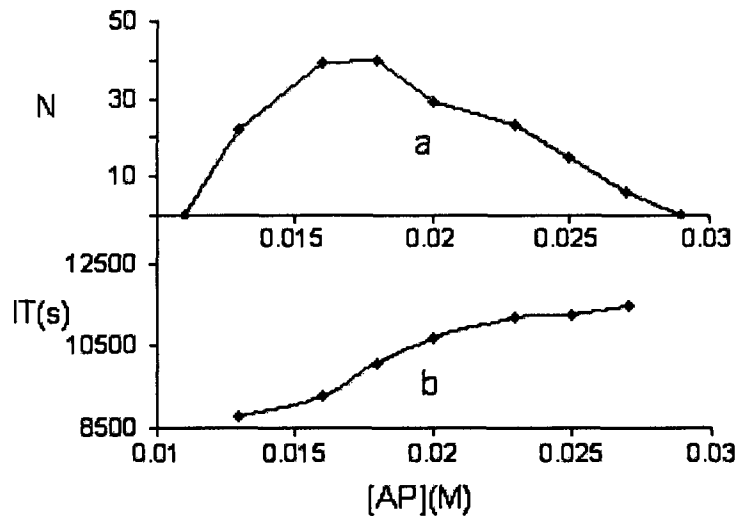
Figure 5.2 Dependence of the induction time (IT) and number of oscillations on the concentration of AP. Other reaction conditions are the same as those used in Fig. 5.1.

Fig. 5.3 presents the evolution of the illuminated bromate-AP reaction recorded simultaneously with a bromide selective electrode and a Pt electrode. In bromate-based chemical oscillators, Br^- plays a critical role via rapidly reacting with the autocatalyst $HBrO_2$ [32,33]. As shown in this Figure, the abrupt increase in the Pt potential coincides with an abrupt increase of the bromide potential. The calibration shows that high bromide electrode potential corresponds to low bromide concentration. The sudden disappearance of the yellow precipitate thus accompanies a sudden decrease of bromide concentration. Such a dramatic process may arise from an autocatalytic production of $HBrO_2$, which consequently consumes bromide via the reaction $HBrO_2 + Br^- + H^+ \rightarrow 2HOBr$. The above measurement also shows that bromide concentration increases slowly during the long induction time and then oscillates toward a higher value. Since the bromide electrode is sensitive to illumination, only a few reactions were recorded simultaneously with the Pt and bromide selective electrodes.
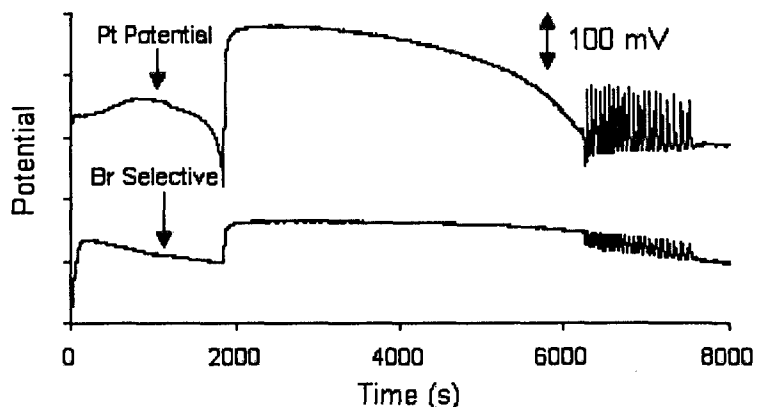
Figure 5.3 Time series recorded simultaneously with a bromide ion selective electrode and a Pt electrode. The reaction conditions are [BrO$_3^-$] = 0.050 M, [H$_2$SO$_4$] = 1.70 M, [AP] = 0.020 M, and light intensity = 150 mW/cm^2.

Fig. 5.4 presents a phase diagram in a bromate and AP concentration plane, where (♦) indicates the conditions under which the system exhibits spontaneous oscillations. At first glance, Fig. 5.4 suggests that the illuminated bromate-AP system is able to oscillate over a broad concentration range of AP and bromate; however, at a fixed concentration of AP (or bromate), the suitable concentration range of bromate (or AP) is quite narrow. The diagonal-structured parameter window suggests that the reaction behaviour is more sensitive to the ratio of [bromate]/[AP] than their actual concentrations. Moreover, this phase diagram illustrates that increasing AP concentration shifts the suitable bromate concentration toward higher values. A useful note is that when the bromate concentration is higher than 0.08 M, the system evolves into the oscillatory window through one process, where the yellow precipitates disappear gradually and there are no sudden increases in the Pt and bromide potentials (Fig. 4.3).
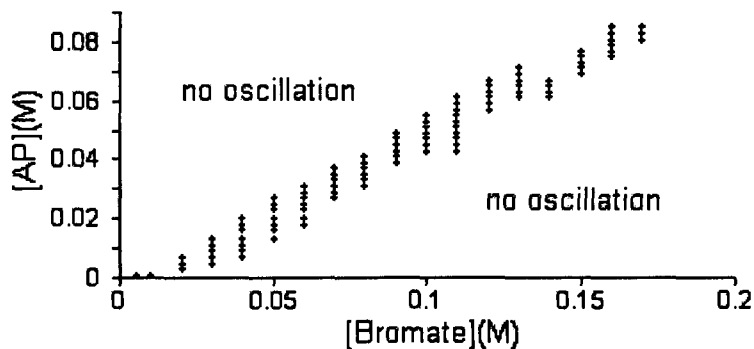
Figure 5.4 Phase diagram in the AP – bromate concentration plane. (♦) indicates the conditions under which the system shows spontaneous oscillations. Other reaction conditions are [H_2SO_4] = 1.70 M and light intensity is 100 mW/cm^2.

The system involves three reactants, namely bromate, 4-aminophenol and acid. Determining the oscillation parameter window in a three-dimensional concentration space represents a tremendous challenge as a huge number of experiments would be required. To partially overcome such a challenge and gain some meaningful insight into the reaction behaviour in a three-dimensional parameter space, Fig. 5.5 presents a primitive three-dimensional phase diagram which was constructed by establishing phase-diagrams in the bromate-AP plane at two concentrations of acid. This primitive 3D plot indicates that the parameter window within which the system exhibits spontaneous oscillations is a thin slab in the bromate-acid-AP concentration space, implying that nonlinear behaviour in the studied system is more sensitive to the ratio of [AP]/[bromate] than their absolute concentrations.
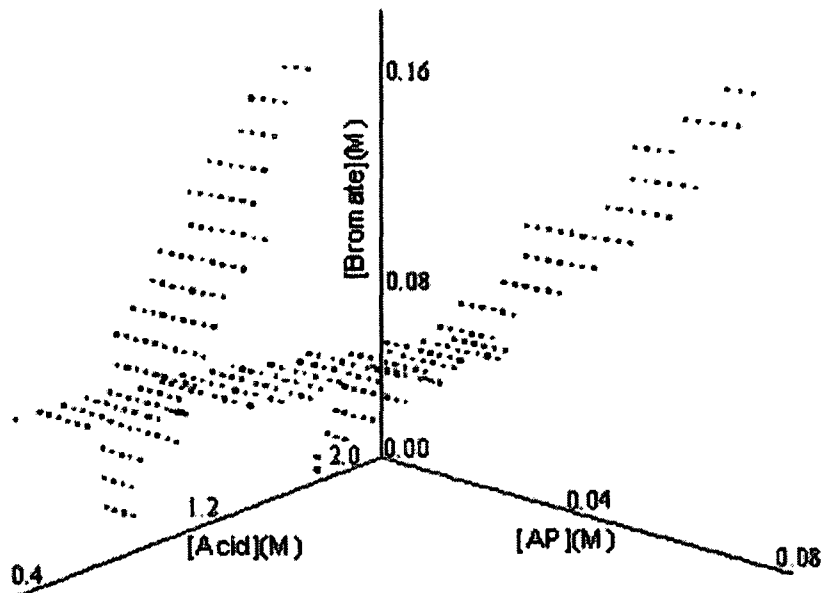
Figure 5.5 Phase diagram in a three-dimensional concentration space. (♦) indicates the conditions under which the system exhibits spontaneous oscillations. The light intensity is 100 mW/cm².

Our experiments illustrate that the dependence of the number of oscillations on bromate concentration is similar to what was obtained when AP concentration was adjusted, suggesting that bromate has similar effects as AP on the oscillatory behaviour. Despite there being an optimum concentration for the largest number of oscillations, the induction time nevertheless increases monotonically with respect to bromate concentration. The study on the influences of acid concentration on the oscillatory behaviour shows that, different from the cases of bromate and aminophenol, the induction time does not exhibit significant change when the acid concentration is adjusted. For both acid and bromate, there is a rapid increase in the induction time when the system moves closer to the upper threshold concentration of the acid or bromate.

It has been reported in the earlier letter that the applied light intensity must be above a threshold value for the system to exhibit significant reactivity, in particular the oscillatory behaviour [28]. The effect of light intensity on the number of oscillations is presented in Fig. 5.6. In this series of experiments, there is no oscillatory phenomenon when the applied light intensity is lower than 30 mW/cm^2. Above such a critical value, the number of peaks increases gradually with the light intensity. Beyond 90 mW/cm^2, however, further increase of light intensity exhibits adverse influences on the oscillatory behaviour, causing a decrease in the number of oscillations. Within the above parameter window, the amplitude of oscillation increases monotonically while the induction time decreases monotonically with increasing light intensity. Limited by the light source, we have not been able to reach the upper limit of the light intensity beyond which the system does not oscillate.
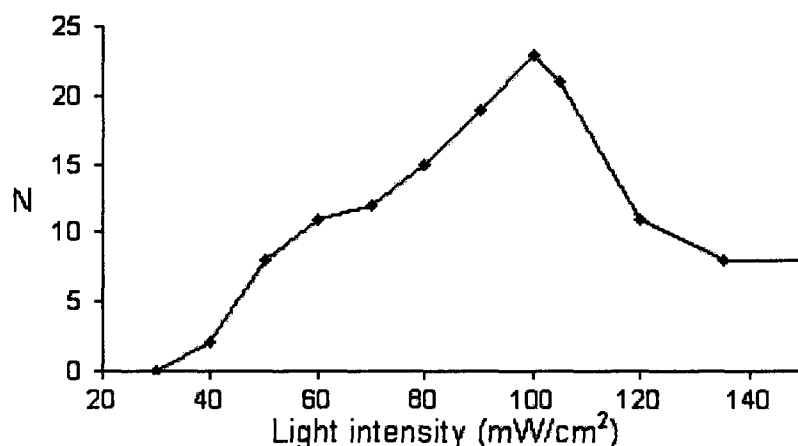
Figure 5.6 Dependence of the number of oscillations on light intensity. Other reaction conditions are [H$_2$SO$_4$] = 1.70 M, [BrO$_3^-$] = 0.050 M, and [AP] = 0.023 M.

The inhibitory effect of aliphatic alcohols on bromate-based chemical oscillators such as the BZ reaction has been reported earlier, in which when small amounts of ethanol were added to an oscillating mixture, the oscillations became strongly damped and after some time the oscillation terminated [34-36]. Figure 5.7 presents the influence of ethanol on the illuminated bromate-AP reaction, where the addition of 4.0×10^{-3} M of ethanol immediately quenches the oscillatory behaviour, whereas the oscillation amplitude is significantly reduced by 1.0×10^{-3} M ethanol. Different from the response to bromide ion perturbation, here the impact of ethanol is irreversible, implying that ethanol is not consumed like bromide ions. Studies with a UV/Vis spectroscopy (at 330 nm) show that ethanol reacts with acidic bromate to produce HOBr, which can act as a radical scavenger through reacting with organic radicals or can directly interact with bromide ions to affect the reaction dynamics. In Fig. 5.7a, the addition of ethanol causes an immediate increase of the Pt potential, which corresponds to a decrease of bromide concentration as illustrated in Fig. 5.3. This suggests that the above observed inhibitory effect of ethanol arises from the production of HOBr, which subsequently consumes bromide ions.

Fig. 5.8 plots the amplitude of oscillations measured with a UV/vis spectrophotometer at different wavelengths. The result shows that intermediates which have strong absorptions within the wavelength between 310 and 430 nm oscillate in time. Known species which have strong absorption within such a range include HOBr (330 nm), Br_2 (390 nm), N-bromo-1,4-benzoquinone-4-imine (250 and 330 nm). No oscillation was achieved when the evolution was followed at other wavelengths, despite the fact that the reaction solution, especially AP, has strong absorption within the UV range.
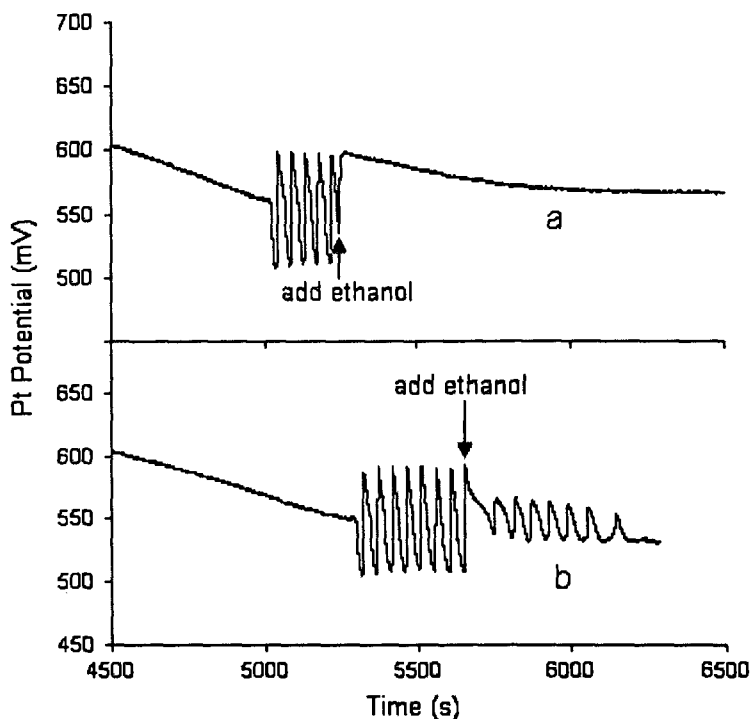
Figure 5.7 Quenching behaviour with the addition of ethanol: (a) 4×10^{-3} M, and (b) 1 $\times 10^{-3}$ M. Other reaction conditions are $[H_2SO_4] = 1.70$ M, $[BrO_3^-] = 0.050$ M, $[AP] = 0.016$ M, and light intensity $= 150$ mW/cm^2.
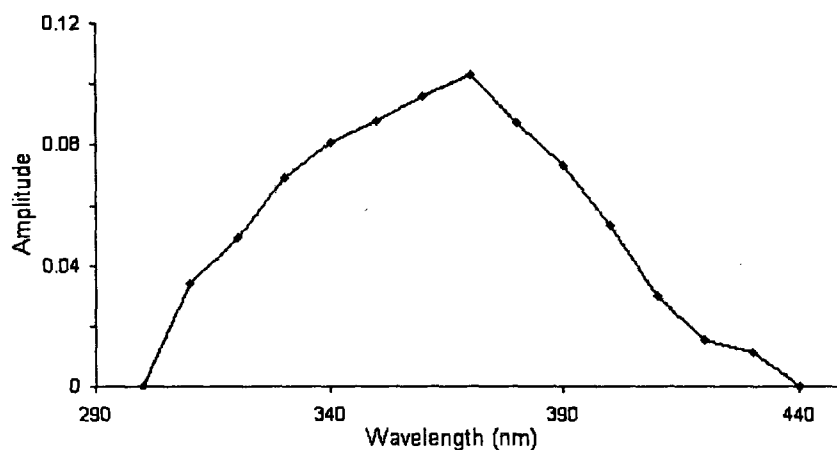
Figure 5.8 The largest amplitude of oscillation measured with a UV/vis spectrophotometer at different wavelengths. Reaction conditions are: $[AP] = 0.023$ M, $[H_2SO_4] = 1.70$ M, $[BrO_3^-] = 0.05$ M, and light intensity $= 150$ mW/cm^2. The spectra were taken by placing a 2.5 ml solution which just started oscillating in a regular reactor into a stirred 1.0 cm path length cuvette. The cuvette was then illuminated with 50 mW/cm^2 light along a vertical direction.

To decipher the mechanism of this illuminated bromate-AP reaction, mass spectrometry (electron impact, direct insertion) and ^{1}H-NMR analysis were performed at different reaction stages denoted respectively by 1, 2 and 3 in Table 5.1. In the earlier work [28], we have identified that N-bromo-1,4-benzoquinone-4-imine, which is referred to as imine hereafter, is the precipitate formed at the beginning of the reaction. Therefore, before spontaneous oscillations commence there are at least two stable organic compounds in the reaction mixture, namely, AP and imine. The sample was analysed when the reaction was stopped at about 300 seconds after mixing all reagents together (i.e. stage 1). To carry out the analysis, the reaction mixture was first filtered to remove imine precipitate and then was extracted with diethyl ether solvent. The extracted solvent was analyzed with the NMR and mass spectroscopy. The second reaction stage is when the yellow imine precipitate has completely dissolved but the oscillation has yet to appear (c.a. 7000 s after mixing all reagents together). Again, the reaction was stopped by adding diethyl ether into the solution. The third stage is when the system starts oscillating. In both of the subsequent stages, the reaction was stopped by adding diethyl ether to the solution and analysed.

Using the same samples for each technique, mass spectra and ^{1}H NMR spectra were acquired, each displaying too many peaks, and making them impossible to interpret completely. However, in CDCl$_3$ solution we could assign the resonance at 6.78 ppm to 1,4-benzoquinone (1,4-BQ), which is the dominant species in solution at stage 1. The ^{13}C NMR spectrum shows two peaks at 138 ppm and 187 ppm that belong to 1,4-BQ [37], and such a conclusion is further supported by DEPT-135 experiments.

Table 5.1 Proposed chemical species on the basis of mass spectra.

Reaction stage	Mass (m/e)	Suggested species
1 and 2	186/188	$(O)C_6H_3Br(O)$
1 and 2	188/190	$(OH)C_6H_3Br(HO)$
1 and 2	264/266/268	$(O)C_6H_2Br_2(O)$
1, 2 and 3	266/268/270	$(OH)C_6H_2Br_2(H_2O)$
1, 2 and 3	282/284/286	$(OH)_2C_6H_2Br_2(HO)$
2 and 3	280/282/284	$(O)C_6H_2Br_2OH(O)$
2	234/236/238	$C_6H_4Br_2$
2	141	$(OH)_3C_6H_2(H_2N)$
2	342/344/346/348	$(O)C_6HBr_3(O)$
2	344/346/348/350	$(OH)C_6HBr_3(OH)$
1 and 2	108	OC_6H_4O
2 and 3	202/204	$(O)C_6H_3BrOH(O)$

The mass spectral data in addition indicate monobrominated molecules of m/e 186/188 and 188/190 and dibrominated species centred at m/e 266 and 268. By stage 2, the ^1H NMR spectrum ($CDCl_3$) displays resonances at 6.82 and 6.94 ppm (each, doublet J = 10.3 Hz) in addition to 1,4-benzoquinone, which are consistent with the presence of a 2,3-unsymmetrically disubstituted quinone, of which 2-bromo-3-hydroxy-1,4-benzoquinone; most likely candidate. ^1H NMR spectroscopy in acetone-d_6 gave greater spectral separation of the components, and reveals the presence of additional resonances consistent with the presence of additional substituted, and likely brominated, quinones. In the ^{13}C NMR spectrum, additional resonances in the 180-190 ppm region are indicative of the additional quinones. The mass spectral studies indicate the continued presence of the 186/188, 188/190, 266 and 268 ions, the 202/204 ions consistent with 2-bromo-3-

hydroxy-1,4-benzoquinone, the appearance of a dibromo-monohydroxylated species centred at m/e 282, and trace amounts of tribrominated ions at 342/344/346/348 and 344/346/348/350; in conjunction with the NMR spectral data, we view these species as most likely likely quinones and hydroquinones, as opposed to protonated quinone imines and aminophenols. By stage 3, the purported 2-bromo-3-hydroxy-1,4-benzoquinone (m/e 202/204) is significant, but most of the same species as stage 2 are present, by both ^{1}H NMR spectroscopy and mass spectroscopy. The dominant reaction route appears to involve oxidation of the 4-aminophenol to N-bromobenzoquinone imine, acidic imine hydrolysis to benzoquinone, and subsequent bromination and hydroxybromination reactions of the 1,4-BQ (Scheme 1).

Scheme 1. Proposed dominant reaction pathway
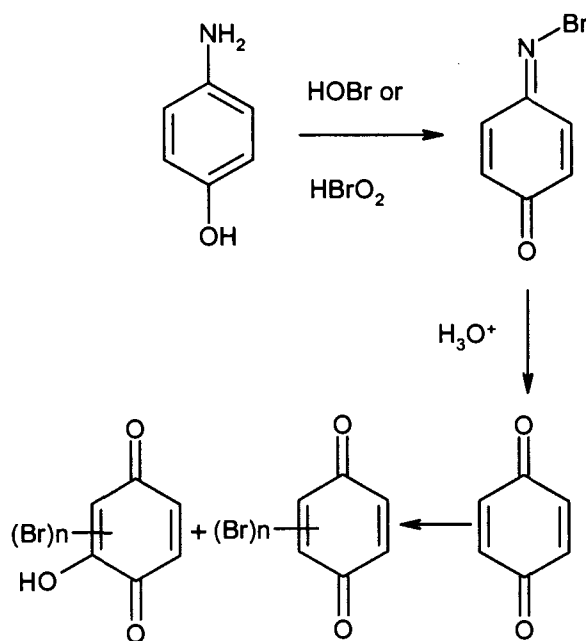
Mechanistic studies with the cyclic voltammetry method show that the redox potential of 4-aminophenol is 235 mV vs $Hg|Hg_2SO_4|K_2SO_4$ electrode, whereas the redox potential of the intermediate imine is -52.5 mV against the same reference electrode (see Fig. 5.9).

Such a result suggests that the intermediate reagent, imine, is a better reducing agent than the initial reactant AP and should be easily oxidized further once formed. As discussed above and listed in Table 1, both mono- and di-bromated organic substances are produced in the reaction process.
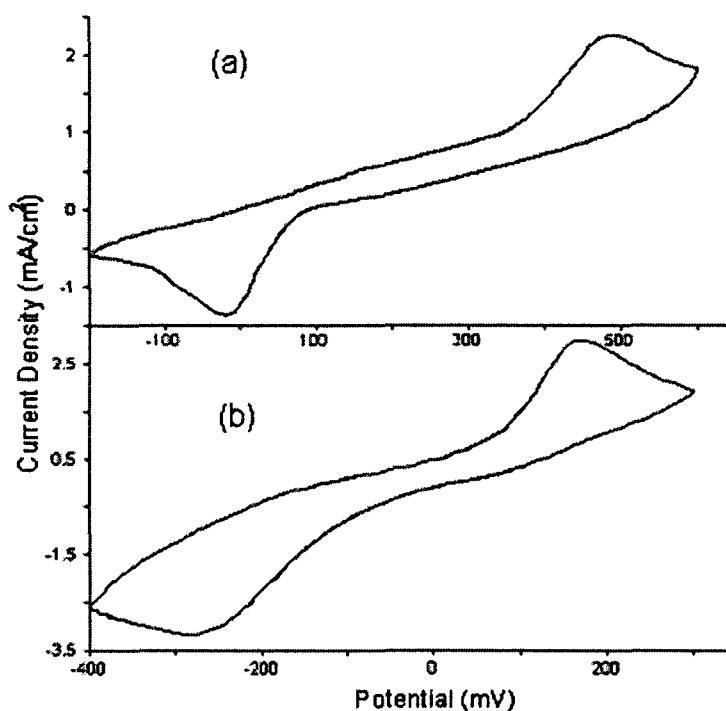
Figure 5.9 Cyclic voltammograms of the (a) AP and (b) imine solution. The measurements were conducted by dissolving 0.023 M AP or imine in a 1.0 M H_2SO_4 solution. The scanning rate is 50 mV/s.

The bromination could take place through the organic substrates reacting with bromine or HOBr. It is worthwhile to mention that HOBr can act as: 1) a bromination agent [38]; 2) an oxidation agent [39]; and 3) a hydroxylation reactant [40-42]. The OKN mechanism has discussed how HOBr acts as a hydroxylation agent [40-42]. The production of 1,4-benzoquinone (1,4-BQ) could happen via the reaction of imine with H_2O in an acidic environment, which is a well-known process [43]. Separate mass spectrometry analysis confirms that bromine reacts with 4-aminophenol producing $(O)C_6H_4(NBr)$ in acidic solution.

Conclusions

This study investigated the kinetics and mechanism of the light-mediated bromate-4-aminophenol reaction and showed that chemical oscillations in the system exist over broad concentration ranges of bromate, 4-aminophenol and sulfuric acid. However, as illustrated by the phase diagrams in a three-dimensional concentration space, the oscillatory behavior is more susceptible to the ratio of $[BrO_3^-]/[AP]$ than their actual concentrations. Within the parameter regime where the system oscillates, increasing the concentration of bromate or AP shows the same kind of influence on the induction time and the number of oscillations as increasing the applied light intensity.

Quenching experiments suggest that the bromate-AP photochemical oscillator is bromide-controlled. Therefore, the autocatalytic production of $HBrO_2$ through the reduction of bromine dioxide radicals by organic substrates could still be responsible here for the nonlinear feedbacks, similar to the bromate-based chemical oscillators reported earlier [24,26,33]. Meanwhile, this photochemical oscillator can also be controlled by ethanol, which reacts with acidic bromate to produce HOBr, an intermediate which reacts

with bromide ions [41] and acts as a radical scavenger to remove organic radicals [6].

Several intermediates are identified in this report with mass spectrometry and NMR

methods. The detection of small amounts of hydroquinones suggests the occurrence of

photoreductions of the quinones [29]. These results should greatly facilitate the further

investigations on the bromate-aromatic compounds reactions, which have exhibited both

subtle photo-sensitivity and interesting reaction dynamics.

References

1. R. J. Field and M. Burger (Eds.), Oscillations and Traveling Waves in Chemical Systems, Wiley-Interscience, New York, 1985.

2. S. K. Scott, Chemical Chaos, Oxford University Press, 1994.

3. I. R. Epstein and J. A. Pojman, An Introduction to Nonlinear Chemical Dynamics, Oxford University Press, New York, 1998.

4. J. Wang, P. G. Sørensen and F. Hynne, J. Phys. Chem. 98, 1994, 725.

5. G. Schmitz, L. Kolar-Anic, S. Anic, T. Grozdic and V. Vukojevic, J. Phys. Chem. A, 110, 2006, 10361.

6. P. I. Kumli, M. Burger, M. J. B. Hauser, S. C. Müller and Z. Nagy-Ungvarai, Phys. Chem. Chem. Phys., 5, 2003, 5454.

7. J. L. Hudson, M. Hart and D. Marinko, J. Chem. Phys., 71, 1979, 1601.

8. R. H. Simoyi, A. Wolf and H. L. Swinney, Phys. Rev. Lett., 49, 1982, 245.

9. M. Dolnik, I. Schreiber and M. Marek, Phys. Lett. A, 100, 1984, 316.

10. R. Blittersdorf, A. F. Munster and F. W. Schneider, J. Phys. Chem., 96, 1992, 5893.

11. V. Petrov, V. Gaspar, J. Masere and K. Showalter, Nature, 361, 1993, 240.

12. G. Rábai and I. Hanazaki, J. Phys. Chem., 98, 1994, 10550.

13. V. Gaspar, G. Bazsa and M.T. Beck, Z. Phys. Chem. – Leipzig, 264, 1983, 43.

14. S. Kéki, G. Székely and M. T. Beck, J. Phys. Chem. A, 107, 2003, 73.

15. J. R. Bamforth, J. H. Merkin, S. K. Scott, R. Toth and V. Gáspár, Phys. Chem. Chem. Phys., 3, 2001, 1435.

16. S. Kadar, J. Wang and K. Showalter, Nature, 391, 1998, 770.

17. O. Steinbock, V. Zykov and S.C. Müller, Nature, 366, 1993, 322.

18. S. L. Kuhnert, K. I. Agladze and V. I. Krinsky, Nature, 337, 1989, 244.

19. S. Kadar, T. Amemiya and K. Showalter, J. Phys. Chem. A, 101, 1997, 8200.

20. V. K. Vanag and I. Hanazaki, J. Phys. Chem. A, 101, 1997, 2147.

21. K. R. Sharma and R. M. Noyes, J. Am. Chem. Soc., 98, 1976, 4345.

22. J. A. Odutola, C. A. Bohlander and R. M. Noyes, J. Phys. Chem., 86, 1982, 818.

23. D. S. Huh, H. S. Kim, J. K. Kang, Y. J. Kim, D. H. Kim, S. H. Park, K. Yadav and J. Wang, Chem. Phys. Lett., 378, 2003, 78.

24. J. Wang, K. Yadav, B. Zhao, Q. Gao and D. Huh, J. Chem. Phys., 121, 2004, 10138.

25. A.K. Horváth, I. Nagypál and I.R. Epstein, J. Am. Chem. Soc., 124, 2002, 10956.

26. B. Zhao and J. Wang, Chem. Phys. Lett., 430, 2006, 41.

27. B. Zhao and J. Wang, J. Photochem. Photobiol. A: Chem., 192, 2007, 204.

28. M. Harati, S. Amiralaei, J. Green andWang, Chem. Phys. Lett., 439, 2007, 337.

29. H. Görner, Photochem. Photobiol., 82, 2006, 71.

30. G. Lente and J. H. Espenson, J. Photochem. Photobiol. A, 163, 2004, 249.

31. I. Amada, M. Yamaji, S. Tsunoda and H. Shizuka, J. Photochem. Photobiol. A, 95, 1996, 27.

32. R. J. Field, E. Körös and R. M. Noyes, J. Am. Chem. Soc., 94, 1972, 8649.

33. I. Szalai and E. Körös, J. Phys. Chem. A, 102, 1998, 6892.

34. Z. Ungvàrai-Nagy and I. Zimányi, React. Kinet. Catal. Lett., 31, 1986, 249.

35. K. Pelle, M. Wittmann, Z. Noszticzius, R. Lombardo, C. Sbriziolo and M. L. Turco Liveri, J. Phys. Chem. A, 107, 2003, 2039.

36. J. Horváth, Z. Ungvàrai-Nagy and S. C. Müller, Phys. Chem. Chem. Phys., 3, 2001, 218.

37. E. Breitmaier and W. Voelter, Carbon-13 NMR Spectroscopy, VCH, Würzburg, 1987.

38. A. Sirimungkala, H. D. Försterling, V. Dlask and R. J. Field, J. Phys. Chem. A, 103, 1999, 1038.

39. E. Chikwana, A. Otoikhian and R. H. Simoyi, J. Phys. Chem. A, 108, 2004, 11591.

40. S. Kawanishi and M. Murata, Toxicology, 221, 2006, 172.

41. M. Orban, E. Körös and R. M. Noyes, J. Phys. Chem., 83, 1979, 3056.

42. P. Herbine and R. J. Field, J. Phys. Chem., 84, 1980, 1330.

43. P. Sukhai and R. A. McClelland, J. Chem. Soc., Perkin Trans. 2, 1996, 1529.

Chapter 6 Breathing, Merging, and Packing Pulses in the Ferroin-Bromate-Pyrocatechol Reaction

Chemical reactions coupled with mass transportations may exhibit various concentration profiles such as pulses in spatially extended media [1-8]. In general, those chemical pulses propagate at a constant speed and amplitude [1]. Theoretical studies have suggested that those propagating pulses may become unstable, leading to the development of breathing and backfiring pulses [9, 10]. Despite the extensive research on this topic, motivated by its potential applications in broad areas such as catalysis, material science and neurobiology [11-13], etc. few reaction systems show the behavior supporting the possible occurrence of the aforementioned instabilities [14-18]. Herein, we present the experimental observation of breathing, merging, and packing pulses in the bromate-pyrocatechol reaction catalyzed by ferroin.

Our investigation was carried out by adding the reactant solution to a capillary tube with an inner diameter of 1.8 mm. The evolution of the spatially extended medium was then monitored with a CCD camera equipped with a zoom lens. The CCD camera was connected to a personal computer running a frame grabber program (Matrox Imaging Library). The reaction solution was prepared by mixing all reagents in a stirred batch reactor, where the reaction was allowed to evolve for 60 minutes before being transported into the tube. The space-time plots presented in the following are generated by sequentially piling up the one-dimensional picture, where the horizontal and vertical axes are, respectively, the space and time. The time evolves in an upward direction. Bright and

dark gray levels correspond to the oxidized and reduced state of the metal catalyst ferroin, respectively.

Figure 6.1 presents a typical scenario where dark colored (i.e., ferroin) waves are developed from the two ends of the capillary tube. These waves appear initially as propagating fronts. Interestingly, both fronts later reverse the propagation direction, showing the features of breathing pulses. Since the medium is a closed reaction system, where no fresh chemicals are supplied, the width of these breathing pulses varies each time and could only repeat a few times. Eventually, they were replaced by stable pulses emitted at the center of the tube. Under the conditions investigated here, the reaction-diffusion medium initially has a light blue color (i.e. white in grayscale), indicating that the system is at an oxidized state. From a kinetic point of view, it implies that the reduction of ferriin by pyrocatechol is slower than its autocatalytic production. Those emerging wave activities therefore correspond to the reduction waves reported earlier in the classic Belousov-Zhabotinsky (BZ) reactions [1]. Figure 6.1 illustrates that for those reduction waves it is the tail, not the front having a sharp interface, which is opposite to the oxidation waves.

Figure 6.1 Space-time plots of propagating pulses achieved under the conditions [NaBrO$_3$] = 0.066 M, [H$_2$SO$_4$] = 1.25 M, [pyrocatechol] = 0.037 M, and [Fe(phen)$_3^{2+}$] = 3.0 x 10^{-3} M. Time period shown here is between 125 and 400 min after injecting the solution into the 250 mm long tube. The length of the solution is 47 mm.

In Figure 6.2, propagating pulses are formed periodically at the two ends of the capillary tube and, similar to other regular chemical waves, annihilate each other upon their collision at the centre of the medium. During the above process, pulses emerging at the left side become noticeably wider each time and eventually become a propagating front. Interestingly, upon its collision with the reduction pulses formed from the right edge, they merge rather than annihilate each other, as indicated by the gradual receding rather than spontaneous disappearance of the propagating front. The merging scenario of a front and a pulse appears to be universal in this chemical system. The transition from a propagating pulse to a propagating front also took place over a broad reaction conditions in the system reported here. As illustrated in Figure 6.2, after the appearance of the propagating front, the medium returns to emit pulses at the left edge.
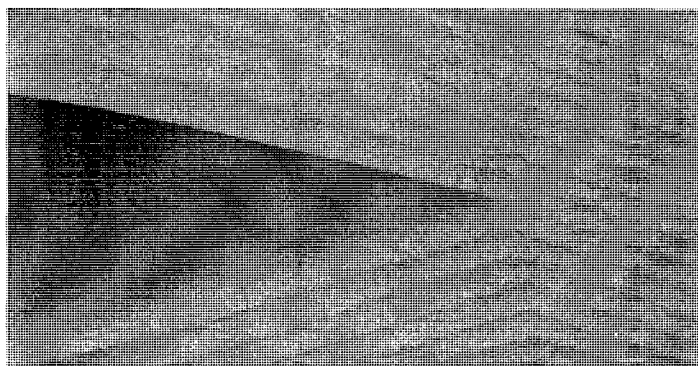
Figure 6.2 Space-time plots showing the merging pulses. Reaction conditions are $[NaBrO_3] = 0.066$ M, $[H_2SO_4] = 1.30$ M, $[pyrocatechol] = 0.037$ M, and $[Fe(phen)_3^{2+}] = 3.0 \times 10^{-3}$ M. Time period shown here is between 300 and 350 min after placing the solution into the 250 mm long tube. The length of the solution is 56 mm.

Also shown in Figure 6.2 is that the propagation of the following pulses is greatly slowed down when it approaches to the merged front, as evidenced by the significant

decrease in the slope of the dark strip, which is the inverse of the propagation velocity. Although the influence of the merged wave activity becomes weaker in time and space, the reduction in the propagation velocity of the preceding pulses shortens the distance between the following pulses, leading to the possible occurrence of packing phenomenon.

In Figure 6.3 wave formation takes place spontaneously both at the centre and at the two free ends of the capillary tube, as a result of increasing the initial concentrations of bromate and pyrocatechol. Because wave activities emerged inside the tube are less frequent than the pulses developed at the ends of the tube, the medium is eventually conquered by these high frequency pulses. During the above transition process, interactions of pulses show strong influence on the following pulse, where the slow down in the propagation of the preceding pulse results in a clear decrease in wavelength, leading to the occurrence of packing scenario [16]. Since this is a closed reaction system, the behaviour could only be achieved within a short period of time. Afterwards, pulses propagating at a constant speed with a constant wavelength are achieved, which last for a few hours until the whole medium turns into a homogeneous red color.

A close examination of the result shown in Figure 6.3 revealed that for those high frequency pulses generated at the right end of the tube, not every one of them could make its way into the tube. Indeed, only every other pulse was able to propagate and collide with the waves emerged at the centre, showing a type of period-doubling behavior. Presumably the failure of propagation is because the medium is still refractory after the passing through of the previous wave and has yet to return to the state where it can support further wave activity.
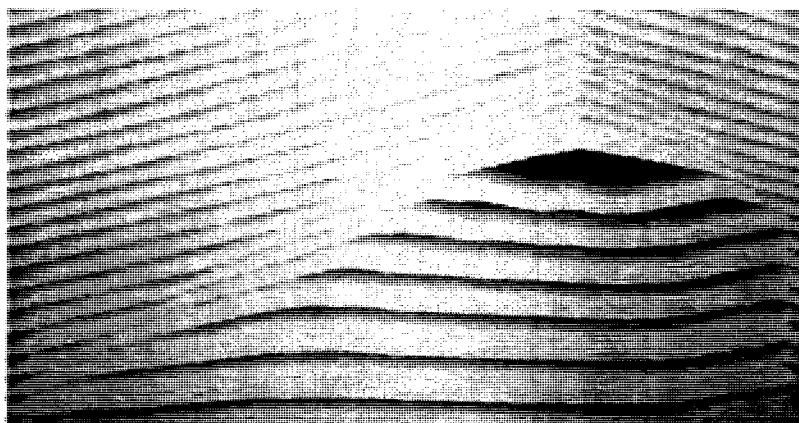
Figure 6.3 Space-time plots showing the packing phenomenon. Reaction conditions are [NaBrO₃] = 0.068 M, [H₂SO₄] = 1.30 M, [pyrocatechol] = 0.040 M, and [Fe(phen)₃²⁺] = 3.0 x 10⁻³ M. Time period shown here is between 90 and 230 min after injecting the solution into the 250 mm long tube. The length of the reaction solution is 48 mm.

Systematic examination of our experiments indicates that the behavior of propagation failure typically takes place during the initial reaction stage. Figure 4 presents an example of propagation failure collected between 150 and 240 min after injecting the reaction solution into the capillary tube. Note that within the first 150 minutes there was no wave activity in the medium. Such a long induction time is consistent with the temporal kinetics in a stirred reactor, in which chemical oscillations of the studied system have a very long induction time.

Our kinetic study also shows that oxygen inhibits the oscillatory phenomena, quenching the system to a reduced state [19,20]. In this spatially extended medium, both ends of the tube are exposed to air. As a result of the oxygen influence, the oxidized solution is quenched to a reduced state. This explains why wave activity (i.e., reduction

waves) always starts at the two free ends of the glass tube. Under the conditions

investigated in Figure 6.4, while the oxygen becomes capable of quenching the oxidation

state at the two ends, the bulk of the medium is still far away from a bifurcation point at

which a transition from an oxidized to oscillatory state could take place. Consequently,

the reduction waves initiated at the two ends could not successfully intrude into the tube.

As the reaction evolves in time, the system eventually reaches the state where reduction

waves are supported by the system. Fig. 6.4 shows that there is no obvious change in how

far the wave can propagate through during the above transition period. Since the

spontaneous initiation of pulses is connected to the interface with air, waves may not

appear simultaneously at the two ends. In addition, it is unnecessary for the pulses to

appear periodically at each end. For example, in Fig. 6.4 the reduction pulse at the left

end emerges irregularly.
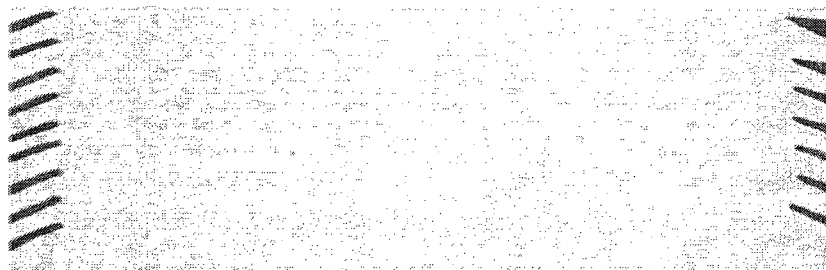
Fig. 6.4 Space-time plots showing the behavior of propagation failure. This is the same experiment as presented in Fig. 2, except that time period shown here is between 150 and 240 after setting up the reaction-diffusion medium.

The propagation failure phenomenon presented in Fig. 6.4 appears to be ubiquitous in

the system studied here. Fig. 6.5 summarizes the dynamical behavior of the propagating

pulses in the pyrocatechol and bromate concentration phase plane, where the conditions at

which the system does produce any wave activity is denoted by x. The color of the no

wave activity medium is red, implying that the system is at the reduced state. Notably,

there is a narrow region between the conditions where no waves could be achieved and

the parameters which support the formation of propagating pulses. Only the propagation

failure phenomena could be seen within such a narrow region denoted by squares.
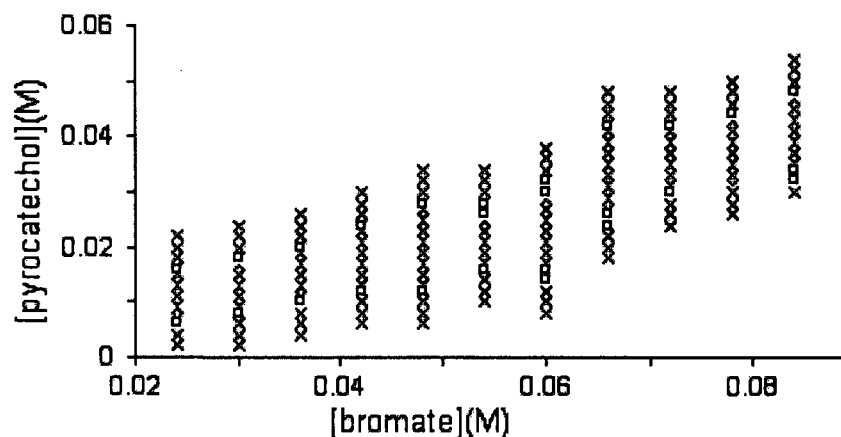
Figure 6.5 Phase diagram showing the behavior of pulse instability in the ferroin-catalyzed bromate-pyrocatechol medium, in which (×): no wave; (□): propagation failure; and (◊) propagation failure and merging. Other reaction conditions are $[H_2SO_4] = 1.40$ M, and $[Fe(phen)_3^{2+}] = 3.0 \times 10^{-3}$ M.

In summary, this study provides an experimental system which is capable of producing

various pulse instabilities. A unique kinetic property of this reaction is that pyrocatechol

and ferroin can both be oxidized auto-catalytically by bromine dioxide radicals, forming

coupled nonlinear feedbacks. It has been emphasized in the earlier report that the co-

existence of two types of metal catalysts was crucial for their observed pulses instability

[16]. This experimental study further highlights that the presence of coupled nonlinear

feedbacks may be essential for the occurrence of pulse instabilities. Considering that there was only limited success in finding a reaction-diffusion medium showing pulse instabilities [14-18], the above information shall greatly facilitate the future study on this important nonlinear behavior.

References

1. R. Kapral and K. Showalter, Eds. Chemical Waves and Patterns (Kluwer, Dordrecht, The Netherlands, 1995).

2. R. Evans, C. R. Timmel, P. J. Hore and M. M. Britton, J. Am. Chem. Soc., 128, 2006, 7309.

3. V. K. Vanag and I. R. Epstein, Proc. Nat. Acad. Sci., 100, 2003, 14635.

4. O. Steinbock, P. Kettunen and K. Showalter, Science, 269, 1995, 1857.

5. A. Magnani, N. Marchettini, S. Ristori, C. Rossi, F. Rossi, M. Rustici, O. Spalla and E. Tiezzi, J. Am. Chem. Soc., 126, 2004, 11406.

6. U. Storb, C. R. Neto, M. Bär and S. C. Müller, Phys. Chem. Chem. Phys., 5, 2003, 2344.

7. M. R. Roussel and J. Wang, Phys. Chem. Chem. Phys., 4, 2002, 1310.

8. A. F. Taylor, B. R. Johnson and S. K. Scott, Phys. Chem. Chem. Phys., 1, 1999, 807.

9. L. Brusch, M. G. Zimmermann, M. Hecker, M. Bär and A. Torcini, Phys. Rev. Lett., 85, 2000, 86.

10. M. Argentina, O. Rudzick and M. G. Velarde, Chaos, 14, 2004, 777.

11. M. O. Vlad, L. L. Cavalli-Sforza and J. Ross, Proc. Nat. Acad. Sci., 101, 2004, 10249.

12. J. Wolff, A. G. Papathanasiou, I. G. Kevrekidis, H. H. Rotermund and G. Ertl, Science, 294, 2001, 134.

13. Y. Masaoka, N. Yoshimura, M. Inoue, M. Kawamura and I. Homma, Neurosci. Lett., 412, 2007, 45.

14. C. Christoph, E. Eiswirth, N. Hartmann, R. Imbihl, I. Kevrekidis and M. Bär, Phys. Rev. Lett., 82, 1999, 1586.

15. N. Manz, S. C. Müller and O. Steinbock, J. Phys. Chem. A, 104, 2000, 5895.

16. N. Manz and O. Steinbock, Chaos, 16, 2006, 037112.

17. L. Yang, A. M. Zhaboinsky and I. R. Epstein, Phys. Chem. Chem. Phys., 8, 2006, 4647.

18. M. Pomprompanya, S. C. Müller, H. Ševčíková, Phys. Chem. Chem. Phys., 4, 2002, 3370.

19. M. Harati and J. Wang, J. Phys. Chem. A, 112, 2008, 4241.

20. M. Harati and J. Wang, Z. Phys. Chem., 222, 2008, 997.

Chapter 7 The Formation of Complex Spatiotemporal Behavior in the Ferroin-Bromate-Pyrocatechol Medium

Introduction

Pattern formation in both excitable and oscillatory systems has been one of the most important issues in the investigation of nonlinear dynamics which are frequently encountered in chemistry [1-12], biology [13-18] as well as other physical systems in nature [19, 20]. Among existing chemical oscillators, the Belousov-Zhabotinsky (BZ) reaction is perhaps the most employed model system for studies of both temporal and spatiotemporal nonlinear behaviors [11, 12, 21-29]. In the study of spatial temporal structures, a drawback of the classical BZ reaction is the production of gas bubbles from the organic substrate malonic acid, which may consequently implement unexpected hydrodynamic effects, leading to the onset of complex patterns [11, 29]. Solving this dilemma, there have been a large number of efforts dedicated to exploring new organic substrates to substitute malonic acid [10, 11, 31]. Unfortunately, those modified BZ reactions have not yielded such a wide range of nonlinear behaviors as observed in the malonic acid-BZ system.

In 1982, Farage et al. reported a long time series of oscillatory behaviour in the uncatalyzed bromate-1,4-cyclohexandione (CHD) reaction, which opened a new door toward studying pattern formation in a bubble free reaction-diffusion medium [31]. Later, Kurin-Csörgei and co-workers demonstrated that bromate-CHD-ferroin media were

capable of producing various traveling waves [32]. Furthermore, Zhabotinsky et al. showed that this modified BZ reaction can support the formation of crossing waves whether the reaction diffusion system constitutes aqueous or gel medium [32]. Recent studies by Steinbock and co-workers on the above system showed that this system could produce wave activity with anomalous dispersion relationship [33, 34].

According to Steinbock et al., the most important factor determining the characteristics of spiral tip motion is the kinetics of the reaction between the organic substrate and bromate [42, 43]. It is therefore interesting to provide examples of meandering spiral waves using different organic substrate and/or oxidizing agents. In last part of this chapter, we investigated the dependence of spiral tip trajectory on various parameters in the pyrocatechol-bromate system. This system does not produce gases and exhibits very long-term chemical wave activity, which makes it an attractive system for further investigation of nonlinear spatiotemporal behaviours such as spiral tip trajectory and anomalous dispersion in a closed, thin-layer system [30, 44].

Recently we reported oscillatory behavior in both uncatalyzed and catalyzed bromate-pyrocatechol reactions and showed the feasibility of chemical wave formation in this gas-free system when ferroin was employed as the metal catalyst. Herein, we investigated pattern formation in this new bubble free reaction-diffusion medium. As presented in the following, in addition to target pattern and spiral waves commonly seen in spatially extended medium, the ferroin-bromate-pyrocatechol system also produces waves with anomalous dispersion relationship, which consequently results in the wave breakup and the formation of complex patterns. The unique dependence of the dynamics of the system on the ratio of bromate and pyrocatechol also leads to the subtle response of the wave propagation speed to the changes of bromate (or pyrocatechol) concentration. Besides, the

great light sensitivity makes this system an appropriate candidate to investigate perturbed wave activities.

Experimental Procedure

Stock solutions of $NaBrO_3$ (Aldrich, 99%), 0.6 M, and sulfuric acid (Aldrich, 95-98%), 4.0 M, were prepared with double-distilled water. Ferroin, 0.025 M, was prepared from a calculated amount of $FeSO_4.7H_2O$ (Aldrich, 99+%) and 1,10-phenanthroline (Aldrich, 99+%). Pyrocatechol (Sigma, 99%) was directly dissolved in the reaction mixture. The reaction solution was prepared by mixing all reagents in a stirred batch reactor, where the reaction was allowed, depending on the study of wave formation, to evolve for about 1 minute. Chemical waves were investigated by spreading the reaction solution mixture in a thin space (0.5 mm) between two microscope slides. Therefore, loosely speaking the studied reaction-diffusion medium has no free surface exposed to air. For those experiments exhibiting spontaneous transition to complex spatial structures, the experiments were repeated several times with 0.3 mm thickness solution layer between the two microscopic slides and the same results were achieved. Throughout this research, evolution of the spatially extended medium was monitored with a CCD camera equipped with a zoom lens. The CCD camera was connected to a personal computer running a frame grabber program (Matrox Imaging Library).

Chemical waves in bead system were investigated by spreading the reaction solution mixture onto a thin layer of cation-exchange resin loaded with ferroin. The analytical grade 100-200 mesh ion-exchange resin (Dowex 50W-X4) was purchased from the Fisher Scientific Co. First, 30 g of ion-exchange resin was washed five times with doubly distilled water to modify its acidity [43]. Then it was filtered and used to load ferroin with

desired concentrations. To load the catalyst ferroin onto the resin, filtered resin was mixed with ferroin solution (30 ml of 0.002 M, unless otherwise mentioned in text) and mixture was stirred vigorously at 600 rpm for overnight. The ferroin solution became transparent at the end of the process, presumably due to the complete absorption of ferroin by the cation bead. The mixture was left unstirred for 30 minutes and then we removed solution on top of bead. Ferroin loaded bead have been washed three more times through adding 60 ml of doubly distilled water and stirring for 10 minutes each time. This washing is useful in removing imperfect bead and any impurities. It is also beneficial in reducing the amount of bead floating on the top of reaction mixture in the Petri dish. To begin our experiments, 22.5 ml of the reaction mixture was mixed with 3.0 (± 0.1) g of the bead loaded with ferroin in a Petri dish (9 cm in diameter), in which the bead formed a thin film of 0.5 (± 0.1) mm on the bottom of the Petri dish. The Petri dish was maintained at room temperature of 20 ± 1°C. Confirming spiral tip movement and abnormal behaviour, some experiments have been repeated for several times.

The perturbation of light was implemented with a halogen lamp equipped with dual bifurcated optic fibers and continuous variable light level (Fisher Scientific, Model DLS-100HD, 150 mW/cm^2). The illumination was implemented by placing one of the fibers on the top of the microscopic glass.

Results and Discussions

We characterized propagations of the first and second stage wave activity in which spatial location of a wave segment have been followed in time. The propagation speed of the second stage wave activity has also been measured at later stages of wave activity and there was a decline in propagation speed. For the first stage, samples were taken from

stirred batch reactor immediately after mixing all chemicals together and spread between two microscopic glasses right away. Initial wave analyzing was done whenever wave activity started in the system. In all cases for the first stage we calculate the speed of propagating waves; while system was also capable of supporting circular wave and wildfire activity which washed out all the wave activity all of sudden in the thin layer. Those patterns last for up to 150 seconds which depending on the initial conditions. Furthermore, the propagating speed of second stage of wave activity also obtained with sampling after 50 minutes of starting the reaction in stirred batch reactor. This new chemical wave activity lasted for up to 360 minutes, depending on initial conditions. We analyzed wave propagation speed after 30 min of their appearance in all cases; conditions further away from oscillatory window caused shorter period of the second stage wave activity. In all cases we measured only the velocity of the oxidizing waves.

Figure 7.1 presents propagation speed of waves in the first stage as function of initial concentration of (a) bromate, (b) sulfuric acid, (c) pyrocatechol, and (d) ferroin, respectively. Considering bromate, in part (a), propagation speed amplified with increasing bromate concentration. When the concentration of bromate was lower than 0.124 M, the system did not exhibit circular wave activity; however, there was just development of propagating waves and wildfire. The propagation speed of the first stage of wave activity under different concentrations of acid is presented in part (b). The propagation speed for the first stage waves change in a semi-circular way as acid concentration increases and then it is almost constant with additional increasing in acid concentration. Furthermore, the speed of propagation decreased toward the end of wave activity. As shown in Fig. 7.1 (c), there is a minimum in wave speed versus pyrocatechol concentration i.e., with increasing the concentration of pyrocatechol wave speed

decreases first and then it increases. In spite of the classic BZ reaction, in this system first

stage wave propagation depends on organic substrate, pyrocatechol [35, 36].
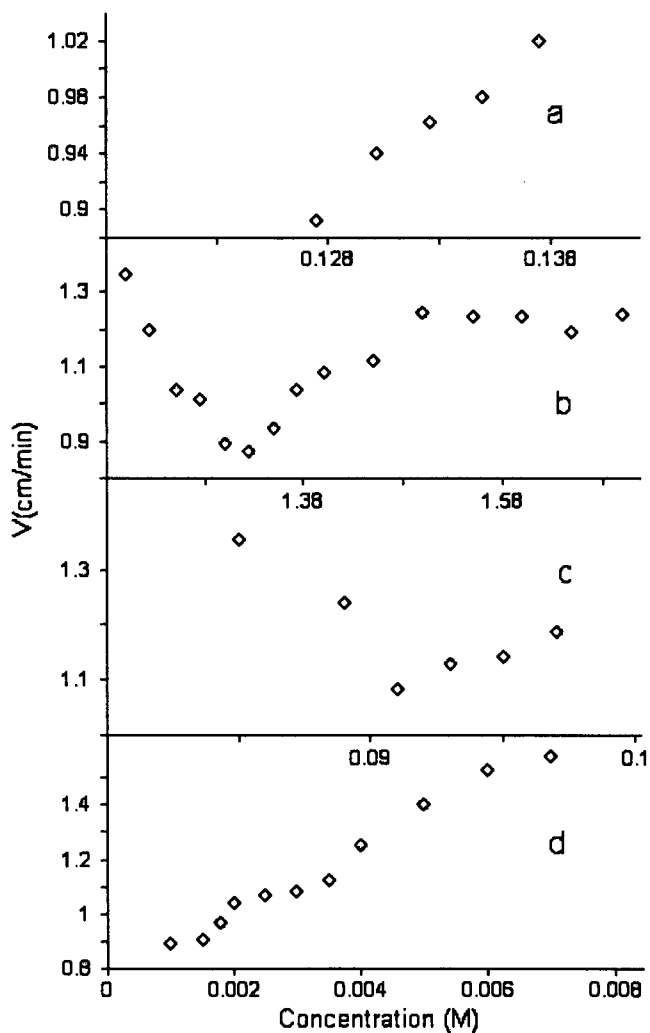
Figure 7.1 Propagation speed of waves in the first stage as function of initial concentration of (a) bromate, (b) sulfuric acid, (c) pyrocatechol, and (d) ferroin, under condition: (a) [pyrocatechol] = 0.091 M, [acid] = 1.40 M and [ferroin] = 0.003 M; (b) [pyrocatechol] = 0.091 M, [bromate] = 0.1248 M and [ferroin] = 0.003 M; (c) [bromate] = 0.1248 M, [acid] = 1.40 M and [ferroin] = 0.003 M; (d) [pyrocatechol] = 0.091 M, [bromate] = 0.1248 M and [acid] = 1.40 M.

As shown in Figure 7.1, Ferroin concentration has different effects on the first and the second stage wave propagation speed shown (Figure 7.1 (d) and 7.2 (d)). According to our observations, higher concentration of ferroin favours the occurrence of wildfire in the first stage. Increase in ferroin concentration increases propagation speed in the first stage.

Figure 7.2 shows changes of second stage wave velocity versus concentration of (a) bromate, (b) acid, (c) pyrocatechol, and (d) ferroin. Increasing concentration of bromate has the same influence on propagating wave speed in the second stage as in the first one. System showed a better contrast in lower concentrations of bromate. The system did not exhibit any wave activity at all when concentration of bromate was lower than 0.115 M. The propagation speed of the second stage waves under different acid concentrations is presented in Figure 7.2 (b). In all cases, the rate was measured 30 minutes after their appearance. This plot indicates that the second stage propagation speed increases as the initial concentration of acid increases. No wave activity was observed when the concentration of acid is higher than 1.70 M or lower than 1.20 M. Increasing pyrocatechol concentration has the opposite effect on wave speed than acid and bromate. Increase in ferroin concentration decreased propagation speed in the second stage. In lower ferroin concentration system displayed higher wave activities but contrast was not adequate for visibility. On the other hand, increasing the ferroin concentration results in better contrast but reduces the lifetime of the patterns formed in the system. Therefore we could not calculate wave speed when concentration of ferroin was below 0.0018 M. In constant ferroin concentration, propagation speed decreased at the later stages.
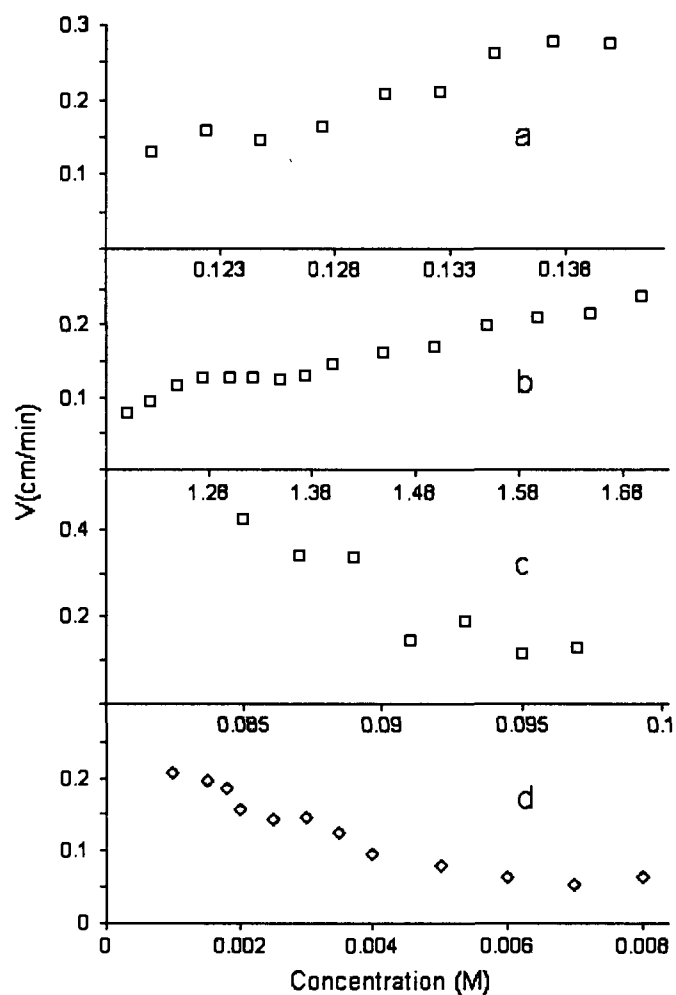
Figure 7.2 Plot of the wave speed the second stage waves as a function of initial concentration of (a) bromate, (b) sulfuric acid, (c) pyrocatechol, and (d) ferroin. All conditions are the same as Fig. 7.1.

For a long time, a universal feature of excitable media was considered to be normal dispersion of excitation waves, until theoretical studies by Elphick et al. and then experimental results reported by Steinbock et al. described the existence of anomalous dispersion [37]. Figure 7.3 shows anomalous dispersion in the ferroin-pyrocatechol-bromate system. Under different experimental conditions, waves propagate faster at the

beginning and then they propagate slower which makes waves having different distances in different areas. This behaviour in the system is not limited to a particular set of initial conditions. However, it mostly has been observed whenever concentration of bromate or acid is very low which implies that the system is far away from oscillatory condition and it is in excitable state.
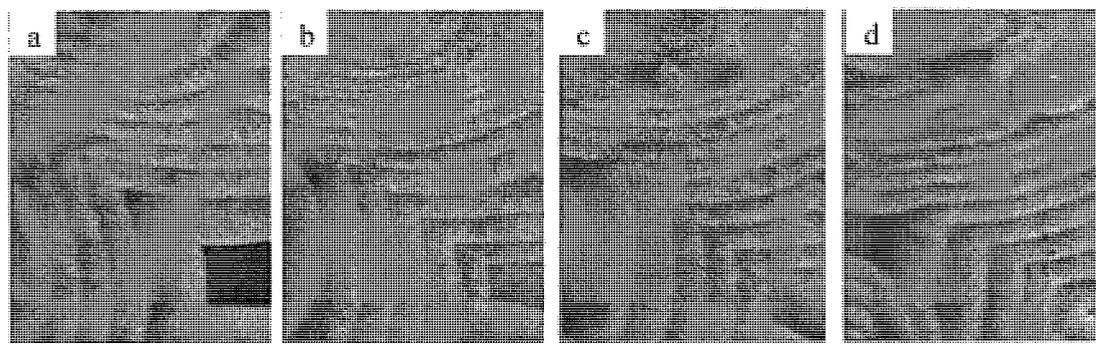
Figure 7.3 Snapshots of anomalous dispersion behaviour, in the second stage, were taken at (a) 151, (b) 164.3, (c) 167, and (d) 192 min after spreading solution between two glasses. The initial reaction conditions are [pyrocatechol] = 0.091 M, [bromate] = 0.1248 M, [acid] = 1.30 M, [ferroin] = 0.003 M.

We carried out some stirred batch reactor experiments and there was no oscillatory behaviour in the system which shows that the system is not in an oscillatory window under reported conditions here,. Because of this abnormal behaviour in wave activity, the distance between a leading wave and its immediate successor usually decreases continuously and consequent to that they can come to direct front-to-back collision which then can lead to wave break-up. This wave break-up behaviour is shown in Figure 7.3 (c) and (d).

Figure 7.4 presents responses of the second stage waves to light illumination, where a beam of halogen light of the intensity 50 mW/cm^2 was applied locally for 1 minute. Figure 7.4 (a) is a snapshot taken right before illumination and other two snapshots were taken at (b) 1, (c) 12 min after removing light. As it is shown in Figure 7.4 (b) which has been taken right after removing the illumination, indicates that the illumination of light is able to quench local wave activity. After a short transitory time, the illuminated area was able to resume its reactivity by becoming a new center for commencing of wave activity spontaneously. Photosensitivity of this new system in homogeneous system is different than either the classical ferroin-catalyzed BZ reaction or bromate-1,4-cyclohexandione-ferroin system [12, 38]. Furthermore, we observed light-quench oscillations in the stirred batch reactor; therefore, we tried global light quench experiment under the same condition as local light quench. Illuminating the system with light intensity of 150 mW/cm^2 globally for 3 minutes quenched all wave activity in the system. It is shown by global quenching experiment that light is able to quench wave activity globally. The system regained its wave activity immediately after removing the light and wave activity after illumination was different from wave pattern before illumination.

As reported in earlier studies, the wave velocity in the BZ reaction is strongly dependent on the initial concentrations of sulfuric acid and sodium bromate [35, 36, 39-41]. The form of the concentration dependence of acid and bromate on velocity is accepted to be the square root of the product of the initial reactant concentrations [35, 36].

For this reason, our results are presented in this form. The calculated best fit for the data with the square root power dependence is of the form

$$v \text{ (cm/min)} = 0.2594 \times ([H_2SO_4]^{1/2}[BrO_3^-]^{1/2}) + 0.1342$$

A linear dependence of wave velocity on the product $[H_2SO_4]^{1/2}[BrO_3^-]^{1/2}$ is shown in Figure 7.5 with correlation factor (R) of 0.8762. Field and Noyes demonstrated that trigger wave propagation in the BZ reaction depends primarily on the autocatalytic generation of $HBrO_2$. A linear least-square fit of the data in Fig. 7.5 in excellent agreement with the experimental velocity dependence found in the BZ reaction. Furthermore, we tried to fit wave velocity data with $[H_2SO_4][BrO_3^-]$ and surprisingly it shows a linear relationship with the same formula mentioned above and its correlation factor was 0.8719. According to these two linear fitting, it seems unlikely that for pyrocatechol-acidic bromate system the autocatalytic generation of $HBrO_2$ is the dominant factor in wave propagation in this system which makes this system different than classical BZ reaction.

The propagation speed of the chemical waves in ferroin loaded-cationic bead has been analyzed at different stages, e.g. the initial stage during which waves just emerged, and the later stage from 100 to 600 minutes after spreading reaction mixture in the Petri dish.
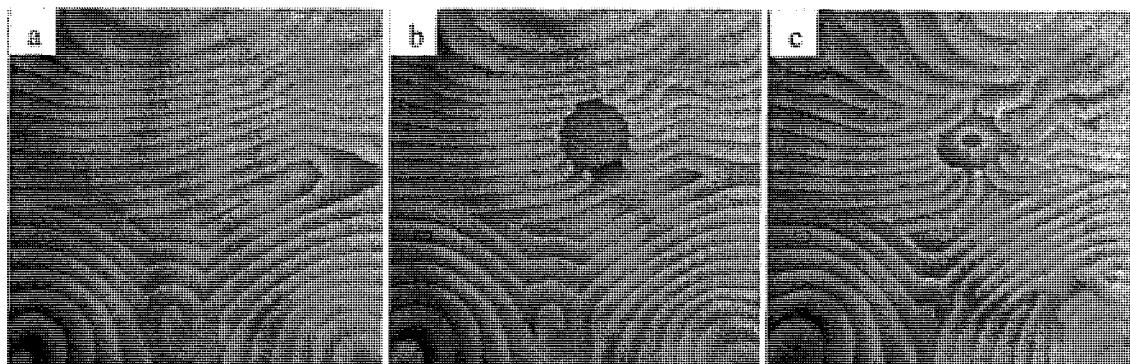
Figure 7.4 Photosensitivity of the second stage waves. Snapshots were taken at (a) 1 minute before illumination, (b) 1, and (c) 12 min after removing light illumination. Composition of the system is [pyrocatechol] = 0.091 M, [bromate] = 0.1248 M, [acid] = 1.40 M, [ferroin] = 0.003 M.
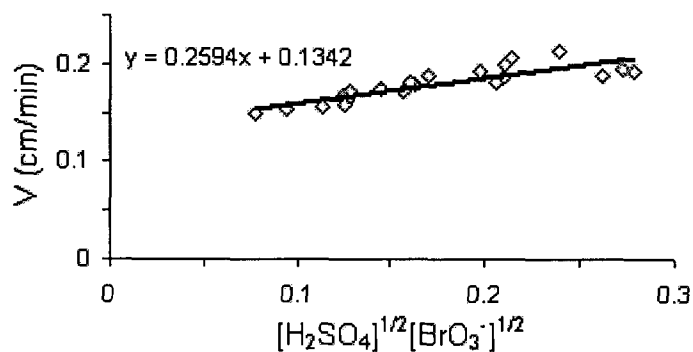
Figure 7.5 Dependence of wave velocity on the $[H_2SO_4]^{1/2}[BrO_3^-]^{1/2}$

Figure 7.6 characterizes the propagation speed of the waves between 200 and 450 minutes, in which the spatial location of a wave segment is plotted versus time. Linearity of these curves indicates a constant wave velocity, independent of time or curvature of the

band in a short period of time. The velocity of successive waves slightly decreases in time because of reactant consumption. This plot shows that wave propagates at average rates of 0.0724 and 0.0629 cm/min at 200 and 450 min, respectively. The decline in wave speed is due to the aging of the reaction mixture. However, within a short time frame, the wave speed is almost constant. The decrease in wave propagation speed as times goes on is one of the common aspects of the closed reaction system. While in most conditions studied here chemical waves last between 600 and 800 min, in some conditions it lasted for up to 1300 minute. In this report, the analysis of chemical wave speed has been done after 200 min of the first appearance of wave activity in the Petri dish.
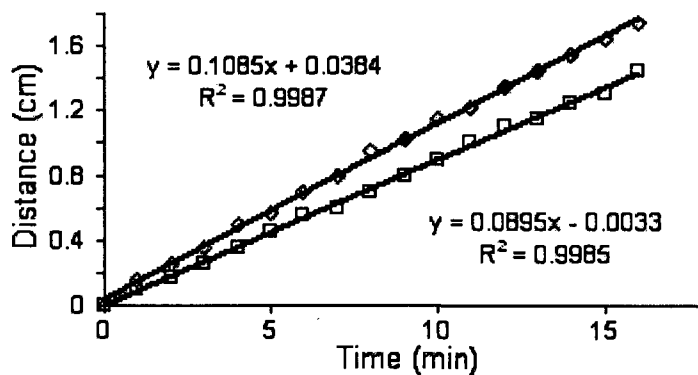
Figure 7.6 Wave propagation speed under reaction conditions: [bromate] = 0.068 M, [acid] = 1.4 M, [pyrocatechol] = 0.035 M, [ferroin] = 0.002 M, and 3.0 g of bead; wave speed was calculated at (◊) 200 min and (□) 450 min after appearing of wave activity.

The dependence of wave velocity on initial concentrations of different reagents is shown in Figure 7.7. This Figure shows that mass of the bead has little effect on wave

velocity. As it is demonstrated in part (a) of this Figure, propagation speed amplifies with increasing bromate concentration. At high concentration of bromate (> 0.075 M) visibility of these waves was not good and when concentration of bromate was larger than 0.08 M the system did not exhibit any wave activity. When the concentration of bromate is higher than 0.072 M the system exhibited target and spiral waves. Although wave activity had a better contrast at low bromate concentration, they lasted for a shorter period of time.

Acid concentration effect on wave propagation speed is shown in Figure 7.7b. Increase in acid concentration from 0.8 to 1.8 M raised wave propagation speed from 0.08 to 1.25 cm/min. Again, in all cases the rate was measured at 200 min after the initial appearance o wave activity in the medium. Higher acid concentrations ($\geq$ 1.6 M) resulted in poor contrast and visibility, but allowed wave activity to survive longer. In low acid concentrations, i.e. lower than 1.2 M, this system only showed target waves. Studies on the effect of initial concentration of ferroin loaded onto ion-exchange resins have also been carried out; result of this study is presented in Fig. 7.7c which illustrates change of wave propagation speed versus ferroin concentration. According to Fig. 7.7c increasing ferroin concentration causes a decrease in wave propagation speed. Performing effect of ferroin concentration studies, concentrations of bromate, acid, and the mass of bead were kept constant at 0.068 M, 1.4 M, and 3.0 g, respectively. Carrying out preliminary studies on the effect of bead mass on chemical wave activity, we kept acid and bromate concentrations constant at 1.4 M and 0.068 M, respectively.
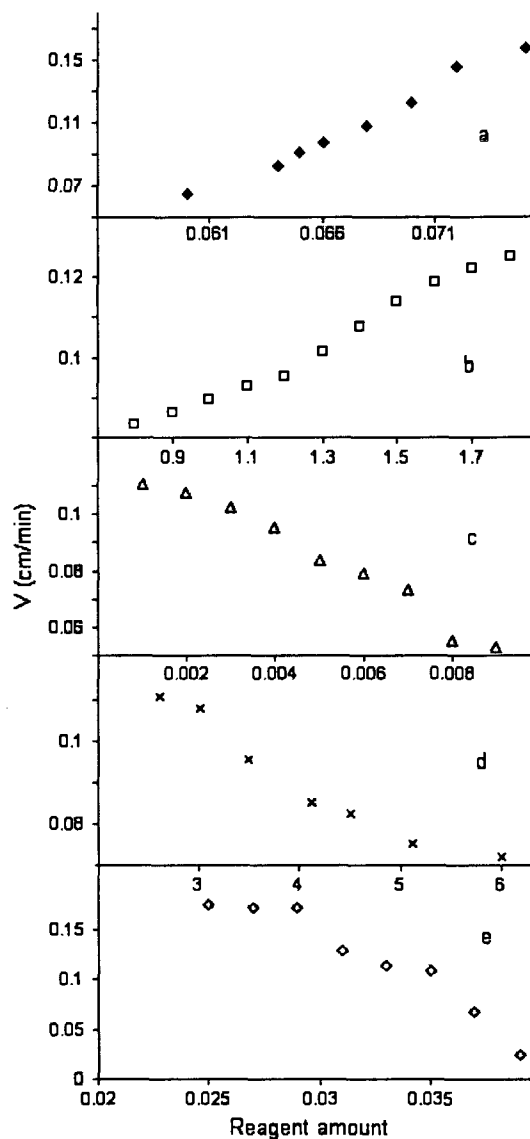
Figure 7.7 Wave propagation speed versus (a) initial bromate concentration while other reagent concentrations were fixed at: [acid] = 1.4 M, [pyrocatechol] = 0.035 M, [ferroin] = 0.002 M, and 3.0 g of bead; (b) initial acid concentration while other reagent concentrations were fixed at: [bromate] = 0.068 M, [pyrocatechol] = 0.035 M, [ferroin] = 0.002 M, and 3.0 g of bead; (c) initial ferroin concentration while other reagent concentrations were fixed at: [bromate] = 0.068 M, [acid] = 1.4 M, [pyrocatechol] = 0.035 M, and 3.0 g of bead and (d) bead mass while other reagent concentrations were fixed at: [bromate] = 0.068 M, [acid] = 1.4 M, [pyrocatechol] = 0.035 M, [ferroin] = 0.002 M. (e) initial pyrocatechol concentration while other reagent concentrations were fixed at: [acid] = 1.4 M, [bromate] = 0.068 M, [ferroin] = 0.002 M, and 3.0 g of bead; Wave speed analyzes have been done after 200 min of appearing wave activity in all cases.

Figure 7.7d plots wave propagation speed as a function of bead mass, in which wave speed decreases as bead mass increases from 2.6 to 6.0 g. Such a result is consistent with the effect of ferroin concentration on the wave propagation rate.

Figure 7.8a shows evolution of spiral tip movement with time as a function of initial bromate concentration. The movement of spiral tip can be classified into a diversity of qualitatively different trajectories including cycloidal curves and simple circles. These behaviours are referred to as meandering and rigid rotation, respectively. When bromate concentration is equal to or less than 0.065 M the system yields rigid spiral tip movement. On the other hand, at high bromate concentrations the medium exhibits meandering spiral tip as well.

Notably, as shown in Figure 7.8, the motion of these spiral tips changes in time, because chemicals are consumed continuously, which consequently alternate the dynamics of the reaction medium. The most variety of chemical wave activities has been observed when bromate concentration was between 0.066 M and 0.070 M. The system exhibited two stages of wave break-up; The first one was the break-up of circular wave to spiral; Subsequently, spirals fell apart from outside toward inside, forming lots of wave segments. The process of spiral segmentation always starts from outer spiral's tail (see Fig. 7.9).
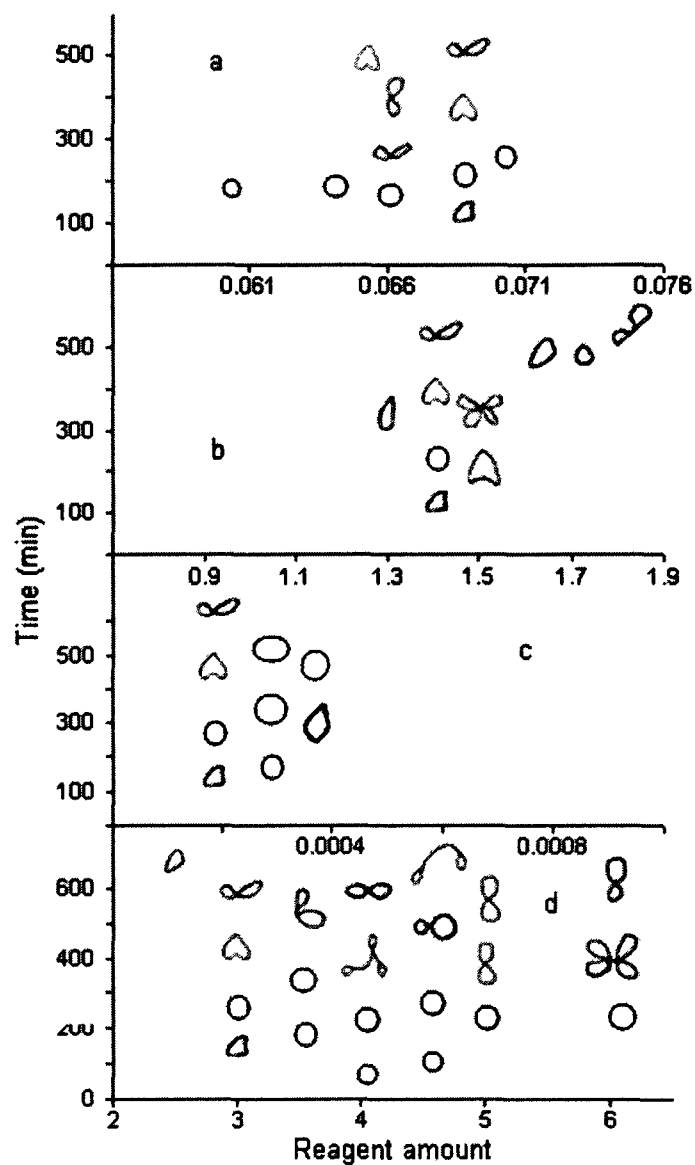
Figure 7.8 Spiral tip trajectory versus (a) initial bromate concentration while other reagent concentrations were fixed at: [acid] = 1.4 M, [pyrocatechol] = 0.035 M, [ferroin] = 0.002 M, and 3.0 g of bead; (b) initial acid concentration while other reagent concentrations were fixed at: [bromate] = 0.068 M, [pyrocatechol] = 0.035 M, [ferroin] = 0.002 M, and 3.0 g of bead; (c) initial ferroin concentration while other reagent concentrations were fixed at: [bromate] = 0.068 M, [acid] = 1.4 M, [pyrocatechol] = 0.035 M, and 3.0 g of bead and (d) bead mass while other reagent concentrations were fixed at: [bromate] = 0.068 M, [acid] = 1.4 M, [pyrocatechol] = 0.035 M, [ferroin] = 0.002 M.
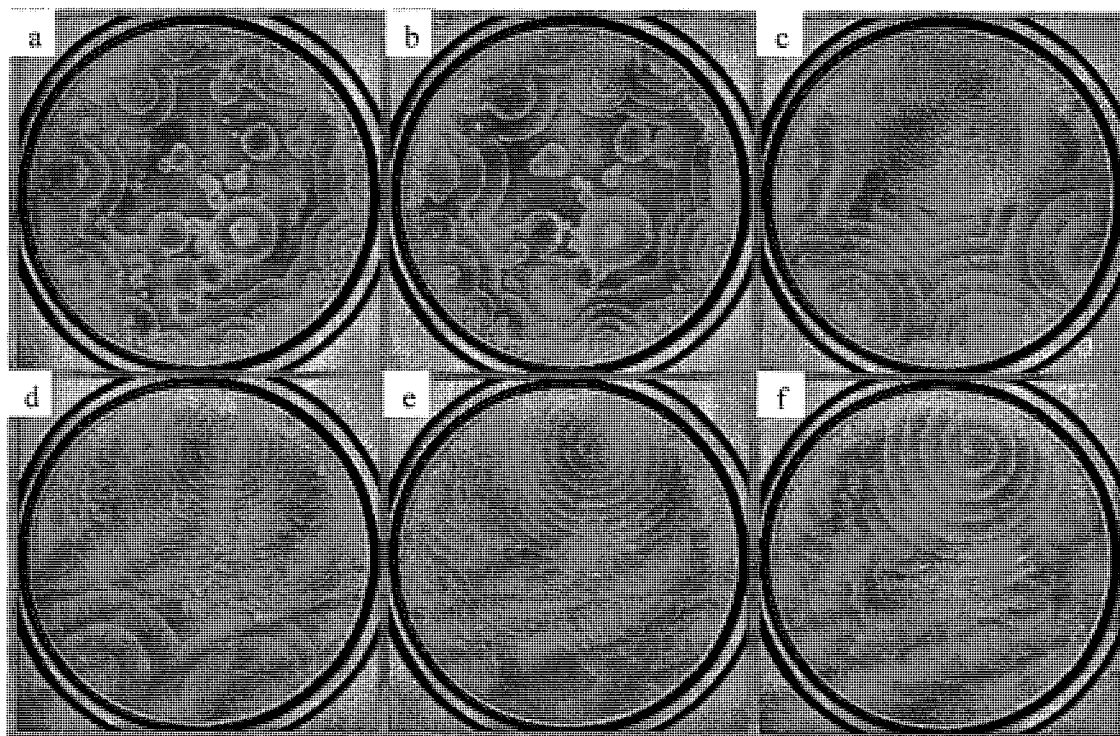
Figure 7.9 Chemical waves at 60 min (a), 70 min (b), 110 min (c), 150 min (d), 200 min (e), and (f) at 262 min. In panel (a) circular wave breaks up to form spirals. In panel (c) spiral starts breaking-up from its tail. Other reaction conditions are [bromate] = 0.068 M, [acid] = 1.4 M, [pyrocatechol] = 0.035 M, [ferroin] = 0.002 M, and 3.0 g of bead.

In Fig. 7.10 at 0.07 M bromate, high frequency waves emerged out of low frequency ones and wave with higher frequency eventually covered the whole medium. In Fig. 7.11, the concentration of bromate is slightly lower than that in Fig. 7.10 (i.e. 0.066 M), where high frequency waves gradually evolved into low frequency ones as a result of the consumption of reactants.

Acid concentration effect on spiral tip trajectory is shown in Figure 7.8b. When acid

concentration is higher than 1.3 M, the system was able to exhibit spirals with

meandering or rigid tip movement. When acid concentration was 1.5 M the trajectory of

the tip looked like a hypocycloid. This complex route can be considered as a

superposition of two circular motions with different radii and rotational frequencies in

contrast to a rigid rotation where the tip rotates with a constant frequency on a circular

pathway with a fixed center [42]. Quantitative analysis of the data reveals an increase in

the number of petals as the concentration of acid is increased.
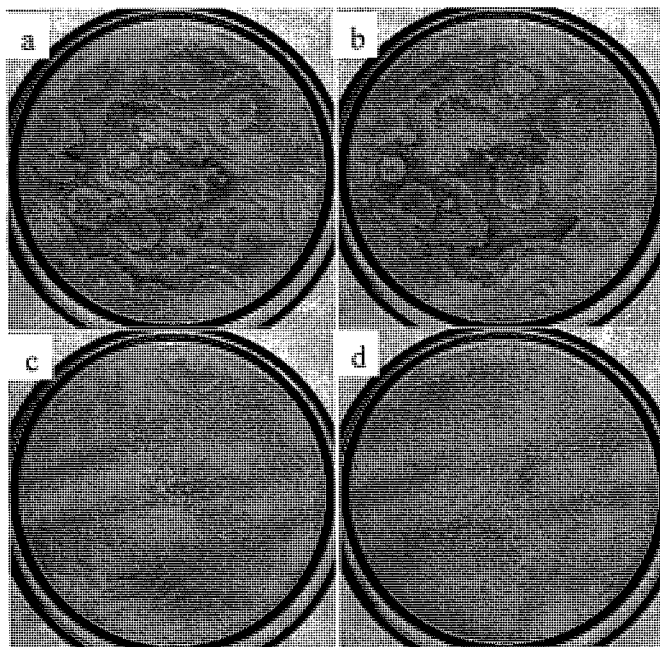
Figure 7.10 (a) Appearance of spiral with high frequency among low frequency waves, 92 min; (b) 103 min, (c) 148 min, and (d) 200 min. Other reaction conditions are [bromate] = 0.070 M, [acid] = 1.4 M, [pyrocatechol] = 0.035 M, [ferroin] = 0.002 M, and 3.0 g of bead.
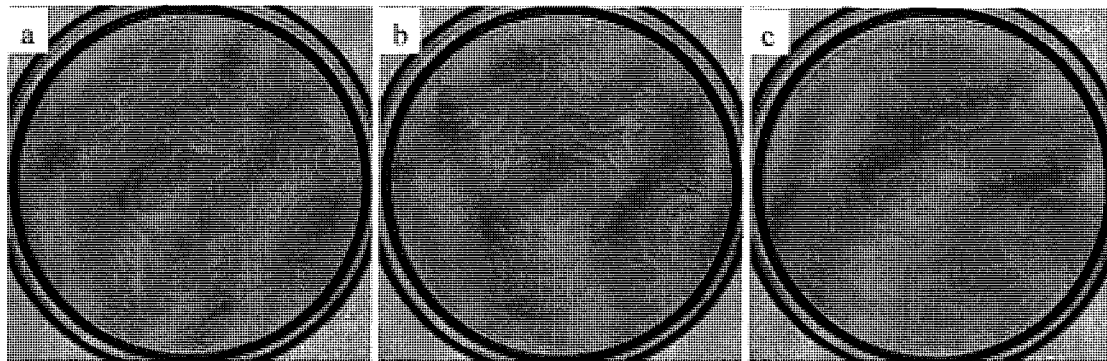
Figure 7.11 (a) Appearance of wave segments in the reaction medium at 1.2M acid concentration at 267 min, (b) 338 min, and (c) 470 min. Other reaction conditions are [bromate] = 0.068 M, [acid] = 1.2 M, [pyrocatechol] = 0.035 M, [ferroin] = 0.002 M, and 3.0 g of bead.
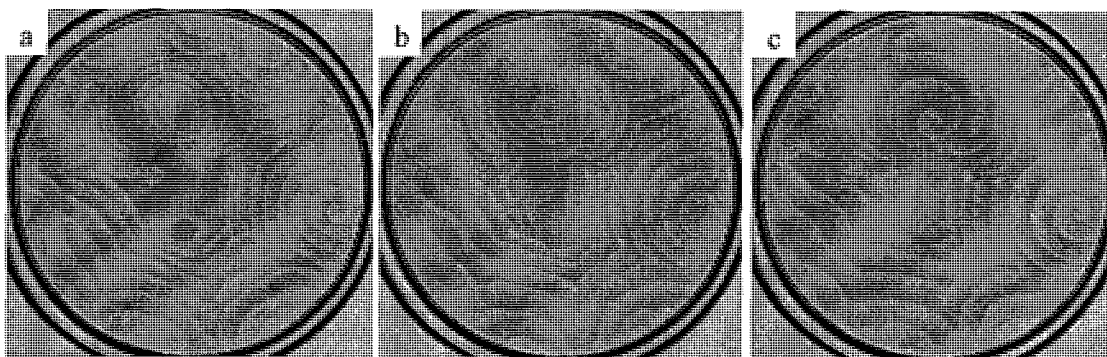
Figure 7.12 (a) Appearing of the meandering spiral which with tip movement causes anomalous abnormal in system (a) 254 min (b) 308 min (c). 408 min. Other reaction conditions are [bromate] = 0.068 M, [acid] = 1.4 M, [pyrocatechol] = 0.035 M, [ferroin] = 0.002 M, and 6.0 g of bead.

The result of ferroin concentration effect on the motion of spirals is presented in Fig. 7.8c. For concentrations of ferroin between 0.003 M and 0.004 M, the reaction-diffusion medium supports a rigidly rotating spiral wave for at least 6 hours. During this time, the size of the spiral core expanded. When ferroin concentration is higher than 0.005 M the system exhibits just target waves with anomalous dispersion behaviour. For a low concentration of ferroin, 0.001 M, there is plenty of wave activity in the system such as anomalous dispersion and spiral tip movement; however, due to visibility dilemma we were not able to follow spiral tip trajectory.

Figure 7.8d shows spiral wave tip trajectory as a function of bead mass, where bead mass was adjusted between 2.6 and 6.0 g. High bead mass was in favour of meandering spiral. At lower bead mass meandering spiral occurred at later stage of wave activity, while at high bead mass meandering behaviour appeared in earlier stages and lasted over 10 hours until the end of wave activity. Another phenomenon that this system is able to support at high bead mass of (> 3.5 g) is abnormal dispersion. According to experimental studies by Steinbock et al. [42, 43] anomalous dispersion happens because of the fact that waves propagate faster at the beginning and then they propagate slower which makes wave trains having different distances in different areas. Another approach that causes anomalous dispersion is the meandering movement of spiral tip in bead-pyrocatechol system. Distance between waves increased in one side and decreased on the other side of the spiral (closer in direction of tip movement) because of the meandering movement of spiral tip [45] (An example is shown in Fig. 7.12). In the described chemical medium spiral waves exist for more than 10 hour during which the size of this meandering pattern increases slowly with the aging of the solution.

As observed in earlier studies [39-41], the wave propagation velocity in the BZ reaction is strongly dependent on the initial concentrations of sulfuric acid and sodium bromate. The form of the concentration dependence on sulfuric acid and sodium bromate is characterized to be the square root of the product of their initial concentrations. For this reason, our results are represented in this form. A linear dependence of wave velocity on the product $[H^+]^{1/2}[BrO_3^-]^{1/2}$ is shown in Fig 7.13. The best two-parameter least-squares line through the points is

$$v \text{ (cm/min)} = 0.4959 \times [H^+]^{1/2}[BrO_3^-]^{1/2} - 0.0445 \qquad (1)$$

We also tried several other fitting procedures, but their correlation coefficients were even worse than the square root of the product of bromate and acid concentrations.
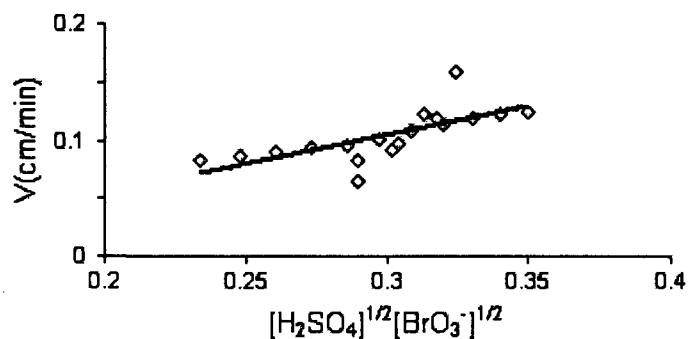
Figure 7.13 Plot of velocity of band propagation vs. square root of product of initial concentrations of sulfuric acid and sodium bromate: [pyrocatechol] = 0.035 M, [ferroin] = 0.002 M, and 3.0 g of bead.

Conclusions

We investigated pattern formation in the ferroin-pyrocatechol-bromate reaction under the conditions where the stirred system does not exhibit oscillatory behaviour. Two separate stages of spontaneous pattern formation were achieved in this system. The first step of wave activity started 5 minutes after mixing all chemicals and injecting sample between two glasses and it lasted for less than 3 minutes and excitability three different kinds of wave activity including circular waves, propagating waves and wildfire. The second stage of wave activity started by taking sample from stirred system after 50 min of starting the reaction and spreading the sample between two glasses: its wave activity lasted for up to six hours. The system was able to support target wave and spiral formation and different kind of complex behaviours such as cross waves, anomalous dispersion and wave break-ups. Dynamics of these two stage wave formations depends on composition of the solution like concentration of acid, bromate, and ferroin. For example, propagation speed increased with increasing bromate concentration. The second stage and the first stage propagation speed increases as the initial concentration of acid and ferroin increases, respectively. Increasing in concentration of ferroin caused a decline of the second stage wave propagation speed. This system is capable of exhibiting complex pattern formations especially when concentration of bromate or acid is low; it is capable of exhibiting anomalous dispersion which in the middle of wave activity window caused waves get close to each other and collide and therefore wave break-ups. Cross waves (CW) observed in this system in the manner that second wave activity appear after the first row and while it is still active. These two wave activities did not have influence on each other according to our experimental results, although they cross each other. This

system is also light sensitive which makes it suitable for perturbation studies and manipulating pattern formation.

We also report preliminary experimental results of chemical wave in the pyrocatechol-bromate bead system. Variation of wave propagation speed and spiral tip trajectory versus four different factors including concentration of bromate, acid, and ferroin concentration and bead mass have been characterized. Depending on reaction conditions, this system exhibits a variety of concentration patterns with long life times of approximately 10 to 12 hours on average. High concentrations of acid and bromate generally favour longer chemical wave activity, but do not favour image contrast. Therefore, following the motion of spiral tip at high concentration of these two reagents is a challenging issue. In these systems spiral tips exhibit both rigid and meandering movement for long times up to 10 h. Chemical wave speed increases with increasing acid and bromate concentration, but decreases with concentration of ferroin and mass of bead. This system needs more investigation on the influence of light and/or laser pulses on spiral tip movement. Also, according to our preliminary studies spiral tip movement speed changes with reaction mixture age.

References

1. R. J. Field and M. Burger (Eds.), Oscillations and Traveling Waves in Chemical Systems, Wiley-Interscience, New York, 1985.

2. A. T. Winfree, The Geometry of Biological Time, Springer, Heidelberg, 2000.

3. S. K. Scott, Chemical Chaos, Oxford University Press, 1994.

4. B. R. Johnson, S. K. Scott and A. F. Taylor, J. Chem. Soc., Faraday Trans., 93, 1997, 3733.

5. I. R. Epstein, J. A. Pojman and O. Steinbock, Chaos, 16, 2006, 037101.

6. V. K. Vanag and I. Hanazaki, J. Phys. Chem. A, 101, 1997, 2147.

7. T. R. Chigwada, P. Parmananda and K. Showalter, Phys. Rev. Lett., 96, 2006, 244101.

8. I. Berenstein, L. Yang, M. Dolnik, A. M. Zhabotinsky and I. R. Epstein, J. Phys. Chem. A, 109, 2005, 5382.

9. S. Grill, V. S. Zykov and S. C. Müller, Phys. Rev. Lett., 75, 1995, 3368.

10. L. Adamčíková, Z. Farbulová and P. Ševčík, New J. Chem., 25, 2001, 487.

11. I. Szalai, K. Kurin-Csörgei and M. Orbán, Phys. Chem. Chem. Phys., 4, 2002, 1271.

12. O. Steinbock and S. C. Müller, Phys. Rev. E, 47, 1993, 1506.

13. E. Fung, W. W. Wong, J. K. Suen, T. Bulter, S. Lee and J. C. Liao, Nature, 435, 2005, 118.

14. K. Horikawa, K. Ishimatsu, E. Yoshimoto, S. Kondo and H. Takeda, Nature, 441, 2006, 719.

15. W. W. Wong, T. Y. Tsai and J. C. Liao, Mol. Syst. Biol., 3, 2007, 1.

16. B. Blasius, A. Huppert and L. Stone, Nature, 399, 1999, 354.

17. S. Danø, P. Sørensen and F. Hynne, Nature, 402, 1999, 320.

18. T. Hideshima, Y. Kato, Biophys. Chem., 124, 2006, 100.

19. P. Mohanty, Nature, 437, 2005, 325.

20. N. J. Abram, M. K. Gagan, Z. Liu, W. S. Hantoro, M. T. McCulloch and B. W. Suwargadi, Nature, 445, 2007, 299.

21. Z. Nagy-Ungvarai, S. C. Müller, J. J. Tyson and B. Hess, J. Phys. Chem., 93, 1989, 2760.

22. L. Kuhnert, H. J. Krug and L. Pohlmann, J. Phys. Chem., 89, 1985, 2022.

23. H. Liao, L. Zhou, C. Zhang and Q. Ouyang, Phys. Rev. Lett., 95, 2005, 238301.

24. C. Oosawa, Y. Fukuta, K. Natsume and K. Kometani, J. Phys. Chem., 100, 1996, 1043.

25. A. E. Bugrim, M. Dolnik, A. M. Zhabotinsky and I. R. Epstein, J. Phys. Chem., 100, 1996, 19017.

26. C. Luengviriya, U. Storb, M. J. B. Hauser and S. C. Müller, Phys. Chem. Chem. Phys., 8, 2006, 1425.

27. H. Guo, L. Li, Q. Ouyang, J. Liu and Z. She, J. Chem. Phys., 118, 2003, 5038.

28. N. Nishiyama and T. Matsuyama, J. Chem. Phys., 106, 1997, 3427.

29. N. Manz, B. T. Ginn and O. Steinbock, J. Phys. Chem. A, 107, 2003, 11008.

30. M. Harati, S. Amiralaei, J. Green and J. Wang, Chem. Phys. Lett., 439, 2007, 337.

31. V. J. Farage and D. Janjic, Chem. Phys. Lett., 93, 1982, 621.

32. K. Kurin-Csörgei, A. M. Zhabotinsky, M. Orbán and I. R. Epstein, J. Phys. Chem., 100, 1996, 5393.

33. N. Manz, S. C. Müller and O. Steinbock, J. Phys. Chem. A, 104, 2000, 5896.

34. C. T. Hamik, N. Manz and O. Steinbock, J. Phys. Chem. A, 105, 2001, 6144.

35. L. Kuhnert and H. J. Krug, J. Phys. Chem.., 91, 1987, 730.

36. R. J. Field and R. M. Noyes, J. Am. Chem. Soc., 96, 1974, 2001.

37. C. Elphick, E. Meron and E. A. Spiegel, Phys. Rev. Lett., 61, 1988, 496.

38. D. S. Huh, Y. J. Kim, H. S. Kim, J. K. Kang and J. Wang, Phys. Chem. Chem. Phys., 5, 2003, 3188.

39. Z. Nagy-Ungvarai, J. J. Tyson and B. Hess, J. Phys. Chem., 93, 1989, 707.

40. P. M. Wood and J. Ross, J. Chem. Phys., 82, 1985, 1924.

41. K. Showalter, J. Phys. Chem., 85, 1981, 440.

42. O. Steinbock and S. C. Müller, Phys. Rev. E, 47, 1993, 1506.

43. N. Manz, B. T. Ginn and O. Steinbock, J. Phys. Chem. A, 107, 2003, 11008.

44. M. Harati and J. Wang, J. Phys. Chem. A, 112, 2008, 4241.

45. H. M. Liao, L. Q. Zhou, C. X. Zhang and Q. Ouyang, Phys. Rev. Lett., 95, 2005, 238301.

Chapter 8 Chemical Wave Studies in the Catalyzed Aminophenol-Bromate System

Introduction

Slow oscillations and waves are subjects of ongoing research in biological systems such as waves in brain and nervous systems [1-3]. Recent studies found that dopamine (DA), a substituted 1,2-quinone, plays an important role in the core molecular mechanism of the Circadian clock, which is a biological chronometer that regulates molecular and physiological rhythms in animals and loops with a periodicity of about 24 hours [4-12]. DA neuronal oscillations have been suggested to play an important role in information processing in the brain. Midbrain DA neurons receive inputs from widely distributed brain areas where the amplitude of these low frequency oscillations is much reduced in the substantia nigra (SN) when compared with those in the ventral tegmental area (VTA) and so is the number of DA neurons qualified as high-SO cells.

If coenzyme Q is reduced by two equivalents, the compound becomes a ubiquinol, denoted QH_2. Brain research result indicates that coenzyme Q1 (CoQ1) recycling depletes nicotinamide dinucleotide phosphate (NAD(P)H) and inhibits ascorbate recycling when cellular energy metabolism is limited by glucose deprivation [13-15]. The oscillating, age-related reduction of ferricytochrome c is sensitive to superoxide dismutase, is inhibited by coenzyme Q and is reduced or absent from sera of younger individuals. The presence of this enzyme at the cell surface and the demonstration of an ability to oxidize reduced quinones of the plasma membrane, e.g. ubiquinol, has offered an opportunity to

formulate, for the first time, a complete electron transport chain from the cytosol to oxygen at the cell surface with the NADH oxidase (NOX) protein acting as the terminal oxidase. The hydroquinone (NADH) oxidase activity and a protein disulfide-thiol interchange activity alternate to generate the 24 min period [14]. The mechanism whereby coenzyme Q blocks the oscillating reduction of ferricytochrome c is unclear. The oscillations are given by both the oxidation of NADH and by the oxidation of ubiquinol.

Experimental Procedure

Stock solutions $NaBrO_3$ (Aldrich, 99%), 0.6 M, and sulfuric acid (Aldrich, 95-98%), 4.0 M, were prepared with double-distilled water. 4-aminophenol (Aldrich, 98+ %) was directly dissolved in the reaction mixture. The volume of the reaction mixture was fixed at 30.0 ml in all experiments. Ferroin, 0.025 M, was prepared from a calculated amount of $FeSO_4 \cdot 7H_2O$ (Aldrich, 99+%) and 1,10-phenanthroline (Aldrich, 99+%). The analytical grade 100-200 mesh ion-exchange resin (Dowex 50W-X4) was purchased from the Fisher Scientific Co. All chemicals were used as received grade without further purification.

To initiate our 2-D experiments, we started the reaction in a stirred batch reactor where the total volume of reaction solution was fixed at 30 ml in all experiments and it was illuminated with 150 mW/cm^2 light until it evolved into oscillatory window. Then we turned off the light and transferred the whole sample to a Petri dish (9 cm in diameter) and mixed with 3.0 (±0.1) g of cation-exchange resin beads (100-200 mesh) loaded with 0.003 M ferroin. To load the catalyst ferroin onto the resin, filtered resin was mixed with ferroin solution and the mixture was stirred vigorously for overnight. The ferroin solution became transparent at the end of the process, presumably due to the complete absorption of ferroin by the cation beads. The mixture was left unstirred for 30 minutes and then we

removed the solution on top of the beads. Ferroin loaded beads were washed three more times through adding 60 ml of doubly distilled water and stirred for 10 minutes each time. This washing procedure is useful in removing imperfect beads, i.e., reducing the amount of beads floating on the top of reaction mixture in the Petri dish. The Petri dish was maintained at room temperature of $24 \pm 1°C$.

Evolution of the spatially extended medium was monitored with a CCD camera equipped with a zoom lens. The CCD camera was connected to a personal computer running a frame grabber program (Matrox Imaging Library). Images were stored on an external hard disk for future analysis. The perturbation of light was implemented with a halogen lamp equipped with dual bifurcated optic fibers and continuous variable light level (Fisher Scientific, Model DLS-100HD, 150 mW/cm^2). The illumination was implemented by placing one of the fibers on top of the Petri dish.

Results and Discussions

Figure 8.1 presents a series of snapshots of chemical waves in the ferroin-aminophenol-acidic bromate system. Our previous earlier kinetic studies in a batch reactor show that in the absence of light not only the uncatalyzed system is not capable of showing oscillatory behaviour but also there is not much progress in the overall reaction [16, 17]. More specifically, turning off the light in the stirred system resulted in an immediate disappearance of the spontaneous oscillation. However, as we take sample from the same reaction mixture and transfer it to a Petri dish filled with beads system loaded with ferroin, the medium is supports wave activity for a very long time even in the absence of light. For example, under the specified conditions used in Fig. 8.1, the system shows wave activity for about 50 hours. Notably, after waves propagate out of the

medium, there is a period of time when there is no wave activity in the reaction-diffusion medium.
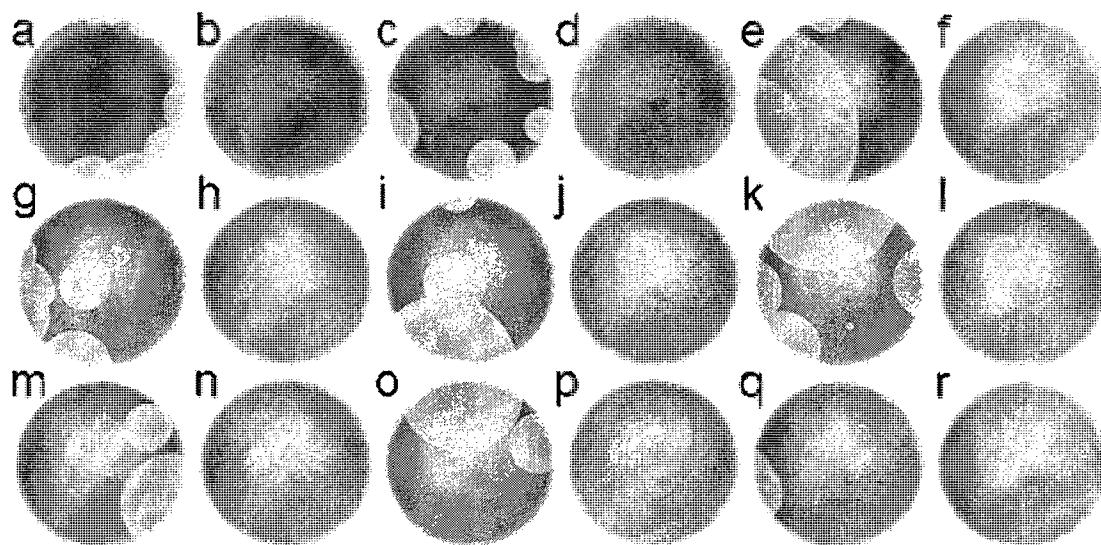
Figure 8.1 Slow wave activity in aminophenol-bromate system under condition: [bromate] = 0.06 M, [acid] = 1.0 M, [AP] = 0.017 M. Snapshots are taken at: (a) 20, (b) 300, (c) 334, (d) 426, (e) 560, (f) 682, (g) 715, (h) 873, (i) 974, (j) 1057, (k) 1146, (l) 1349, (m) 1383, (n) 1608, (o) 1642, (p) 1916, (q) 1952, (r) 2137, times are in minutes.

In Figure 8.1b, once the waves disappear the medium exhibits a distinctive, uniform red color indicating that ferroin is in its reduced state. In general, quenching of wave activity is believed to be due to the consumption of reactants, but after awhile, the unperturbed reaction medium showed another wave activity and this scenario reiterated for 9 times under the conditions studied here. Notably, the longest and shortest stages of pattern propagation last for 240 min and 74 min, respectively; and shortest and longest quiescent windows (no wave activity) persist for 72 min and 225 min, respectively. The

illuminated system just shows one oscillatory stage and one stage of wave activity if transferred to a beads loaded Petri dish filled with beads loaded with ferroin.

As it is mentioned earlier in the uncatalyzed bromate-aminophenol reaction in a stirred batch reactor if we turn off the light spontaneous oscillations stopped immediately. The system exhibits the same kind of behaviour even if ferroin is added to the system. Yet, waves developed in the beads system loaded with ferroin even in the absence of light. To gain insight into the above surprising phenomenon we carried out a series of studies in a stirred batch reactor via adding ferroin to the reaction mixture after turning off the light. These experiments show that when the concentration of ferroin reaches 0.002 M, the catalyzed system would exhibit low frequency oscillations. Summary of this systematic study is presented in Figure 8.2.
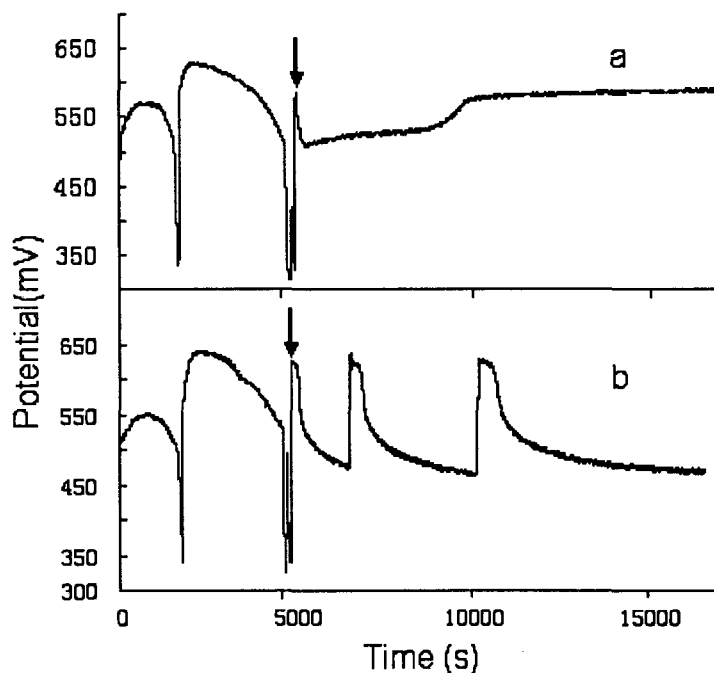
Figure 8.2 Time series of aminophenol-bromate system under condition: [bromate] =0.06 M, [acid] = 1.0 M, [AP] = 0.016 M, concentration of added ferroin is (a) 5×10^{-4} M and (b) 3×10^{-3} M. ferroin is added to the system immediately after turning off the light.

Propagation speed of the waves under different concentrations of reagents is presented

in Figure 8.3. The propagation speed was measured in each stage and there was a

minuscule decrease in the speed as reaction evolves in time (Fig. 8.4). The propagation

rate increases as the concentration of bromate or acid increases, bur decreases with the

increase of aminophenol concentration. In all cases, wave propagates slower in each

subsequent stage. The lifetime of each stage of wave activity decreases with the longest

lifetime of 30 h for the first stage (presented in Fig. 8.5).
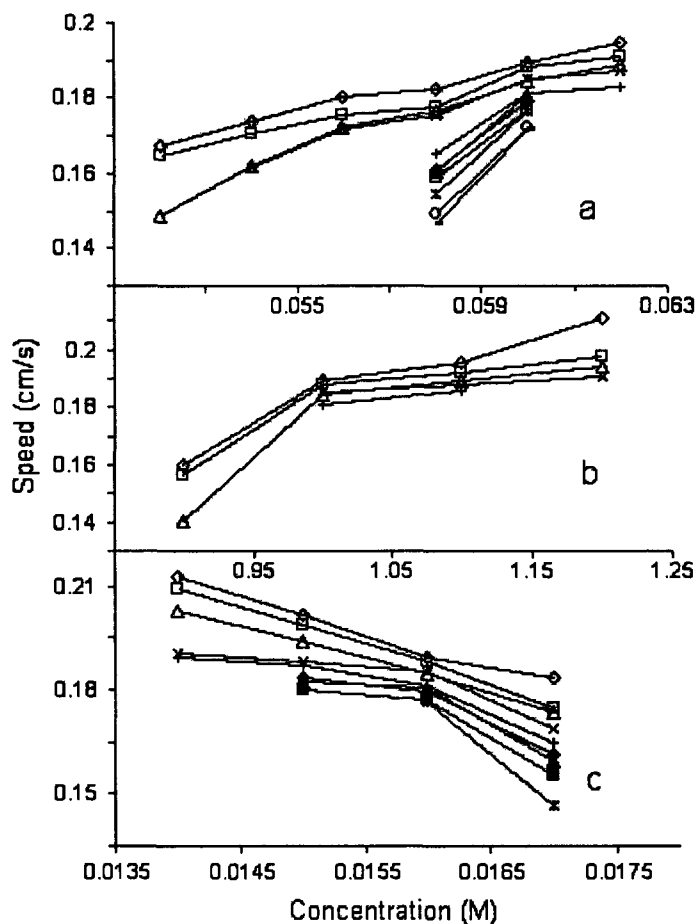
Figure 8.3 Plot of the propagation speed versus (a) bromate, (b) acid, and (c) aminophenol concentration, M, under condition: (a) [acid] = 1.0 M and [AP] = 0.016 M, (b)[bromate] = 0.06 M and [AP] = 0.016 M, and (c)[bromate] =0.06 M and [acid] = 1.0 M, in which (◊) First, (■) second, (Δ) third, (×) fourth, (+) fifth, (♦) sixth, (■) seventh, (▲) eighth, (*) ninth, (●) tenth, and (-) eleventh stage.
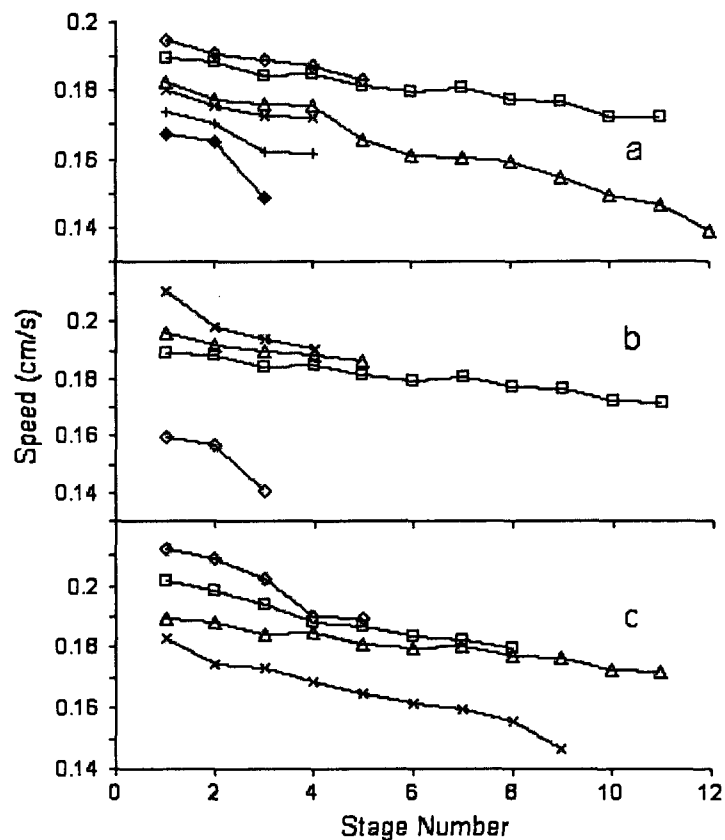
Figure 8.4 Plot of the propagation speed versus stage number in which (a) bromate, (b) acid, and (c) aminophenol concentration. In (a) conditions are: [acid] = 1.0 M, [aminophenol] =0.016 M, and [bromate] is equal to ($\Diamond$) 0.062 M, ($\square$) 0.060 M, ($\triangle$) 0.058 M, ($\times$) 0.056 M, (+) 0.054 M, and ($\blacksquare$) 0.052 M. In (b) conditions are [bromate] = 0.060 M, [aminophenol] = 0.016 M, and [acid] is equal to ($\Diamond$) 0.90 M, ($\square$) 1.0 M, ($\triangle$) 1.10 M, and ($\times$) 1.20 M. In (c) conditions are: [bromate] = 0.016 M, [acid] = 1.0 M, and [aminophenol] is equal to: ($\Diamond$) 0.014 M, ($\square$) 0.015 M, ($\triangle$) 0.016 M, and ($\times$) 0.017 M.

The lifetime of quiescent window, the stage that the medium does not have wave activity, has a reverse relationship in comparison with the lifetime, of wave activity. The last quiescent window is the longest one in each experiment and can last for up to 11 h,

depending on the reaction conditions. Illuminating system for a short time, 1 min, during

wave activity causes lots of wave activity in just one stage (detailed results presented in

Fig. 8.7).
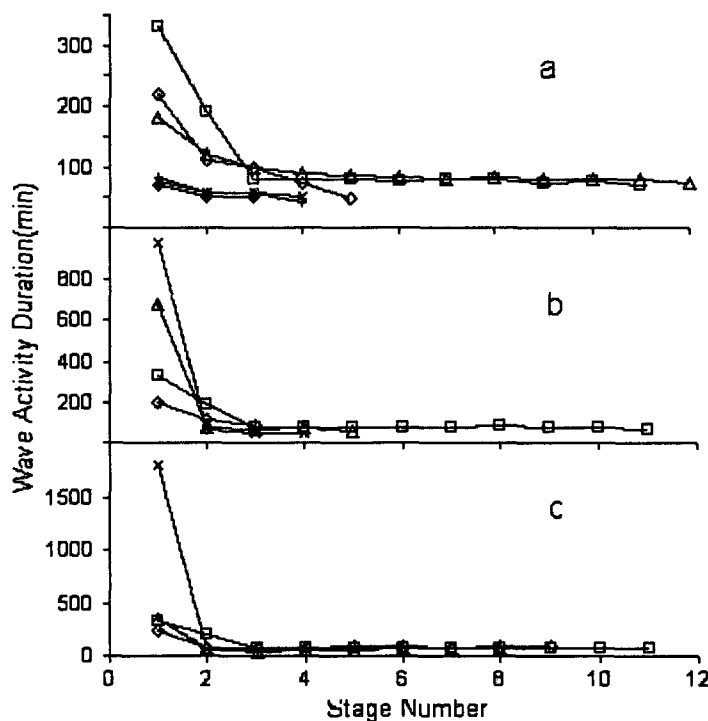
Figure 8.5 Plot of wave activity duration versus stage number in (a) bromate, (b) acid, and (c) aminophenol. In (a) conditions are: [acid] = 1.0 M, [aminophenol] =0.016 M, and [bromate] is equal to (◊) 0.062 M, (□) 0.060 M, (△) 0.058 M, (×) 0.056 M, (+) 0.054 M, and (■) 0.052 M. In (b) conditions are [bromate] = 0.060 M, [aminophenol] = 0.016 M, and [acid] is equal to (◊) 0.90 M, (□) 1.0 M, (△) 1.10 M, and (×) 1.20 M. In (c) conditions are: [bromate] = 0.016 M, [acid] = 1.0 M, and [aminophenol] is equal to: (◊) 0.017 M, (□) 0.016 M, (△) 0.015 M, and (×) 0.014 M.
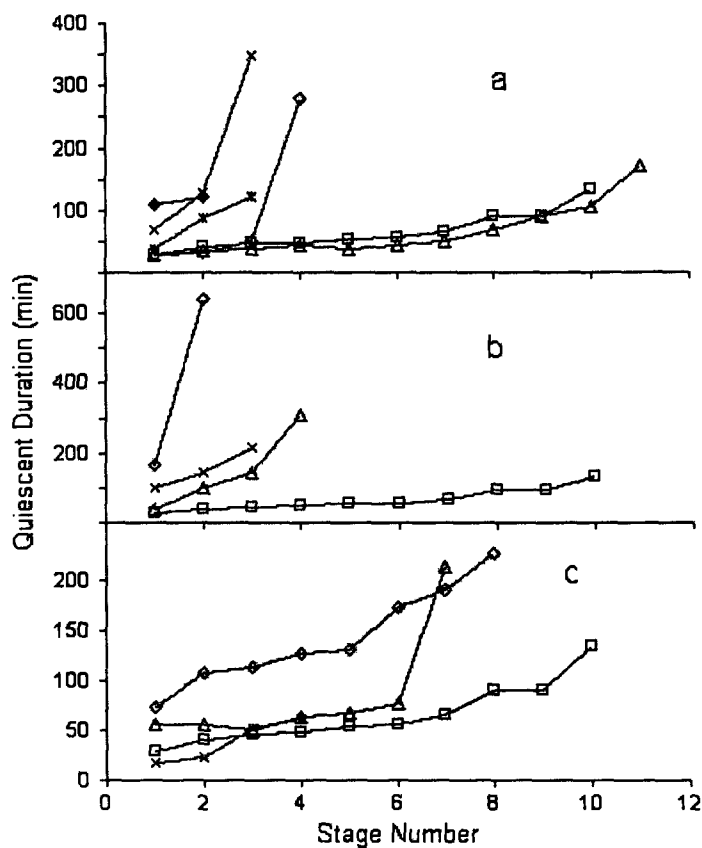
Figure 8.6 Plot of quiescence duration versus stage number in (a) bromate, (b) acid, and (c) aminophenol. In (a) conditions are: [acid] = 1.0 M, [aminophenol] =0.016 M, and [bromate] is equal to (◊) 0.062 M, (□) 0.060 M, (Δ) 0.058 M, (×) 0.056 M, (+) 0.054 M, and (■) 0.052 M. In (b) conditions are [bromate] = 0.060 M, [aminophenol] = 0.016 M, and [acid] is equal to (◊) 0.90 M, (□) 1.0 M, (Δ) 1.10 M, and (×) 1.20 M. In (c) conditions are: [bromate] = 0.016 M, [acid] = 1.0 M, and [aminophenol] is equal to: (◊) 0.017 M, (□) 0.016 M, (Δ) 0.015 M, and (×) 0.014 M.

Light perturbation studies have been carried out using two different strategies: first we examined the influence of illumination on existing wave activity. As it is shown in Figure 8.7 we illuminated the system with one fiber for 60 seconds with the light density of 100

mW/cm^2. At the beginning it seems that light quenches wave activity (see fig. 8.7c), however, after a short time, system exhibits wave activity at the illuminated place which ends up to form a pair of spirals. This newly formed spiral eventually dominated the whole media in which the high frequency waves last for about 35 hr. Recall that the non-illuminated system show several stages of wave activity. Here, when illuminated by light and after dying out of the spiral wave, system did not exhibit further wave activity. The system exhibited the same behaviour when the illumination is as short as 10 seconds, indicates that the aminophenol oscillatory system is highly photosensitive.
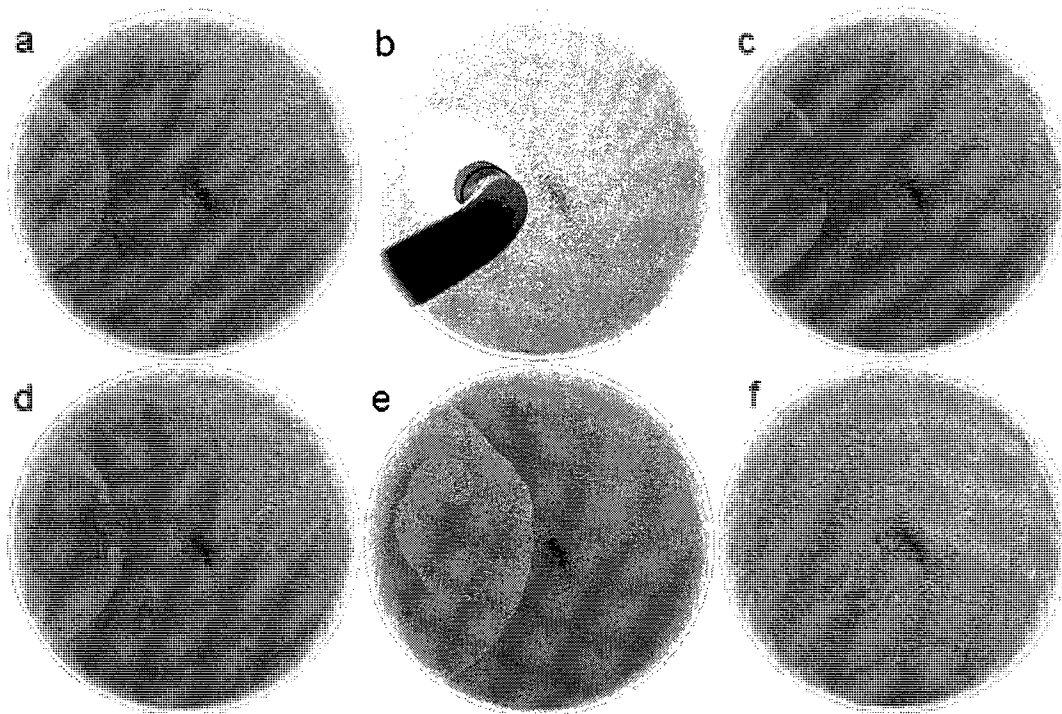
Figure 8.7 Light perturbation experiment under the condition: [bromate] = 0.06 M, [acid] = 1.0 M, and [AP] = 0.016 M, light intensity = 100 mW/cm^2 and just one fiber used for illumination. Images are taken after (a) 158 min, (b) 159 min, (c) 160 min, (d) 161 min, (e) 179 min, and (f) 218 min of injecting reaction solution in the Petri dish.

The second protocol was to illuminate the system when the medium did not exhibit wave activity. Note that the light intensity and illumination time in terms used here are the same as those employed in protocol one. After illuminating the system locally for 60 seconds, there was one propagating wave inhibited (fig. 8.8d). When this single propagating wave moved out of Petri dish and system moved to quiescent window as seen in Fig. 8.8; however, the system showed another propagating front after a brief period of delay and continued to exhibit slow wave activity similar to the scene in Fig. 8.1. To test the behaviour of the light-induced wave activity, we illuminated the system for the second time in the same manner as the first time. System formed spiral with just one stage wave activity, similar to behaviour shown in Figure 8.7. The way that the system responds to light illumination, does not change in 48 hours after spreading the reaction mixture into the beads-filled Petri-dish. Note that when the system is illuminated during quiescent period, high frequency waves does not form and each time just one propagating front forms. Furthermore, a light-induced pattern formation can be obtained, even 3 days after the disappearance of the last stage.
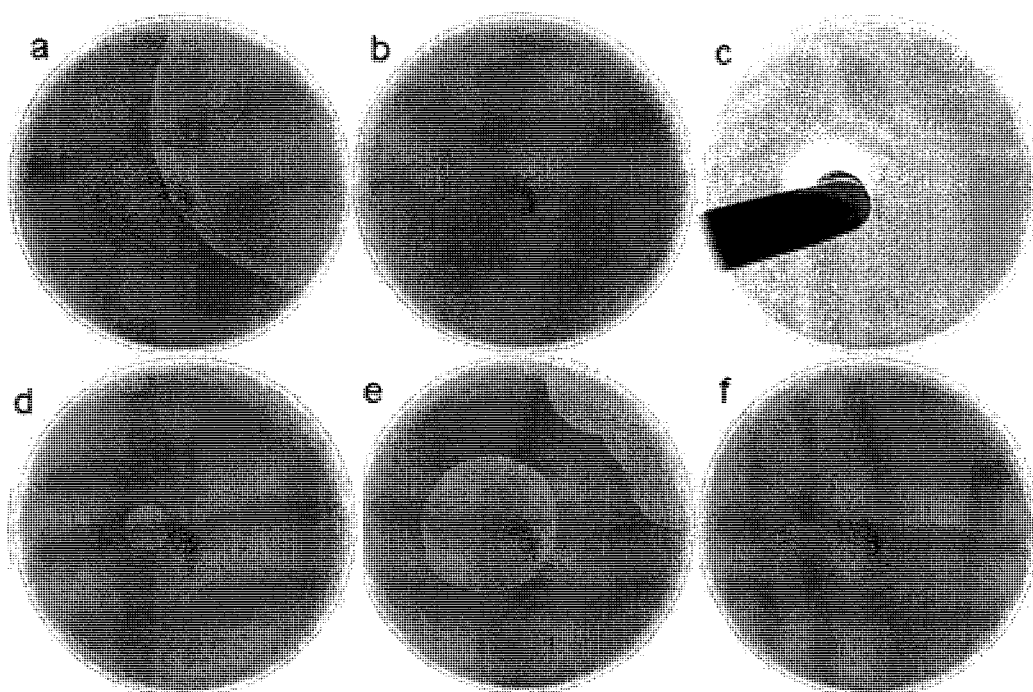
Figure 8.8 Light perturbation experiment under the condition: [bromate] = 0.06 M, [acid] = 1.0 M, and [AP] = 0.016 M, light intensity = 100 mW/cm^2 and just one fiber used for illumination. Images are taken after (a) 437 min, (b) 470 min, (c) 471 min, (d) 473 min, (e) 482 min, and (f) 512 min of injecting reaction solution in the Petri dish.

Conclusions

This preliminary exploration illustrates that the bromate-aminophenol system can be used to explore pattern formation. When the concentration of metal catalyst is high, wave formation with an extremely low frequency can be obtained even in the absence of illumination. The property of spontaneous pattern formation with such a low frequency is particularly interesting. For one, we are not aware of any report on such kind of wave behaviour in chemical reaction-diffusion medium. The long recovery period normally

implies that waves have a large refractory tail. It thus offers a unique chance for explore

its interaction with various external perturbations. It may be worth to point out that many

biological systems exhibit slow wave activity with extremely long recovery periods,

largely resembling what happens in this system. Despite the fact that biological and

chemical waves occur in very different media, they share several features in common.

Therefore, the investigation of wave activity in this highly photosensitive reaction system

may provide a venue to gain new insights into similar behaviour in other physical and

biological systems. These should be pursued in the future research.

References

1. W. E. Lowry, C. Blanpain, J. A. Nowak, G. Guasch, L. Lewis and E. Fuchs, Genes and Dev., 19, 2005, 1596.

2. J. Huelsken, R. Vogel, B. Erdmann, G. Cotsarelis and W. Birchmeier, Cell, 105, 2001, 533.

3. C. L. Celso, D. M. Prowse and F. M. Watt, Development, 131, 2003, 1787.

4. D. J. Morré, P. Chueh, J. Pletcher, X. Tang, L. Wu and D. Morré, Biochemistry, 41, 2002, 11945.

5. V. Yuferov, E. R. Butelman and M. J. Kreek, Eur. J. Hum. Genet., 13, 2005, 1101.

6. D. M. Morré, F. Guo and D. J. Morré, Mol. Cell. Biochem., 254, 2003, 101.

7. I. H. Riedel-Kruse, C. Müller and A. C. Oates, Science, 317, 2007, 1911.

8. C. B. Green and M. Menaker, Science, 301, 2003, 319.

9. J. D. Levine, P. Funes, H. B. Dowse and J. C. Hall, Science, 298, 2002, 2010.

10. J. C. Dunlap, Science, 311, 2006, 184.

11. M. U. Gillette and T. J. Sejnowski, Science, 309, 2005, 1196.

12. M. G. Murer, K. Y. Tseng, F. Kasanetz, M. Belluscio and L. A. Riquelme, Cell. Mol. Neurobiol., 22, 2002, 611.

13. C. D. Fiorillo, P. N. Tobler and W. Schultz, Behav. Brain Func., 1, 2005, 7.

14. D. J. Morré, R. Pogue and D. M. Morré, BioFactors, 9, 1999, 179.

15. M. Dragan, S. J. Dixon, E. Jaworski, T. S. Chan, P. J. O'Brien and J. X. Wilson, Brain Res., 1078, 2006, 9.

16. M. Harati, S. Amiralaei, J. Green and J. Wang, Chem. Phys. Lett., 439, 2007, 337.

17. M. Harati, S. Amiralaei, J. R. Green and J. Wang, J. Photochem. Photobiol. A: Chem., 198, 2008, 92.

Chapter 9 General Discussions and Conclusions

Discovery of new chemical oscillators is still an active and attractive subject in the study of macroscopic chemical reaction dynamics [1-7]. I have successfully discovered two new bromate-based chemical oscillatory reactions in a stirred batch reactor. Since then I carried out systematic investigations on the catalyzed systems using ferroin, cerium (III), and manganese (II). Then upon observing periodic colour change in the ferroin-catalyzed systems, I transferred both systems from the stirred batch reactor to reaction-diffusion media and studied wave formation during the rest of the course of my Ph.D. studies [8-12].

In chapter 2, I reported for the first time observing spontaneous chemical oscillatory behaviour in the uncatalyzed pyrocatechol-bromate reaction in sulfuric acid medium in the stirred batch reactor upon extensive searches in the concentration phase space [9]. This uncatalyzed bromate-pyrocatechol reaction has been investigated earlier by Orbàn and Körös, but no oscillatory behaviour was observed [13-15]. This system exhibits a clock reaction at the beginning which is accompanied by a dramatic color change from transparent to deep red and then gradually turns into yellow within the next two hours which is followed by oscillatory behaviour when the right reagent concentration is chosen. Long induction time in this system occurs, which perhaps is because of more stable bromated species in spite of malonic acid in the BZ reaction. This hypothesis can be examined by addition of HOBr or brominated pyrocatechol as an initial reagent to the reaction mixture. The long induction time seen in this uncatalyzed bromate-oscillator is insensitive to the initial presence of brominated species i.e., initial addition of bromide, which leads to the rapid production of bromine

and consequently causes the bromination of organic substrates. Mass spectrometry studies suggest the formation of bromo-1,2-benzoquinone from the reaction between pyrocatechol and bromine. Furthermore, our primary spectroscopic studies indicate that portion of pyrocatechol undergoes reactions or structure changes through, possibly, the formation of dimers or trimers with the pyrocatechol radicals produced through the initial excursion. The phase diagram in the bromate – pyrocatechol concentration phase space shows that the oscillatory behaviour is more sensitive to the ratio of [bromate]/[pyrocatechol] than their actual concentrations. The time series recorded with bromide selective electrode illustrates that at the initial stage of the reaction, there is a sudden drop in bromide concentration and subsequently the bromide concentration increases gradually through the long induction time period. We have proposed a mechanism for the system where our numerical simulations qualitatively reproduced the oscillations. The simulation further shows that experimental results of light-induced and light-quenched oscillatory behaviours can be qualitatively reproduced with light-mediated dissociation of bromine molecules. The proposed model can also qualitatively reproduce effects of bromate concentration on the oscillations seen in experiments, but is unable to account for variations of the induction time with respect to bromate concentration. This proposed mechanism and model need more detail investigation, such as considering reactions between bromine dioxide and organic substrate.

In chapter 3, we have examined effect of three different catalysts on the bromate-pyrocatechol reaction conducted in the stirred batch reactor. The induction time is insensitive to the presence of ferroin, but is greatly shortened by Ce(III) or Mn(II) [8]. On the other hand, the number of oscillations is significantly increased by ferroin, while it is less sensitive to Ce(III) and Mn(II). Interestingly, when catalysts

are added after oscillations have finished, the addition of ferroin was able to revive the oscillation, while adding the same amounts of cerium or magnesium ions at the same point did not show any observable influence on the reaction behaviour. This difference is due to the reduction potential of catalysts. The ferroin-catalyzed system also exhibits strong photosensitivity, in which illumination could quench the oscillatory behaviour. Whether the enhanced photosensitivity arises from ferroin or is due to changes in the reaction dynamics definitely worth to be explored in the future, as it may shed light on the photochemistry of several related systems.

Chemical wave studies carried out in the ferroin-catalyzed pyrocatechol-bromate system display different kinds of phenomena. Experiments in 1-D capillary tubes present various types of pulse instabilities which include breathing, propagation failure and merging pulses. Interactions of the propagating pulses further lead to the packing phenomenon. Systematic examination of our experiments indicates that the behaviour of propagation failure typically takes place during the initial reaction stage. A unique kinetic property of this reaction is that pyrocatechol and ferroin can both be oxidized auto-catalytically by bromine dioxide radicals, forming coupled nonlinear feedbacks. Considering that there was only limited success in finding a reaction-diffusion medium showing pulse instabilities [16-18], the above information shall greatly facilitate the future study on this important nonlinear behaviour. Chemical pattern formation investigated in 2-D media shows that the ferroin-pyrocatechol-bromate system exhibits two stages of wave activity, in which the first stage wave activity propagates several times faster than that of the second stage waves. Different from the classic BZ reaction [19], the first stage wave speed depends on the concentration of organic substrate, where wave speed decreases first and then increases as the concentration of pyrocatechol is increased. The second stage

wave activity survives for a significantly longer time than the initial waves, which lasts for up to 360 minutes depending on the initial conditions. In comparison to the ferroin-catalyzed BZ medium, the studied system exhibits greater photosensitivity, where photo-quenched (photo-initiated) behaviour could be conveniently achieved. We also reported in this thesis, our preliminary experimental result of chemical waves in the pyrocatechol-bromate system when ferroin was loaded onto cation beads. This thesis work illustrates that waves propagate faster in homogeneous pyrocatechol-bromate system than in the beads medium.

In chapter 4, chemical oscillations have been uncovered in the photo-mediated 4-aminophenol –bromate reaction [11]. The presence of light is found essential both to the extent of the reaction and the oscillatory behaviour, where turning-off (on) the light results in an immediate disappearance (revival) of the oscillation. When mixing all reactants together the reaction solution goes from colorless to yellow, mixed with precipitate. Formation of the precipitate is greatly accelerated in the presence of illumination. Phase diagrams show that illumination with intense light allows the otherwise non-oscillatory system to exhibit oscillations over broad 4-aminophenol, bromate and sulfuric acid concentrations. Phase diagram in a three-dimensional concentration space illustrates that the oscillatory behaviour is more sensitive to the ratio of $[AP]/[BrO_3^-]$ than their actual concentrations. Results of recording the potential simultaneously with both bromide selective electrode and Pt electrode indicate that the abrupt increase in the Pt potential matches with an abrupt increase of the bromide potential which corresponds to decrease of bromide concentration. Also, the sudden disappearance of the yellow precipitate accompanies a sudden decrease of bromide concentration which may be due to an autocatalytic production of $HBrO_2$, which consequently consumes bromide. This measurement also demonstrates that

bromide concentration increases slowly during the long induction time and then oscillates toward a higher value. The yellow precipitates have been analyzed with several methods including thin layer chromatography (TLC), mass spectrometry, ^{1}H NMR spectrometry, ^{13}C NMR spectrometry, elemental analysis, and measuring melting point. These characterization studies suggest that the reaction involves the production of N-bromo-1,4-benzoquinone-4-imine. To gain insight into the mechanism, mass spectrometry (electron impact, direct insertion), ^{1}H NMR, and ^{13}C NMR analysis were also performed at different reaction stages and several intermediates were identified such as: 1,4-benzoquinone and 2-bromo-3-hydroxy-1,4-benzoquinone.

The uncatalyzed bromate-aminophenol reaction does not display oscillatory behaviour in the absence of light. However, if we turn off the light and then add ferroin to the reaction mixture, the system exhibits slow oscillatory behaviour when the concentration of ferroin is higher than 0.002 M. When studied in reaction-diffusion media due to low reactivity of the medium, when the subsequent wave appears the previous one had already left the Petri dish, resulting the scenario of multistage pattern formation.

The two systems reported in this thesis need investigations on their mechanism and simulation of their wave formation. Especially the pyrocatechol-beads system needs more investigation in detail on the influence of light and/or laser pulses on spiral tip movement. Wave studies on the aminophenol-bromate in 1-D have been carried out, which were not covered in this thesis. However, the results show a very long lasting wave activity, more than 24 hours in general, along with wave instabilities and global breathing phenomena. Furthermore, we have used white light in all our experiments

on the aminophenol system; using a more selective light source would be beneficial in understanding the reaction mechanism.

Dopamine plays an important role in the brain and in the nervous systems. Therefore, at the beginning our primary goal was to investigate whether dopamine is capable of supporting oscillatory behaviour. Since chloride ions act as inhibitor in the BZ reaction and dopamine is only commercially available in hydrochloride form, we did not investigate dopamine directly and it would be the subject of future studies. Instead, we studied pyrocatechol and 4-aminophenol, which are very similar in structure with dopamine.

References

1. I. R. Epstein and J. A. Pojman, An Introduction to Nonlinear Chemical Dynamics, Oxford University Press, New York, 1998.

2. K. Kovacs, R.E. McIlwaine, S. K. Scott and A. F. Taylor, Phys. Chem. Chem. Phys., 9, 2007, 3711.

3. R. McIlwaine, K. Kovacs, S. K. Scott and A. F. Taylor, Chem. Phys. Lett., 417, 2006, 39.

4. K. Kurin-Csörgei, I. R. Epstein and M. Orbán, J. Phys. Chem. B, 108, 2004, 7352.

5. N. Okazaki, G. Rábai and I. Hanazaki, J. Phys. Chem. A, 103, 1999, 10915.

6. M. Tóthová, A. Nagy and L. Treindl, Chem. Phys. Lett., 299, 1999, 243.

7. K. Kovacs, R. E. McIlwaine, S. K. Scott and A. F. Taylor, J. Phys. Chem. A, 111, 2007, 549

8. M. Harati and J. Wang, J. Phys. Chem. A, 112, 2008, 4241.

9. M. Harati and J. Wang, Z. Phys. Chem., 222, 2008, 997.

10. M. Harati and J. Wang, Chaos, submitted.

11. M. Harati, S. Amiralaei, J. Green and J. Wang, Chem. Phys. Lett., 439, 2007, 337.

12. M. Harati, S. Amiralaei, J. R. Green and J. Wang, J. Photochem. Photobiol. A: Chem., 198, 2008, 92.

13. E. Körös and M. Orbán, Nature, 273, 1978, 371.

14. M. Orbán and E. Körös, J. Phys. Chem., 82, 1978, 1672.

15. M. Orbán and E. Körös, React. Kinet. Catal. Lett., 8, 1978, 273.

16. N. Manz and O. Steinbock, Chaos, 16, 2006, 037112.

17. N. Manz, S. C. Müller and O. Steinbock, J. Phys. Chem. A, 104, 2000, 5895.

18. M. Pomprompanya, S. C. Müller, H. Ševčíková, Phys. Chem. Chem. Phys., 4, 2002, 3370.

19. L. Kuhnert and H. J. Krug, J. Phys. Chem., 91, 1987, 730.

Appendix A Code of the Simulation in Table 2.1

METHOD STIFF

STARTTIME = 0
STOPTIME= 60000
DT = 0.02
TOLERANCE = 0.000001

H = 2.8
H2O = 55.6

```
{ 1: BrO3+Br+2H <--> HBrO2+HOBr }
    RXN1 = K1f*BrO3*Br*H^2 - K1r*HBrO2*HOBr
    K1f = 2.1
    K1r = 10000
    INIT Br = 1e-15
    INIT BrO3 =0.085
    INIT HBrO2 = 1e-8
    INIT HOBr = 1e-8
    d/dt(Br) = -RXN1-RXN2+RXN7-RXN8+3*RXN9
    d/dt(BrO3) = -RXN1-RXN3+RXN5
    d/dt(HBrO2) = +RXN1-RXN2-RXN3+RXN4-2*RXN5+RXN13
    d/dt(HOBr) = +RXN1+2*RXN2+RXN5-RXN6-RXN8-RXN10

{ 2: HBrO2+Br+H <--> 2HOBr }
    RXN2 = K2f*HBrO2*Br*H - K2r*HOBr^2
    K2f = 2e+009
    K2r = 0

{ 3: BrO3+HBrO2+H <--> 2BrO2+H2O }
    RXN3 = K3f*BrO3*HBrO2*H - K3r*BrO2^2*H2O
    K3f = 10000
    K3r = 2e+007
    INIT BrO2 = 1e-8
    d/dt(BrO2) = +2*RXN3-RXN4-RXN13

{ 4: BrO2+HArOH2 <--> HBrO2+HArOHO }
    RXN4 = K4f*BrO2*HArOH2 - K4r*HBrO2*HArOHO
    K4f = 700
```

```
    K4r = 0
    INIT HArOH2 = 0.041
    INIT HArOHO = 1e-8
    d/dt(HArOH2) = -RXN4-RXN9-RXN10-RXN11+RXN12
    d/dt(HArOHO) = +RXN4-RXN6-RXN7-RXN11-2*RXN12-RXN13


{ 5: 2HBrO2 <--> BrO3+HOBr+H }
    RXN5 = K5f*HBrO2^2 - K5r*BrO3*HOBr*H
    K5f = 4e+007
    K5r = 0


{ 6: HOBr+HArOHO <--> C+HArO2 }
    RXN6 = K6f*HOBr*HArOHO - K6r*C*HArO2
    K6f = 5500
    K6r = 2e+006
    INIT C = 1e-8
    INIT HArO2 = 1e-8
    d/dt(C) = +RXN6-RXN7+2*RXN14
    d/dt(HArO2) = +RXN6+RXN7+RXN12+RXN13


{ 7: C+HArOHO <--> Br+HArO2+H }
    RXN7 = K7f*C*HArOHO - K7r*Br*HArO2*H
    K7f = 5.5e+006
    K7r = 1050


{ 8: HOBr+Br+H <--> Br2+H2O }
    RXN8 = K8f*HOBr*Br*H - K8r*Br2*H2O
    K8f = 8e+009
    K8r = 110
    INIT Br2 = 1e-8
    d/dt(Br2) = +RXN8-2*RXN9-RXN14


{ 9: 2Br2+HArOH2 <--> BrArOH2+3Br+3H }
    RXN9 = K9f*Br2^2*HArOH2 - K9r*BrArOH2*Br^3*H^3
    K9f = 0.05
    K9r = 0
    INIT BrArOH2 = 1e-8
    d/dt(BrArOH2) = +RXN9+RXN10


{ 10: HOBr+HArOH2 <--> BrArOH2+H2O }
    RXN10 = K10f*HOBr*HArOH2 - K10r*BrArOH2*H2O
    K10f = 1
    K10r = 0


{ 11: HArOHO+HArOH2 <--> Complex }
    RXN11 = K11f*HArOHO*HArOH2 - K11r*Complex
    K11f = 1e+006
```

```
   K11r = 1
   INIT Complex = 0
   d/dt(Complex) = +RXN11

{ 12: 2HArOHO <--> HArOH2+HArO2 }
   RXN12 = K12f*HArOHO^2 - K12r*HArOH2*HArO2
   K12f = 0
   K12r = 0

{ 13: HArOHO+BrO2 <--> HBrO2+HArO2 }
   RXN13 = K13f*HArOHO*BrO2 - K13r*HBrO2*HArO2
   K13f = 5000
   K13r = 0

{ 14: Br2 <--> 2C }
   RXN14 = K14f*Br2 - K14r*C^2
   K14f = 0
   K14r = 0.
```

Appendix B Copyright Releases J. Phys. Chem. A

American Chemical Society's Policy on Theses and Dissertations

Thank you for your request for permission to include your paper or portions of text from your paper in your thesis. Permission is now automatically granted; please pay special attention to the implications paragraph below. The Copyright Subcommittee of the Joint Board/Council Committees on Publications approved the following:

<u>Copyright permissions for published and submitted material from theses and dissertations</u>
ACS extends blanket permission to students to include in their theses and dissertations their own articles, or portions thereof, that have been published in ACS journals or submitted to ACS journals for publication, provided that the ACS copyright credit line is noted on the appropriate page(s).

<u>Publishing implications of electronic publication of theses and dissertation material</u>
Students and their mentors should be aware that posting of theses and dissertation material on the Web prior to submission of material from that thesis or dissertation to an ACS journal <u>may</u> affect publication in that journal. Whether Web posting is considered prior publication may be evaluated on a case-by-case basis by the journal's editor. Is an ACS journal editor considers Web posting to be "prior publication", the paper will not be accepted for publication in that journal. If you intend to submit your unpublished paper to ACS for publication, check with the appropriate editor prior to posting your manuscript electronically.

Appendix C Copyright Releases Chem. Phys. Lett.

ELSEVIER LICENSE
TERMS AND CONDITIONS

Oct 19, 2008

This is a License Agreement between Mohammad Harati ("You") and Elsevier ("Elsevier"). The license consists of your order details, the terms and conditions provided by Elsevier, and the payment terms and conditions.

Supplier	Elsevier Limited The Boulevard,Langford Lane Kidlington,Oxford,OX5 1GB,UK
Registered Company Number	1982084
Customer name	Mohammad Harati
Customer address	150 Park St. west
	Windsor, ON N9A7A2
License Number	2052830987806
License date	Oct 19, 2008
Licensed content publisher	Elsevier
Licensed content publication	Chemical Physics Letters
Licensed content title	Chemical oscillations in the 4-aminophenol–bromate photoreaction
Licensed content author	Mohammad Harati, Sheida Amiralaei, James Green and Jichang Wang
Licensed content date	11 May 2007
Volume number	

Issue number

Pages	0
Type of Use	Thesis / Dissertation
Portion	Full article
Format	Print
You are an author of the Elsevier article	Yes
Are you translating?	No

Purchase order number

Expected publication date	Dec 2008
Elsevier VAT number	GB 494 6272 12
Permissions price	0.00 USD
Value added tax 0.0%	0.00 USD
Total	0.00 USD

Terms and Conditions

INTRODUCTION

1. The publisher for this copyrighted material is Elsevier. By clicking "accept" in connection with completing this licensing transaction, you agree that the following terms and conditions apply to this transaction (along with the Billing and Payment terms and conditions established by Copyright Clearance Center, Inc. ("CCC"), at the time that you opened your Rightslink account and that are available at any time at <http://myaccount.copyright.com>).

GENERAL TERMS

2. Elsevier hereby grants you permission to reproduce the aforementioned material subject to the terms and conditions indicated.

3. Acknowledgement: If any part of the material to be used (for example, figures) has appeared in our publication with credit or acknowledgement to another source, permission must also be sought from that source. If such permission is not obtained then that material may not be included in your publication/copies. Suitable acknowledgement to the source

must be made, either as a footnote or in a reference list at the end of your publication, as follows:

"Reprinted from Publication title, Vol /edition number, Author(s), Title of article / title of chapter, Pages No., Copyright (Year), with permission from Elsevier [OR APPLICABLE SOCIETY COPYRIGHT OWNER]." Also Lancet special credit - "Reprinted from The Lancet, Vol. number, Author(s), Title of article, Pages No., Copyright (Year), with permission from Elsevier."

4. Reproduction of this material is confined to the purpose and/or media for which permission is hereby given.

5. Altering/Modifying Material: Not Permitted. However figures and illustrations may be altered/adapted minimally to serve your work. Any other abbreviations, additions, deletions and/or any other alterations shall be made only with prior written authorization of Elsevier Ltd. (Please contact Elsevier at permissions@elsevier.com)

6. If the permission fee for the requested use of our material is waived in this instance, please be advised that your future requests for Elsevier materials may attract a fee.

7. Reservation of Rights: Publisher reserves all rights not specifically granted in the combination of (i) the license details provided by you and accepted in the course of this licensing transaction, (ii) these terms and conditions and (iii) CCC's Billing and Payment terms and conditions.

8. License Contingent Upon Payment: While you may exercise the rights licensed immediately upon issuance of the license at the end of the licensing process for the transaction, provided that you have disclosed complete and accurate details of your proposed use, no license is finally effective unless and until full payment is received from you (either by publisher or by CCC) as provided in CCC's Billing and Payment terms and conditions. If full payment is not received on a timely basis, then any license preliminarily granted shall be deemed automatically revoked and shall be void as if never granted. Further, in the event that you breach any of these terms and conditions or any of CCC's Billing and Payment terms and conditions, the license is automatically revoked and shall be void as if never granted. Use of materials as described in a revoked license, as well as any use of the materials beyond the scope of an unrevoked license, may constitute copyright infringement and publisher reserves the right to take any and all action to protect its copyright in the materials.

9. Warranties: Publisher makes no representations or warranties with respect to the licensed material.

10. Indemnity: You hereby indemnify and agree to hold harmless publisher and CCC, and their respective officers, directors, employees and agents, from and against any and all claims arising out of your use of the licensed material other than as specifically authorized

pursuant to this license.

11. No Transfer of License: This license is personal to you and may not be sublicensed, assigned, or transferred by you to any other person without publisher's written permission.

12. No Amendment Except in Writing: This license may not be amended except in a writing signed by both parties (or, in the case of publisher, by CCC on publisher's behalf).

13. Objection to Contrary Terms: Publisher hereby objects to any terms contained in any purchase order, acknowledgment, check endorsement or other writing prepared by you, which terms are inconsistent with these terms and conditions or CCC's Billing and Payment terms and conditions. These terms and conditions, together with CCC's Billing and Payment terms and conditions (which are incorporated herein), comprise the entire agreement between you and publisher (and CCC) concerning this licensing transaction. In the event of any conflict between your obligations established by these terms and conditions and those established by CCC's Billing and Payment terms and conditions, these terms and conditions shall control.

14. Revocation: Elsevier or Copyright Clearance Center may deny the permissions described in this License at their sole discretion, for any reason or no reason, with a full refund payable to you. Notice of such denial will be made using the contact information provided by you. Failure to receive such notice will not alter or invalidate the denial. In no event will Elsevier or Copyright Clearance Center be responsible or liable for any costs, expenses or damage incurred by you as a result of a denial of your permission request, other than a refund of the amount(s) paid by you to Elsevier and/or Copyright Clearance Center for denied permissions.

LIMITED LICENSE

The following terms and conditions apply to specific license types:

15. **Translation**: This permission is granted for non-exclusive world **English** rights only unless your license was granted for translation rights. If you licensed translation rights you may only translate this content into the languages you requested. A professional translator must perform all translations and reproduce the content word for word preserving the integrity of the article. If this license is to re-use 1 or 2 figures then permission is granted for non-exclusive world rights in all languages.

16. **Website**: The following terms and conditions apply to electronic reserve and author websites:
Electronic reserve: If licensed material is to be posted to website, the web site is to be password-protected and made available only to bona fide students registered on a relevant

course if:

This license was made in connection with a course,

This permission is granted for 1 year only. You may obtain a license for future website posting,

All content posted to the web site must maintain the copyright information line on the bottom of each image,

A hyper-text must be included to the Homepage of the journal from which you are licensing at http://www.sciencedirect.com/science/journal/xxxxx or the Elsevier homepage for books at http://www.elsevier.com , and

Central Storage: This license does not include permission for a scanned version of the material to be stored in a central repository such as that provided by Heron/XanEdu.

17. **Author website** for journals with the following additional clauses:

This permission is granted for 1 year only. You may obtain a license for future website posting,

All content posted to the web site must maintain the copyright information line on the bottom of each image, and

The permission granted is limited to the personal version of your paper. You are not allowed to download and post the published electronic version of your article (whether PDF or HTML, proof or final version), nor may you scan the printed edition to create an electronic version,

A hyper-text must be included to the Homepage of the journal from which you are licensing at http://www.sciencedirect.com/science/journal/xxxxx , or the Elsevier homepage for books at http://www.elsevier.com and

Central Storage: This license does not include permission for a scanned version of the material to be stored in a central repository such as that provided by Heron/XanEdu.

18. **Author website** for books with the following additional clauses:

Authors are permitted to place a brief summary of their work online only.

A hyper-text must be included to the Elsevier homepage at http://www.elsevier.com

This permission is granted for 1 year only. You may obtain a license for future website posting,

All content posted to the web site must maintain the copyright information line on the bottom of each image, and

The permission granted is limited to the personal version of your paper. You are not allowed to download and post the published electronic version of your article (whether PDF or HTML, proof or final version), nor may you scan the printed edition to create an electronic version,

A hyper-text must be included to the Homepage of the journal from which you are licensing at http://www.sciencedirect.com/science/journal/xxxxx , or the Elsevier homepage for books at http://www.elsevier.com and

Central Storage: This license does not include permission for a scanned version of the material to be stored in a central repository such as that provided by Heron/XanEdu.

19. **Website** (regular and for author): "A hyper-text must be included to the Homepage of the journal from which you are licensing at http://www.sciencedirect.com/science/journal/xxxxx."

20. **Thesis/Dissertation**: If your license is for use in a thesis/dissertation your thesis may be submitted to your institution in either print or electronic form. Should your thesis be published commercially, please reapply for permission. These requirements include permission for the Library and Archives of Canada to supply single copies, on demand, of the complete thesis and include permission for UMI to supply single copies, on demand, of the complete thesis. Should your thesis be published commercially, please reapply for permission.

v1.2

21. **Other conditions:**

None

Appendix D Copyright Releases J. Photochem. Photobiol. A: Chem

ELSEVIER LICENSE
TERMS AND CONDITIONS

Oct 19, 2008

This is a License Agreement between Mohammad Harati ("You") and Elsevier ("Elsevier"). The license consists of your order details, the terms and conditions provided by Elsevier, and the payment terms and conditions.

Supplier	Elsevier Limited The Boulevard,Langford Lane Kidlington,Oxford,OX5 1GB,UK
Registered Company Number	1982084
Customer name	Mohammad Harati
Customer address	150 Park St. west
	Windsor, ON N9A7A2
License Number	2052850035267
License date	Oct 19, 2008
Licensed content publisher	Elsevier
Licensed content publication	Journal of Photochemistry and Photobiology A: Chemistry
Licensed content title	Nonlinear instabilities in the light-mediated bromate–4-aminophenol reaction
Licensed content author	Mohammad Harati, Sheida Amiralaei, James R. Green and Jichang Wang
Licensed content date	5 July 2008
Volume number	198
Issue number	1

Pages	6
Type of Use	Thesis / Dissertation
Portion	Full article
Format	Print
You are an author of the Elsevier article	Yes
Are you translating?	No
Purchase order number	
Expected publication date	Dec 2008
Elsevier VAT number	GB 494 6272 12
Permissions price	0.00 USD
Value added tax 0.0%	0.00 USD
Total	0.00 USD

Terms and Conditions

INTRODUCTION

1. The publisher for this copyrighted material is Elsevier. By clicking "accept" in connection with completing this licensing transaction, you agree that the following terms and conditions apply to this transaction (along with the Billing and Payment terms and conditions established by Copyright Clearance Center, Inc. ("CCC"), at the time that you opened your Rightslink account and that are available at any time at <http://myaccount.copyright.com>).

GENERAL TERMS

2. Elsevier hereby grants you permission to reproduce the aforementioned material subject to the terms and conditions indicated.

3. Acknowledgement: If any part of the material to be used (for example, figures) has appeared in our publication with credit or acknowledgement to another source, permission must also be sought from that source. If such permission is not obtained then that material

may not be included in your publication/copies. Suitable acknowledgement to the source must be made, either as a footnote or in a reference list at the end of your publication, as follows:

"Reprinted from Publication title, Vol /edition number, Author(s), Title of article / title of chapter, Pages No., Copyright (Year), with permission from Elsevier [OR APPLICABLE SOCIETY COPYRIGHT OWNER]." Also Lancet special credit - "Reprinted from The Lancet, Vol. number, Author(s), Title of article, Pages No., Copyright (Year), with permission from Elsevier."

4. Reproduction of this material is confined to the purpose and/or media for which permission is hereby given.

5. Altering/Modifying Material: Not Permitted. However figures and illustrations may be altered/adapted minimally to serve your work. Any other abbreviations, additions, deletions and/or any other alterations shall be made only with prior written authorization of Elsevier Ltd. (Please contact Elsevier at permissions@elsevier.com)

6. If the permission fee for the requested use of our material is waived in this instance, please be advised that your future requests for Elsevier materials may attract a fee.

7. Reservation of Rights: Publisher reserves all rights not specifically granted in the combination of (i) the license details provided by you and accepted in the course of this licensing transaction, (ii) these terms and conditions and (iii) CCC's Billing and Payment terms and conditions.

8. License Contingent Upon Payment: While you may exercise the rights licensed immediately upon issuance of the license at the end of the licensing process for the transaction, provided that you have disclosed complete and accurate details of your proposed use, no license is finally effective unless and until full payment is received from you (either by publisher or by CCC) as provided in CCC's Billing and Payment terms and conditions. If full payment is not received on a timely basis, then any license preliminarily granted shall be deemed automatically revoked and shall be void as if never granted. Further, in the event that you breach any of these terms and conditions or any of CCC's Billing and Payment terms and conditions, the license is automatically revoked and shall be void as if never granted. Use of materials as described in a revoked license, as well as any use of the materials beyond the scope of an unrevoked license, may constitute copyright infringement and publisher reserves the right to take any and all action to protect its copyright in the materials.

9. Warranties: Publisher makes no representations or warranties with respect to the licensed material.

10. Indemnity: You hereby indemnify and agree to hold harmless publisher and CCC, and their respective officers, directors, employees and agents, from and against any and all claims arising out of your use of the licensed material other than as specifically authorized

pursuant to this license.

11. No Transfer of License: This license is personal to you and may not be sublicensed, assigned, or transferred by you to any other person without publisher's written permission.

12. No Amendment Except in Writing: This license may not be amended except in a writing signed by both parties (or, in the case of publisher, by CCC on publisher's behalf).

13. Objection to Contrary Terms: Publisher hereby objects to any terms contained in any purchase order, acknowledgment, check endorsement or other writing prepared by you, which terms are inconsistent with these terms and conditions or CCC's Billing and Payment terms and conditions. These terms and conditions, together with CCC's Billing and Payment terms and conditions (which are incorporated herein), comprise the entire agreement between you and publisher (and CCC) concerning this licensing transaction. In the event of any conflict between your obligations established by these terms and conditions and those established by CCC's Billing and Payment terms and conditions, these terms and conditions shall control.

14. Revocation: Elsevier or Copyright Clearance Center may deny the permissions described in this License at their sole discretion, for any reason or no reason, with a full refund payable to you. Notice of such denial will be made using the contact information provided by you. Failure to receive such notice will not alter or invalidate the denial. In no event will Elsevier or Copyright Clearance Center be responsible or liable for any costs, expenses or damage incurred by you as a result of a denial of your permission request, other than a refund of the amount(s) paid by you to Elsevier and/or Copyright Clearance Center for denied permissions.

LIMITED LICENSE

The following terms and conditions apply to specific license types:

15. **Translation**: This permission is granted for non-exclusive world **English** rights only unless your license was granted for translation rights. If you licensed translation rights you may only translate this content into the languages you requested. A professional translator must perform all translations and reproduce the content word for word preserving the integrity of the article. If this license is to re-use 1 or 2 figures then permission is granted for non-exclusive world rights in all languages.

16. **Website**: The following terms and conditions apply to electronic reserve and author websites:
Electronic reserve: If licensed material is to be posted to website, the web site is to be password-protected and made available only to bona fide students registered on a relevant

course if:
This license was made in connection with a course,
This permission is granted for 1 year only. You may obtain a license for future website posting,
All content posted to the web site must maintain the copyright information line on the bottom of each image,
A hyper-text must be included to the Homepage of the journal from which you are licensing at http://www.sciencedirect.com/science/journal/xxxxx or the Elsevier homepage for books at http://www.elsevier.com , and
Central Storage: This license does not include permission for a scanned version of the material to be stored in a central repository such as that provided by Heron/XanEdu.

17. **Author website** for journals with the following additional clauses:
This permission is granted for 1 year only. You may obtain a license for future website posting,
All content posted to the web site must maintain the copyright information line on the bottom of each image, and
The permission granted is limited to the personal version of your paper. You are not allowed to download and post the published electronic version of your article (whether PDF or HTML, proof or final version), nor may you scan the printed edition to create an electronic version,
A hyper-text must be included to the Homepage of the journal from which you are licensing at http://www.sciencedirect.com/science/journal/xxxxx , or the Elsevier homepage for books at http://www.elsevier.com and
Central Storage: This license does not include permission for a scanned version of the material to be stored in a central repository such as that provided by Heron/XanEdu.

18. **Author website** for books with the following additional clauses:
Authors are permitted to place a brief summary of their work online only.
A hyper-text must be included to the Elsevier homepage at http://www.elsevier.com
This permission is granted for 1 year only. You may obtain a license for future website posting,
All content posted to the web site must maintain the copyright information line on the bottom of each image, and
The permission granted is limited to the personal version of your paper. You are not allowed to download and post the published electronic version of your article (whether PDF or HTML, proof or final version), nor may you scan the printed edition to create an electronic version,
A hyper-text must be included to the Homepage of the journal from which you are licensing at http://www.sciencedirect.com/science/journal/xxxxx , or the Elsevier homepage for books at http://www.elsevier.com and
Central Storage: This license does not include permission for a scanned version of the material to be stored in a central repository such as that provided by Heron/XanEdu.

19. **Website** (regular and for author): "A hyper-text must be included to the Homepage of the journal from which you are licensing at http://www.sciencedirect.com/science/journal/xxxxx."

20. **Thesis/Dissertation**: If your license is for use in a thesis/dissertation your thesis may be submitted to your institution in either print or electronic form. Should your thesis be published commercially, please reapply for permission. These requirements include permission for the Library and Archives of Canada to supply single copies, on demand, of the complete thesis and include permission for UMI to supply single copies, on demand, of the complete thesis. Should your thesis be published commercially, please reapply for permission.

v1.2

21. **Other conditions:**

None

APPENDIX E Copyright Releases Z. Phys. Chem.

From: "Prof. H. Baumgaertel" <baum@chemie.fu-berlin.de>

Subject: Re: Third email, Policy on Dissertation

Date: Mon, 13 Oct 2008 12:50:37 +0200

To: "Mohammad Harati" <harati@uwindsor.ca>

Re: Third email, Policy on Dissertation
Dear Mohammad Harati,

we are apologizing for our delayed answer to your e-mails.

We agree that you use the material of the recent publication (Z. Phys. Chem, 222 (2008) 997-1011) in your Ph.D. Thesis.

Sincerely Yours

Prof. Dr. H. Baumgärtel
(Editor in Chief)

VITA AUCTORIS

NAME	Mohammad Harati
PLACE OF BIRTH	Tehran, Iran
YEARS OF BIRTH	1974
EDUCATION	Saadat High School, Bushehr 1988-1992 Ferdowsi University of Mashhad, Mashhad, Iran 1992-1996 B.Sc. Sharif University of Technology, Tehran, Iran 1999-2001 Univeristy of Windsor, Ontaio, Canada 2005-2008